

**Department of Civil Engineering**

**Bioelectrochemical Reactor Technology for the Treatment of  
Alkaline Waste Streams of Alumina Industry**

**Tharanga Nimashanie Weerasinghe Mohottige**

**This thesis is presented for the Degree of  
Doctor of Philosophy  
of  
Curtin University**

**September 2017**

## **Declaration**

To the best of my knowledge and belief, this thesis contains no material previously published by and other person except where due acknowledgement has been made.

This thesis contains no material which has been accepted for the award of any other degree or diploma in any university.

Signature:



Tharanga Nimashanie Weerasinghe Mohottige

Date: 22<sup>nd</sup> September 2018

## **Abstract**

Aluminium is one of the most commercially utilized metals in the world due to its light weight, high strength and excellent corrosion resistance. Aluminium does not occur in its metallic form and refining is required to produce aluminium from its mineral ore. Bauxite is the most commonly used aluminium ore and it is refined in Bayer process to produce alumina ( $\text{Al}_2\text{O}_3$ ). In brief, the major steps of the Bayer process are (1) the digestion of bauxite in a hot concentrated caustic ( $\text{NaOH}$ ) solution; (2) the recovery of aluminium hydroxide ( $\text{Al(OH)}_3$ ) with seeded precipitation at low temperature; and (3) the calcination of aluminium hydroxide to produce alumina.

The accumulation of organic impurities into the process liquor is a major challenge in Bayer processing. Bauxite contains a range of organic substances, which are extracted into process liquor during the digestion step. After precipitation of aluminium hydroxide, the liquor part (spent liquor) is recycle back to digestion step for reuse of the remaining caustic. However, this recirculation of the spent liquor increases the organics concentration of the process liquor. Among the organic impurities, sodium oxalate ( $\text{Na}_2\text{C}_2\text{O}_4$ ) is detrimental, as oxalate co-precipitates with  $\text{Al(OH)}_3$  and reduces the product quality and process efficiency. In Western Australia typical alumina refinery can produce approximately 40 t/d oxalate, which requires environmentally feasible treatment option.

Biological processes have been considered as an environmentally sustainable solution for complete degradation of sodium oxalate. The commercial scale aerobic bioreactors are in operation at some refineries in Western Australia. Although the aerobic biodegradation of oxalate is a proven treatment solution, it does not allow the recovery of caustic soda. Therefore, the main objective of this study was to investigate an alternative technology, as bioelectrochemical systems (BES), to biodegrade oxalate and recover caustic soda from solutions that represent Bayer liquor in its alkalinity, salinity and oxalate concentration. The other objective of this research was to investigate the use of nitrogen fixing bacteria in both aerobic bioreactors and BES reactor to alleviate the need for external nitrogen supplementation for oxalate biodegradation.

A series of laboratory scale experiments were carried out to: 1) prove the concept of organics removal in BES using alkaline and saline solution under both N-

supplemented and N-deficient conditions, 2) investigate and compare the caustic recovery under N-supplemented and N-deficient conditions, 3) enrich a haloalkaliphilic oxalate degrading biofilm in an aerobic reactor under both N-supplemented and N-deficient conditions, 4) optimise the aerobic process under different operational parameters (pH, dissolve oxygen concentration (DO) and oxalate concentration) and 5) investigate the oxalate degradation in BES using aerobically acclimatised biofilm. Comparative analysis of N-deficient systems vs. N-supplemented systems was conducted to evaluate whether nitrogen fixing microorganisms provide competitive performance as compared to N-supplemented microbial communities. During the entire study, a synthetic solution that stimulate the Bayer liquor alkalinity, salinity and oxalate content was used as the feed solution.

As the proof of concept, the feasibility of using BES to oxidise oxalate in the anodic chamber of BES at alkaline and saline conditions with and without N source (reactor R1 with N source, reactor R2 without N source) was investigated. Two identical duel chamber laboratory scale BES reactors (operated > 300 days) filled with graphite granules as the anode and cathode material were used in this experiment. Activated sludge was used as the inoculum source to establish an electrochemically active haloalkaliphilic biofilms. Even though the biofilms in R1 and R2 were unable to anodically oxidise oxalate under the operating conditions (pH 9.0, NaCl 25 g/L and anode potential +200 mV vs. Ag/AgCl), acetate and formate were readily oxidised in the BES. After adding sodium acetate as a co-substrate, the R1 and R2 biofilms produced maximum currents of  $227 \pm 6.5$  mA (Chemical oxygen demand (COD) removal 31%, organic loading rate (OLR) 15.3 kg COD/m<sup>3</sup>.d) and  $135 \pm 4$  mA (COD removal 38 %, OLR 5.1 kg COD/m<sup>3</sup>.d), respectively. However, the oxalate removal efficiency was very low (< 5%) compared to complete acetate removal regardless of N supplementation. Further, the results showed that although the bioanode potentials in both R1 and R2 were mostly maintained at +200 mV vs. Ag/AgCl during the start-up, both biofilms were able to generate maximal anodic current at a much lower anode potentials (-300 mV vs. Ag/AgCl for R1; -200 mV vs Ag/AgCl for R2). The microbial community analysis revealed that the inefficient oxalate removal was likely due to the lack of oxalotrophic strains responsible for catalysing the decarboxylation of oxalate.

The same two BES reactors were used to investigate the cathodic caustic production under N-supplemented and N-deficient conditions. The BES anodic compartments

were fed continuously with oxalate and acetate containing saline and alkaline solution simulating the salinity and alkalinity of Bayer liquor (0.4 M NaCl, pH 10), and the anolyte was actively maintained at pH 9 by dosing NaOH. Cathodes were operated in fed-batch mode with 0.4 M NaCl (2 L) as the catholyte.  $\text{Na}^+$  transfer % to catholyte was higher in N-deficient BES reactor (95.8%) compared to N-supplemented BES (94.9%). Both reactors were able to produce coulombic efficiency (CE) of >75% for caustic generation. The energy input for the caustic production was lower than reported in previous studies conducted by using BES for caustic recovery.

To overcome the difficulty in oxalate oxidation for established biofilm inoculated with activated sludge in BES reactors, two aerobic bioreactors were setup to enrich oxalate degrading biofilms. Two packed bed column reactors filled with graphite granules as biofilm carriers were used as aerobic bioreactors (operated > 265 days) for the experiments. Soil samples collected from coastal sediments and rhizosphere from a nature reserve were used as an inoculum source. The graphite granules (conductive material) were used as the biofilm carriers with the aim to use the granules as anode material for later BES experiments. Comparative analysis was carried out to characterise and optimise different operational parameters with N-supplemented and N-deficient conditions. In one set of experiments, oxalate degradation rates and oxygen uptake rates (OUR) were determined at different bulk water DO set-points. The results revealed that oxalate removal rates (33 – 111 mg/h.g biomass) linearly correlated with OUR (0 – 70 mg O<sub>2</sub>/h.g biomass) in the N-supplemented reactor. However, in the N-deficient reactor, a linear increase of oxalate removal was recorded only with DO up to  $\leq$  3 mg/L. Surprisingly, anaerobic oxalate removal was evident even in the presence of up to 8 mg/L DO in both reactors. Further investigation revealed formate, acetate and methane as by-products of anaerobic oxalate removal in both reactors.

Although an N-deficient culture appears beneficial (no requirements to supplement N) this culture is yet to be fully characterised and compared against the N-supplemented cultures used by the industry. As Bayer liquor is an alkaline solution, the knowledge about the influence of pH is necessary for the industry to consider and adopt haloalkaliphilic nitrogen fixers as a preferable microbial culture. Hence, the influence of pH on oxalate removal efficiencies of two biofilms enriched under N-deficient and supplemented conditions was comparatively examined. Although, N-deficient biofilm

was acclimatised at pH 9, the highest oxalate removal rate was over a pH range of 7 to 8 possibly due to the inhibition of nitrogenase activity at pH > 8. In contrast, the N-supplemented reactor showed the highest removal rate at pH 9. Further, the effect of other simple organic compounds (sodium acetate, sodium formate, sodium succinate and sodium malonate) present in Bayer process on aerobic oxalate oxidation was evaluated and the results suggested that no influence from the other organics on oxalate oxidation in aerobic reactor regardless of N availability.

Until now, there has been paucity of information available on oxalate degradation kinetics, although it is a key design factor for developing bioreactor processes. In this study, Michaelis-Menten kinetics was used to determine the oxalate degradation kinetics in N-deficient and N-supplemented cultures. The N-deficient reactor had a higher affinity ( $K_m$ ) towards oxalate and showed higher maximum specific oxalate oxidation rates ( $V_{max}$ ) compared to the N-supplemented reactor. The derived kinetic parameters were used to propose a novel two step treatment process to remove oxalate from an oxalate slurry side stream of an alumina refinery. The prospective bioreactor will require two units, yet with a smaller reactor foot print, especially suitable for a low oxalate discharge with effluent. Microbial community analysis suggested that the composition of the two cultures were uniquely different.

The aerobically acclimatised oxalotrophic biofilm was used to inoculate a BES reactor for further study the oxalate degradation. A rapid reactor start-up was recorded, as the biofilm was able to instantly switch the electron acceptor from oxygen to solid electrode surface. The performance of the BES was evaluated at a range of hydraulic retention times (HRTs) (3 - 24 h), set anode potentials (-600 to +200 mV Ag/AgCl) and concentrations of sodium acetate (5 - 30 mM) as a co-substrate. The maximum current production was  $122 \pm 0.6$  mA at 3 h HRT and coulombic efficiency (CE) was 70% at all tested HRTs. The anodic biofilm produced maximum current at -300 mV vs. Ag/AgCl and was capable of complete oxidation of acetate and oxalate simultaneously with 80% CE. The analysis of microbial communities revealed that known oxalate degraders from *Oxalobacteraceae* family were present in the biofilm.

Overall, in this thesis, the feasibility of biological oxalate and other organics removal was explored in two different contexts, aerobic bioreactors and BES reactors under alkaline, saline, N-supplemented and N-deficient conditions. Both biological

processes were competent in efficient organics destruction under the tested conditions. Specifically, this study revealed the potential of BES technology, not only as an efficient organics removal method, but also for the recovery of caustic from alkaline, saline organic-rich water. Further research is needed to investigate the feasibility of the BES process using real waste streams from alumina industry.

## **Acknowledgement**

Hereby, I would like to express my sincere gratitude to those mentioned below who supported to complete my PhD studies.

First and foremost, I would like to thank all my supervisors for their valuable advice, guidance and encouragement throughout the course of my studies. I thank Dr, Ranjan Sarukkalige for giving this opportunity to me and his continuous encouragement throughout my studies. I really appreciate the understanding and flexibility of Dr. KaYu Cheng for sharing his knowledge in bio electrochemical systems and writing skills. His invaluable guidance helped me to improve on my academic and soft skills. I thank Dr Maneesha Ginige for the detail explanations on academic matters, which helped me to build my confidence in the new environment and for encouraging me to finish my work. I admire his knowledge and passion for research. I am also grateful to Dr Anna Kaksonen for her friendly guidance and quick feedbacks. I thank her for inspiring me to become efficient and accurate in work. I feel fortunate to do my PhD under such some elite group of supervisors.

I would also like to take this opportunity to thank all my colleagues whom I worked closely at CSIRO. They have become my second family during the past few years, assisting me in various ways. Penny Wong, Sara Salehi and Hassan Mohammadi Khalfbadam for their helping hands and friendship. Trevor Bastow and Yasuko Gaste for assistance in chemical analysis and friendly discussions. Jason Wylie, Naomi Boxall and Cristina Morris for sharing their knowledge on microbial analysis and techniques. Robert Woodbury, Aino-Maija Lakaniemi and other lunch table friends for the friendly and educational lunch time discussions. I cherished every moment of your company.

I would not have reached this far and completed my PhD, if it was not for the efforts of all my former tutors at my alma maters. I would like remember and extend my sincere gratitude to all of them for their extraordinary support.

I don't want to forget all my friends in Perth, especially, Thanuja, Lalinda, Dilka and Amila for helping me in many ways and being very close to me for the past few years.

Last but not least, I would like to thank my family for always being with me and encouraging me. I am extremely grateful to my parents, for the mental support which

helped me immensely to persevere this work. I would also like to thank my sister, Nimasha who encouraged me to do a PhD, and my brother-in-law Charitha for his valuable support throughout the course of my studies. I thank my parents-in-law who has been very supportive throughout completing this study. It would not have been possible, if it's not for the support and patience of my loving husband Avantha. Thanks for your understanding and love.

## **Items derived from this thesis**

### **Journal publications included as chapters**

Weerasinghe Mohottige, T.N., Ginige, M.P., Kaksonen, A.H., Sarukkalige, R. and Cheng, K.Y. (2017) Bioelectrochemical oxidation of organics by alkali-halotolerant anodophilic biofilm under nitrogen-deficient, alkaline and saline conditions. *Bioresource Technology*. DOI: <https://doi.org/10.1016/j.biortech.2017.08.157>.

Weerasinghe Mohottige, T.N., Cheng, K.Y., Kaksonen, A.H., Sarukkalige, R. and Ginige, M.P. (2017) Oxalate degradation by alkaliphilic biofilms acclimatized to nitrogen-supplemented and nitrogen-deficient conditions. *Journal of Chemical Technology and Biotechnology*. DOI: 10.1002/jctb.5424.

Weerasinghe Mohottige, T.N., Ginige, M.P., Kaksonen, A.H., Sarukkalige, R. and Cheng, K.Y. (2017) Rapid start-up of a bioelectrochemical system under alkaline and saline conditions for efficient oxalate removal. *Bioresource Technology*, doi:10.1016/j.biortech.2017.11.009.

Weerasinghe Mohottige, T.N., Cheng, K.Y., Kaksonen, A.H., Sarukkalige, R. and Ginige, M.P. (2017) Influences of pH and organic carbon on oxalate removal by mixed bacterial cultures acclimatized to Nitrogen-deficient and supplemented conditions. *Journal of Cleaner Production*. Revision Under Review.

Weerasinghe Mohottige, T.N., Kaksonen, A.H., Cheng, K.Y., Sarukkalige, R. and Ginige, M.P. (2017) A comparative study on the kinetics of oxalate degradation and microbial communities of aerobic bioreactors operated under nitrogen supplemented and deficient conditions. To be submitted.

# Table of Contents

Declaration	i
Abstract	ii
Acknowledgment	vii
Items derived from this thesis	ix
Table of Contents	x
List of Figures	xvi
List of Tables	xxi
Abbreviations	xxii
<b>Chapter 1 - Introduction and scope of research</b>	1
1.1 Aluminium Industry	1
1.2 Aluminium production	3
1.3 Bayer Process	3
1.3.1 Digestion	4
1.3.2 Clarification	4
1.3.3 Precipitation	5
1.3.4 Calcination	5
1.4 Caustic loss in the Bayer process and importance of caustic recovery	6
1.5 Organics in bauxite and their impact on Bayer process	7
1.6 Organic removal processes	8
1.6.1 Biodegradation of oxalate and organic impurities in Bayer process liquor	9
1.6.2 Bioelectrochemical systems	10
1.7 Nitrogen fixation by microorganisms	13
1.8 Aim and objectives of this study	15
1.9 Thesis structure	16
<b>Chapter 2 - Bioelectrochemical oxidation of organics by alkali-halotolerant anodophilic biofilm under nitrogen-deficient, alkaline and saline conditions</b>	18
Chapter Summary	18
2.1 Introduction	19
2.2 Materials and Methods	21
2.2.1 Bioelectrochemical systems, process set-up and general operation	21
2.2.2 Synthetic alkaline-saline medium (anolyte) and catholyte media	23
2.2.3 Experimental procedures	24
2.2.3.1 Reactor start-up and acclimatisation of electrochemically active anodic biofilm	24
2.2.3.2 Supplementation of sodium acetate to facilitate bioanode establishment	24
2.2.3.3 Ability of the established biofilm to oxidise other organics commonly present in Bayer liquor	25

2.2.3.4 Characterisation of the BES performance under stable operations	26
2.2.3.4.1 Effect of organic loading rates (OLR) on reactor performance	26
2.2.3.4.2 Effect of anode potential on BES performance	26
2.2.4 Chemical analyses	27
2.2.5 Microbial community analysis	27
2.3 Results and Discussion	29
2.3.1 Activated sludge was unable to start-up both R1 and R2 with oxalate as the sole carbon source	29
2.3.2 The established biofilms could readily generate current using other organics	31
2.3.3 Characterisation of the BES performance with the established anodic biofilm	33
2.3.3.1 Effect of HRT on the electrochemical and treatment performance	33
2.3.3.2 Effect of poised anode potential on the electrochemical and treatment performance	36
2.3.4 Microbial community composition of the alkali-halotolerant biofilms	38
2.3.5 Implication of the findings	41
2.4 Conclusions	42
<b>Chapter 3 - Bioelectrochemical system for caustic soda recovery from alkaline-saline wastewater under nitrogen supplemented and deficient environments</b>	43
Chapter Summary	43
3.1 Introduction	44
3.2 Materials and Methods	46
3.2.1 Bioelectrochemical systems set-up and general operation	46
3.2.2 Synthetic liquor and reactor electrolyte	48
3.2.3. Experimental Procedures	48
3.2.3.1. Reactor start-up and acclimatisation of electrochemically active anodic biofilm	48
3.2.3.2 Evaluating alkalinity increase and caustic production capacity from alkaline and saline solution	49
3.2.4. Chemical Analysis	50
3.3 Results and Discussion	51
3.3.1 Alkalinity increase of catholyte and caustic recovery	51
3.3.1.1 Catholyte alkalinity increased over time at steady current production – Comparison of two reactors	51
3.3.1.2 Higher Na <sup>+</sup> transfer to catholyte in N-deficient reactor than N-supplemented reactor	54
3.3.1.3 Caustic recovery from high pH (> 12) feed solution in N-supplemented (R1) reactor	55
3.3.2 Implications of the study	57

3.4 Conclusions	59
<b>Chapter 4 - Oxalate degradation by alkaliphilic biofilms acclimatised to nitrogen-supplemented and nitrogen-deficient conditions</b>	60
Chapter Summary	60
4.1 Introduction	61
4.2 Materials and methods	63
4.2.1 Aerobic bioreactor systems	63
4.2.2 Synthetic Bayer Process Liquor	65
4.2.2.1 Influent for N-supplemented reactor	65
4.2.2.2 Influent for N-deficient reactor	65
4.2.3 Reactor start up	65
4.2.4 Cyclic studies	66
4.2.5 Investigating the oxygen uptake rate of established biofilm	67
4.2.6 Anaerobic oxalate degradation	68
4.2.7 Assessment of nitrogen-deficient conditions	69
4.2.7.1 Concentrations of soluble nitrogen species	69
4.2.7.2 Acetylene reduction assays	69
4.2.8 Sample analysis	70
4.2.8.1 Estimation of dry biomass weight in reactors	70
4.2.8.2 Analysis of nitrogen species and organic carbon	70
4.2.8.3 Gas analysis	71
4.3. Results and Discussion	71
4.3.1 Start-up of the N-supplemented and N-deficient reactors	71
4.3.2 Detailed studies revealed that both N-supplemented and N-deficient biofilms had a similar capacity to degrade oxalate	73
4.3.3 Presence/absence of an easily used nitrogen source influence pathway of methanogenesis during alkaline fermentation of oxalate	78
4.3.4 Are nitrogen requirements of N-deficient reactor fulfilled with atmospheric nitrogen fixation?	80
4.3.5 Implications of findings	82
4.4 Conclusions	82
<b>Chapter 5 - Influences of pH and organic carbon on oxalate removal by mixed bacterial cultures acclimatized to Nitrogen-deficient and supplemented conditions.</b>	83
Chapter Summary	83
5.1 Introduction	84
5.2 Materials and methods	86
5.2.1 Aerobic bioreactor systems	86
5.2.2 Influent for N-supplemented and N-deficient reactors	87
5.2.3 Reactor start up	88
5.2.4 Cyclic studies	89
5.2.5 Effect of in-reactor pH on oxalate degradation rate	90
5.2.6 Removal of other organics and their influence on oxalate removal	90

5.2.7 Assessment of N-deficient conditions	91
5.2.7.1 In-reactor ammonia-N, nitrite-N and nitrate-N concentrations	91
5.2.7.2 Acetylene reduction assay	91
5.2.8 Analysis of samples	92
5.2.8.1 Analysis of organic carbon and nitrogen species	92
5.2.8.2 Gas analysis	92
5.2.8.3 Estimation of dry biomass weight in reactors	93
5.3. Results and Discussion	93
5.3.1 Highly alkaline conditions impacted N-deficient reactor more than N-supplemented one	93
5.3.2 The acetylene reduction assay on N-deficient biomass confirmed low nitrogenase activity	95
5.3.3 The performance of the N-deficient reactor improved at close to neutral pH	96
5.3.4 A continuous influent flow can facilitate the maintenance of optimum pH	97
5.3.5 The N-supplemented reactor was irreversibly impacted when in-reactor pH values exceeded 11	98
5.3.6 Short-term exposure to optimal pH conditions has a long-lasting impact with higher rates of oxalate removal in N-deficient reactor	100
5.3.7 Other organic impurities in Bayer liquor could potentially increase the performance of N-deficient reactor	101
5.3.8 Implication of the findings	104
5.4. Conclusions	104
<b>Chapter 6 - A comparative study on the kinetics of oxalate degradation and microbial communities of aerobic bioreactors operated under nitrogen supplemented and deficient conditions</b>	106
Chapter Summary	106
6.1 Introduction	107
6.2 Materials and methods	109
6.2.1 Aerobic bioreactor set up	109
6.2.2 Synthetic Medium	110
6.2.3 Microbial inoculum	111
6.2.4 Reactor start up	111
6.2.5 Investigating the effect of initial oxalate concentration on oxalate degradation	112
6.2.6 Determination of biomass dry weight	112
6.2.7 Kinetic calculations	113
6.2.8 Assessment of N deficient conditions	114
6.2.9 Chemical analysis	114
6.2.10 Microbial Analysis	114
6.2.10.1 DNA extraction	115
6.2.10.2 Microbial community analysis	115
6.3 Results and Discussion	116

6.3.1 Bioreactor performance	116
6.3.2 Oxalate degradation kinetics	118
6.3.3 A side stream two-step continuous biological treatment process for efficient removal of oxalate	120
6.3.4 Kinetic differences reflect the differences in microbial community composition	124
6.4. Conclusions	128
<b>Chapter 7 - Rapid start-up of a bioelectrochemical system under alkaline and saline conditions for efficient oxalate removal</b>	129
Chapter Summary	129
7.1 Introduction	130
7.2 Materials and methods	133
7.2.1 Bioelectrochemical systems and general process operation	133
7.2.2 Synthetic refinery process water (anolyte) and BES catholyte	135
7.2.3 Experimental Procedures	135
7.2.3.1 Process start-up with the aerobic biofilm coated graphite granules	135
7.2.3.2 Effect of Hydraulic Retention Time (HRT) on BES performance	136
7.2.3.3 Effect of anode potential on BES performance	136
7.2.3.4 Effect of increasing acetate concentration on oxalate degradation rate and BES performance	136
7.2.4 Chemical analyses	137
7.2.5 Biofilm samples collection and DNA extraction	137
7.2.5.1 Microbial community analysis	138
7.3 Results and Discussion	139
7.3.1 The aerobic oxalotrophic biofilm could readily switch from using oxygen to graphite as electron acceptor	139
7.3.2. Increasing hydraulic loading increased current and oxalate removal when the anolyte had a pH of ~9	140
7.3.3. The oxalotrophic biofilm remained proficient in generating current even at low anode potentials	143
7.3.4. Simultaneous acetate degradation by the established oxalotrophic anodic biofilm	144
7.3.5. Changes in microbial community compositions at different stages of the BES operation	146
7.3.6. Implication of the findings	149
7.4. Conclusions	153
<b>Chapter 8 - Conclusions and suggestions for future research</b>	154
8.1 Main findings of the study	154
8.2 The practical implementation of biological oxalate removal processes in alumina refinery	156
8.3 Suggestions for Future Research	159

<b>References</b>	162
Appendix 1	178
Appendix 2	182
Appendix 3	184

## List of Figures

<b>Figure 1.1.</b> World alumina production total from January 2016 to January 2017 per year. Total production 126,024 thousand metric tonnes (Values given in thousand metric tonnes, Oceania: Australia)	2
<b>Figure 1.2.</b> Geographic distribution of world production of bauxite and alumina in 2015.	2
<b>Figure 1.3.</b> Aluminium production processes from bauxite to cast aluminium	3
<b>Figure 1.4.</b> Bayer process flow chart	6
<b>Figure 1.5.</b> Schematic of a bioelectrochemical system	12
<b>Figure 2.1.</b> Schematic diagram of the bioelectrochemical process. WE= working electrode; CE= counter electrode; RE= reference electrode.	22
<b>Figure 2.2.</b> Start-up performance of the two BES reactors during the initial 54 days period. (A, B) Current production in R1 and R2 with sodium oxalate as the main carbon source; (C) Oxalate concentration of the influent and effluent of R1 and R2. The anode potentials in both reactors were maintained at +200mV. Influent pH was 10. The reactors were operated in continuous mode from day 1 to 26 with one day HRT and from day 38 to 44 with two days HRT. Different vertical arrows indicate additions of different agents: activated sludge (30 mL); yeast extract (50 mg); acetate (2.5 mmol).	30
<b>Figure 2.3.</b> Current responses of the biofilms to (A) sodium acetate, and (B) sodium formate in the presence of sodium oxalate (25 mM). Both R1 and R2 were operated in batch mode. The addition of sodium acetate (2.5 mmoles) was carried out on day 83, whereas the addition of sodium formate (2.5 mmoles and 5 mmoles) was carried out on day 86. Note: Corresponding CE (coulombic efficiency) values were calculated based on the amount of electrons in the organic added versus that recovered from the triggered current (i.e. electrons available from the oxalate were excluded).	32
<b>Figure 2.4.</b> Effect of HRT on the performance of R1: N-supplemented BES. (A) Changes in HRT and COD loading rate over time; (B) Current production and catholyte electrical conductivity over the time; (C) Oxalate, acetate and COD removal percentages at different COD loading rates; (D) CE % based on both COD loading and COD removal at different HRTs. The bioanode potential was -300 mV, pH 9.0 and with both sodium oxalate and sodium acetate as electron donors. In (B), the catholyte was refreshed (25 g NaCl/L) on 5.8 d.	34
<b>Figure 2.5.</b> Effect of HRT on the performance of R2: N-deficient BES. (A) Changes in HRT and COD loading rate over time; (B) Current production and catholyte electrical conductivity over the time; (C) Oxalate, acetate and COD removal percentages at different COD loading rates; (D) CE % based on both COD loading and COD removal at different HRTs. The bioanode potential was -300 mV, pH 9.0 and with both sodium oxalate and sodium acetate as electron donors.	35
<b>Figure 2.6.</b> Linear relationship between current density and COD removal rate for R1: N-supplemented BES; and R2: N-deficient BES. Data were obtained from the experiments as shown in Figures 2.4 and 2.5, respectively.	36

**Figure 2.7.** Effect of anode potential on the performance of R1: N-supplemented (A-C) and R2: N-deficient (D-F) BES reactors. (A, D) Current production and anode potential over the experimental time period. (B, E) Variation of average current produced at different poised anode potentials. (C, F) Oxalate, acetate and COD removal percentages at the experimented range of anode potentials. The anolyte was maintained at pH 9.0 with sodium oxalate and sodium acetate as electron donors on day 111 for R1, and day 170 for R2. HRT was 3 h. 37

**Figure 2.8.** Relative abundance of microbial taxa classified at the family level based on 454 sequencing of 16S rRNA genes for biofilm samples collected from the bioanodes of (A) R1: N-supplemented; and (B) R2: N-deficient after 200 days of operation. Families that represent less than 3% of the total microbial community composition were classified as “others”. 40

**Figure 3.1.** A schematic diagram of the BES bioreactor system consisting of anodic cell and cathodic cell filled with graphite granules, a recirculation line and a computer for process monitoring and control. RE – Reference electrode, WE – Working electrode (Anode) and CE – Counter electrode (Cathode). 47

**Figure 3.2.** Reactor R1 catholyte caustic generation at anode potential -300 mV, anolyte pH 9.0 and COD loading rate 5.1 kg COD/m<sup>3</sup>.d (HRT 3 hr) with sodium oxalate and sodium acetate as electron donors on day 141. (A) Steady current production and anode and cathode electrode potentials. (B) Increase of catholyte Na<sup>+</sup> and NH<sub>4</sub><sup>+</sup> ion concentration. (C) Oxalate and acetate removal percentages (D) Anolyte and catholyte pH. (E) Increase of catholyte total alkalinity and catholyte electrical conductivity. (F) Cumulative energy input into the system during the experiment. 52

**Figure 3.3.** Reactor R2 catholyte caustic generation at anode potential -300 mV, anolyte pH 9.0 and COD loading rate 5.1 kgCOD/m<sup>3</sup>.d (HRT 3hrs) with sodium oxalate and sodium acetate as electron donors on day 187. (A) Current production and anode and cathode electrode potentials over the experimental time period. (B) Increase of catholyte Na<sup>+</sup> and NH<sub>4</sub><sup>+</sup> ion concentration during the experimental time. (C) Oxalate and acetate removal percentages during the experiment. (D) Anolyte and catholyte pH varying with the time. (E) Increase of catholyte total alkalinity and catholyte electrical conductivity over the experimental time. (F) Cummulative energy input into the system during the experiment. 53

**Figure 3.4.** Distribution of cations migrated from anode to cathode to balance the electron flow. 55

**Figure 3.5.** Reactor R1 catholyte caustic generation at anode potential -300 mV, anolyte pH 9.0 and COD loading rate 2.55 kgCOD/m<sup>3</sup>.d (HRT 6hrs) with sodium oxalate and sodium acetate as electronne donors. (A) Steady current production and anode and cathode electrode potentials over the experimental time period. (B) Increase of catholyte Na<sup>+</sup> and NH<sub>4</sub><sup>+</sup> ion concentration during the experimental time. (C) Oxalate, acetate and COD removal percentages during the experiment. (D) Anolyte, catholyte and feed solution pH varying with the time. (E) Increase of catholyte total alkalinity and catholyte electrical conductivity over the experimental time. (F) Cummulative energy input into the system during the experiment. 56

**Figure 4.1.** Schematic diagram of the aerobic bioreactor system used in the study. 64

<b>Figure 4.2.</b> Change of influent oxalate concentration and cycle length of (A) N-supplemented and (B) N-deficient reactors at the start-up of the reactors, and (C) Oxalate removal efficiencies of the N-supplemented and the N-deficient reactor inoculated with the same starting inoculum.	72
<b>Figure 4.3.</b> Effect of (A and D) DO concentration on the removal of oxalate; (B and E) DO concentration on the removal rate of oxalate; (C and F) Oxygen uptake rate on the removal rate of oxalate; (G) Correlations of oxygen consumed and oxalate removed for N-supplemented and N-deficient reactors. The tests were carried out from day 146 for N-supplemented reactor and from day 224 for N-deficient reactor.	76
<b>Figure 4.4.</b> Influence of oxalate spikes on oxygen uptake rates in (A) N-supplemented reactor on day 288 and (B) N-deficient reactor on day 365. (C) Correlations of oxygen consumed and oxalate removed for N-supplemented and N-deficient reactors.	77
<b>Figure 4.5.</b> Conversion of carbon in N-supplemented and N-deficient reactors during anaerobic fermentation of oxalate. $C/C_0$ = molar ratio of carbon in degradation products versus initial oxalate carbon concentration. C – Carbon moles in degradation products (such as oxalate, acetate, formate or methane) and $C_0$ – Carbon moles in initial oxalate concentration.	79
<b>Figure 4.6.</b> Production of methane during anaerobic exposure to $H_2/CO_2$ in the absence of oxalate.	80
<b>Figure 5.1.</b> A schematic diagram and a photographic image of the aerobic packed bed bioreactor.	87
<b>Figure 5.2.</b> Oxalate concentrations during oxalate degradation and various initial pH values in the (A) N-supplemented reactor from day 167 and (B) N-deficient reactor from day 267. The influence of pH on oxalate removal rate in (C) N-supplemented and (D) N-deficient reactors as calculated based on initial 2 h of oxalate removal.	97
<b>Figure 5.3.</b> Reversible and irreversible inhibition of oxalate removal by N-supplemented reactor at in-reactor pH 7 and pH 12, respectively.	100
<b>Figure 5.4.</b> Intermittent exposure to a favourable pH and its impact on the removal of oxalate after the exposed to an unfavourable pH from day 298.	101
<b>Figure 5.5.</b> The efficacy of N-supplemented and N-deficient biofilms to oxidise organics other than oxalate and the influence of other organics on oxalate removal. The tests were carried out for N-supplemented reactor from day 229 and for N-deficient reactor from day 413.	103
<b>Figure 6.1.</b> A schematic diagram of the laboratory-scale aerobic packed bed bioreactor.	110
<b>Figure 6.2.</b> Profiles of in-reactor oxalate concentration, oxygen uptake rate (OUR) and pH during a 3.5 h aerobic reactor reaction time.	117
<b>Figure 6.3.</b> (A) Effect of initial oxalate concentration (S) on specific oxalate degradation rate (V) in N-supplemented and N-deficient reactors. Linearization of results with (B) Lineweaver-Burk plot (C) Hanes plot, and (D) Eadie-Hofstee plot. The experimental tests were carried out for N-supplemented reactor from day 196 and for N-deficient reactor from day 360.	119
<b>Figure 6.4.</b> A schematic diagram of a side stream continuous biological oxalate removal one-stage process.	121
<b>Figure 6.5.</b> A schematic diagram of a side stream continuous biological oxalate removal two-stage process.	122

**Figure 6.6.** Similarity analysis (at 97% sequences similarity) of microbial communities in N-supplemented and N-deficient reactors 3 weeks after inoculation and during stable operation based on unweighted Unifrac. (A) Principal coordinates analysis (PCoA). (B) Unweighted pair group method with arithmetic mean (UPGMA) cluster analysis. The values on branches show the similarity of the microbial communities. 125

**Figure 6.7.** (A) Relative abundance of microbial class (having a  $\geq 3\%$  abundance) observed in N-supplemented and N-deficient reactors. (B) Specific oxalate removal rates of the two reactors at the time sample collection for microbial community analysis. 126

**Figure 6.8.** Change of abundance of microbial genera during the operation of N-supplemented and N-deficient reactors. (A) A comparison of relative abundance of genera *Azoarcus* and *Paracoccus*. (B) Other bacterial genera that showed a positive increase of abundance - N-supplemented reactor. (C) Other bacterial genera that showed a positive increase of abundance - N-deficient reactor. 128

**Figure 7.1.** A schematic diagram of the BES process consisting of anodic cell and cathodic cell filled with graphite granules, a recirculation line and a computer for process monitoring and control. 134

**Figure 7.2.** (A) BES current generation and pH profile during start up with biofilm granules from aerobic bioreactor, using influent with 25 mM sodium oxalate. The anode potential was +200 mV and HRT of 1 day for first 4 days. (B) Oxalate concentration in anolyte inflow and outflow streams for the first 4 days. 140

**Figure 7.3.** BES performance at various HRTs at an anode potential of -300 mV vs. Ag/AgCl, in-reactor pH of ~ 9 and with sodium oxalate as only electron donor. (A) Variation of HRT and current production over time. An enlarged view of area covered by red dotted box is given in (B). (C) Average current and CE (%) at various HRTs. (D) Oxalate removal percentage and average current produced at various COD loading rates. 142

**Figure 7.4.** BES performance at various poised anode potentials from -600 mV to +200 mV vs. Ag/AgCl at in-reactor pH of 9 – 9.5 with 25 mM sodium oxalate as only electron donor and anodic chamber HRT of 6 h. (A) Current production and electrode potentials over time. (B) Average current produced, oxalate removal percentage and CE (%) at various poised anode potentials. (C) Positive linear relationship between current and oxalate removal rate. 144

**Figure 7.5.** Increase in current production with increasing acetate concentrations in the feed with sodium oxalate (25 mM) at anode potential of -300 mV vs. Ag/AgCl, HRT of 12 h and in-reactor pH of 9.5. (A) Increase in oxalate to acetate ratio over time. (B) Current production, and influent oxalate and acetate concentrations over time. (C) Oxalate and acetate removal efficiencies over time. (D) Relationship of average current production and CE with oxalate to acetate ratio. 146

**Figure 7.6.** (A) Principle component analysis (PcoA) profile (unweighted Unifrac) for samples collected from the aerobic bioreactor (BR-1 and BR-2) and BES (BES-21D, BES-75D, BES-99D to BES-103D) indicating clustering of samples. (B) Unweighted pair group method with arithmetic mean (UPGMA) dendrogram of unweighted unifrac distances sample set. The values at the branches show the similarity of the samples. The two plots highlight the clustering of samples according to reactor type and carbon source available. (C) Stacked bar plot of the relative abundance bacterial families in the aerobic bioreactor and BES fed with oxalate and oxalate + acetate. Family that represent less than 3% of the total microbial community composition were classified as “others”.

## List of Tables

<b>Table 1.1.</b> Minimum, average and maximum content of main elements and total organic carbon (TOC) in bauxite	1
<b>Table 3.1.</b> Comparison of studies on cathodic caustic generation in electrochemical systems	58
<b>Table 6.1.</b> Michaelis-Menten constants ( $K_m$ ) and maximum specific oxalate degradation rates ( $V_{max}$ ) for N-supplemented and N-deficient reactor systems obtained with three different linearization approaches.	120
<b>Table 6.2.</b> Design parameters for one stage and two stage bioreactor processes assuming oxalate generation of 40 t/d (McSweeney 2011) and influent oxalate concentration of 100 g/L	122
<b>Table 7.1.</b> Comparison of oxalate removal performance of various aerobic and bioelectrochemical reactor processes.	152
<b>Table 8.1.</b> Estimated footprint for the removal of daily oxalate production of 40 t/day – A comparison of aerobic reactor and BES	158
<b>Table 8.2.</b> Comparison of energy input cost for BES to produce 1 T of caustic with the market price of caustic.	159

## Abbreviations

Bioelectrochemical systems	BES
Brunauer-Emmett-Teller method	BET
Cation exchange membrane	CEM
Chemical oxygen demand	COD
Coefficient of determination	R <sup>2</sup>
Coulombic efficiency	CE
critical oxalate concentration	COC
Dissolve oxygen concentration	DO
Ethylenediaminetetraacetic acid	EDTA
Flame ionisation detector	FID
Hydraulic retention time	HRT
Initial oxalate concentration	S
Initial specific rate of oxalate removal	V
Ion chromatography	IC
Ion sphere particles	ISP
Maximum initial oxalate oxidation rate	V <sub>max</sub>
Michaelis-Menten constant	K <sub>m</sub>
Microbial electrolysis cell	MEC
Microbial fuel cell	MFC
Mixed liquor suspended solid	MLSS
Nitrogen	N
Not applicable	n.a
Operational taxonomic unit	OTU
Organic loading rate	OLR
Organic removal rate	ORR
Oxygen uptake rate	OUR
Principal coordinate analysis	PCoA
Quantitative insights into microbial ecology	QIIME
Reagent free ion chromatography	RFIC
Returned activated sludge	RAS
Suspended solids	SS
Total ammonia nitrogen	TAN

Total organic carbon	TOC
total suspended solids	TSS
Unweighted pair group method with arithmetic mean	UPGMA
Upflow anaerobic sludge blanket	UASB
Volatile suspended solids	VSS

# 1 INTRODUCTION

## 1.1 Aluminium Industry

Aluminium is one of the most utilized metals in the world, which is demanded in major industries such as construction, transportation, electronics and packaging (International Aluminium, 2017; Power et al., 2011a). This high demand is a reason of its unique properties: light weight, corrosion resistance, flexibility, recyclability and durability (Hind et al., 1999; Miller et al., 2000; Piña & Cervantes, 1996). These chemical and physical properties can be further increased by mixing aluminium with other metals such as magnesium, nickel, copper and zinc for extensive applications from household commodities to spacecraft manufacturing.

Aluminium is extracted from alumina containing ores, typically bauxite, and converted to metallic aluminium by series of chemical and electrolytic processes. Bauxite is formed as a result of intense chemical weathering in hot and humid zones (Bogatyrev et al., 2009). Table 1.1 shows the content of main elements and total organic carbon (TOC) in bauxite. Bauxite ores contain aluminium oxide and aluminium hydroxide in the range of 25-60% (w/w %). Main aluminium mineral types contained in bauxite are gibbsite ( $\text{Al}(\text{OH})_3$ ), boehmite ( $\gamma\text{-AlO(OH)}$ ) and diasporite ( $\alpha\text{-AlO(OH)}$ ) (Whelan et al., 2003).

**Table 1.1.** Minimum, average and maximum content of main elements and total organic carbon (TOC) in bauxite (Atasoy, 2005; Gräfe et al., 2009; Power & Loh, 2010).

Element	Content (wt %)		
	Minimum	Average	Maximum
Al	10	13-32	37
Fe	0.35	7-24	45
Ti	0.06	1-2	15
Si	0.05	2-4	7
TOC (%)	0.15	0.27	1.11

Alumina production in various regions of the world in 2016 is shown in figure 1.1 and the countries with largest bauxite and alumina production are listed in figure 1.2. China is the leading alumina producer contributing 48% of world alumina production in 2015 and continuously increasing its share on global alumina production. For the first time, in year 2012, world alumina production reached 100,000 thousand metric tonnes per annum (International Aluminium, 2017).



**Figure 1.1.** World alumina production total from January 2016 to January 2017 per year. Total production 126,024 thousand metric tonnes (Values given in thousand metric tonnes, Oceania: Australia) (International Aluminium, 2017).

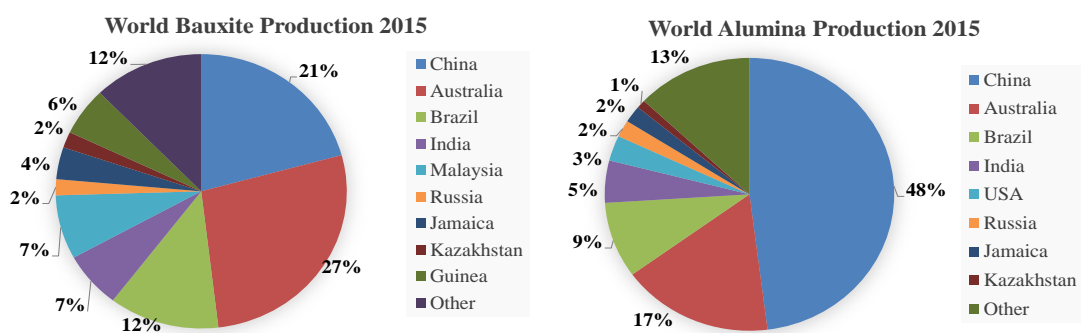


**Figure 1.2.** Geographic distribution of world production of bauxite and alumina in 2015. (Adapted from <https://minerals.usgs.gov/minerals/pubs/commodity/bauxite/> on November 2016)

Australia started producing alumina and aluminium from imported bauxite in 1955 (Hind et al., 1999). Today, Australia is one of the World's largest Bauxite producers and refiners (Figure 1.2). Australia has increased its share in bauxite production from 20 to 32% over the last 40 years from 1970 to 2010 (Nappi, 2013). Australia has three major bauxite mining areas: Darling Range in Western Australia, Gove in Northern territory and Weipa in Queensland. The mined bauxite is refined at seven large scale refineries at Gove, Gladstone, Yarwun, Kwinana, Pinjarra, Wagerup and Worsley. Western Australia contributes to 58% of Australian alumina production and 11% of global alumina production. However, Western Australian bauxite has low alumina content and high organic content compared to bauxite mined in other places (Australian Aluminium Council, 2010; Hind et al., 1999).

## 1.2 Aluminium production

The most commonly used methods for aluminium production are Bayer process and Hall-Heroult process. The Bayer process is used to produce alumina ( $\text{Al}_2\text{O}_3$ ) from bauxite and Hall-Heroult process is used to produce molten aluminium from alumina (Figure 1.3). In year 1887, Karl Josef Bayer discovered a new method of extracting aluminium hydroxide from bauxite through Bayer processing, and still aluminium industry uses the same principal approach with minor modifications (Meyers, 2004; Power et al., 2011b).

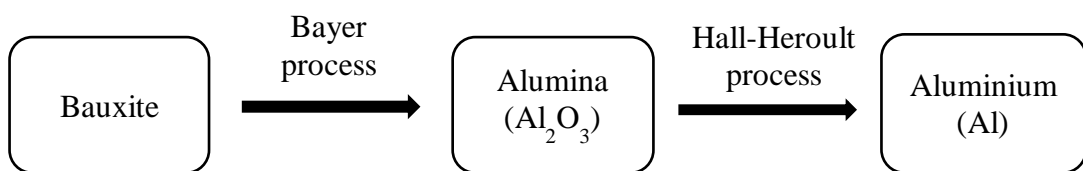


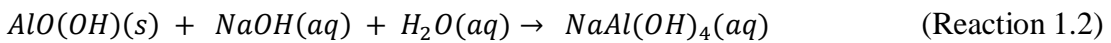
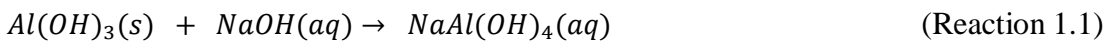
**Figure 1.3.** Aluminium production processes from bauxite to cast aluminium

## 1.3 Bayer Process

Bayer process can be briefly categorized into 4 major steps; namely digestion, clarification, precipitation and calcination (Figure 1.4). Each of these are described briefly below.

### **1.3.1 Digestion**

In digestion, crushed bauxite is mixed with concentrated 3.5 - 5 M caustic (NaOH) solution at temperature of 100 – 240 °C (Gräfe et al., 2009; Whelan et al., 2003). Mostly, this concentrated caustic solution constitutes a majority of the spent liquor from the process, which is recycled to digestion step for multiple times. The key parameters of the digestion process include temperature, pressure and caustic concentration, which can vary depending on aluminium hydroxide type and content present in the bauxite. Bauxite composed mainly of gibbsite (aluminium trihydroxide,  $\text{Al(OH)}_3$ ) is digested at 145 °C (Reaction 1.1), whereas bauxites composed of boehmite and diaspore (aluminium oxyhydroxides,  $\text{AlO(OH)}$ ) require higher temperatures (up to 255 °C) and high pressures for digestion (Reaction 1.2) (Hind et al. 1999).



Caustic consumption in digestion processes mainly depends on the alumina and silica contents of the bauxite. The presence of silicate minerals in bauxite forms sodium alumino-silicates (known as desilication products) at high  $\text{Na}^+$  concentration. These desilication products need to be removed from the Bayer liquor and as a result, caustic and alumina loss is taking place (Power et al., 2011a). The digestion step highly affects the productivity of the entire Bayer process as key objective of the digestion step is to enrich the caustic solution with maximum of alumina for recovery in subsequent steps (Den Hond et al., 2007; Raghavan et al., 2011).

### **1.3.2 Clarification**

Super saturated sodium aluminate ( $\text{NaAl(OH)}_4$ ) solution discharged from the digestion process is sent to clarification process, which includes several settling and filtration steps to separate sand and insoluble (inorganic and organic) residue called red mud from the sodium aluminate solution before aluminium trihydroxide ( $\text{Al(OH)}_3$ ) precipitation (Den Hond et al., 2007; Hind et al., 1999; Power et al., 2011a). The red mud mostly contains inorganic substances originated from the bauxite, such as iron

oxide, quartz, calcium carbonate, titanium dioxide, sodium aluminosilicate and calcium aluminate. The red mud is further washed to recover entrained NaOH and  $\text{NaAl(OH)}_4$ . The amount of residue produced from bauxite is mainly dependent on bauxite quality and digestion conditions as caustic concentration. Typically 0.7 - 2 tonnes of both organic and inorganic residue are produced per tonne of alumina produced. The disposal of this bauxite residue is a serious environmental issue, mainly because of high alkalinity of the residue and dispose in large quantities. Considering the alkalinity of residue due to entrapment of caustic, the disposal cause negative impacts on ground water quality and risk of contact with ecosystems. Apart from environmental risks, the loss of caustic and alumina with residue disposal affect the economies of the Bayer process. Hence, research efforts have been directed to developing environmentally friendly disposal methods and resource recovery (International Aluminium Institute and European Aluminium, 2014).

### 1.3.3 Precipitation

In the precipitation step, aluminium trihydroxide ( $\text{Al(OH)}_3$ ) is precipitated from the cooled pregnant liquor at approximately 60 °C by seeding the liquor with aluminium trihydroxide (Reaction 1.3) (McSweeney 2011).



The initial caustic concentration is crucial for the aluminium trihydroxide precipitation and the determination of caustic strength depends on various operational parameters and bauxite quality. However, to achieve maximum precipitation yield the caustic concentration is likely to be below 300 g/L  $\text{Na}_2\text{CO}_3$  (Den Hond et al., 2007; Hind et al., 1999). After the precipitation step the spent liquor is heated and concentrated, and is recycled to the digestion process.

### 1.3.4 Calcination

The calcination process removes water from the precipitated aluminium trihydroxide at 1100 °C to produce powdered alumina (Balomenos et al., 2011). The reaction taking place in calcination process (Meyers, 2004) is given in reaction 1.4.



(Reaction 1.4)

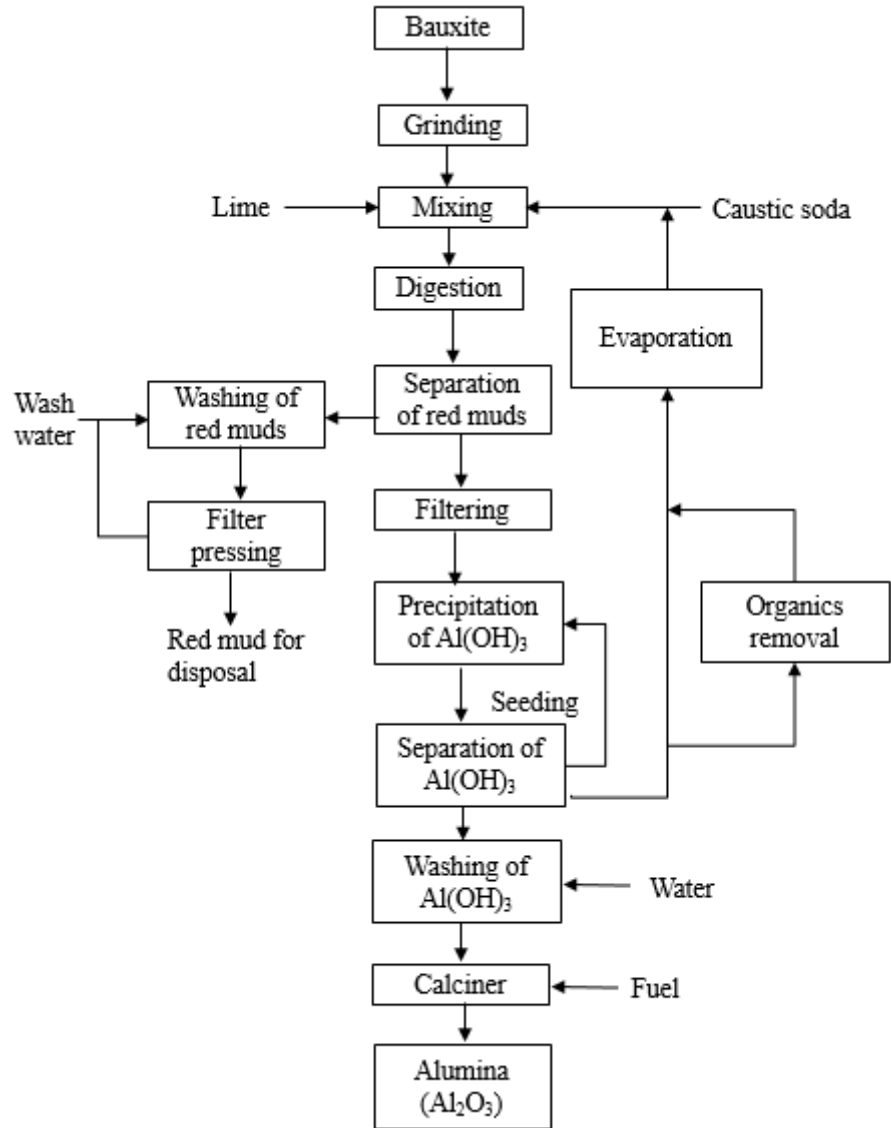


**Figure 1.4.** Bayer process flow chart (adapted from (Hind et al., 1999; Meyers, 2004)).

## 1.4 Caustic loss in the Bayer process and importance of caustic recovery

Caustic soda ( $NaOH$ ) is the main chemical agent used in Bayer process to extract alumina from bauxite. The alumina digestion yield and precipitation yield are largely dependent on caustic concentration (Den Hond et al., 2007). Hence, careful controlling of caustic concentration is important to improve the process economics. The spent

liquor, which is rich in caustic soda, is recycled to the digestion step after the  $\text{Al(OH)}_3$  precipitation for the reuse of caustic (Songqing, 2013). Theoretically, caustic concentration of pregnant liquor and spent liquor should be the same according to reactions 1.1 and 1.3. However, caustic losses occur at residue separation and addition of water for washing, resulting in lower caustic concentration in spent liquor stream (Den Hond et al., 2007). The spent liquor is concentrated by energy intensive evaporation process at high temperature to increase the caustic concentration before adding to digestion phase. However, with the recirculation of spent liquor, the organics accumulate in the process liquor, which detrimentally impacts the alumina product quality and yield (Hind et al., 1999).

## 1.5 Organics in bauxite and their impact on Bayer process

Bauxite contains typically 0.1 - 0.3% organics, and in some ores organics content can be up to 1% (Table 1.1). The organics present in bauxite are consisted of a wide range of organic compounds from very complex high molecular weight humic substances to simple organic acids (Power et al., 2012). According to McSweeney (2011), Western Australian (WA) bauxite contains high concentrations of humic substances. The organic matter contained in bauxite is extracted into the Bayer process liquor during digestion step (Hind et al., 1999; Whelan et al., 2003). It has been reported, this percentage of organics extraction can be over 50% during the digestion (Gnyra & Lever, 1979). At clarification step, insoluble organic matter is separated from the liquor. However, some organics are soluble in the Bayer liquor and remain in the system. The larger molecule organics are degraded into simple organic compounds such as acetate, formate and oxalate due to high temperature and alkaline nature of Bayer process liquor. In perfect conditions, the final product of the organics degradation is carbonate. However, some simple organic compounds such as acetate, oxalate and succinate are sufficiently stable and tend to be the final product of some reaction sequences (Power & Loh, 2010). Even though the recirculation of spent liquor is effective in decreasing caustic consumption, it results in the accumulation of organics in the process liquor (Den Hond et al., 2007; Wellington & Valcin, 2007).

The accumulated organic compounds create various problems that can lead to diminished overall process efficiency and productivity. The consequences include lower alumina yield, generation of fine alumina particles, increased content of impurities in alumina, loss of caustic due to the formation of organic sodium salts and increase in scale formation (Soucy et al., 2013). According to Power and Loh (2010), the organic impurities in Bayer process liquor incur a cost of more than AUS\$ 500 million to the Australian Alumina industry per year.

Among the organic impurities in Bayer process liquor, sodium oxalate is the most detrimental (Gnyra & Lever, 1979; Power et al., 2012) and average size WA alumina refinery produces oxalate 40 t/d (McSweeney, 2011). Depending on the digestion conditions, 5 - 10% of the organic carbon is typically converted to sodium oxalate (Sipos et al., 1999). If not controlled, oxalate concentration rises to saturation point resulting in co-precipitation with the aluminium trihydroxide at precipitation stage. In order to quantify the supersaturation concentration of oxalate crystallisation, industry determines critical oxalate concentration (COC) as the precipitation threshold depends on refinery operational conditions, process liquor organic content and thermodynamic properties of oxalate solubility (Power et al., 2012; Sipos et al., 1999). This COC value is a variable and unpredictable, and can be increased up to 3-4 g/L (Hiralal et al., 1994; Sipos et al., 1999). Oxalate also causes caustic loss due to sodium oxalate crystallization and excessive scaling of pipes. Therefore, it is necessary to remove and reduce the oxalate concentration for smooth operation of the Bayer process.

## 1.6 Organic removal processes

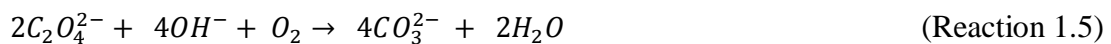
Many biological and non-biological strategies have been used to remove sodium oxalate ( $\text{Na}_2\text{C}_2\text{O}_4$ ) and other organic impurities from Bayer process liquor (Tadanori et al., 1975; Williams & Perrotta, 1998). Some of the patented organic control processes are wet oxidation, membrane filtration, liquor calcination, precipitation by seeding and biodegradation (Soucy et al., 2013). The most widely practiced methods to remove oxalate in industrial scale are liquor calcination (burning) and precipitation of sodium oxalate by seeding.

In liquor burning process, a side stream of Bayer process liquor is mixed with alumina dust and heated to a temperature of approximately 1000 °C inside a kiln. At high temperature organic impurities are combusted, releasing CO<sub>2</sub> and other oxides. However, the process is expensive and requires additional controls to minimise environmental impacts (McKinnon & Baker, 2012). Precipitation of sodium oxalate by seeding with sodium oxalate crystals is another strategy to remove harmful sodium oxalate from the Bayer process liquor (Brown, 1991; Rosenberg et al., 2004). Precipitated sodium oxalate crystals are disposed of in residue areas. This method is unable to completely destroy the sodium oxalate, and hence large storage space is needed to store the disposed sodium oxalate and long term storage poses a hazard to the surrounding environment. Biodegradation of organics has been identified as a more sustainable solution to completely destroy the organic impurities, and to mitigate the environmental concerns.

### **1.6.1 Biodegradation of oxalate and organic impurities in Bayer process liquor**

In previous studies, various oxalotrophic bacteria able to oxidise oxalate as a carbon source have been isolated from a number of living and environmental sources such as human gastrointestinal tracts, sheep rumen, rhizosphere soil and aquatic sediments. However, biodegradation of oxalate is challenging due to its chemical nature, low energy yield (impacts bacterial growth) and toxicity (inhibiting bacterial activity) (Sahin, 2003; Svedruzic et al., 2005). Three main class of enzymes present in oxalotrophic bacterial strains are involved in catalysing the oxalate degradation by cleaving the C-C bond between carbon atoms, namely oxalate oxidase, oxalate decarboxylase and oxalyl-CoA decarboxylase (Svedruzic et al., 2005).

Recently, the alumina industry has explored biological processes to destruct oxalate. Biological oxidation of oxalate under high pH results in carbonate generation (Reaction 1.5).



Industrial bioprocess for biological oxalate oxidation was first reported and patented by Alcan International Limited in 1989. The bioprocess was based on the use of biofilms in a three compartment rotating biological contractor containing 73 rotating

disks with a total surface area of 3.7 m<sup>2</sup>. The reactor was inoculated with Pseudomonas or Pseudomonas-like microorganisms isolated from rhizosphere of oxalate producing plants. Due to the intolerance of the isolated bacteria to high pH, the influent pH needed to be adjusted to a pH value of 7.5 (Brassinga et al., 1989). The bioreactor successfully decreased an initial oxalate concentration of 2600 mg/L to 50 mg/L within a residence time of 5 h. Following this study, many other studies were carried out under different conditions to examine the efficiencies of other oxalate degrading bacterial strains. For example, Worsley Alumina Pty Limited for the first time examined the efficacies of an alkaliphilic bacilli to oxidise oxalate. The alkaliphilic bacilli strain was able to tolerate a pH range of 9-11, eliminating the need to neutralise the influent of refinery lake water (> 12.4 pH) (Morton et al., 1991).

However, one of the main drawback in aerobic oxidation of oxalate is reduction of alkalinity due to carbonate production. Hence, additional causticisation step (Adding Ca(OH)<sub>2</sub> to convert Na<sub>2</sub>CO<sub>3</sub> to NaOH) is required to increase the alkalinity of the effluent. As caustic is the main chemical agent used in alumina refineries to extract alumina, the recovery of caustic from the process liquor is beneficial to decrease processing costs. Hence, more versatile biological processes, such as bioelectrochemical systems, are required to allow simultaneous organics destruction and caustic recovery.

### **1.6.2 Bioelectrochemical systems**

Bioelectrochemical systems (BESs) combine biological and electrochemical processes to produce electricity or useful products, such as hydrogen gas. Bioelectrochemical systems can be divided into two main categories: microbial fuel cells (MFCs) and microbial electrolysis cells (MECs). MFCs are designed to produce electricity by using microorganisms to convert chemical energy into electrical energy. In MECs microorganisms decompose organic matter by using external electrical energy and generate hydrogen or methane gas (Davis & Yarbrough, 1962; Rao et al., 1976).

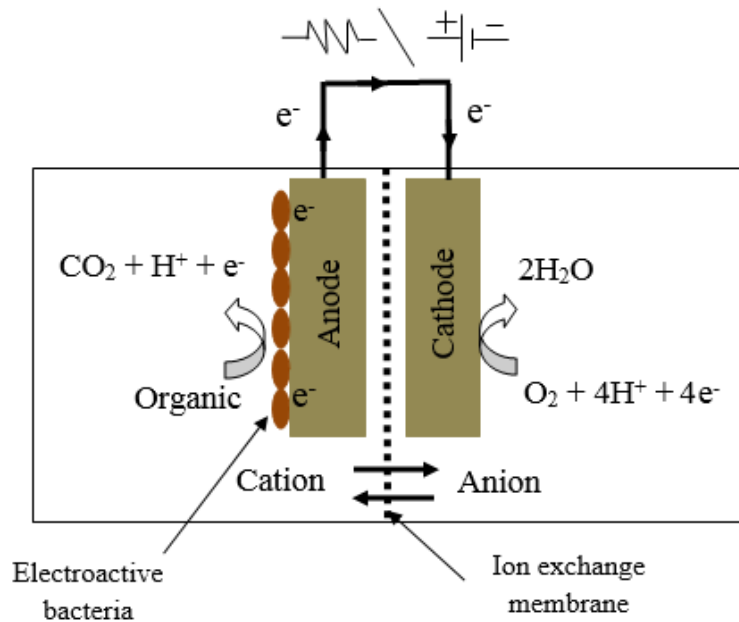
BES consists of an anode and a cathode placed in an aqueous solution and connected by an external electric circuit (Figure 1.5). Often the two cells are separated by a cation exchange membrane (Allen & Bennetto, 1993; Logan et al., 2006; Rabaey et al., 2007;

Virdis et al., 2011). Microorganisms in an anode biofilm oxidise organic matter and liberate the electrons and protons. The electrons are transferred from the anode to the cathode through the external circuit and the protons are transferred from the anodic compartment through the membrane to the cathodic compartment. At the cathode, electrons react with oxidants allowing the BES to generate electricity (Cheng et al., 2012; Das & Mangwani, 2010; Logan et al., 2006; Rabaey et al., 2007). The mechanism by which electricity can be produced directly from the degradation of organic matter in an MFC is still not completely understood. Heterotrophic bacteria liberate energy from the oxidation of organic matter in the process known as catabolism. When bacteria oxidize a compound, they capture the electrons and transfer them to a series of respiratory enzymes within the cell. Typically, these electrons are then released to an external electron acceptor such as ferric iron, nitrate, sulfate or oxygen. However, in BES bacteria can transfer the electrons to an anode (Chang et al., 2006; McKinlay & Zeikus, 2004; Rabaey et al., 2007). Various bacteria have been used as biocatalysts in BESs. Shewanella, Pseudomonas and Geobacter species and bacteria originating from wastewater are the most commonly used microorganisms in BES processes (Sharma and Kundu 2010). In wastewater based BESs, mixed cultures are mostly used.

BES performance is affected by several factors, which include the type of inoculum (the source of bacterial culture and bacterial strain(s) used at the anode) (Badalamenti et al., 2013; Ishii et al., 2013; Liu et al., 2010), the substrate and its concentration (Gil et al., 2003), pH value of the anodic and cathodic compartments (Gil et al., 2003; He et al., 2008; Raghavulu et al., 2009; Zhuang et al., 2010b), temperature (Larrosa-Guerrero et al., 2010), internal resistance of the system (Cheng et al., 2014; Pei-Yuan & Zhong-Liang, 2010) and materials used for anode, cathode and membrane (Ahn et al., 2014; Cheng et al., 2006; Rozendal et al., 2006).

BES anodic reaction is a proton generating process and cathodic reaction is a proton consuming process, resulting in a pH gradient between the two compartments. Proton consumption in the cathodic chamber increases pH and alkalinity. Cations such as sodium ( $\text{Na}^+$ ) and potassium ( $\text{K}^+$ ) present in the anolyte, migrate through the membrane to the cathodic compartment. These migrated cations together with  $\text{OH}^-$  ion in the cathodic compartment produce a caustic solution. Rabaey et al. (2010) demonstrated the successful recovery of a caustic solution in cathodic chamber of BES

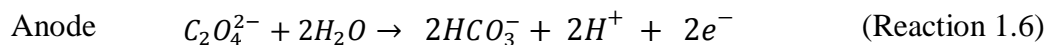
treating Brewery wastewater. The strength of recovered caustic stream ( $\text{NaOH}$ ) can be increased by increasing the anolyte sodium concentration (Pikaar et al., 2013). The migration of other cations, such as  $\text{NH}_4^+$ ,  $\text{Ca}^{2+}$ , and  $\text{Mg}^{2+}$ , lowers the quality of recovered caustic and the coulombic efficiency of caustic generation.

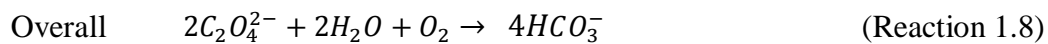
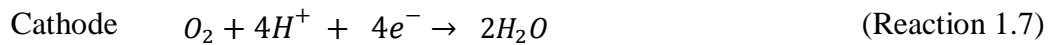


**Figure 1.5.** Schematic of a bioelectrochemical system

Recently, (Bonmati et al., 2013) have demonstrated the use of BES for oxalate degradation under non-saline and possibly neutral pH conditions (pH not mentioned) (Bonmati et al., 2013). In their study, dual chamber BES reactor was used with graphite granules as anode and cathode for the experiments. BES was inoculated with a mixed culture microbial consortium enriched in acetate fed MFC and biomass from upflow anaerobic sludge blanket (UASB) reactor treating brewery wastewater. The anode potential was controlled at +100 to -100 mV vs. standard hydrogen electrode (SHE). At the start up, acetate was used as a co-substrate to stimulate oxalate degradation. Even though the coulombic efficiency (CE) was low ( $21 \pm 2\%$ ) with oxalate as the only carbon source, the oxalate removal was 100%.

The possible half reactions at anode and cathode for oxalate oxidation could be written as follows (Reactions 1.6 - 1.8):





The use of alkaliphilic microorganisms to catalyse anodic processes in BES has been investigated in several studies (Badalamenti et al., 2013; Liu et al., 2010; Ma et al., 2012; Yong et al., 2013; Zhuang et al., 2010a). Zhang et al. (2016) was able to operate glucose fed air-cathode MFC at stable power output of 140 mW/m<sup>2</sup> at pH 11. These studies clearly indicated that alkaliphilic microorganisms can couple their metabolism using insoluble electrodes with concomitant generation of electrical current under alkaline condition.

BES is a promising technology for destructing organics common for Bayer process liquors. From a thermodynamic standpoint, the alkaline nature of the oxalate stream is favourable to the anodic electrochemical reaction of a bioelectrochemical system (Theoretically, a gain of anodic potential of -59 mV/ pH rise of one unit). The oxalate containing waste stream derived from the Bayer process normally has a pH ranging from 12 to 13 and contain excessive amount of sodium salts of the organic compounds ranging at about 4 g/L. Hence, it is worth testing whether an oxalate-degrading culture can be enriched with an anode as the sole microbial electron acceptor using the alkaline Bayer process liquor as a feedstock. If successful, such a process approach would offer a unit process for organics removal and possibly also electrical energy recovery from Bayer liquors. Further, high salinity of Bayer liquor would help to reduce the internal resistance of the BES (Jin et al., 2016; Rousseau et al., 2013).

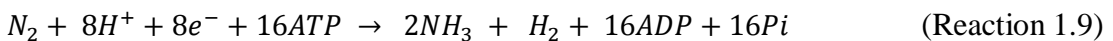
Moreover, the high sodium concentration in Bayer liquor offers an excellent opportunity to recover caustic soda in BES cathode. The recovery of organic free concentrated caustic solution with BES technology would facilitate caustic reuse and decrease the caustic demand of the overall Bayer process.

## 1.7 Nitrogen fixation by microorganisms

Hostile conditions of Bayer process liquor, such as nitrogen (N) deficiency, can negatively impact biological treatment processes. As N is a key nutrient for biological metabolism and cell growth, N supplementation is necessary for biological treatment

of N-deficient wastewater. At present N requirements of full-scale biological treatment plants are typically met with an external dose of N source such as urea (McSweeney, 2011). Urea is a suitable nitrogen source for bulk use, due to its relatively low cost (Bezerra et al., 2012). However, for bacteria to gain access to the N in urea, urea has to be first hydrolysed to form ammonia and in high alkaline aerated bioreactors, much of this ammonia is likely to get volatised, limiting its availability for bacterial metabolism. Therefore, urea are often supplied at a quantity far beyond the theoretical N requirements of the biological oxidation process. Further, the oversupply of urea not only incurs a significant cost but also poses a challenge to achieve a desired effluent quality from the biological process. Maintaining a non-N limiting environment while managing losses due to volatilisation of ammonia is challenging, and hence, over usage of urea has been considered unavoidable.

The use of N-fixing bacteria could provide a more sustainable alternative to the use of external N sources. Under extreme N limitation, N-fixing bacteria are capable of converting atmospheric N<sub>2</sub> to ammonia to fulfil the N requirements for their cell growth (Nair, 2010; Peoples et al., 1995). Nitrogenase enzyme catalyses the biological N fixation activity in certain microorganisms. The chemical reaction of N<sub>2</sub> reduction activity taking place in N fixation is given in Reaction 1.9.



An N-fixing inoculum eliminates the need to maintain a non-limiting concentration of N in the process liquor and assist in overcoming current challenges faced by the industry in N supplementation. So far, the N-fixing bacterial culture has not been studied for biological oxalate destruction in both aerobic and anaerobic conditions. Moreover, the high salinity and alkalinity of the Bayer process liquor would impact on application of N-fixing bacterial culture. However, Wong et al. (2014) demonstrated the successful use of N-fixing bacteria to degrade glucose in BES anode to treat N-deficient wastewater under neutral pH conditions.

## **1.8 Aim and objectives of this study**

This thesis aimed to improve the existing practice of aerobic organics destruction, as well as to exploit new option (i.e. BES) for the Alumina industry. A new bacterial culture (N-deficient) was studied and characterised to improve the oxalate degradation rate of the aerobic bioprocesses. Further, this study explored the feasibility of BES technology for the destruction of organic impurities present in Bayer process and the recovery of caustic from organic rich wastewater that resembles Bayer liquor in its alkalinity and salinity. The effects of N limitation, microbial community composition and operational parameters on oxalate removal were studied in both BES and aerobic bioreactors.

The specific objectives of the work were to:

1. Explore and compare the use of BES inoculated with activated sludge to oxalate destruction in alkaline and saline medium under N-supplemented and N-deficient conditions (Chapter 2).
2. Examine the caustic recovery and cation migration in BES reactor operated at alkaline condition with and without N supplementation. The feasibility of caustic recovery from the established BES reactor process is important for the economies of the process as recovered caustic can be reused in the Bayer process (Chapter 3).
3. Establish an oxalate degrading biofilm in aerobic bioreactors and determine the effect of dissolved oxygen concentration on the performance of aerobic bioreactors and oxalate removal pathways of the established biofilm under N-supplemented and N-deficient conditions (Chapter 4).
4. Evaluate the effect of pH and various organic compounds on aerobic oxalate degradation rate (Chapter 5).
5. Determine the kinetics of oxalate degradation and microbial community composition in the aerobic bioreactors (Chapter 6).
6. Investigate the use of aerobic biofilm formed on conductive material as inoculum for the BES reactor (Chapter 7).

## 1.9 Thesis structure

This thesis comprises eight chapters including introduction, experimental chapters and conclusion. The introduction (**Chapter 1**) contains an overview of aluminium industry, Bayer process, problems caused by organic impurities and use of biological processes for organics destruction. The chapter also reviews previous studies on aerobic oxalate removal, fundamentals of BES and biological nitrogen fixation.

**Chapter 2** reports the initial attempt to start-up a bioelectrochemical reactor using activated sludge as the microbial inoculum to degrade oxalate and other simple organics common for Bayer process liquor. Microbial communities of the established biofilms were characterised to justify the oxalate removal limitations of the reactors. The effect of N deficiency was also evaluated, considering that omission of the requirement of dosing N (e.g. ammonium chloride) to maintain the bioprocess could be seen as a practical advantage of the process.

**Chapter 3** documents the process characteristic of the BES process established in the previous chapter (under both N-supplemented and N-deficient conditions) for recovering caustic soda.

Since **Chapter 2** suggested that bioelectrochemical oxidation of oxalate was inefficient, a more robust or reliable method should be adopted to facilitate the prime goal of oxalate destruction. Hence, two conventional aerobic bioreactors were set up and assessed for their ability to destruct oxalate under alkaline and saline conditions (**Chapter 4**). Again, the effect of N deficiency was assessed for the rationale as mentioned above. It was useful to further characterise the established aerobic reactors (specifically N-deficient reactor) to improve the oxalate removal efficiencies, as full scale aerobic bioreactors are already used at some refineries to degrade oxalate. Hence, various process parameters were comparatively examined to find out the suitability of N-deficient biofilm to treat alkaline and saline wastewater. The effect of bulk water dissolve oxygen concentration on oxalate degradation rate was examined and oxalate fermentation pathways were explored for the established biofilms.

Following the successful development of the aerobic bio-treatment unit, **Chapter 5** explored the physiological characteristic of the established aerobic biofilm in terms of its response to pH changes and its ability to degrade other organic compounds

commonly present in Bayer liquor (e.g. sodium acetate, sodium formate, sodium malonate and sodium succinate).

**Chapter 6** further elucidated the kinetics of oxalate degradation in both the N-supplemented and N-deficient bioreactors. The determined key kinetics parameters (Michaelis-Menten constants ( $K_m$ ) and maximum specific oxalate degradation rate ( $V_{max}$ )) of the biofilms were used to propose a novel two step oxalate removal process that capitalises on higher specific oxalate removal rates to effectively remove oxalate from alumina refineries. The two cultures were characterised using DNA-based methods and the bacterial genera were identified that could be directly or indirectly responsible for the removal of oxalate in both cultures.

It was hypothesized that the inability of activated sludge to bioanodically oxidise oxalate was due to a lack of key oxalotrophic microorganisms, which are responsible for catalysing decarboxylation of oxalate into formate. Thus, with the established aerobic oxalate degrading biofilm (on graphite granules) (which assumed to contain suitable microorganisms), **Chapter 7** aimed to test if such pre-acclimatised biofilm could be a better source of microbial inoculum for starting up a BES anodic process. Moreover, the changes in the microbial community structure under various operating conditions were reported.

**Chapter 8**, the final chapter, summarised the major findings of the experimental work and their implications for industrial applications. Further, recommendations for future studies and limitations of this study were discussed.

## **2 BIOELECTROCHEMICAL OXIDATION OF ORGANICS BY ALKALI-HALOTOLERANT ANODOPHILIC BIOFILM UNDER NITROGEN-DEFICIENT, ALKALINE AND SALINE CONDITIONS**

Extended from

Weerasinghe Mohottige, T.N., Ginige, M.P., Kaksonen, A.H., Sarukkalige, R. and Cheng, K.Y. (2017) Bioelectrochemical oxidation of organics by alkali-halotolerant anodophilic biofilm under nitrogen-deficient, alkaline and saline conditions. *Bioresource Technology*. DOI: <https://doi.org/10.1016/j.biortech.2017.08.157>

### **Chapter Summary**

This work aimed to study the feasibility of using bioelectrochemical systems (BES) for organics removal under alkaline-saline and nitrogen (N) deficient conditions. Two BES inoculated with activated sludge were examined for organics (oxalate, acetate, formate) oxidation under alkaline-saline (pH 9.5, 25 g/L NaCl) and N deficient conditions. One reactor (R1) received ammonium chloride as an N-source, while the other (R2) without. The reactors were initially loaded with only oxalate (25 mM), but start-up was achieved only when acetate was added as co-substrate (5 mM). Maximum current were R1:  $908 \pm 26$  mA/m<sup>3</sup> (organic removal rate (ORR) 4.61 kg COD/m<sup>3</sup>.d) and R2:  $540 \pm 17$  mA/m<sup>3</sup> (ORR 2.06 kg COD/m<sup>3</sup>.d). Formate was utilised by both anodic biofilms, but the inefficient oxalate removal was likely due to the paucity of microorganisms that catalyse decarboxylation of oxalate into formate. Further development of this promising technology for the treatment of alkaline-saline wastewater is warranted.

## 2.1 Introduction

Alumina (aluminium oxide,  $\text{Al}_2\text{O}_3$ ) is produced from bauxite ore in a process known as the Bayer process, which involves mixing the ores with caustic solutions under elevated temperature (Meyers, 2004; Whelan et al., 2003). Many bauxite ores, particularly those in Australia contain a wide range of organic compounds, which can detrimentally affect the Bayer process by (1) reducing the availability of caustic in the Bayer liquor (due to incorporation of sodium into organic compounds), and (2) reducing aluminium trihydroxide ( $\text{Al}(\text{OH})_3$ ) precipitation rate (due to crystallization poisoning) (Den Hond et al., 2007; Wellington & Valcin, 2007). These organics are generally considered as unwanted waste components for the alumina industry. Therefore, effective removal of organic compounds from the process water of the alumina refining circuit (Bayer process) is essential.

Amongst all the organics present in Bayer process liquor, sodium oxalate ( $\text{Na}_2\text{C}_2\text{O}_4$ ) is the key detrimental compound (Power et al., 2012). As the Bayer liquor is typically recycled within the refinery circuit, sodium oxalate concentration in the liquor would gradually reach a level that triggers the aforementioned problems. Preferably, the oxalate from the Bayer circuit should be permanently destroyed in an economical and environmentally sustainable manner (McKinnon & Baker, 2012). One option to destroy oxalate from the Bayer circuit is by adopting microbial oxidation processes such as aerobic bioreactor processes (McKinnon and Baker, 2012). Although effective in terms of oxalate destruction, aeration requirement in aerobic processes would incur significant energy demand. Further, aerobic bioreactor processes do not normally facilitate recovery of resources (e.g. energy and caustic) (Rabaey et al., 2010). Hence, alternative treatment processes that allow energy saving and resources recovery should be considered.

Although not yet embraced by the alumina industry, bioelectrochemical systems (BES) have been widely explored as an advanced microbial oxidative process for removing organic contaminants and recovering resources from wastewaters (Rabaey et al., 2010; Rozendal et al., 2008). Recently, the use of BES for oxalate removal has been demonstrated by Bonmati et al. (2013). They successfully established an oxalate-degrading bioanode with both acetate and oxalate as the carbon and electron sources, and found that the anodic biofilm could oxidise oxalate under neutral pH and non-

saline conditions (coulombic efficiency 34%) (Bonmati et al., 2013). In fact, alkaliphilic microorganisms have been shown as being able to generate anodic current in BESs (Badalamenti et al., 2013; Liu et al., 2010). For instance, Liu et al. (2010) showed that a Gram-positive alkaliphile (*Corynebacterium* sp.) could utilise formate as an electron donor at pH 9. Badalamenti et al. (2013) also recently reported two pure haloalkaliphilic strains (*Geoalkalibacter ferrihydriticus* DSM 17813 and *Geoalkalibacter subterraneus* DSM 23483) that could produce current under either alkaline (pH 9.3) (8.3 A/m<sup>2</sup>) or saline (17 g/L NaCl) (3.3 A/m<sup>2</sup>) conditions with acetate as an electron donor. Since the oxalate waste from alumina refineries is both saline (up to 25 g/L of sodium chloride) and alkaline (>pH 13), it would be desirable to develop a BES process for oxalate removal under both alkaline and saline conditions.

Besides, as Bayer process water is typically deficient in nitrogen (N), external dosing of N into aerobic oxalate removing bioreactors is commonly practiced since N is an essential element for microbial growth. However, this not only incurs additional costs, but excessive dosage can lead to undesirable build-up and release of ammonia (particularly under alkaline conditions), causing odour issues. Since the required conditions (presence of organic carbon, absence of inorganic N and low concentrations of dissolved oxygen (Gauthier et al., 2000)) for biological N fixation are ubiquitous in the Bayer process water, it would be worth testing if anodophilic microorganisms could grow in an alkaline-saline BES without external supplementation of N. Omission of this requirement would be attractive in terms of reducing treatment costs.

In light of the above, this study aimed to examine the use of BES for the treatment of synthetic liquor mimicking Bayer process water in its alkalinity (pH 10) and salinity (25 g/L NaCl) under N-deficient conditions. The specific research questions were: (1) Can anodic biofilms be established using activated sludge as a microbial inoculum to remove oxalate under alkaline and saline conditions? (2) Can the supply of ammonium chloride as N source be omitted to establish an anodic biofilm for organics removal under alkaline-saline conditions? (3) Can the established biofilm be used to remove organic compounds present in Bayer liquor, such as acetate, formate, succinate and malonate under alkaline and saline conditions? These questions were answered for the first time by operating two parallel laboratory-scale, dual-chamber BES reactors, with one supplied with ammonium chloride (NH<sub>4</sub>Cl) as an external N source and the other not. Activated sludge was selected as the microbial inoculum considering its board

microbial diversity and availability from sewage treatment plants (McKinnon and Baker, 2012). There is also a previous report of using activated sludge as a start-up inoculum for a full scale aerobic oxalate degrading bioreactor (McSweeney, 2011). An alkaline (pH 10) and saline (25 g/L NaCl) media mimicking the alkalinity and salinity of a typical Bayer process water was continuously loaded into the two reactors for a period of >350 days. The effects of various process parameters, such as anode potential, hydraulic retention time (HRT) and anolyte pH on the BES performance (anodic current, organics removal rate, coulombic efficiencies) were quantified.

## 2.2 Materials and Methods

### 2.2.1 Bioelectrochemical systems, process set-up and general operation

Two dual-chamber BES reactors were used in this study. Reactor 1 (R1) was fed with an ammonium-N supplemented synthetic Bayer liquor and reactor 2 (R2) was fed with a synthetic Bayer liquor that lacked ammonia-N (Figure 2.1). Each reactor consisted of two identical half cells (14 cm × 12 cm × 2 cm), which were separated by a cation exchange membrane (surface area 168 cm<sup>2</sup>) (Ultrex CMI-7000, Membrane International Inc.). Both half cells were loaded with identical conductive graphite granules (285 g, 3-5 mm diameter, KAIYU Industrial (HK) Ltd.). This reduced the liquid volume of each half cell from 336 to 250 mL. The specific surface area of the graphite granules was  $1.308 \pm 0.003 \text{ m}^2/\text{g}$  as determined by using Brunauer-Emmett-Teller (BET) method (CSIRO Process Science and Engineering, Waterford, Western Australia). Four graphite rods (5 mm diameter, length 12 cm) were used as current collectors in each half cell to enable electric connection between the graphite granules and the external circuit. The reactors were operated as a three-electrode system coupled with a potentiostat (VMP3, BioLogic) (Cheng et al., 2010). Only the anodic half cell was inoculated with microorganisms and the electrode therein is termed as the working electrode (here anode). The electrode in another half cell is termed as the counter electrode (cathode). The working electrode was polarized against a silver-silver chloride (Ag/AgCl) reference electrode (MF-2079 Bioanalytical Systems, USA) at a defined potential using the potentiostat. The reference electrode was mounted in the working chamber and was located close (< 1 cm) to the granular graphite working

electrode. In this study, the BES processes were operated with a potentiostat to ensure that the anodic process could be examined without being influenced by factors such as ohmic resistance and cathodic reduction reaction. A total liquid volume of 0.5 and 2.0 L was continuously recirculated through the anodic and the cathodic chambers via two separate external recirculation bottles (0.25 and 2.0 L), respectively, at a recirculation rate of approximately 14 L/h. The anodic recirculation bottle was intermittently (every 20 min for 30 second) purged with nitrogen gas to create an anaerobic environment in the anodic chamber and to enable availability of dissolved N<sub>2</sub> for R2. The process was operated under ambient conditions at 22 ± 2°C.

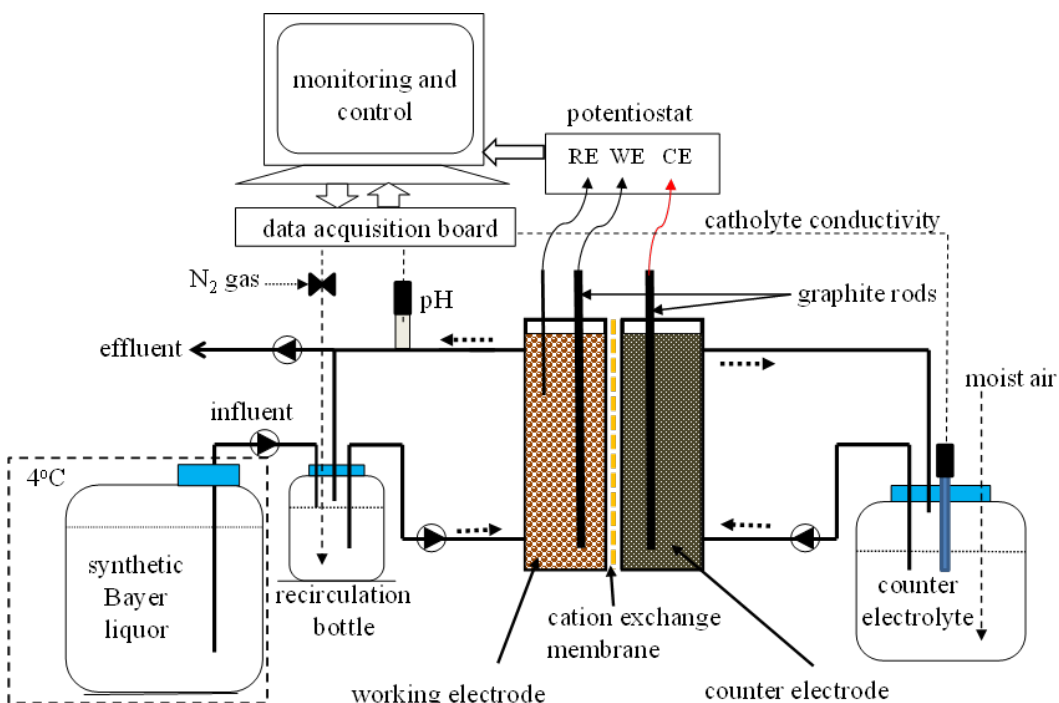


**Figure 2.1.** Schematic diagram of the bioelectrochemical process. WE = working electrode; CE = counter electrode; RE = reference electrode.

The anodic chambers of both reactors were operated in either batch or continuous modes, as specified in the text below. When the reactors were operated in continuous mode, fresh anolyte (maintained at 4 °C in a refrigerator) was continuously introduced at a specified flow rate into the anodic recirculation bottle and an equal volume of the working anolyte was extracted (and discarded) from the recirculation line using a peristaltic pump (Masterflex® Cole-Parmer L/S pump drive fitted with a Model

77202-60 Masterflex® pump head; Norprene® tubing 06404-14). The cathodic chambers of the reactors were exclusively operated in batch mode. The catholyte was occasionally renewed according to experimental requirements. The BES process was continuously monitored and controlled using a computer program (LabVIEW™). The electrode potentials and the electrical current of the BES reactors were monitored via the potentiostat. All electrode potentials (mV) reported in this paper refer to values against Ag/AgCl reference electrode (ca. +197 mV vs. standard hydrogen electrode (Bard & Faulkner, 2001)). The pH of the working electrolyte was continuously monitored using in-line pH sensors (TPS Ltd. Co., Australia). All signals were regularly recorded to an Excel spreadsheet via the LabVIEW™ programme interfaced with a National InstrumentTM data acquisition unit (Compact Rio®).

## **2.2.2 Synthetic alkaline-saline medium (anolyte) and catholyte media**

A synthetic medium that mimicked the highly saline and alkaline conditions of the Bayer process liquor was used as the anolyte for both R1 and R2 reactors. Unless stated otherwise, sodium oxalate 3.35 g/L (25 mM) and/or sodium acetate (5 mM) were used as the carbon source. Sodium chloride (25 g/L) was added to increase the solution salinity equivalent to that of a typical Bayer liquor (Hind et al., 1997). This level of salinity was maintained throughout the entire study. The pH value of the feed solution was maintained at above 10 by adding 2 M NaOH. The synthetic liquor used for R1 consisted of (mg/L): NH<sub>4</sub>Cl, 265; NaHCO<sub>3</sub>, 125; MgSO<sub>4</sub>·7H<sub>2</sub>O, 51; CaCl<sub>2</sub>·2H<sub>2</sub>O, 15; and K<sub>2</sub>HPO<sub>4</sub>·3H<sub>2</sub>O, 20.52 and 1.25 mL/L of trace element solution which had the composition of (g/L): ZnSO<sub>4</sub>·7H<sub>2</sub>O, 0.43; FeSO<sub>4</sub>·7H<sub>2</sub>O, 5; CoCl<sub>2</sub>·6H<sub>2</sub>O, 0.24; MnCl<sub>2</sub>·4H<sub>2</sub>O, 0.99; CuSO<sub>4</sub>·5H<sub>2</sub>O, 0.25; NaMoO<sub>4</sub>·2H<sub>2</sub>O, 0.22; NiCl<sub>2</sub>·6H<sub>2</sub>O, 0.19; NaSeO<sub>4</sub>·10H<sub>2</sub>O, 0.21; ethylenediaminetetraacetic acid (EDTA) 15, H<sub>3</sub>BO<sub>3</sub>, 0.014; and NaWO<sub>4</sub>·2H<sub>2</sub>O, 0.05 (Cheng et al., 2010). R2 received the same influent as the anolyte, but without NH<sub>4</sub>Cl to deprive the microorganisms of nitrogen source. Unless stated otherwise, this medium was used as the anolyte in the anodic chambers of R1 and R2 throughout the entire study. A NaCl solution (25 g/L) was used as the catholyte of both reactors (R1 and R2).

### **2.2.3 Experimental procedures**

#### **2.2.3.1 Reactor start-up and acclimatisation of electrochemically active anodic biofilm**

The anodic chambers of both reactors (R1 and R2) were inoculated with returned activated sludge (RAS) collected from a municipal wastewater treatment plant in Perth, Western Australia to initiate establishment of an electrochemically active biofilm. Activated sludge was chosen in this study as the microbial inoculum because of its diverse microbial community and availability from sewage treatment plants (McKinnon & Baker, 2012). There is also a previous report of using activated sludge as a start-up inoculum for a full scale aerobic oxalate degrading bioreactor (McSweeney, 2011). The RAS was filtered through a metal screen to remove large particles (< 1 mm). The inoculation was done by injecting a predefined volume (30 mL, mixed liquor suspended solid (MLSS) concentration was 33.9 g/L) of the filtered sludge into the anodic recirculation line. During initial start-up period (i.e. the first 54 days), yeast extract (50 mg/L final concentration) was intermittently introduced to the anolyte (Figure 2.2) to assist establishment of the electrochemically active bacteria of both reactors. Both the anolyte and catholyte were renewed regularly (weekly or prior to each specific experiment) to avoid accumulation of unwanted chemical species. After the microbial inoculation, the working electrode (anode) was maintained at a constant potential of +200 mV vs Ag/AgCl, which was successfully used to establish an effective nitrogen fixing anodophilic biofilm (Wong et al., 2014). The synthetic medium was continuously loaded into the anodic chamber to maintain a hydraulic retention time (HRT) of one day. Over this start-up period (i.e. the first 54 days), sodium oxalate was used as the main carbon and electron source and the influent was maintained at pH 10.

#### **2.2.3.2 Supplementation of sodium acetate to facilitate bioanode establishment**

Since no remarkable current production (< 2 mA) was recorded, both R1 and R2 were switched into batch mode operation (from day 27 to day 38, and from day 44 to 54). Fixed amounts (5 mmol/L) of sodium acetate (1.25 mL from a 2 M stock solution) were injected into the anodic recirculation line of each reactor on days 35, 43, 48 and

51 to test if the biofilm could readily utilise acetate (a commonly used electron donor) for current generation. Since the addition of acetate readily triggered current production, from day 54 onwards the synthetic medium was amended to additionally include sodium acetate (5 mM) as a co-substrate. Instead of using a more alkaline influent, the in-reactor pH was maintained at 9 by computer-feedback dosing of NaOH (0.5 M) to neutralise the extra protons liberated from the anodic acetate oxidation reaction. This approach of pH control was adopted to prevent any possible over-loading of alkalinity. The operational parameters of different time periods were given in Table S2.1 and S2.2 (see appendix 1) for reactor R1 and R2, respectively.

### **2.2.3.3 Ability of the established biofilm to oxidise other organics commonly present in Bayer liquor**

Separate tests were carried out to examine the ability and coulombic conversion efficiencies of the established anodic biofilm to oxidise other organic compounds likely present in typical Bayer process water, namely sodium acetate, sodium formate, sodium succinate and sodium malonate. Prior to each separate test, the two reactors were operated in batch mode to exhaust any residual acetate, as indicated by a low and stable background current of < 1 mA. Thereafter, a known quantity of the organic compound was injected to the anodic chamber to test if current could be triggered. During this test, oxalate was maintained at a similar level (25 mM), as at the time of the test both reactors were unable to allow notable current production using oxalate as the sole electron donor. Accordingly, once a steady background current was established, 1.25 mL from 2 M sodium acetate solution was injected to create an in-reactor concentration of 5 mM in both reactors on day 83. Similarly, on day 86, 2.5 mL of 1 M sodium formate solution was injected to create an in-reactor concentration of 5 mM in both R1 and R2 reactors. Once the current reached a stable background level, sodium formate (1 M, 5 mL) was added for the second time to give an in-reactor formate concentration of 10 mM. The current peaks triggered by the addition of the organic compounds were integrated to determine coulombic efficiencies corresponded to acetate and formate tested (i.e. coulombs recorded from the triggered current versus the coulombs added as a spike). The coulombs from the background oxalate were excluded in this calculation. On days 230 and 245, R1 and R2 were each injected with

2.5 mL of 1 M sodium succinate solution (in-reactor concentration 5 mM) to test if current could be produced. Similarly the effect of sodium malonate was tested by adding 2.5 mL of 1 M sodium malonate solution (in-reactor concentration 5 mM), on day 233 and 250 for reactor R1 and R2, respectively.

#### **2.2.3.4 Characterisation of the BES performance under stable operations**

The two BES reactors were operated continuously for over 300 days (Figure S2.1 in appendix 1). During this period, the effects of various operational settings (HRT and anode potential) were examined with oxalate (25 mM) and acetate (5 mM) as the substrates as detailed below. The reactors were given sufficient time to run at each tested setting until a stable trend of anodic current generation was attained.

##### **2.2.3.4.1 Effect of organic loading rates (OLR) on reactor performance**

To study the effect of organic loading rates (OLR), both R1 and R2 were operated at various HRTs (0.5 – 48 h). The corresponding chemical oxygen demand (COD) loading rates were ranging from 0.32 kg/m<sup>3</sup>.d to 45.9 kg/m<sup>3</sup>.d. The oxalate and acetate removal rates at different OLRs were quantified by analysing the influent and effluent concentrations. The reactors were operated at each HRT set point until a stable current was recorded. Based on the outcome of the previous experiment, a constant anode potential of +200 mV was maintained and the anolyte pH was also controlled at 9.0 ± 0.2 on both reactors.

##### **2.2.3.4.2 Effect of anode potential on BES performance**

Unlike many other BES processes that were operated under pH circumneutral condition, the BESSs in this study were operated under alkaline condition. Therefore, it was likely that the anodic reaction in our alkaline BES processes would remain energetically favourable even at a lower anode potential. Hence, it would be meaningful to examine the response of the established biofilm to different poised anode potentials. The following experiment was carried out on R1 and R2 reactors on

day 111 and day 170, respectively. During these tests, the reactors were operated in continuous mode at 3 h HRT in order to prevent substrate limitation during the experiment. The BES was first allowed to operate in open circuit mode for at least 12 h until the open circuit voltage was stable. Thereafter, the anode potential was adjusted to different set points, ranging from -600 mV to +300 mV. Steady currents were recorded and plotted against the respective anode potential set points.

#### **2.2.4 Chemical analyses**

Performance of the BES reactors was quantified by measuring the changes of COD, oxalate and acetate concentrations over time. Anolyte pH and catholyte conductivity were also monitored throughout the experiment. Liquid samples collected from the BES were immediately filtered through a 0.22 µm filter (0.8/0.2 µm Supor® Membrane, PALL® Life Sciences) upon collection and were stored at 4 °C prior to analysis. Acetate, oxalate, and other anions were analysed using a Dionex ICS-3000 reagent free ion chromatography (RFIC) system equipped with an IonPac® AS18 4 x 250 mm column. Potassium hydroxide was used as an eluent at a flow rate of 1 mL/min. The eluent concentration was 12-45 mM from 0-5 min, 45 mM from 5-8 min, 45-60 mM from 8-10 min and 60-12 mM from 10-13 min. Ammonium ( $\text{NH}_4^+$  - N) and other cations were measured with the same RFIC with a IonPac® CG16, CS16, 5 mm column. Methansulfonic acid was used as an eluent with a flow rate of 1 mL min-1. The eluent concentration was 30 mM for 29 min. The temperature of the two columns was maintained at 30°C. Suppressed conductivity was used as the detection signal (ASRS ULTRA II 4 mm, 150 mA, AutoSuppression® recycle mode). COD was measured using a closed reflux dichromate COD method (HACH Method 8000, HACH Ltd).

#### **2.2.5 Microbial community analysis**

Biofilm samples were collected from the reactors at specific time points during the operation for microbial community analysis. Sampling of the biofilm was carried out by dislodging the biomass from the granular anode for approximately 3 min using a clean Teflon tubing (length 250 mm, internal diameter 3 mm) connected to a 50 ml

sterile syringe (liquid agitation by repeated forward-backward movement of the syringe piston) (Wong et al., 2014). Samples were collected from both BES reactors after 200 days when the reactors were producing steady current with both oxalate and acetate as the substrates.

DNA was extracted from 250 µL of suspended biomass using Power Soil DNA isolation kit (MO BIO laboratories, Inc) following manufacturer's instructions. The extracted DNA was quantified using a Qubit fluorometer and stored at -20°C prior to 454 sequencing at School of Pathology and Laboratory Medicine, University of Western Australia. The sequencing was carried out as described in (Nagel et al., 2016). In brief, microbial 16S rRNA genes were amplified from 1 ng aliquots of the extracted DNA using V4/5 primers (515F: GTGCCAGCMGCCGCGTAA and 806R: GGACTACHVGGGTWTCTAAT) (Caporaso et al., 2010a). A mixture of gene-specific primers and gene-specific primers tagged with Ion Torrent-specific sequencing adaptors and barcodes were used. The tagged and untagged primers were mixed at a ratio of 90:10. Using this method, the amplification of all samples was achieved using 18 – 20 cycles, thus minimising primer-dimer formation and allowing streamlined downstream purification. Amplification was confirmed by agarose gel electrophoresis and quantified by fluorometry. Up to 100 amplicons were diluted to equal concentrations and adjusted to a final concentration of 60 pM. Templated Ion Sphere Particles (ISP) were generated and loaded onto sequencing chips using an Ion Chef (Thermofisher Scientific) and sequenced on a PGM semiconductor sequencer (Thermofisher Scientific) for 650 cycles using a 400 bp sequencing kit that yields a modal read length of 309 bp. Data collection and read trimming/filtering were performed using TorrentSuite 5.0.

The post sequencing was done by using the open source software package QIIME (Quantitative Insights Into Microbial Ecology). The fasta, qual and mapping files were analysed using downstream computational pipelines in QIIME. The chimeric reads were filtered using USEARCH61 algorithm against a reference database (Greengene) at 97 % sequence similarity. The sequences were assigned operational taxonomic units (OTU) at 97 % sequence similarity using the same reference database file. Once a representative sequence was appointed for each of the OTUs, a taxonomic assignment was carried out using the RDP classifier version 2.2 in reference to the greengene database.

## **2.3 Results and Discussion**

### **2.3.1 Activated sludge was unable to start-up both R1 and R2 with oxalate as the sole carbon source**

After inoculation with activated sludge, the two reactors were operated with sodium oxalate as the main source of carbon and electrons (Figure 2.2). When oxalate was the sole carbon and electron source (start-up period of first 54 days), the currents in both R1 and R2 were very low (< 5 mA), and no notable consumption of oxalate was recorded (Figure 2.2C). After approximately two weeks (at ~day 14), yeast extract was occasionally added to the anolyte in both reactors to stimulate biofilm growth (Figure 2.2) during the start-up period. However, as no notable improvement of oxalate removal was achieved, on day 37 a concentrated acetate solution was spiked into both reactors to test if the biofilms could readily produce a current. The addition of acetate immediately triggered current production in both reactors even with processes previously not adapted to acetate (Figure 2.2A, B). Since no notable degradation of oxalate was recorded in both systems, the produced currents were not attributed to the anodic oxidation of oxalate (Figure 2.2C). This result suggested that the activated sludge could not be readily acclimatised using oxalate as a sole electron donor under the tested conditions. In other words, activated sludge may not be a suitable microbial inoculum for the described alkaline-saline BES processes.

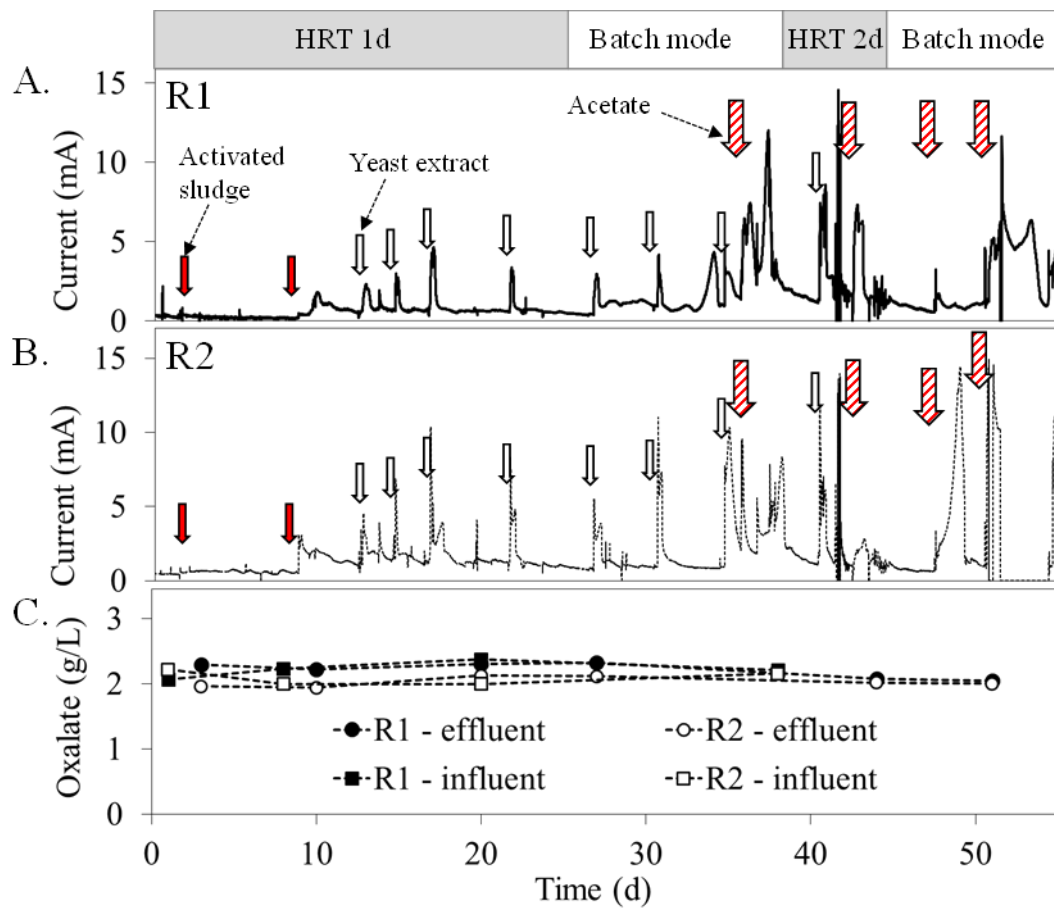


**Figure 2.2.** Start-up performance of the two BES reactors during the initial 54 days period. (A, B) Current production in R1 and R2 with sodium oxalate as the main carbon source; (C) Oxalate concentration of the influent and effluent of R1 and R2. The anode potentials in both reactors were maintained at +200mV. Influent pH was 10. The reactors were operated in continuous mode from day 1 to 26 with one day HRT and from day 38 to 44 with two days HRT. Different vertical arrows indicate additions of different agents: activated sludge (30 mL); yeast extract (50 mg); acetate (2.5 mmol).

Given that the biofilms in both R1 and R2 could readily respond to acetate additions (current generation), and that acetate was successfully used by Bonmati et al. (2013) as a co-substrate for a successful start-up of an oxalate-degrading BES, from day 54 onwards the synthetic medium was supplemented with acetate (5 mM) to facilitate process start-up in both reactors. Further, Allison et al. (1985) investigated that well-known oxalate degrading bacteria *Oxalobacter formigenes* requires small amount of acetate as a growth requirement. Since Bayer liquor typically contains a range of soluble organics including sodium acetate (Cardwell & Laughton, 1994; Power et al.,

2012; Power et al., 2011c), the addition of sodium acetate as co-substrate to the reactors can be justified.

### **2.3.2 The established biofilms could readily generate current using other organics**

After supplemented with acetate, the biofilms in both R1 and R2 showed a gradual improvement toward production of current (see Figure S2.1B, days 60-80 in appendix 1). Hence, the biofilms were examined for their ability to generate anodic current with the addition of specific organic compounds that are known to be present together with oxalate (Figure 2.3).

As observed during the start-up phase, the addition of acetate immediately triggered current peaks in both R1 and R2 (Figure 2.3A). Comparison of the amount of electrons added as acetate with that recovered from the acetate-triggered current peaks (i.e. electrons available from the background oxalate were excluded) revealed a coulombic efficiency (CE) of 77% for R1. This value agrees well with other studies that used acetate as the sole energy donor (Cheng et al., 2008; Rabaey et al., 2005). For instance, with acetate as a sole electron donor, Cheng et al. (2008) reported a CE of 83% for their anodic biofilm. Similarly, a high CE was recorded for R2. However, the value was beyond 100% (106%), suggesting that there were more electrons received by the anode than available from the added acetate. Since oxalate was the only other electron donor available during the test, the extra electrons recorded were likely originated from the oxalate. It was unclear why such a high CE% was only observed in R2 (i.e. under N-deficient condition), but the result implied that anodic oxalate oxidation might be facilitated by the presence of acetate. In fact, previous studies have shown that acetate is a growth supplement for anaerobic oxalate degrading bacteria such as *Oxalobacter formigenes*, which in the presence of acetate was able to produce CO<sub>2</sub> and formate from oxalate degradation Allison et al. (1985).

On the other hand, apart from being abundant in Bayer liquor, formate is indeed a key metabolic intermediate of microbial oxalate degradation (Dawson et al., 1980b; Dehning & Schink, 1989) (Reaction 2.1). Our results suggested that similar to acetate, formate was readily converted into anodic current in both R1 and R2. Figure 2.3B clearly shows that the addition of the two formate spikes (2.5 and 5 mmol) triggered

spontaneous current production in both systems. High CE values (ranging from 94 to 101%) were obtained with these spikes, suggesting that the observed anodic conversions were highly efficient.

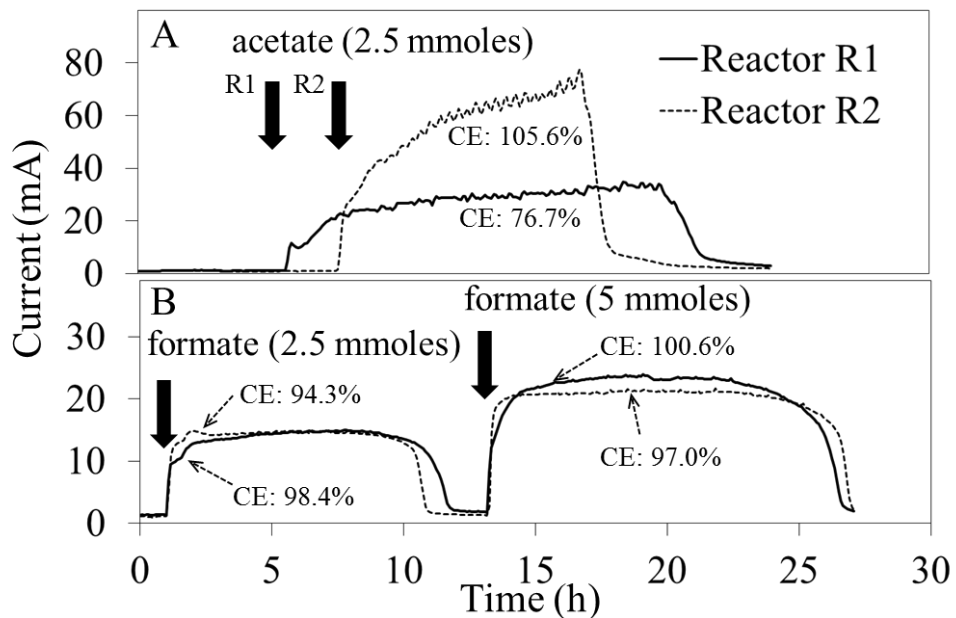
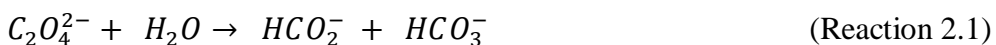


**Figure 2.3.** Current responses of the biofilms to (A) sodium acetate, and (B) sodium formate in the presence of sodium oxalate (25 mM). Both R1 and R2 were operated in batch mode. The addition of sodium acetate (2.5 mmoles) was carried out on day 83, whereas the addition of sodium formate (2.5 mmoles and 5 mmoles) was carried out on day 86. Note: Corresponding CE (coulombic efficiency) values were calculated based on the amount of electrons in the organic added versus that recovered from the triggered current (i.e. electrons available from the oxalate were excluded).

Unlike, the current production from acetate and formate addition, the current produced from the addition of sodium succinate was significantly low. Although measurable currents were recorded in both reactors (maximum current of 7.8 mA and 6.2 mA in R1 and R2, respectively), the CEs of the succinate-triggered current peaks were remarkably lowered (22.5 % and 20.0 % for reactor R1 and R2, respectively) (data not shown). For malonate, no notable increase in current was recorded after the addition of sodium malonate (data not shown), suggesting that both biofilms were unable to electrochemically oxidise malonate.





Formate and CO<sub>2</sub> are the main products of oxalate decarboxylating pathway by anaerobic bacteria (Dehning & Schink, 1989). The failure of both R1 and R2 in retrieving electrons from oxalate could be explained by the paucity of microbial strains capable of catalysing the conversion of oxalate into formate (reaction 2.1) (Dehning & Schink, 1989). Supposedly, if the conversion of oxalate to formate (reaction 2.1) in both reactors was efficient, both reactors should display a much higher background anodic current (prior to formate addition), as the anodic formate oxidation was highly efficient in both reactors (reaction 2.2) (Figure 2.3B). However, the extremely low background current (<2 mA) recorded in both R1 and R2 suggested that such a conversion was indeed negligible. Decarboxylating oxalate to formate is challenging, as specific enzymes in oxalotrophic bacteria are required to catalyse the cleavage of C-C bond in oxalate (Stewart et al., 2004; Svedruzic et al., 2005). It was likely that the inoculum (activated sludge) used in this study was a poor source of these crucial oxalotrophic microbial strains (e.g. *Oxalobacter vibrioformis*, *Clostridium oxalicum* (Dehning & Schink, 1989); *Oxalobacter formigenes* (Allison et al., 1985)).

### 2.3.3 Characterisation of the BES performance with the established anodic biofilm

#### 2.3.3.1 Effect of HRT on the electrochemical and treatment performance

The electrochemical and organics removal performance of the two BES reactors were further characterised by varying the hydraulic loading rates (Figures 2.4 and 2.5). The results suggested that both biofilms responded readily to the changing hydraulic loads, as indicated by the distinct shifts in the steady-state current in both R1 and R2 at various HRTs (Figures 2.4B and 2.5B). The different electrochemical (CE, current) and treatment (oxalate, acetate and COD removal) parameters were further related to the HRTs to visualise their relationships (Figures 2.4C, D and 2.5C, D). Oxalate removal efficacies in both reactors were notably low at all the HRTs tested (<10%). However, near complete acetate removal was recorded again when both reactors were given sufficient time to process the liquor (HRT ≥ 3 h) (Figures 2.4C and 2.5C). When the HRT was too short (HRT<1 h and <3 h, for R1 and R2, respectively), both the

current and COD (acetate) removal efficacies in the two reactors decreased remarkably, likely due to substrate overloading (Figures 2.4C and 2.5C).

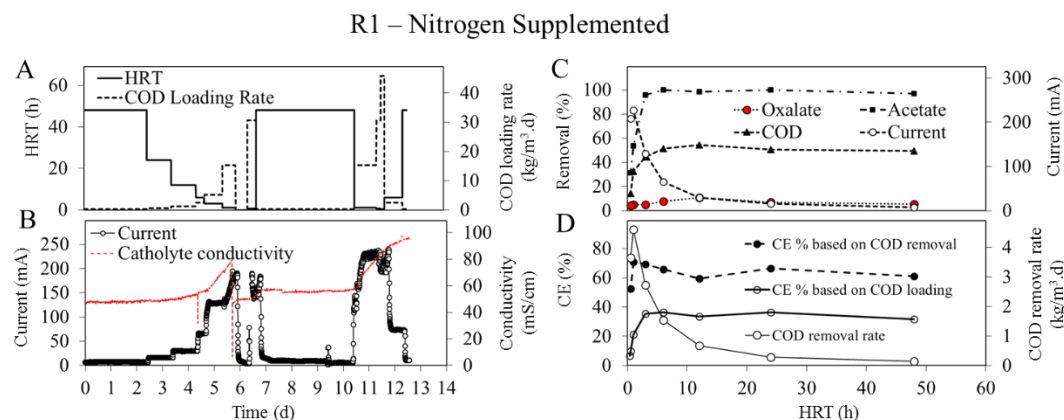


**Figure 2.4.** Effect of HRT on the performance of R1: N-supplemented BES. (A) Changes in HRT and COD loading rate over time; (B) Current production and catholyte electrical conductivity over the time; (C) Oxalate, acetate and COD removal percentages at different COD loading rates; (D) CE % based on both COD loading and COD removal at different HRTs. The bioanode potential was -300 mV, pH 9.0 and with both sodium oxalate and sodium acetate as electron donors. In (B), the catholyte was refreshed (25 g NaCl/L) on 5.8 d.

The results also indicated that the columbic efficiencies (CE) were dependent on HRT (Figures 2.4D and 2.5D). In this study, two methods were used to calculate CE for the two BES reactors: (1) based on the total COD loaded; and (2) based on the actual COD removed. Since the disappearance of COD in both reactors was predominately due to acetate removal, both reactors displayed relatively low CEs (<40%) with Method 1; whereas with Method 2 higher CEs (maximum of 71% and 75%, respectively for R1 and R2) were obtained (Figures 2.4D and 2.5D). Similar to other process parameters, CEs in both R1 and R2 were markedly decreased when the HTR was too low (HRT<3 h) (Figure 2.4D and 2.5D). Therefore, selection of HRT is critical for optimising the treatment performance.

### R2 – Nitrogen Deficient

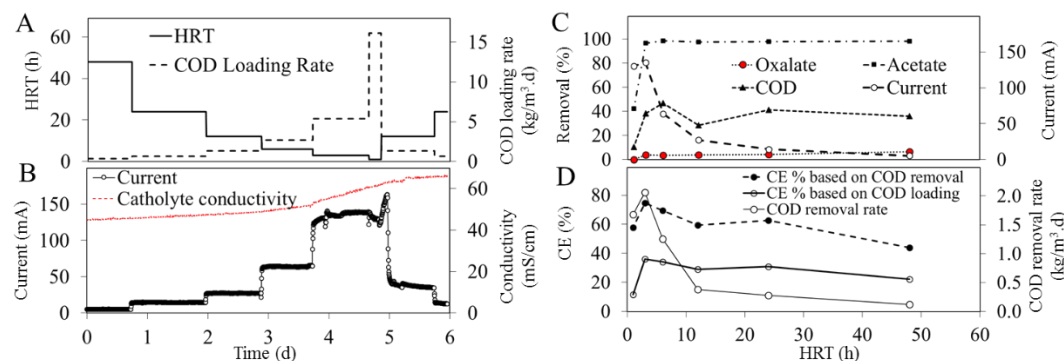


**Figure 2.5.** Effect of HRT on the performance of R2: N-deficient BES. (A) Changes in HRT and COD loading rate over time; (B) Current production and catholyte electrical conductivity over the time; (C) Oxalate, acetate and COD removal percentages at different COD loading rates; (D) CE % based on both COD loading and COD removal at different HRTs. The bioanode potential was -300 mV, pH 9.0 and with both sodium oxalate and sodium acetate as electron donors.

To further compare the COD removing performance between R1 and R2, the relationships between COD removal rate and current density for the two reactors were established (Figure 2.6). The COD removal rates linearly correlated with the current densities of both reactors ( $R^2 > 0.96$ ). However, R1 bioanode appeared to be more active than that of R2 as it enabled a higher maximal COD removal rate (up to 4.61 vs. 2.06  $\text{kg/m}^3\text{d}$ ) and a volumetric current density ( $908 \pm 26$  vs.  $540 \pm 17 \text{ A/m}^3$  anodic void volume) (Figure 2.6). This result suggested that although the establishment of an alkali-halotolerant anodic biofilm necessarily do not require an external N source, the presence of external N may still be advantageous to optimise treatment efficiencies of the described process.

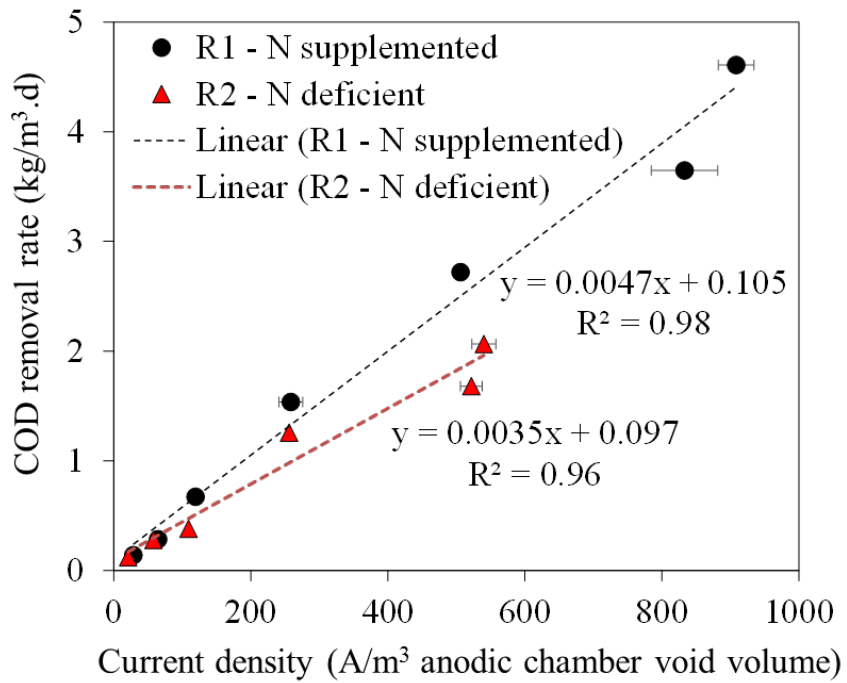


**Figure 2.6.** Linear relationship between current density and COD removal rate for R1: N-supplemented BES; and R2: N-deficient BES. Data were obtained from the experiments as shown in Figures 2.4 and 2.5, respectively.

### 2.3.3.2 Effect of poised anode potential on the electrochemical and treatment performance

Understanding the dependencies of the current production of the established biofilms is useful, as this would enable the selection of the most suitable electrode potential to facilitate anodic substrate conversion (Cheng et al., 2008). To explore such a relationship for the established biofilms, an experiment was carried out by changing the bioanode potentials stepwise in both R1 and R2 (Figure 2.7). The results showed that although the bioanode potential in both R1 and R2 were predominately maintained at +200 mV during the start-up, both biofilms were able to generate maximal anodic current at a much lower anode potential (-300 mV for R1; -200 mV for R2) (Figures 2.7B and 2.7E). This ability of the biofilms is desirable as a lower (more negative) optimal anode potential infers a lower overpotential of the anodic reaction, which in turn enables a lower electrical energy input to operate the BES process (Aelterman et al., 2008; Cheng et al., 2008). The results also indicated that the two biofilms were able to produce similar maximal current densities (~ 480 A/m<sup>3</sup> void volume of the

anodic chamber). As such, it can be concluded that the omission of external N did not hinder the R2 bioanode to convert organic substrates into current. In other words, the biofilm in R2 was able to fulfil its N requirement without relying on an external N source.

In terms of organics removal (oxalate and acetate), both R1 and R2 achieved nearly complete removal of acetate (100% when the current was at maximum) (Figures 2.7C and 2.7F). However, as with the previous results (Figures 2.2, 2.4 and 2.5) very poor oxalate removal was recorded in both reactors, leading to a low overall COD removal of only 40%. Nonetheless, low yet notable levels of oxalate removal were recorded (~4%) in both reactors, indicating that the established biofilms were able to oxidise oxalate to some extent. Whilst inadequate oxalate removal appeared unsatisfactory, it was promising that the anodic biofilm established in R2 did not require an external N source to facilitate bioanodic oxidation of organics for a prolonged period (> 3 months) of time.

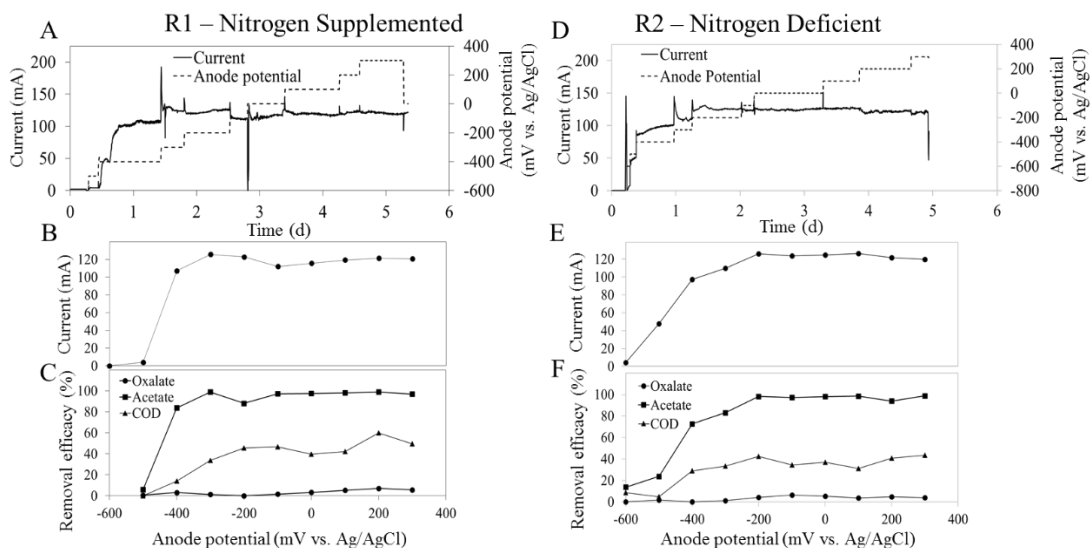


**Figure 2.7.** Effect of anode potential on the performance of R1: N-supplemented (A-C) and R2: N-deficient (D-F) BES reactors. (A, D) Current production and anode potential over the experimental time period. (B, E) Variation of average current produced at different poised anode potentials. (C, F) Oxalate, acetate and COD removal percentages at the experimented range of anode potentials. The anolyte was maintained at pH 9.0 with sodium oxalate and sodium acetate as electron donors on day 111 for R1, and day 170 for R2. HRT was 3 h.

The ability of an anodophilic biofilm to fix dinitrogen ( $N_2$ ) has been recently explored (Wong et al., 2014). In their study, Wong et al. (2014) adopted a similar biofilm enrichment approach as the present study, namely by depriving the supply of external N source from the influent for an extended period and the occasional displacement of anodic headspace with  $N_2$  gas. However, unlike in the present study an energy-rich substrate (glucose) was used as the carbon and energy source and their BES was operated under non-saline and pH neutral (pH 7) conditions. Since N-fixation is a very energy intensive process (630 kJ/mol  $N_2$ ) demanding 16 ATP per mole of  $N_2$  (Atkinson, 1977), the use of glucose was considered favourable for the anode-associated  $N_2$  fixation process (Wong et al., 2014). Interestingly, our result suggested that even with a lower energy-yielding C2 substrate (here acetate, which yields only one-third of the energy of that from glucose), an active alkali-halotolerant anodic biofilm could meet its N requirement plausibly via  $N_2$  fixation. Although further experiments (e.g. acetylene reduction assay) are needed to confirm the  $N_2$  fixing activity of the anodic biofilm, the present finding is intriguing from a bio-treatment perspective as it implies that the cost associated with external nutrient addition may be avoided.

### **2.3.4 Microbial community composition of the alkali-halotolerant biofilms**

The results of the 16S rRNA sequencing showed that the microbial communities of the anodic biofilms enriched in both R1 and R2 were remarkably different (Figure 2.8). Rarefaction curves of the samples sequenced indicated that sequencing depth was adequate to capture bacterial diversity present in the samples (data not shown).

In R1, the most dominant bacterial families were *Oceanospirillaceae* (36.6%) and *Halomonadacea* (17.2%). *Nitrincola* and *Halomonas* were identified as the dominant genera of these families, respectively (data not shown). In literature, members of these two groups have been reported as halophilic (Joshi et al., 2016; McSweeney et al., 2011b). For instance, McSweeney et al. (2011b) found that 22% of a microbial community enriched in a full-scale moving bed reactor that could efficiently degrade oxalate in a real (alkaline (~ pH 9.7) and saline) alumina refinery process water was dominated by genus *Halomonas*. However, in our study the presence of genus *Halomonas* did not facilitate an efficient anodic oxalate oxidation in R1. Plausibly,

this was due to their inability to catalyse the conversion of oxalate into formate (reaction 2.1) under the anodic condition tested. Nevertheless, since the biofilm in R1 was acclimatised with both oxalate and acetate, the predominant presence of the species under *Halomonas* in R1 suggested that these microbes could be actively utilising acetate as their energy source. Indeed, the ability of *Halomonas* species to metabolise acetate with anode as electron acceptor has been previously reported (Erable et al., 2009).

The biofilm acclimatised under N-deficient conditions (R2) had a more diversified bacterial community than the N-supplemented biofilm (Figure 2.8B). The dominant bacterial families were *Rhodocyclaceae* (15.7%), *Haloplasmataceae* (12.5%) and *Idiomarinaceae* (10.1%). Within the family *Rhodocyclaceae*, the most abundant genus was identified as *Zoogloea* (15.7%). Some bacterial species of genus *Zoogloea* have been reported as being able to carry out nitrogen fixation with acetate as the carbon source (Ghulam et al., 2007; Xie & Yokota, 2006). The result was in line with the lack of known N<sub>2</sub>-fixing species in R1, where the microorganisms were not required to fulfil their N requirement via N<sub>2</sub>-fixation (Figure 2.8A). The bacterial families *Haloplasmataceae* and *Idiomarinaceae* have been reported as halophilic microorganisms (Albuquerque & da Costa, 2014; Antunes, 2014). However, no previous study has affirmed their ability to degrade oxalate under alkaline-saline environments.

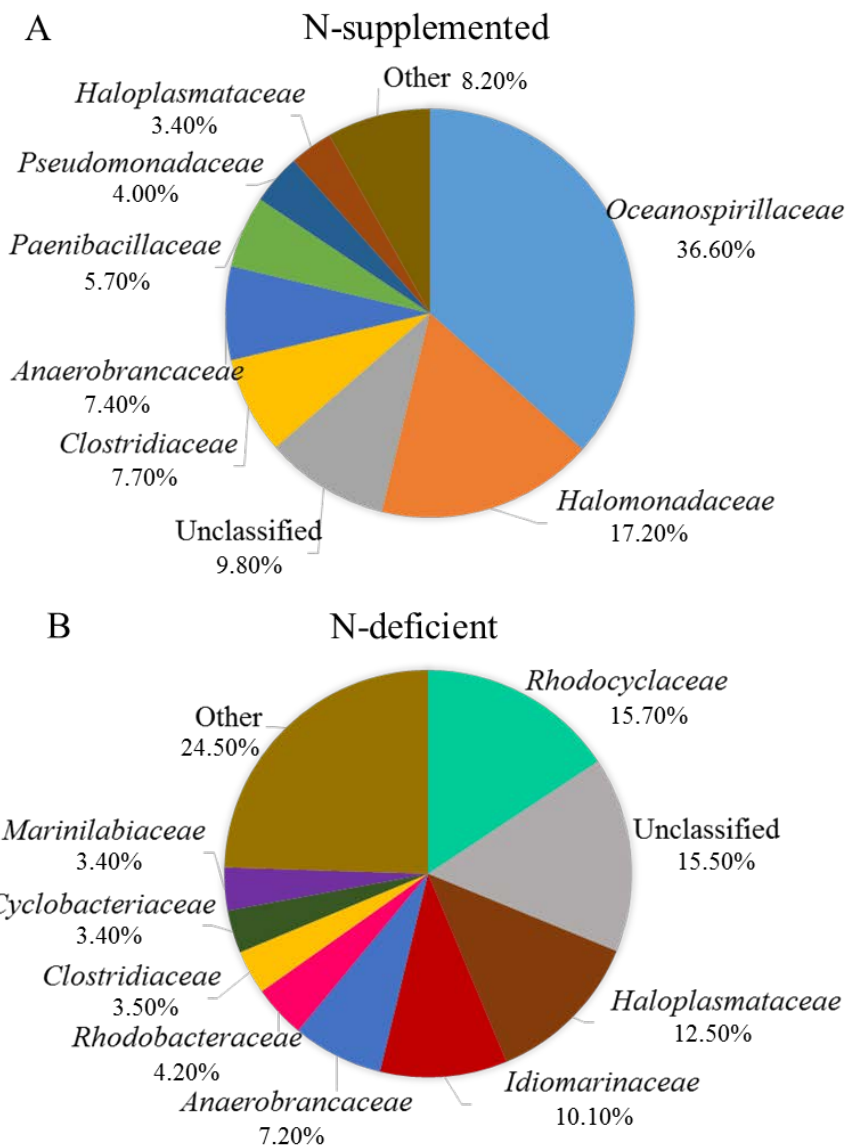


**Figure 2.8.** Relative abundance of microbial taxa classified at the family level based on 454 sequencing of 16S rRNA genes for biofilm samples collected from the bioanodes of (A) R1: N-supplemented; and (B) R2: N-deficient after 200 days of operation. Families that represent less than 3% of the total microbial community composition were classified as “others”.

Given that the two biofilms enriched in this study contained no members under the family of *Oxalobacteraceae* (e.g. *Oxalobacter vibrioformis*, *Oxalobacter formigenes*), which have been considered as the main group of microorganisms capable of decarboxylating oxalate to formate (Svedruzic et al., 2005), the poor oxalate removal in both R1 and R2 may be due to the lack of these important species. Again, this result

supports that activated sludge was not a suitable microbial inoculum for oxalate removal under the tested conditions.

### **2.3.5 Implication of the findings**

To our knowledge, this study is the first to exploit BES technology for the treatment of alkaline-saline process water mimicking those originated from alumina refineries. This study is the first to exploit BES for the treatment of alkaline-saline process water mimicking those in alumina refineries. In the literature, several studies have explored the use of BES for anodic removal of various organic substrates under alkaline and/or saline conditions (Liu et al., 2010; Margaria et al., 2017; Miller & Oremland, 2008; Paul et al., 2014; Zhuang et al., 2010b). Unlike here where activated sludge (which had not been adapted to saline-alkaline condition) was used, most BESs were inoculated with microorganisms already acclimatized to alkaline and/or saline environments (e.g. soda lakes, sea water). The highest current density reported thus far was 140 A/m<sup>3</sup> (65% CE) (Zhuang et al., 2010), where brewery wastewater (pH 10, salinity 0.5%) was treated. Considering in this study a 5-fold higher current density (675 A/m<sup>3</sup> for the N-supplemented reactor) was achieved, activated sludge may still be a suitable inoculum for BES treating alkaline-saline liquor impacted by organics other than oxalate.

Apart from being able to remove organics, the technology also has the potential to recover caustic soda from the alkaline process water. In this work, a linear dependence was observed between the ionic strength in the catholyte and anodic current in both reactors (R1 and R2) (see Figure S2.2 in appendix 1). The increase in both ionic strength and alkalinity in the separate stream (catholyte) also suggested that the process may be favourably used as a caustic recovery unit (data not shown). Further studies are warranted to develop the technology for this attractive application. This is sensible as the reclaimed caustics can be readily returned to the refinery process and as such represents a cost saving to the operation.

Regardless of whether nitrogen was sufficiently present or not (deficient), the desirable removal (anodic oxidation) of oxalate was poor. The fact that both acetate and formate could be readily oxidised, while oxalate was recalcitrant suggests paucity of oxalate

degrading microorganisms in the reactors and the microbial inoculum used (activated sludge). For this, alternative microbial sources from suitable oxalate-laden, alkaline-saline environments (e.g. Soda lake or residue lake within an alumina plant) should be considered as inoculums in future tests. Nonetheless, our finding that external nitrogen supplementation was not needed to sustain a prolonged functioning of an alkali-halotolerant anodophilic biofilm implies that, BES is a promising technology for treating other alkaline waste streams that are deficient in nitrogen. Further development of this promising technology is warranted.

## 2.4 Conclusions

The feasibility of using BES for organics removal under alkaline-saline and nitrogen deficient conditions was examined for the first time. It was concluded that under the tested alkaline-saline conditions, activated sludge was an unsuitable inoculum to facilitate oxalate removal. Establishment of alkali-halotolerant anodic biofilms under both N-supplemented and N-deficient condition was possible only when acetate was used as the main electron donating substrate. The established biofilms could also efficiently convert formate into current under alkaline-saline condition. The inefficient oxalate removal was likely due to the paucity of oxalotrophic strains responsible to catalyse decarboxylation of oxalate into formate.

# **3 BIOELECTROCHEMICAL SYSTEM FOR CAUSTIC SODA RECOVERY FROM ALKALINE-SALINE WASTEWATER UNDER NITROGEN SUPPLEMENTED AND DEFICIENT ENVIRONMENTS**

## **Chapter Summary**

This study focuses on the use of bioelectrochemical systems (BES) for recover caustic solution from nitrogen (N) deficient, alkaline-saline wastewater such as alumina refinery process liquor. The use of ion-selective membranes in the BES may facilitate the recovery of organic free caustic solution from the wastewater, which can be reuse in the refinery process. In the present study, two dual-chamber BES reactors were used (R1: with ammonia; R2: without ammonia) to compare the caustic recovery efficiency. Anodic granules were potentiostatically controlled at -300 mV Ag/AgCl. The anodic compartment was fed continuously with oxalate and acetate containing saline and alkaline solution simulating the salinity and alkalinity of alumina refinery process liquor (0.4 M NaCl, pH 10), and the anolyte was actively maintained at pH 9 by adding NaOH. Cathodes were operated in fed-batch mode with 0.4 M NaCl (2 L) as the catholyte.  $\text{Na}^+$  transfer % to catholyte was higher in N-deficient BES reactor. Both reactors were able to produce coulombic efficiency (CE) of > 75% for caustic generation. The energy input for the caustic production was lower than reported in previous studies conducted by using BES for caustic recovery.

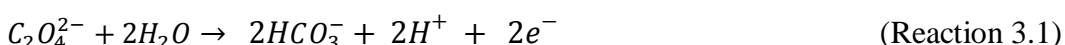
### 3.1 Introduction

Among the organic impurities in bauxite, sodium oxalate is most detrimental to the Bayer process as above critical concentration it co-precipitates with gibbsite at the precipitation process. The formation of needle type oxalate structures in gibbsite particles reduce the product quality and process efficiency (Power et al., 2012).

The spent liquor recirculation is economically important to achieve high process productivity. However, due to several washing and solid separation steps throughout the entire process the spent caustic liquor becomes more diluted. Costly evaporation techniques are often used to re-concentrate the spent caustic liquor to desirable levels of approximately 3 - 3.5 M NaOH for bauxite digestion (Wellington & Valcin, 2007; Whelan et al., 2003). The development of an economical and environmentally sustainable technique for improving quality of recycling caustic solution would improve the sustainability of Bayer processing.

In recent past, bioelectrochemical systems (BES) have been applied to achieve simultaneous organic degradation and caustic recovery from waste streams (Rabaey et al., 2010). BES technology can also have potential for recovering caustic from organic rich spent Bayer process liquors.

In brief, BES use microorganisms as catalysts for the oxidation of organics (electron donor) present in waste streams. Solid anode surface accepts electrons released from organics oxidation and convey them through an external circuit towards the cathode. With the flow of negative charge, to maintain the electroneutrality, protons and other cations in anode cell are migrated to the cathode cell through cation exchange membrane. This electron flow from anode to cathode is driven by potential gradient. Depending on energy input to the system or energy gain from the system, the cathodic activity varies. In microbial electrolysis cells (MEC), external energy is required to trigger the cathodic reaction, such as the reduction of protons to produce hydrogen ( $H_2$ ) gas. In microbial fuel cells (MFC), electron flow from anode generates electrical energy and MFC cathode can reduce oxidized substances such as  $O_2$  to  $H_2O$  or  $NO_3^-$  to  $N_2$  (Cheng, 2009; Logan et al., 2006; Rozendal et al., 2008).



BES anodic reaction is a proton generating process (Reaction 3.1) and cathodic reaction is a proton consuming process (Reaction 3.2), hence pH gradient is created between the two cells during BES operation. Cations such as sodium ( $\text{Na}^+$ ) and potassium ( $\text{K}^+$ ) present in the anolyte, migrate to cathodic cell through the membrane. These migrated cations together with  $\text{OH}^-$  ion in the cathodic cell produce a caustic solution. Rabaey et al. (2010) demonstrated the successful recovery of a caustic solution in the cathodic chamber of a BES treating Brewery wastewater. The strength of the recovered caustic stream can be increased by increasing the anolyte sodium concentration (Pikaar et al., 2013).

However, in cathodic caustic recovery, the other cations present in the anolyte feed solution also migrated to the cathodic chamber alongside the sodium ions. The migration of undesirable cations, such as  $\text{NH}_4^+$ ,  $\text{Ca}^{2+}$ ,  $\text{Mg}^{2+}$  lower the quality of recovered caustic stream and decrease the coulombic efficiency (CE) of the caustic generation (Pikaar et al., 2013). Even though  $\text{NH}_4^+$  ion migration negatively impacts the cathodic caustic recovery,  $\text{NH}_4^+$  is an essential nutrient required for biofilm growth on the BES anode. The use of nitrogen (N)-fixing bacteria could be an alternative to avoid the need for external  $\text{NH}_4^+$  supplementation in anolyte for microbial growth. Wong et al. (2014) successfully demonstrated the use of N-fixing bacteria in BES anode to treat the N-deficient wastewater.

In this study, two dual chamber BES reactors were used to examine the caustic production from synthetic alkaline (pH 10) and saline ( $\text{NaCl}$  25 g/L) organics (acetate and oxalate) rich wastewater that represented Bayer liquor in its salinity and alkalinity. One reactor (R1) was supplemented with N source ( $\text{NH}_4\text{Cl}$ ) and the other reactor (R2) was deficient of N source. Further, this study explored and compared the strength of recovered caustic solution and the energy requirement for the caustic recovery using N-supplemented and N-deficient BES reactors.

## 3.2 Materials and Methods

### 3.2.1 Bioelectrochemical systems set-up and general operation

In this study, two dual-chamber BES reactors were used for the experiments as described in chapter 2. Reactor 1 (R1) was fed with an ammonium-N supplemented synthetic liquor, whereas Reactor 2 (R2) was operated with an ammonium-N-deficient synthetic liquor. Each reactor was divided into two identical half cells (14 cm × 12 cm × 2 cm) by a cation exchange membrane (surface area 168 cm<sup>2</sup>) (Ultrex CMI-7000, Membrane International Inc.). Both half cells were loaded with identical conductive graphite granules 285 g each (3-5 mm diameter, KAIYU Industrial (HK) Ltd.), which reduced the void volume of each half cell from 336 to 250 mL. The specific surface area of the graphite granules was  $1.308 \pm 0.003 \text{ m}^2/\text{g}$  as determined by using BET (Brunauer-Emmett-Teller) method (CSIRO Mineral Resources, Waterford, Western Australia). Four graphite rods which were embedded in each cell, (5 mm diameter and length 12 cm) were used as current collectors to enable electric connection between the graphite granules and the external circuit. The reactors were operated as a three-electrode system coupled to a potentiostat (VMP3, BioLogic) (Cheng et al., 2010). Only one half cell (anodic half cell) was inoculated with bacteria and the electrode therein is termed as the working electrode (here anode). The electrode in the counter half cell is termed as the counter electrode (which functioned mostly as a cathode). The working electrode was polarized against a silver-silver chloride (Ag/AgCl) reference electrode (MF-2079 Bioanalytical Systems, USA) at a defined potential using the potentiostat. The reference electrode was embedded within the granular graphite in the working electrode cell. Total liquid volumes of 0.5 and 2.0 L were continuously recirculated through the anodic and the cathodic chambers via two separate external recirculation bottles (0.25 and 2.0 L), respectively, at a recirculation rate of approximately 14 L/h (Figure 3.1). The nitrogen was intermittently sparged (every 20 min for 30 s) into the anode recirculation bottle to create an anaerobic environment in the anodic chamber and to facilitate biological nitrogen fixation in reactor R2. The process was operated at  $22 \pm 2^\circ\text{C}$ .

The anodic chambers were operated in either batch or continuous modes, as specified below. During the continuous mode operation, fresh anolyte (maintained at 4 °C in a

refrigerator) was continuously introduced at a specified flow rate into the external recirculation bottle and an equal volume of the old anolyte was extracted (and discarded) from the recirculation line using a peristaltic pump (Masterflex® Cole-Parmer L/S pump drive fitted with a Model 77202-60 Masterflex® pump head; Norprene® tubing 06404-14). Throughout the entire experimental period, the cathodic chambers of the reactors were operated in batch mode. The catholyte was occasionally renewed as specified below. LabVIEW computer program was used for continuous monitoring and controlling of the BES processes. The working electrode potential and current of the BES were monitored via the potentiostat. All electrode potentials (mV) reported in this paper refer to values against Ag/AgCl reference electrode (ca. +197 mV vs. standard hydrogen electrode (Bard & Faulkner, 2001)). The pH values of the anolyte was continuously monitored using in-line pH sensor (TPS Ltd. Co., Australia). All signals were regularly recorded to an Excel spreadsheet via the computer programme interfaced with a National InstrumentTM data acquisition card.

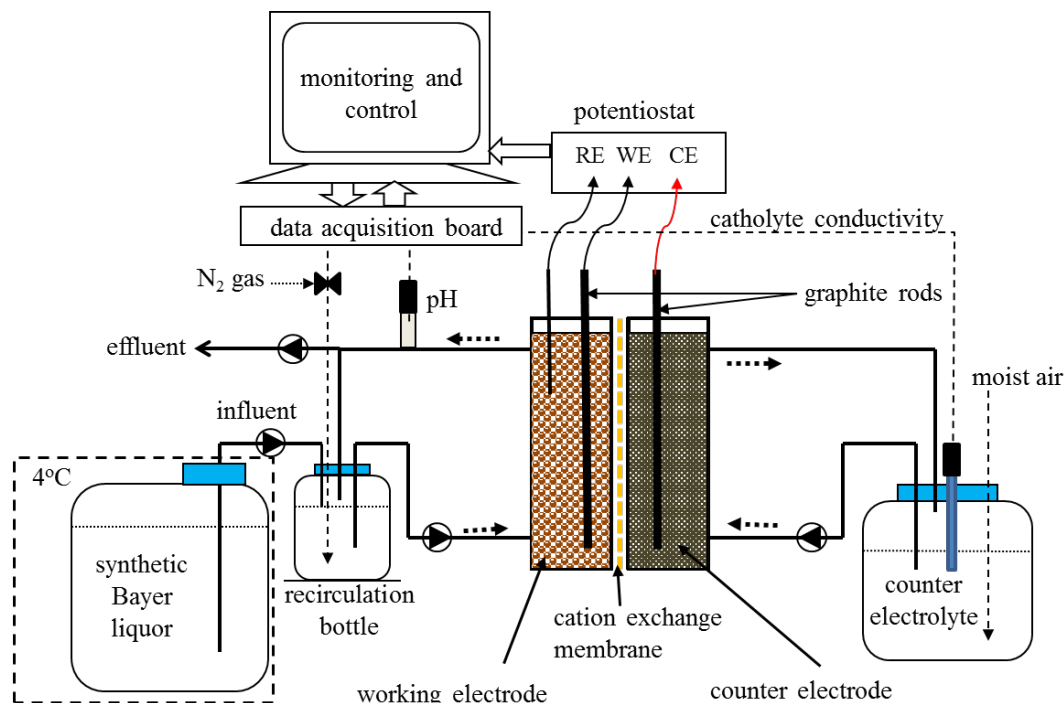


**Figure 3.1.** A schematic diagram of the BES bioreactor system consisting of anodic cell and cathodic cell filled with graphite granules, a recirculation line and a computer for process monitoring and control. RE – Reference electrode, WE – Working electrode (Anode) and CE – Counter electrode (Cathode).

### **3.2.2 Synthetic liquor and reactor electrolyte**

A synthetic medium that simulated Bayer process stream in its alkalinity and salinity was used as the influent of the BES reactors. Unless stated otherwise, sodium oxalate 3.35 g/L (25 mM) and sodium acetate (5 mM) were used as the carbon sources, and NaCl 25 g/L was added to increase the solution salinity. The pH value of the feed solution was maintained at above 10 by adding 2 M NaOH solution according to the experimental requirements. The nutrients medium used for R1 consisted of (mg/L): NH<sub>4</sub>Cl, 130; NaHCO<sub>3</sub>, 125; MgSO<sub>4</sub>·7H<sub>2</sub>O, 51; CaCl<sub>2</sub>·2H<sub>2</sub>O, 15; and K<sub>2</sub>HPO<sub>4</sub>·3H<sub>2</sub>O, 20.52, and 1.25 mL/L of trace element solution containing (g/L): ZnSO<sub>4</sub>·7H<sub>2</sub>O, 0.43; FeSO<sub>4</sub>·7H<sub>2</sub>O, 5; CoCl<sub>2</sub>·6H<sub>2</sub>O, 0.24; MnCl<sub>2</sub>·4H<sub>2</sub>O, 0.99; CuSO<sub>4</sub>·5H<sub>2</sub>O, 0.25; NaMoO<sub>4</sub>·2H<sub>2</sub>O, 0.22; NiCl<sub>2</sub>·6H<sub>2</sub>O, 0.19; NaSeO<sub>4</sub>·10H<sub>2</sub>O, 0.21; ethylenediaminetetraacetic acid (EDTA) 15, H<sub>3</sub>BO<sub>3</sub>, 0.014; and NaWO<sub>4</sub>·2H<sub>2</sub>O, 0.05. (Cheng et al., 2010). The same nutrient medium without NH<sub>4</sub>Cl was used as the influent of the anodic chamber for R2. Unless stated otherwise, this medium was used as the electrolyte in the anodic chamber throughout the entire study. The catholyte of both reactors (R1 and R2) also contained a similar NaCl concentration of 25 g/L as the anolyte. This was chosen with the anticipation that after the organic content is removed, the anodic effluent would form the influent stream of the cathodic chamber.

### **3.2.3. Experimental Procedures**

#### **3.2.3.1. Reactor start-up and acclimatisation of electrochemically active anodic biofilm**

The anodic chambers of both reactors (R1 and R2) were inoculated by adding a returned activated sludge (RAS) collected from a municipal wastewater treatment plant (ca. 2 g MLSS/L) in Perth, Western Australia to establish electrochemically active biofilms. The RAS was filtered through a metal screen to remove large particles (> ca. 1 mm). The inoculation was done by injecting a predefined volume (30 mL) of the filtered sludge into the anodic recirculation line using a 60 mL plastic syringe. As a bacterial growth supplement, yeast extract was added to the anolyte (50 mg/L final concentration) during the initial start-up period. Both the anolyte and catholyte were renewed regularly (and prior to each specific experiments as described below) to avoid

accumulation of unwanted chemical species. After inoculation with the activated sludge, the circuit was closed and the working electrode (anode) was maintained at a constant potential of +200 mV. The synthetic liquor was continuously fed into the anodic chamber to obtain a hydraulic retention time (HRT) (Anolyte volume (500 mL) was void volume of anode chamber + volume of recirculation bottle) of one day. The feed pH was maintained according to the experimental requirements. The in-reactor pH was maintained at 9 by external dosing of NaOH (0.5 M) or alkaline feed flow rate according to the experimental requirements to overcome anodic acidification. Anodic current production and carbon source removal rate in the anolyte were used as the parameters to indicate the establishment of biofilm activity over the start-up period.

### **3.2.3.2 Evaluating alkalinity increase and caustic production capacity from alkaline and saline solution**

A set of experiments was carried out to examine the alkalinity increase of the catholyte and caustic recovery from the BES. The two reactors were operated at 3 hr HRT to achieve a continuous stable current of approximately 130 mA for 10 days. The influent stream pH was maintained at 10 and the anolyte pH was controlled at 9.0 by adding 0.5 M NaOH as an external alkalinity source to neutralise the acidity building up in the anodic chamber. Cathodic chamber was operated in batch mode with a total liquid volume of 2 L and recirculation at a rate of 0.225 L/min. First, both reactors were operated in open circuit mode and subsequently changed to closed circuit mode with poised anode potentials of -300 mV. The catholyte electrical conductivity increase was continuously monitored by a conductivity probe. Liquid samples were collected from catholyte for alkalinity and cation analysis.

Another experiment was carried out with N-supplemented R1 reactor for 7 days with increased influent pH. In this experiment, instead of external dosing of NaOH to control the in-reactor pH at 9, a more alkaline influent stream (pH 12.3) was continuously supplied to control the acidity building up in the anolyte. This experiment was carried out at 6 h HRT with stable current of 60 mA and in-reactor pH of ~ 9. Poised anode potential was -300 mV vs Ag/AgCl. The cathodic chamber was operated in batch mode with fresh 25 g/L NaCl solution (volume 2 L), which was recirculated at the rate of 0.225 L/min.

### **3.2.4. Chemical Analysis**

Performance of the BES reactors was monitored by measuring the changes of chemical oxygen demand, oxalate, acetate and cation concentrations over time. Anolyte pH (pH sensor - TPS Ltd. Co., Australia) and catholyte conductivity (Conductivity sensor - TPS Ltd. Co., Australia) were also monitored continuously throughout the experiment. The pH change of catholyte was checked daily. Alkalinity was determined by potentiometric titration with 0.1 M HCl to pH 8.3 and pH 4.5 according to the standard methods (American Public Health Association. et al., 1995).

Liquid samples collected from the BES were immediately filtered through a 0.22 µm filter (0.8/0.2 µm Supor® Membrane, PALL® Life Sciences) upon collection and were stored at 4 °C prior to analysis. Acetate and oxalate were analyzed using a Dionex ICS-3000 reagent free ion chromatography (RFIC) system equipped with an IonPac® AS18 4 x 250 mm column. Potassium hydroxide was used as an eluent at a flow rate of 1 mL/min. The eluent concentration was 12-45 mM from 0-5 min, 45 mM from 5-8 min, 45-60 mM from 8-10 min and 60-12 mM from 10-13 min. Ammonium ( $\text{NH}_4^+$ -N), sodium ( $\text{Na}^+$ ) and other cations was measured with the same RFIC with a IonPac® CG16, CS16, 5 mm column. The eluent was 30 mM methansulfonic acid with a flow rate of 1 mL/min for 29 min. The two columns were maintained at a temperature of 30°C during the run. Suppressed conductivity was used as the detection signal (ASRS ULTRA II 4 mm, 150 mA, AutoSuppressioin® recycle mode). COD was measured using a closed reflux dichromate COD method (HACH Method 8000, HACH Ltd).

### **3.2.5 Calculations**

The electrical energy input to the BES process was calculated as given in equation 3.1.

$$\begin{aligned} \text{Energy input (Wh)} = \\ \text{Applied voltage (V)} \times \text{Current (A)} \times \text{time (h)} \end{aligned} \quad (\text{Equation 3.1})$$

The calculation of coulombic efficiency (CE) for caustic production was given in equation 3.2.

$$\text{CE of caustic production (\%)} = \frac{\text{Recovered caustic in the catholyte (mol)}}{\text{Transferred electron as current (mol)}} \quad (\text{Equation 3.2})$$

In this calculation, the recovered caustic (NaOH) strength was assessed by using pH measurements of the catholyte.

### **3.3 Results and Discussion**

#### **3.3.1 Alkalinity increase of catholyte and caustic recovery**

##### **3.3.1.1 Catholyte alkalinity increased over time at steady current production – Comparison of two reactors**

This experiment was designed to examine the catholyte caustic generation under alkaline and saline conditions. In this experiment, the anolyte pH was controlled at pH 9 by adding NaOH to compensate for the anodic H<sup>+</sup> production. As spent Bayer liquor contains NaOH > 1 M, the addition of NaOH can be justified. Alkalinity increase and Na<sup>+</sup> migration to the catholyte were recorded at stable current production during the experimental period.

During the experiment, two reactors were operated at 3 h HRT to produce higher stable current (~ 130 mA±8.7) to drive the efficient cathodic caustic production (Figures 3.2 and 3.3). An immediate increase in current production after close the circuit indicated the efficiency of microbial oxidation of organic carbon by electrochemically active biofilms (Figures 3.2A and 3.3A). For reactors R1 and R2, working electrode (anode) potentials were controlled at -300 mV. In R1, counter electrode (cathode) potential decreased from -1200 mV to -1400 mV and in R2 reactor, the counter electrode (cathode) potential decreased from -1300 mV to -1500 mV (Figure 3.2A and 3.3A). Cause for the decrease in cathode potential during the experimental period could be an increase in internal resistance.

As expected, in R1, catholyte Na<sup>+</sup> and NH<sub>4</sub><sup>+</sup> ion concentration increased over time with the migration of cations from anolyte to balance the negative charge transfer (Figure 3.2B). The initial concentrations of other cations (K<sup>+</sup>, Ca<sup>2+</sup> and Mg<sup>2+</sup>) in the influent solution were very low, therefore, the concentration build up in the catholyte over experimental period was negligible. As a result of cation migration, there was a continuous increase in both Na<sup>+</sup> and NH<sub>4</sub><sup>+</sup> ion concentrations in the catholyte resulting from the migration through the cation exchange membrane (Rozendal et al., 2006).

The cation migration was further confirmed by increase in catholyte electrical conductivity during the experiment (Figure 3.2E). As, there was negligible difference in anion concentrations in the catholyte and no pH control in catholyte, this catholyte conductivity increase was mainly caused by  $\text{Na}^+$  and  $\text{NH}_4^+$  ion migration. As R2 reactor was operated without any  $\text{NH}_4^+$  supplementation, the catholyte did not contain any  $\text{NH}_4^+$  (Figure 3.3B). However, similar to R1, the  $\text{Na}^+$  migration from anode chamber to cathode chamber, increased the catholyte  $\text{Na}^+$  concentration (Figure 3.3B). Hence, the R2 reactor was able to produce more pure caustic solution compared to R1 reactor.

Even though the oxalate removal was very low (1 - 10%), acetate removal was approximately 95% (Figure 3.2C and 3.3C). While the reactors was operating in open circuit mode, the acetate removal percentage was very low. After switching to closed circuit mode, the current production immediately increased as a result of acetate oxidation by electrochemically active biofilm.

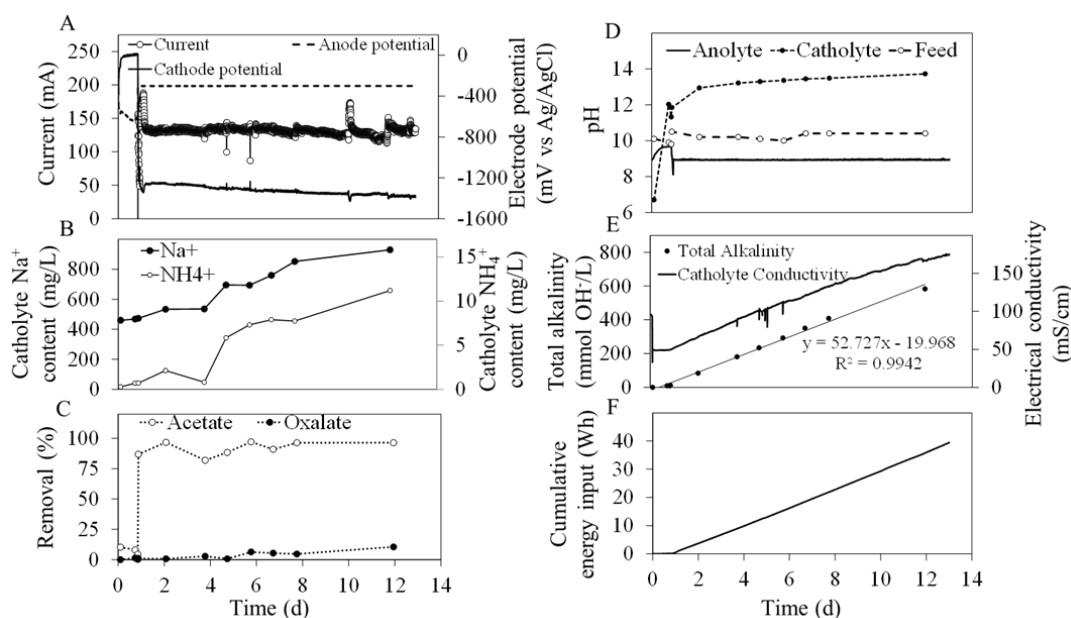


**Figure 3.2.** Reactor R1 catholyte caustic generation at anode potential -300 mV, anolyte pH 9.0 and COD loading rate 5.1 kg COD/m<sup>3</sup>.d (HRT 3 hr) with sodium oxalate and sodium acetate as electron donors on day 141. (A) Steady current production and anode and cathode electrode potentials. (B) Increase of catholyte  $\text{Na}^+$  and  $\text{NH}_4^+$  ion concentration. (C) Oxalate and acetate removal percentages (D) Anolyte and catholyte pH. (E) Increase of catholyte total alkalinity and catholyte electrical conductivity. (F) Cumulative energy input into the system during the experiment.

At the beginning of experiment, catholyte (NaCl solution 25 g/L) pH was ~ 6.8 and with the current production the catholyte pH increased gradually during the experimental period (Figure 3.2D and 3.3D) because of the proton consumption in the cathode chamber (Rozendal et al., 2008). In R1 reactor, the final pH of the catholyte was 13.7 after 12 days and in R2 reactor catholyte pH increased to 13.5 with 8 days of experiment (Figure 3.2D and 3.3D). A linear increase in alkalinity was detected over time with  $R^2 > 0.98$  in two reactors (Figure 3.2E and 3.3E). Reactor R1, catholyte total alkalinity reached a maximum value of 580 mmol OH<sup>-</sup>/L at the end of the 12 days of operation. Na<sup>+</sup> concentrations were very high in catholytes comparison to other cations. Hence the recovered alkaline catholyte was considered as caustic soda (NaOH) solution (Rabaey et al., 2010). Energy input for R1 to produce 0.58 M caustic solution within 12 days was 35.7 Wh (Figure 2F). After 8 d of operation the reactor R2 was able to produce total alkalinity of 400 mM OH<sup>-</sup>/L in catholyte and energy requirement to produce 0.4 M caustic solution in R2 within 8 days was 26.5 Wh (Figure 3.3F). These results confirmed the capacity of the BES technology of generating caustic solution in catholyte by using alkaline and saline feed stream from BES technology.

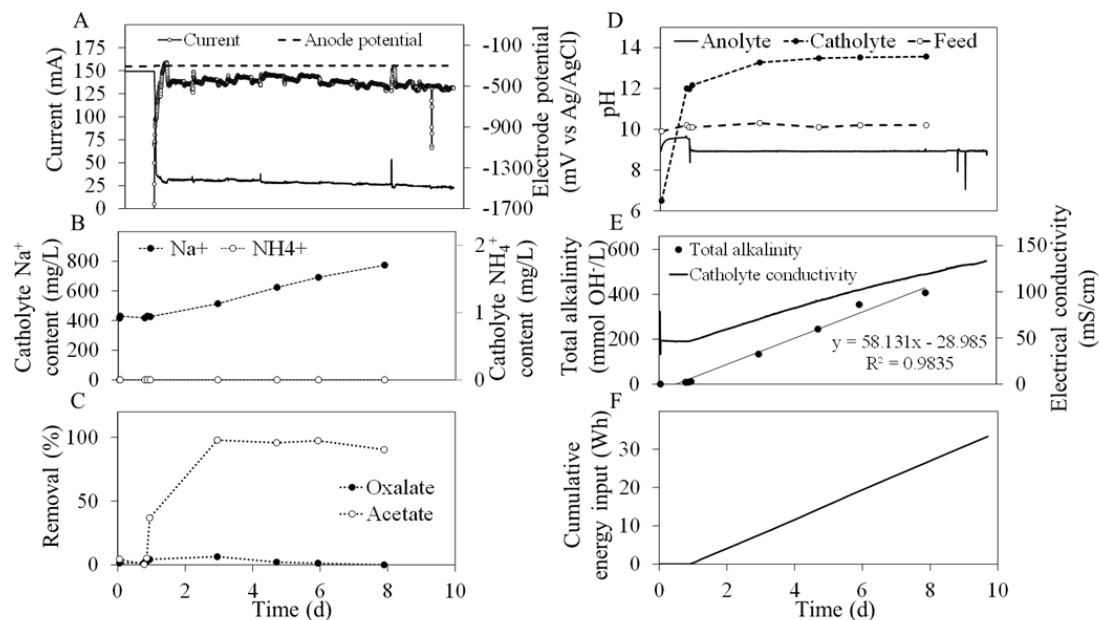


**Figure 3.3.** Reactor R2 catholyte caustic generation at anode potential -300 mV, anolyte pH 9.0 and COD loading rate 5.1 kgCOD/m<sup>3</sup>.d (HRT 3hrs) with sodium oxalate and sodium acetate as electron donors on day 187. (A) Current production and anode and cathode electrode potentials over the experimental time period. (B)

Increase of catholyte  $\text{Na}^+$  and  $\text{NH}_4^+$  ion concentration during the experimental time. (C) Oxalate and acetate removal percentages during the experiment. (D) Anolyte and catholyte pH varying with the time. (E) Increase of catholyte total alkalinity and catholyte electrical conductivity over the experimental time. (F) Cummulative energy input into the system during the experiment.

### **3.3.1.2 Higher $\text{Na}^+$ transfer to catholyte in N-deficient reactor than N-supplemented reactor**

In caustic recovery, the effect of other cation migration could not be neglected (Pikaar et al., 2013). The  $\text{NH}_4^+$ ,  $\text{Mg}^{2+}$  and  $\text{Ca}^{2+}$  ions negatively impact on caustic strength and quality. Hence, catholyte was analysed for cations content over the experimental time period. The Figure 3.4 shows the contribution of each cation for the total charge transfer in the system

To support the hypothesis of caustic recovery as  $\text{NaOH}$ , the transferred cation concentrations as a percentage were analysed in the catholyte during the experimental time period (Figure 3.4). According to the results, the catholyte mostly contained  $\text{Na}^+$ , as compared to  $\text{Na}^+$  concentration of more than 700 mM, the other cation concentrations were negligible. In both reactors, soluble  $\text{Mg}^{2+}$  and  $\text{Ca}^{2+}$  concentrations in the catholyte were below detection limit ( $< 0.1$  mM). However, in reactor R1,  $\text{NH}_4^+$  was responsible for 1.7% from total charge transferred. As a result, in reactor R2  $\text{Na}^+$  account for a larger percentage of overall charge transfer (95.8%) compared to R1 reactor. Consequently, reactor R2 produced more pure caustic solution compared to reactor R1.

The high  $\text{Na}^+$  content in the feed and cation migration from anolyte to catholyte supported the assumption that hydroxide alkalinity increase can be expressed as  $\text{NaOH}$ . Hence, the caustic recovery as  $\text{NaOH}$  was possible in both N-supplemented and N-deficient BES reactors under alkaline and saline conditions.

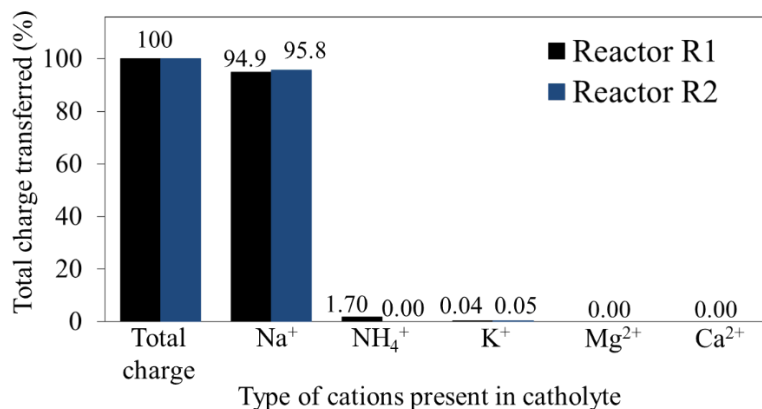


**Figure 3.4.** Distribution of cations migrated from anode to cathode to balance the electron flow.

### 3.3.1.3 Caustic recovery from high pH (> 12) feed solution in N-supplemented (R1) reactor

One of the main challenges in practical applications of BES is membrane pH gradient due to poor transport of  $\text{H}^+$  ion from anode to cathode through the membrane. In the presence of other cations,  $\text{H}^+$  transport is low and as a result pH drops in anode chamber. This pH drop limits the current production by microbial oxidation of organic matter (Dhar & Lee, 2013; Kim et al., 2007; Rozendal et al., 2008; Torres et al., 2008). Hence, it is very important to overcome this issue, when considering practical application of Bayer liquor organic destruction.

As mentioned earlier, Bayer spent liquor is highly alkaline (> 13) and has a high NaOH concentration. The Bayer liquor alkalinity can be used to neutralise the  $\text{H}^+$  generated at the anode without external addition of NaOH. During a stable current production, the anolyte pH can be controlled at desirable level by continuous feeding of the alkaline solution. This alleviates the need to use a buffer or adding a base to maintain in-reactor anolyte pH at a constant level.

To confirm above mentioned strategy, R1 was operated at 6 h HRT with 2.55 kg COD/m<sup>3</sup>.day with increased influent pH (pH 12.3) at controlled anode potential of -300 mV. Catholyte alkalinity increase and caustic generation were quantified (Figure 3.5). As shown in Figure 3.5A, the current production was stable at 60 mA for this 7 d experimental run.

The results in Figure 3.5 confirmed that, reactor R1 performance was similar to the previous experiment results in Figure 3.2. Importantly, Figure 3.5D shows, in-reactor anolyte pH was controlled at ~ 9.5 level under tested conditions without adding any buffer or base solution and the feed pH value was ~ 12.25. During the 7 days of operation the alkalinity increase was 0.2 mmol OH<sup>-</sup>/L at energy consumption of 9 Wh.

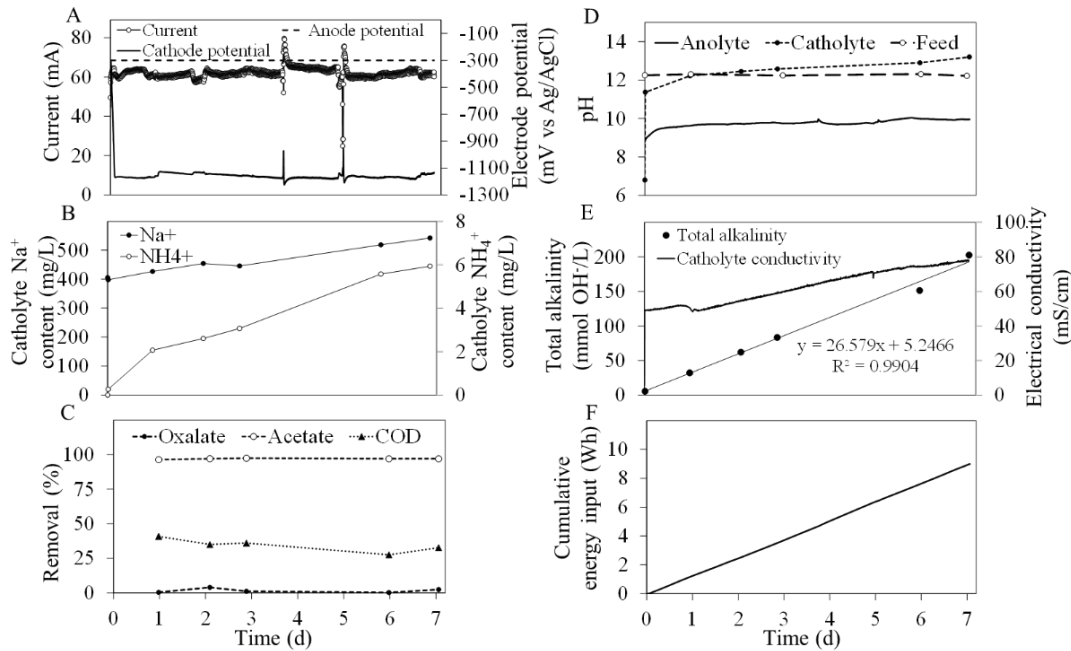


**Figure 3.5.** Reactor R1 catholyte caustic generation at anode potential -300 mV, anolyte pH 9.0 and COD loading rate 2.55 kgCOD/m<sup>3</sup>.d (HRT 6hrs) with sodium oxalate and sodium acetate as electron donors. (A) Steady current production and anode and cathode electrode potentials over the experimental time period. (B) Increase of catholyte Na<sup>+</sup> and NH4<sup>+</sup> ion concentration during the experimental time. (C) Oxalate, acetate and COD removal percentages during the experiment. (D) Anolyte, catholyte and feed solution pH varying with the time. (E) Increase of catholyte total alkalinity and catholyte electrical conductivity over the experimental time. (F) Cummulative energy input into the system during the experiment.

### **3.3.2 Implications of the study**

The results of this study were compared with two other previous studies on caustic recovery from waste streams (Table 3.1). The caustic strength was calculated using pH measurements of the catholyte similar to Rabaey et al. (2010). The caustic strength (as a weight %) of the recovered stream is dependent of different variables such as anolyte caustic concentration, anode and cathode compartment flow rates and current generation. However, Rabaey et al. (2010) was able to recover a caustic solution 3.4% of strength at current generation of  $0.71 \pm 0.10$  A by using a lamellar BES in total volume of 3.313 L (Rabaey et al., 2010). The CEs of caustic production (Equation 3.2) of this study are similar to Rabaey et al. (2010) study. From the experiments in this study, the experiment done in R1 with high pH (12.3) feed solution, was able to achieve the highest CE of caustic production of 81% with lowest energy input. Further, compared to other studies the energy input in this study was rather low. However, a direct comparison between different studies is inappropriate due to different characteristics of the reactor configurations and different operational conditions.

**Table 3.1.** Comparison of studies on cathodic caustic generation in electrochemical systems

<b>Reactor type</b>	<b>Feed type</b>	<b>Caustic strength (wt%)</b>	<b>CE of caustic production (%)</b>	<b>Energy Input (kWh/kg caustic)</b>	<b>Reference</b>
<b>Lamellar BES</b>	Sodium acetate solution	3.4	76	1.06	(Rabaey et al., 2010)
<b>Two chamber electrochemical cell</b>	Sewage	0.61	51	5.25	(Pikaar et al., 2011)
<b>Two chamber BES</b>	Sodium acetate + Sodium oxalate	2.1	75	0.85	This study R1 reactor (with NaOH dosing)
<b>Two chamber BES</b>	Sodium acetate + Sodium oxalate	1.45	77	0.91	This study R2 reactor (with NaOH dosing)
<b>Two chamber BES</b>	Sodium acetate + Sodium oxalate	0.63	81	0.64	This study R1 reactor (With high pH feed solution)

### **3.4 Conclusion**

This study for the first time examined cathodic caustic recovery under N-deficient conditions in a BES operated with alkaline and saline wastewater. As expected, the N-deficient reactor (R2) was able to produce a cleaner caustic stream, which was free from  $\text{NH}_4^+$ .  $\text{Na}^+$  represented over 94% of the charge transfer in the both reactors. The coulombic efficiency of the caustic production was > 75% for the both reactors. The results confirmed efficient cathodic caustic production from alkaline and saline wastewater in BES reactors.

# **4 OXALATE DEGRADATION BY ALKALIPHILIC BIOFILMS ACCLIMATISED TO NITROGEN- SUPPLEMENTED AND NITROGEN- DEFICIENT CONDITIONS**

Extended from

Weerasinghe Mohottige, T.N., Cheng, K.Y., Kaksonen, A.H., Sarukkalige, R. and Ginige, M.P. (2017) Oxalate degradation by alkaliphilic biofilms acclimatised to nitrogen-supplemented and nitrogen-deficient conditions. Journal of Chemical Technology and Biotechnology. DOI: 10.1002/jctb.5424.

## **Chapter Summary**

Aerobic microbial degradation of oxalate has been considered an eco-friendly treatment option for organics removal in Bayer waste streams. Given that Bayer process liquor is typically deficient in nitrogen (N), this study, for the first time examines oxalate degradation under N deficient conditions in a comparative study using two parallel biofilm-reactors. The two packed-bed bioreactors were operated with an alkaline, saline synthetic Bayer process liquor for >250 days, one N-supplemented and the other under N-deficient conditions. Oxalate degradation rates and oxygen uptake rates (OUR) were determined at different bulk water dissolve oxygen concentration (DO) set-points. The results revealed that oxalate removal rates (33 – 111 mg/h.g biomass) linearly correlate with OUR (0 – 70 mg O<sub>2</sub>/h.g biomass) in the N-supplemented reactor. However, in the N-deficient reactor, a linear increase of oxalate removal was recorded only with DO upto  $\leq$  3 mg/L. Surprisingly, anaerobic oxalate removal was evident even in the presence of DO (up to 8 mg/L) in both reactors. Further elucidation revealed formate, acetate and methane by-products during anaerobic oxalate removal in both reactors. This study revealed for the first time the oxalate fermentation pathway under alkaline and N-deficient conditions.

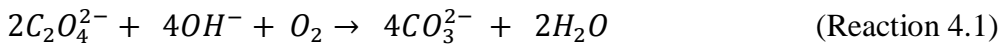
## 4.1 Introduction

Bauxite ore is typically refined in a process known as the Bayer process to produce alumina (aluminium oxide). In brief, the Bayer process involves the digestion of crushed bauxite in a hot concentrated solution of sodium hydroxide (NaOH). During digestion most aluminium containing minerals such as gibbsite ( $\text{Al(OH)}_3$ ), boehmite ( $\gamma\text{-AlO(OH)}$ ) and diasporite ( $\alpha\text{-AlO(OH)}$ ), are solubilised to form sodium aluminate ( $\text{NaAlO}_2$ ) (Whelan et al., 2003; Yamada et al., 1980). Any insoluble impurities are subsequently separated via settling and filtration of process liquor. To recover the solubilised Aluminium (Al), the process liquor is cooled and an  $\text{Al(OH)}_3$  crystallisation seed is introduced to trigger crystallisation of Al. Finally, the spent NaOH is recycled back to the beginning of the process (Meyers, 2004).

Recycling of spent NaOH-rich liquor is important for the Bayer process to be economical. Continuous recycling of NaOH-rich liquor, however, results in the build-up of metals (e.g. gallium (Ga) and vanadium (V)) and organics (naturally abundant in bauxite) in the process liquor. The total organic carbon (TOC) content of bauxite is typically ranging from 0.02 to 0.2 % (w/w) in the other regions of the world (Power & Loh, 2010). However, in Australia, the bauxite ores can have a much higher TOC content in the range of 0.15 to 0.5 % (w/w) (Hind et al., 1999; Power & Loh, 2010; Whelan et al., 2003). The organic compounds in bauxite (e.g. polybasic acids, polyhydroxy acids, alcohols and phenols, humic and fulvic acids, and other carbohydrates) form organic sodium salts during the Bayer process, and of these organic salts, sodium oxalate ( $\text{Na}_2\text{C}_2\text{O}_4$ ) has been identified as the most detrimental to the process (Hind et al., 1997; Power & Loh, 2010). The recycling of spent Bayer liquor results in a build-up of  $\text{Na}_2\text{C}_2\text{O}_4$  in the process liquor. Once supersaturation concentrations are reached,  $\text{Na}_2\text{C}_2\text{O}_4$  tends to crystallise together with  $\text{Al(OH)}_3$ , impacting the quality, quantity and production cost of  $\text{Al(OH)}_3$  (Gnyra & Lever, 1979; Power et al., 2012; Soucy et al., 2013; Yingwei et al., 2011). Therefore, effective removal of  $\text{Na}_2\text{C}_2\text{O}_4$  from the Bayer process liquor is important for alumina refineries.

Different strategies have been adopted to facilitate  $\text{Na}_2\text{C}_2\text{O}_4$  removal from Bayer process liquors (Soucy et al., 2013). The most common strategies involve crystallisation of  $\text{Na}_2\text{C}_2\text{O}_4$  and liquor burning in a side stream process (Brown, 1991; McKinnon & Baker, 2012; Rosenberg et al., 2004). However, these conventional

approaches suffer from a range of problems such as high energy consumption and emission of air pollutants. Recently, the alumina industry has embraced biological processes as a more environmentally benign alternative to oxidise Na<sub>2</sub>C<sub>2</sub>O<sub>4</sub> (McSweeney et al., 2011a; McSweeney et al., 2011b). This process involves the use of microorganisms to drive aerobic oxidation of Na<sub>2</sub>C<sub>2</sub>O<sub>4</sub> into carbonate (Reaction 4.1).



Biological oxidation of Na<sub>2</sub>C<sub>2</sub>O<sub>4</sub> was first reported by Alcan International Limited in 1989 (Brassinga et al., 1989). The company patented an aerobic bioreactor process, which consisted of a three compartment rotating biological contractor (with 73 rotating disks and a total biofilm surface area of 3.7 m<sup>2</sup>) inoculated with Pseudomonas-like isolates from rhizospheres of oxalate producing plants. Due to the intolerance of the isolates to high pH, the pH of the bioreactor influent had to be adjusted to 7.5 (Brassinga et al., 1989; Tilbury, 2003). The bioreactor successfully decreased an initial oxalate concentration of 2,600 mg/L to 50 mg/L within a short residence time of 5 hours. Following this study, other reactor systems and microbial strains have been explored under various conditions for biological oxalate removal (McKinnon & Baker, 2012; Morton et al., 1991; Tilbury, 2003). Today, some alumina refineries have successfully adopted full-scale biological treatment plants to degrade oxalate and other organic impurities from Bayer process liquor.

Although rich in biodegradable carbons, the process liquor of the alumina industry is deficient of nitrogen (N). Nitrogen is a major essential element required for the growth of all living organisms including bacteria. At present nitrogen requirements of biological treatment plants in alumina refineries are met with an external dose of N, and a commonly used nitrogen source is urea (McSweeney et al., 2011a). Compared to ammonium, urea is relatively stable under alkaline conditions. However, for bacteria to gain access to the nitrogen in urea, urea has to be first hydrolysed to form ammonia. At alkaline conditions, much of this ammonia can be easily stripped-off (by aeration) from the bioprocess via volatilisation. Therefore, urea is typically supplied to the bioreactor in excess to avoid N limitations (McSweeney et al., 2011a). However, excessive dosage of urea is not only costly, the elevated ammonia volatilisation may

also cause undesirable emission of odours, leading to health and safety hazards in the refinery.

One alternative would be to explore the use of alkaliphilic bacteria capable of fixing atmospheric dinitrogen ( $N_2$ ) to facilitate oxidation of oxalate and other organic impurities in process liquor. To our knowledge, no previous attempt has been made to oxidise organic impurities present in Bayer process liquor under nitrogen deficient conditions. Hence, a comparative assessment of the performance of N-deficient and N-supplemented microbial communities is imperative to ascertain whether the alumina industry could capitalise from the use of N-fixing inocula for bio-treatment of Bayer process liquor. Therefore, the aim of this study was to compare oxalate degradation under N-supplemented and N-deficient conditions in two packed bed biofilm reactors. The two bioreactors were operated aerobically for a period of 275 days using a synthetic medium that simulated the Bayer process liquor in terms of salinity and alkalinity. The effect of dissolved oxygen (DO) concentration on the oxalate degradation was evaluated under N-supplemented and N-deficient conditions. This study will offer insights on the pros and cons of adopting N-fixing microorganisms to remove organics in Bayer liquor.

## 4.2 Materials and methods

### 4.2.1 Aerobic bioreactor systems

Two identical laboratory-scale aerobic bioreactor systems, consisting of packed bed columns and recirculation bottles were setup and operated as detailed below (Figure 4.1). The columns (total volume 650 mL) had an internal diameter and height of 55 mm and 400 mm, respectively, and were packed with graphite granules (3-5 mm diameter, KAIYU Industrial (HK) Ltd) to a bed volume of 600 mL. The weight of the air-dried graphite granules in each column was 480 g and once packed, the void volume of the granular column was 210 mL. The graphite granular media in the column reactors was exposed to a synthetic Bayer liquor that was continuously aerated in a 2 L glass recirculation bottle. The two systems were operated in sequencing-batch mode with a cycle length of 4 h. In the first 2 mins of the cycle, concentrated solutions (carbon and nutrients) were pumped in together with deionised water into the 2 L bottle

to form 1.3 L of fresh influent. Thereafter, to maintain a near saturation level of DO, compressed air was sparged through the liquid in the 2 L bottle throughout the entire cycle. The liquor (a total working volume of approximately 1.5 L) was continuously recirculated through the packed bed column in an up-flow direction at a flow rate of 9.6 L/h. At the end of each cycle, the liquid (~1.3 L) in the 2 L bottle was decanted, while the packed column remained submerged (~200 mL).

The reactors were monitored and controlled using data acquisition and control hardware (CompactRio National Instruments, USA) and software (Labview, National Instrument, USA). Online monitoring of DO and pH was carried out using a luminescent DO probe (PDO2, Barben Analyzer Technology, USA) and an intermediate junction pH probe (Ionode IJ44, Ionode Pty Ltd, Australia), respectively. Two DO probes were used to measure the DO concentrations before and after the pack column, with one immersed in the liquid of the 2 L bottle and the other placed at the outlet of the column reactor (Figure 4.1). All experiments were carried out at room temperature (~23°C).

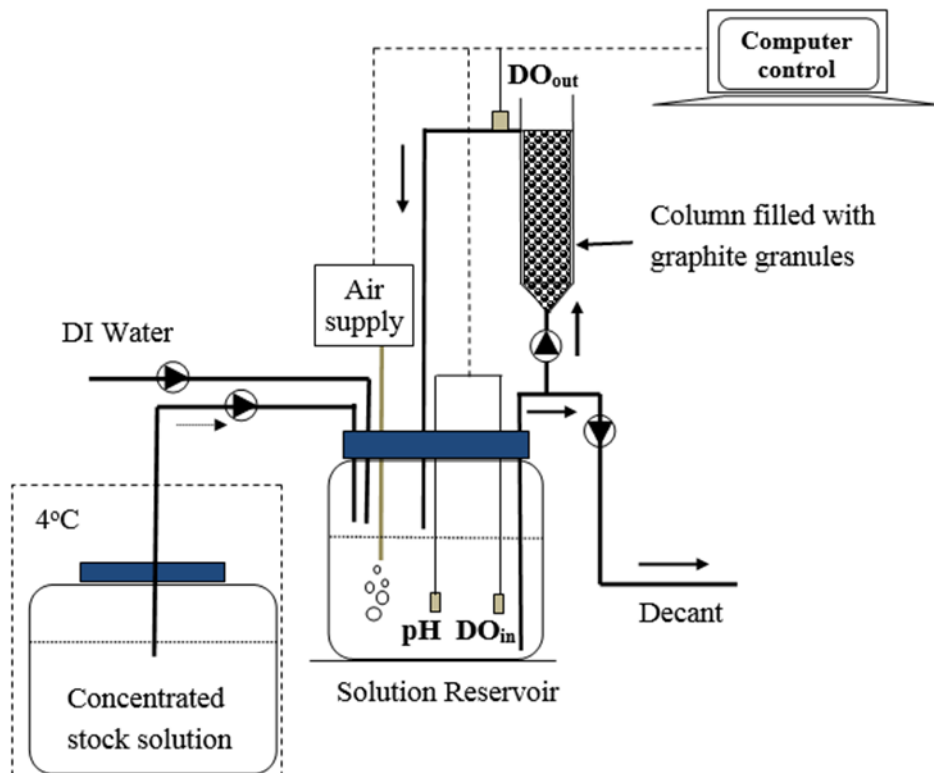


**Figure 4.1.** Schematic diagram of the aerobic bioreactor system used in the study.

## **4.2.2 Synthetic Bayer Process Liquor**

### **4.2.2.1 Influent for N-supplemented reactor**

The feed solution contained 2.0 g/L of Na<sub>2</sub>C<sub>2</sub>O<sub>4</sub> as the carbon source and 25 g/L of NaCl (salinity 2.5 %) in order to simulate the salinity of Bayer liquor. The pH of the solution was adjusted to 9.0 - 9.5 with 2 M NaOH. Additionally, the solution contained (per L): 25 mg NH<sub>4</sub>Cl, 125 mg NaHCO<sub>3</sub>, 51 mg MgSO<sub>4</sub>·7H<sub>2</sub>O, 15 mg CaCl<sub>2</sub>·2H<sub>2</sub>O, 20.5 mg K<sub>2</sub>HPO<sub>4</sub>·3H<sub>2</sub>O, and 1.25 mL of trace element solution. The trace element solution contained (per L): 0.43 g ZnSO<sub>4</sub>·7H<sub>2</sub>O, 5 g FeSO<sub>4</sub>·7H<sub>2</sub>O, 0.24 g CoCl<sub>2</sub>·6H<sub>2</sub>O, 0.99 g MnCl<sub>2</sub>·4H<sub>2</sub>O, 0.25 g CuSO<sub>4</sub>·5H<sub>2</sub>O, 0.22 g NaMoO<sub>4</sub>·2H<sub>2</sub>O, 0.19 g NiCl<sub>2</sub>·6H<sub>2</sub>O, 0.21 g NaSeO<sub>4</sub>·10H<sub>2</sub>O, 15 g ethylenediaminetetraacetic acid (EDTA), 0.014 g H<sub>3</sub>BO<sub>3</sub>, and 0.05 g NaWO<sub>4</sub>·2H<sub>2</sub>O.

### **4.2.2.2 Influent for N-deficient reactor**

The feed solution for the N-deficient bioreactor system was otherwise similar to that of the N-supplemented bioreactor, except that the Na<sub>2</sub>C<sub>2</sub>O<sub>4</sub> concentration was only 0.8 g/L depending on maximum oxalate removal capacity, NH<sub>4</sub>Cl was omitted, and 10 mg/L of yeast extract was added to supplement specific nutrient requirements such as amino acids.

## **4.2.3 Reactor start up**

The inoculum for the bioreactors was sourced from two locations. One sediment sample was collected from a local beach (Floreat Beach) and another two were collected from Perry Lake Reserve of Western Australia. An equal weight (75 g) of sediment from each location was mixed together and suspended in two separate 2 L glass vessels, which contained a 1.5 L of N-supplemented and N-deficient feed solutions, respectively. The Na<sub>2</sub>C<sub>2</sub>O<sub>4</sub> concentrations in the working solutions were initially maintained low (100 mg/L) to prevent substrate inhibition. The two vessels were aerated at room temperature for 3 weeks to enrich aerobic oxalate degrading microorganisms. During the enrichment, aeration was regularly (weekly) terminated

for a period of 1 h to allow settling of the reactor contents. Subsequently, the supernatants (1 L) were discarded and replenished with respective fresh feed solutions.

After the enrichment, the sediments in both bottles were vigorously disturbed by shaking to dislodge microbial cells from the sediment material. Subsequently, the two column reactors were connected to the two vessels as illustrated in figure 4.1. The feed solutions with the dislodged biomass were re-circulated through the column reactors to facilitate biofilm formation on the graphite granules. With intermittent disturbance of the sediment in each of the bottles, the reactors were operated with sediment in the vessels for another 2-3 d. Thereafter, all sediment material in each of the bottles was completely removed and microbial enrichment in column reactors were allowed to continue with weekly replenishment of feed solutions (1.3 L) in the 2 L bottles.

During the enrichment period, oxalate removal in the reactors was monitored every two weeks and the cyclic length of reactors were decreased as oxalate removal performance improved. Once a 4 h cycle length was achieved, the oxalate loading rate was increased (by increasing oxalate concentration in the feed) until no further increase of oxalate removal rate was detected. The final feed  $\text{Na}_2\text{C}_2\text{O}_4$  concentrations in the N-deficient and N-supplemented reactors during stable performance were 0.8 g/L and 2.0 g/L, respectively.

#### **4.2.4 Cyclic studies**

Cyclic studies were performed both during enrichment and steady state operation of reactors. Cyclic studies were performed every two weeks and the frequency of sampling during a cycle depended on cycle length. Hourly sampling was carried out when cyclic studies were carried out on 4 h cycles. During sampling, 3 mL samples were withdrawn from the 2 L bottles and were immediately filtered through 0.22  $\mu\text{m}$  pore size syringe filters (Cat. No. SLGN033NK, Merck Pty Ltd, Australia) into 2 mL Eppendorf tubes. The samples were then stored at 4 °C prior to analyses.

#### 4.2.5 Investigating the oxygen uptake rate of established biofilm

Once a stable reactor performance was reached, the oxygen uptake rate of the biofilm was examined by exposing the biofilm to different influent DO concentrations (between 0 and 8 mg/L) in the column reactors. All of these experiments were carried out at an influent pH of 9.5 and with oxalate concentrations used during normal operation of reactors. DO set points were feedback-maintained by sparging compressed air or nitrogen into the 2 L vessel. The DO probe in the vessel ( $DO_{in}$ ) was used as the input variable for the feedback control algorithm and together with the second DO probe ( $DO_{out}$ ) located at the outlet of the column reactor, specific oxygen uptake rates (OUR) of biofilm were determined in accordance to equation 4.1.

$$OUR = \frac{DO_{in} - DO_{out}}{HRT \times \text{Weight of dry biomass}} \times \text{Reactor liquid volume} \quad (\text{Equation 4.1})$$

Where  $DO_{in}$  and  $DO_{out}$  are influent and effluent dissolved oxygen concentrations (mg O<sub>2</sub>/L), HRT (h) is the hydraulic retention time of the column reactor, the reactor liquid volume (L) is the total liquid volume of the reactor and weight of dry biomass (g) is the dry weight of biofilm attached onto graphite media. HRT was calculated as follows (Equation 4.2):

$$HRT (h) = \frac{\text{Volume of liquid in column reactor (L)}}{\text{Recirculation flow rate (L/h)}} \quad (\text{Equation 4.2})$$

The biofilm was exposed to each influent DO set point over a single 4 h cycle. In the subsequent 5 cycles, the biofilm was allowed to recover using normal operational conditions (i.e. at a DO of 8 mg/L) before the impact of the next DO concentration was examined. During these studies hourly liquid samples were collected and immediately filtered through 0.22 µm syringe filters (Cat No SLGNO33NK, Merck Millipore, USA) for analyses for oxalate and chemical oxygen demand.

The effect of initial oxalate concentration on OUR was also investigated by determining the OUR of the biofilm exposed to various initial concentrations of oxalate (80 – 550 mg). At first the biofilm was exposed to an influent DO concentration of 8 mg/L in complete absence of oxalate. Once a steady background OUR was observed, varying initial concentrations of Na<sub>2</sub>C<sub>2</sub>O<sub>4</sub> were introduced into the reactor at different time intervals and the response of the biofilm was quantified by measuring

OUR, residual oxalate and COD concentrations. The total oxygen consumed (mmol) for a given quantity of Na<sub>2</sub>C<sub>2</sub>O<sub>4</sub> removed (mmol) was calculated by integrating the area under the OUR profile.

#### **4.2.6 Anaerobic oxalate degradation**

Anaerobic removal of oxalate was examined by withdrawing two subsets of biofilm coated granules from each reactor (16 mL and 20 mL of media from N-supplemented and N-deficient reactor respectively) at the end of a reactor cycle. The granules from the two reactors were then transferred into two 150 mL serum bottles that contained their respective growth media but without the presence of oxalate. The serum bottles were subsequently capped (using butyl rubber stoppers) and crimped with aluminium seals and flushed for 3 min using N<sub>2</sub>. To begin the time-course experiment, specified volumes of an oxalate stock solution (22 g/L) were added to the N-supplemented and N-deficient serum bottles to obtain an initial oxalate concentrations of 1200 and 930 mg/L, respectively. The initial pH was 9 and liquid volume was 50 mL. Liquid and headspace gas sampling were carried out from both anaerobic bottles at time intervals of 32, 48, 72, 96 and 120 h. The liquid samples were immediately filtered through 0.22 µm syringe filters (Cat No. SLGNO33NK, Merck Millipore, USA) and the filtrates were analysed for residual oxalate. The head space gas samples were analysed for methane gas. The experiment was carried out in duplicate to examine reproducibility of the results.

To explore possible routes of methanogenesis, another duplicate set of biomass samples of N-supplemented and N-deficient reactors were exposed to H<sub>2</sub>/CO<sub>2</sub> in complete absence of oxalate. Similar to previous experiment, the serum bottles with respective biomass (16 - 20 mL of media) and growth media were capped (using butyl rubber stoppers) crimped (with aluminium seals) and flushed for 3 min using N<sub>2</sub>. Subsequently, the head space of each bottle was flushed again using a H<sub>2</sub>/CO<sub>2</sub> mixture for another 3 min. Headspace gas sampling for analysis of methane was then carried out at time intervals of 0, 16, 24, 40 and 48 h.

#### **4.2.7 Assessment of nitrogen-deficient conditions**

Two methods were used to monitor prevalence of N-deficient and N-supplemented conditions in the reactors, namely concentrations of soluble nitrogen species in the reactors, and acetylene reduction assays.

##### **4.2.7.1 Concentrations of soluble nitrogen species**

$\text{NH}_4^+$ -N,  $\text{NO}_2^-$ -N and  $\text{NO}_3^-$ -N concentrations in both N-deficient and N-supplemented reactors were frequently analyzed using ion chromatography (IC). Approximately 2 mL solution samples were withdrawn and immediately filtered through 0.22  $\mu\text{m}$  syringe filters (Cat No SLGNO33NK, Merck Millipore, USA) and the filtrates were stored at 4 °C until analysed.

##### **4.2.7.2 Acetylene reduction assays**

A modified assay of Sprent (1990) was used for the acetylene reduction assay. Six and two biofilm coated granules samples (16 - 20 mL medium) were withdrawn from the N-deficient and N-supplemented reactors respectively and the samples were placed in eight 150 mL bottles. Subsequently, 50 mL of N-deficient and N-supplemented growth media (pH 9) were introduced into the corresponding bottles. Two of the N-deficient and two of the N-supplemented bottles received 2 g/L oxalate. Of the remaining four N-deficient bottles, two received 1.2 g/L of acetate and the other two received 1.2 g/L of formate. All bottles were subsequently capped (using butyl rubber stoppers), crimped (with an aluminium seal) and flushed with helium for 3 min to remove any  $\text{N}_2$  from the samples. Thereafter, 2 % of the headspace helium was removed and replaced with pure oxygen in one N-supplemented bottle and one oxalate, one acetate and one formate containing N-deficient bottle. In the remaining four bottles, the headspace was completely flushed with pure oxygen. Finally, 2 % headspace volumes of all eight bottles were replaced with acetylene (produced by reacting tap water with calcium carbide in a 1 L conical flask and acetylene captured with displacement of water in a measuring cylinder). The bottles were then incubated in an environmental shaker at 28 °C. Liquid and headspace gas sampling were carried out on all eight

bottles at time intervals of 3, 16, 24, 40 and 48 h. The liquid samples were immediately filtered through 0.22 µm syringe filters (Cat No SLGNO33NK, Merck Millipore, USA) and the filtrates were stored at 4 °C until analysed.

#### **4.2.8 Sample analysis**

##### **4.2.8.1 Estimation of dry biomass weight in reactors**

The amount of biomass coating the graphite media in the reactors was determined by removing a known volume of media from each of the reactors. The graphite media was then immersed in a known volume of deionized water in a 50 mL Falcon tube and sonicated in an ultrasonic water bath (Sanophon ultrasonic cleaner - 90 watts and 50 Hz) for 3 min to dislodge the attached biofilm. The suspension was then collected in a new Falcon tube (50 mL) and the graphite media was sonicated once more for 3 min in fresh deionized water. The suspensions from the two sonications were combined and suspended solids (SS) and volatile suspended solids (VSS) of the suspension were measured using standard methods (American Public Health Association. et al., 1995).

##### **4.2.8.2 Analysis of nitrogen species and organic carbon**

A Dionex ICS-3000 reagent free ion chromatography (RFIC) system equipped with an IonPac® AS18 4 x 250 mm column was used to measure oxalate, acetate, formate, nitrite and nitrate in liquid samples. Potassium hydroxide was used as an eluent at a flow rate of 1 mL/min. The eluent concentration was 12-45 mM from 0-5 min, 45 mM from 5-8 min, 45-60 mM from 8-10 min and 60-12 mM from 10-13 min. Ammonium ( $\text{NH}_4^+ \text{-N}$ ) was measured with the same RFIC but with a IonPac® CG16, CS16, 5 mm column. Methansulfonic acid was used as an eluent with a flow rate of 1 mL/min. The eluent concentration was 30 mM for 29 min. The temperature of the two columns were maintained at 30 °C. Suppressed conductivity was used as the detection signal (ASRS ULTRA II 4 mm, 150 mA, AutoSuppressioin® recycle mode).

A closed reflux dichromate method (HACH Method 8000, HACH Ltd) was used in accordance to manufacturer's instructions to measure chemical oxygen demand in the liquid samples.

#### **4.2.8.3 Gas analysis**

Headspace gas analysis was carried out using a Trace 1300 gas chromatograph (ThermoFisher Scientific, USA) fitted with a flame ionisation detector (FID). Methane, acetylene and ethylene gases were measured using a Rt®-U-BOND (30 m, 0.32 mm ID, 10 µm film, Cat.# 19752, Restek, USA) capillary column. A gas volume of 100 µL was manually transferred using a gas tight syringe into a split injector (split flow 40 mL/min) maintained at 200 °C. Helium was used as the carrier gas and the flow rate through the capillary column was maintained at a constant pressure of 53.1 kPa. The initial oven temperature was set at 100 °C for 1 min. Subsequently the temperature was raised to 150 °C at a rate of 25 °C/min and was finally held for 4 min. FID temperature was maintained at 230 °C and analysis was carried out using Chromeleon software (Version 7.1.2.1478).

### **4.3. Results and Discussion**

#### **4.3.1 Start-up of the N-supplemented and N-deficient reactors**

Although started with the same inoculum and operating conditions, the oxalate removal rates recorded for the two reactors were notably different (Figure 4.2). The N-supplemented reactor demonstrated immediate ability to oxidise oxalate (~ 34 mg/L.h), whereas the N-deficient reactor only demonstrated a measureable oxalate-degrading activity after approximately 75 d. Since the difference between the two reactors was the availability of ammonium, the inability of the N-deficient reactor to readily acclimatise an active oxalate-degrading culture was likely due to the lack of ammonium.

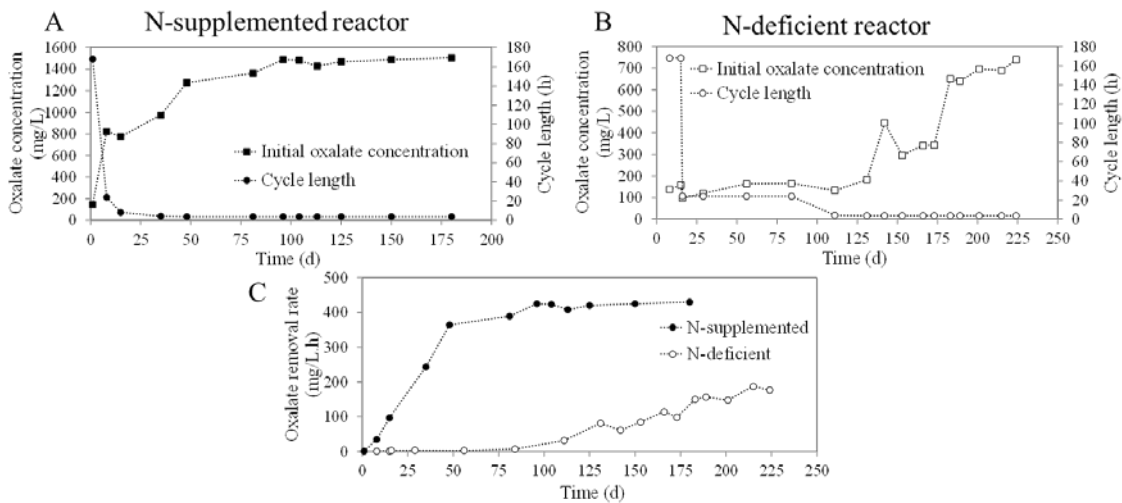


**Figure 4.2.** Change of influent oxalate concentration and cycle length of (A) N-supplemented and (B) N-deficient reactors at the start-up of the reactors, and (C) Oxalate removal efficiencies of the N-supplemented and the N-deficient reactor inoculated with the same starting inoculum.

The oxalate removal rate of the N-supplemented reactor rapidly increased (with a linear increase from 34 to 364 mg/L.h ( $R^2 = 0.98$ )) during the first 48 d of reactor operation. During this period, the cycle length was gradually shortened down to 4 h and the oxalate concentrations in the feed was systematically increased. At a cycle length of 4 h, the highest oxalate degradation rate was 430 mg/L.h and the system completely removed an initial oxalate  $\text{Na}_2\text{C}_2\text{O}_4$  concentration of 2 g/L. In contrast, a slow increase of oxalate removal (from 7 to 187 mg/L.h) was noted after a prolonged operation (after 84 d) of N-deficient reactor, and a relatively stable performance was only observed after 224 d of operation. The acclimatisation period of the N-deficient reactor was five times longer than that of the N-supplemented reactor. Moreover, the N-deficient reactor only could remove approximately half (0.8 g/L) the quantity of oxalate that was fed into the N-supplemented reactor (2 g/L).

The lower oxalate degradation rate in the N-deficient reactor was likely attributed to the lower concentration of biomass as compared to the N-supplemented reactor. The VSS and specific oxalate removal rate of N-supplemented reactor (9.6 mg/mL of graphite media and 111 mg-oxalate/h. g-biomass respectively) was found to be approximately 1.25 times higher than that of N-deficient reactor (7.6 mg/mL of graphite media and 87 mg-oxalate /h. g-biomass respectively). The slow increase of

oxalate removal rate in the N-deficient reactor during the period of enrichment, could be a result of low initial abundance and/or slow growth rates of microorganisms capable of oxidising oxalate under N-deficient conditions. In general, the growth rates of nitrogen fixing bacteria are magnitude lower than the growth rates of bacteria that can assimilate ammonia (Susan Hill, 1972). While slower growth rates of N-fixing microorganisms may have contributed towards the long enrichment period, potentially sub-optimal environmental conditions (e.g. pH, temperature etc.) for growth may also have contributed to the observed outcome.

#### **4.3.2 Detailed studies revealed that both N-supplemented and N-deficient biofilms had a similar capacity to degrade oxalate**

Only a comparative assessment of oxalate degradation between an N-supplemented and an N-deficient processes can reveal whether the N-deficient process could perform as well as the N-supplemented process. This study, for the very first time compared the degradation rates of an N-supplemented and an N-deficient reactor mineralising oxalate. The studies on degradation rates were executed once both reactors achieved a stable performance at a cycle length of 4 h.

Understanding the dependence of biodegradation rates on oxygen transfer or availability is useful for optimising aerobic biofilm treatment processes (Beyenal & Lewandowski, 2005; Bishop et al., 1995; Casey et al., 1999). Hence, the effect of dissolved oxygen (DO) concentration on oxalate degradation was examined by exposing the N-supplemented and N-deficient biofilms to different bulk water DO concentrations (Figure 4.3). The responses of the N-supplemented and N-deficient biofilms to various DO concentrations were notably different. The N-supplemented reactor showed a higher oxalate removal rate with an increase in bulk water DO concentration (Figures 4.3A and 4.3B), and the highest removal rate was observed with a bulk water DO concentration of 8 mg/L (Figure 4.3B). Linear relationships were recorded between DO concentration and (1) oxalate removal rate ( $R^2 = 0.94$ ) and (2) OUR ( $R^2 = 0.99$ ) (Figure 4.3B). These results indicated that oxalate degradation in the N-supplemented reactor was limited by DO availability.

In contrast, the N-deficient reactor did not show an increase of oxalate removal with an increase of bulk water DO concentration. Oxalate degradation improved until DO concentrations reached 3 mg/L, but no further increase occurred at higher DO concentrations (Figures 4.3D and 4.3E). A linear correlation ( $R^2 = 0.99$ ) between increase of bulk water DO concentration and oxalate removal rate was only observed up to a bulk water DO concentration of approximately 3 mg/L.

In addition to aerobic degradation of oxalate, oxalate also can be degraded anaerobically to form methane (Dawson et al., 1980a). Even at saturated concentrations of DO, anaerobic pockets may still be present in biofilm reactors as reported in literature (Santegoeds et al., 1998). The experimental oxalate removal and the theoretically expected aerobic oxalate removal (calculated according to reaction 4.1) were plotted against the total experimental oxygen consumption at different DO concentrations (Figure 4.3G). The amount of oxalate degraded was higher in both reactors compared to the expected amounts of oxalate removed based on the actual oxygen consumption. Moreover, both reactors were capable of removing oxalate in complete absence of DO (0 mg/L, Figure 4.3G). Compared to the N-supplemented reactor, the anaerobic removal of oxalate was marginally lower (3 mmol) in N-deficient reactor. Approximately 7.5 mmoles of oxalate was anaerobically removed alongside aerobic oxalate degradation in the N-supplemented reactor at all tested DO concentrations. This result suggested that even a high DO concentration of 8 mg/L failed to eliminate the occurrence of anaerobic pockets in the biofilm of N-supplemented reactor. A linear relationship ( $R^2 = 0.91$ ) between OUR and oxalate removal rate (Figure 4.3C) confirms that oxygen was limiting in this reactor allowing anaerobic removal of oxalate also to continue. With an increase of DO from 0 to 8 mg/L, the percentage of (%) anaerobic removal  $(\frac{\text{Total oxalate removed} - \text{Theoretical aerobic removal of oxalate}}{\text{Total oxalate removed}} \times 100)$  decreased from 100 to 45 % (due to increase of aerobic oxalate removal) suggesting that anaerobic removal of oxalate was a significant component in N-supplemented reactor even at a higher concentration of DO.

In contrast, the N-deficient reactor only showed a linear relationship ( $R^2 = 0.99$ ) between OUR and oxalate removal rate (Figure 4.3F) with bulk water DO concentrations lower than 3 mg/L. When the bulk water DO concentration was above 3 mg/L, the increase in OUR did not corroborate with an increase in oxalate removal

rate, which largely remained unchanged (80 mg/h.g biomass). At higher OUR (e.g. at 68 mg O<sub>2</sub>/h.g biomass; ~ at DO 8 mg/L), the N-deficient reactor showed a low constant oxalate removal rate (83 mg/h.g biomass) compared to an increasing removal rate noted in N-supplemented reactor (110 mg/h.g biomass).

The graph showing oxalate degradation versus oxygen consumption for N-deficient reactor was also parallel to theoretical oxygen consumption graph when oxygen consumption was below 1.8 mmol (Figure 4.3G). Approximately 4.5 mmoles of oxalate were anaerobically removed alongside aerobic degradation of oxalate even in the N-deficient reactor when oxygen consumption was below 1.8 mmol. An increase of OUR with no increase of oxalate removal rate at oxygen consumption above 1.8 mmol suggested an increase of aerobic and a simultaneous decrease of anaerobic removal of oxalate maintaining a constant net removal of oxalate (~ 10 mmol) in the N-deficient reactor (Figure 4.3G). This indicated that oxygen limitation in the N-deficient reactor was not as severe as in the N-supplemented reactor at higher bulk water DO concentrations. This observation was perhaps due to the low biomass concentration (thinner biofilm) in the N-deficient reactor (1.25 times lower than that of N-supplemented reactor), enabling maintenance of possibly a much thinner biofilm in the reactor. Higher biomass densities on the other hand induce higher oxygen demands and also reduce void spaces in packed bed column reactors. A reduction of void spaces also results in short circuiting flow paths and anaerobic conditions in N-supplemented reactor was likely induced by all of the above factors.

In summary, both reactors showed a much higher level of oxalate removal (specifically at bulk water DO concentrations of less than 3 mg/L, or total oxygen consumption below 1.8 mmol) compared to the theoretical estimations of aerobic oxalate degradation (Figure 4.3G). This suggests that anaerobic degradation of oxalate also occurred in both reactors in the presence of oxygen. Anaerobic oxalate degradation, however, decreased with an increase of bulk water DO concentrations in the N-deficient reactor whereas this was not evident in N-supplemented reactor. Moreover, for all DO concentrations tested, the N-supplemented reactor was able to remove a marginally higher quantity of oxalate compared to the N-deficient reactor (Figure 4.3G). Overall the oxalate removal efficiencies of both reactor can be further enhanced by eliminating anaerobic pockets and enhancing mass transfer by replacing the packed bed columns with suspended biomass (e.g. activated sludge) or biofilm carriers.

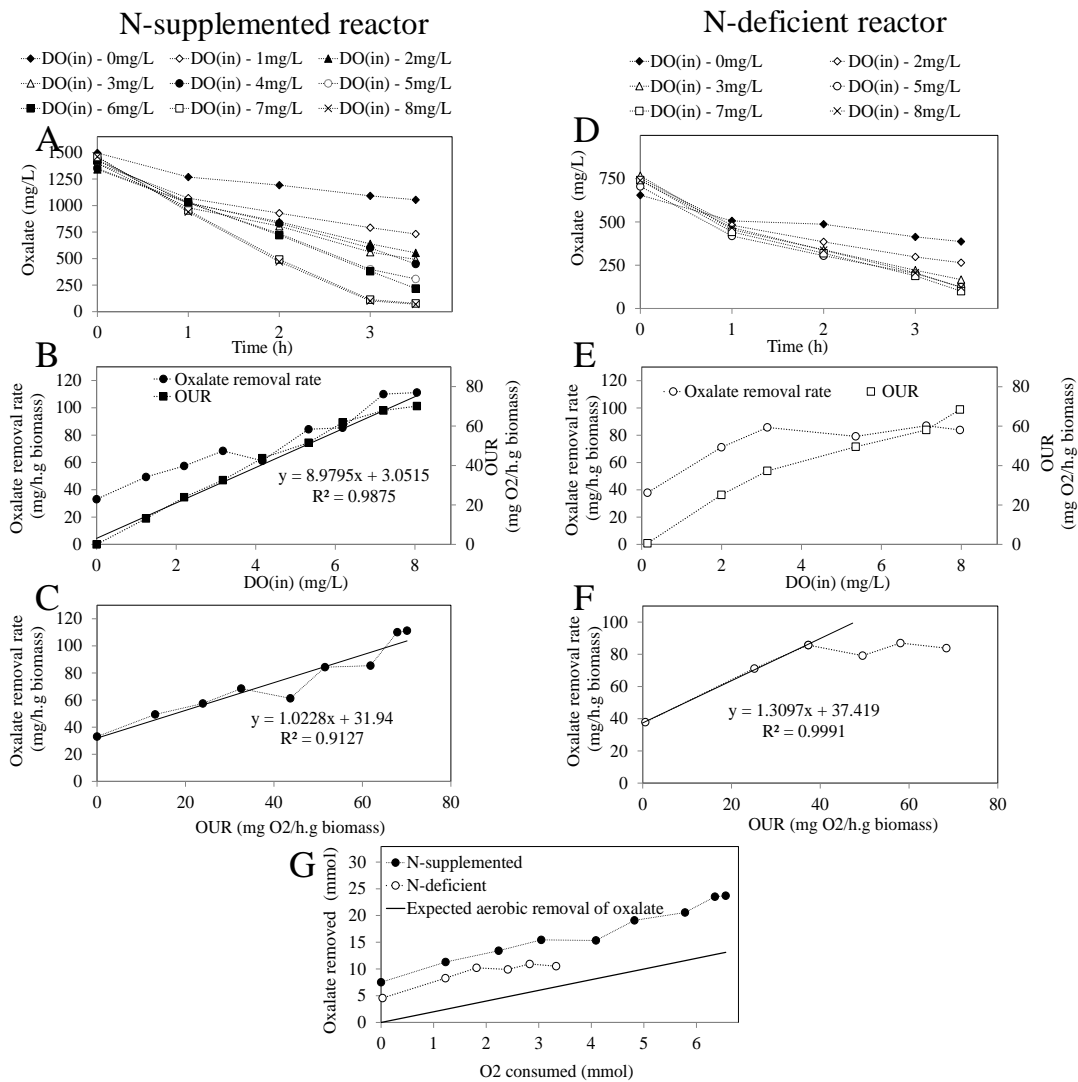


**Figure 4.3.** Effect of (A and D) DO concentration on the removal of oxalate; (B and E) DO concentration on the removal rate of oxalate; (C and F) Oxygen uptake rate on the removal rate of oxalate; (G) Correlations of oxygen consumed and oxalate removed for N-supplemented and N-deficient reactors. The tests were carried out from day 146 for N-supplemented reactor and from day 224 for N-deficient reactor.

To further verify whether the N-supplemented reactor was more efficient at removing oxalate, an alternative method was used to determine the relationship between oxygen consumption and oxalate removal in both N-supplemented and N-deficient reactors (Figure 4.4). This experiment enabled accurate quantification of oxygen demand (at a bulk water DO of 8 mg/L) for a spike of a known quantity of oxalate, and this was facilitated with an integration of area under the derived OUR curve. Both reactors,

when starved of oxalate for an extended period of time, showed an endogenous, base line oxygen consumption rate of approximately 20 mg/h.g biomass (Figures 4.4A and 4.4B). Compared to the N-deficient reactor, the oxalate removal efficiency of the N-supplemented reactor was found to be approximately 1.3 times higher at a given level oxygen consumption (Figure 4.4C). Nitrogen fixation was likely the main mechanism by which biological nitrogen requirements were met in the N-deficient reactor. The high energy demand of nitrogen fixation (Schulze et al., 1994), may have negatively impacted oxalate removal efficiency of the N-deficient reactor. Future research should focus on developing strategies to improve the oxalate removal efficiency in N-deficient reactors.

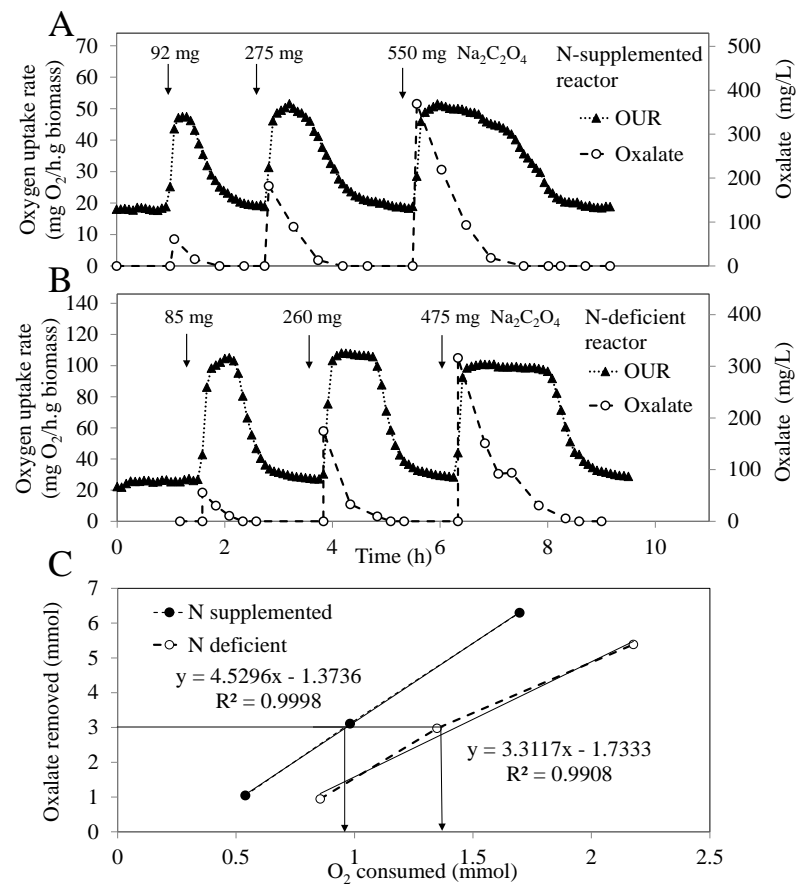


**Figure 4.4.** Influence of oxalate spikes on oxygen uptake rates in (A) N-supplemented reactor on day 288 and (B) N-deficient reactor on day 365. (C) Correlations of oxygen consumed and oxalate removed for N-supplemented and N-deficient reactors.

#### **4.3.3 Presence/absence of an easily utilisable nitrogen source influence pathway of methanogenesis during alkaline fermentation of oxalate**

Anaerobic fermentation of oxalate to methane is reported in literature (Dawson et al., 1980a). However, studies have not revealed the methane generation pathways, specifically when fermenting oxalate under alkaline and N-deficient conditions. Our study for the first time, compared fermentation of oxalate in an N-supplemented and an N-deficient reactor to determine the methane generation pathways of these two reactors. A separate serum bottle experiment was conducted to determine the anaerobic oxalate degradation pathway in each N-supplemented and N-deficient reactors. The N-supplemented and N-deficient bottles were exposed to an initial oxalate concentration of ~ 1 g/L under anaerobic conditions. Both samples showed a good removal of oxalate under anaerobic conditions (Figure 4.5). The initial anaerobic oxalate fermentation rates in the N-supplemented and N-deficient reactors were 8.9 and 6.7 mg/h.g biomass, respectively. When oxalate concentrations decreased to ~100 mg/L, the oxalate fermentation rates in the N-supplemented and N-deficient reactors reduced to 0.5 and 0.6 mg/h.g biomass respectively. The decrease in anaerobic oxalate fermentation rate also coincided with a peak concentration of formate (510 and 202 mg/L in N-supplemented and N-deficient reactors, respectively), which is an intermediate by-product of both aerobic and anaerobic oxalate degradation (Dawson et al., 1980a; Dijkhuizen et al., 1978; Stewart et al., 2004). However, it remains unclear whether the decrease in oxalate fermentation was due to the build-up of formate (which might have inhibited oxalate fermentation) or the exhaustion of oxalate in both reactors.

Acetate accumulation was also detected in both reactors, but unlike formate, the concentration of acetate did not decrease over time (Figures 4.5A and 4.5B). Guyot and Brauman (1986) report the ability of bacteria to ferment formate to acetate. The detection of both formate and acetate in both N-supplemented and N-deficient reactors suggested two possible mechanisms of anaerobic oxalate mineralisation: (1) by a single bacterium having necessary metabolic pathways to ferment oxalate to acetate via the intermediate by-product formate and (2) by a group of bacteria (individually lacking a complete metabolic pathway) interacting symbiotically. If a single bacterium was responsible, the fermentation of formate to acetate appears to be the rate limiting step of the process resulting in a momentary accumulation of formate in the medium.

The decrease in the formate concentration over time suggested the presence of hydrogenotrophic methanogens since some hydrogenotrophic methanogens are known to be capable of utilising formate as a substrate (Guyot & Brauman, 1986; Sakai et al., 2010).

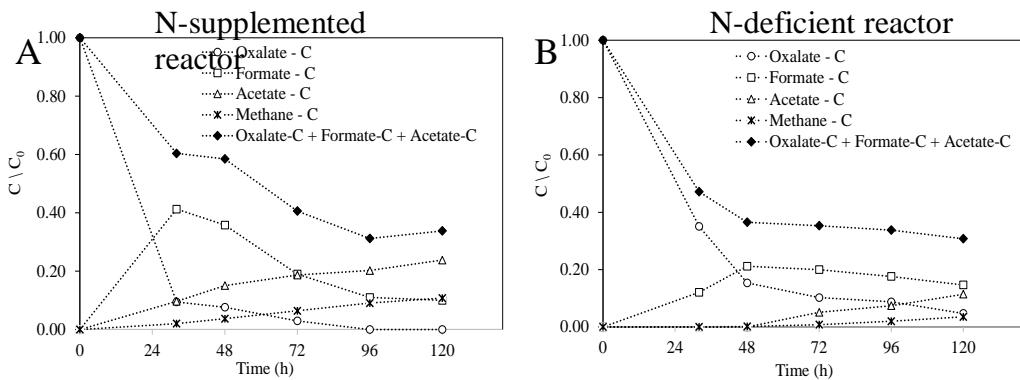


**Figure 4.5.** Conversion of carbon in N-supplemented and N-deficient reactors during anaerobic fermentation of oxalate.  $C/C_0$  = molar ratio of carbon in degradation products versus initial oxalate carbon concentration. C – Carbon moles in degradation products (such as oxalate, acetate, formate or methane) and  $C_0$  – Carbon moles in initial oxalate concentration.

The formate and acetate that accumulated, far exceeded the amount of methane produced in both N-supplemented and N-deficient reactors during anaerobic fermentation of oxalate (Figure 4.5). The N-supplemented reactor has a higher methane production rate (0.125 mg/h.g biomass) than the N-deficient reactor (0.05 mg/h.g biomass). While a low emission of methane could be an inherent feature of N-deficient systems, a difference in the thickness of biofilm in the two systems may also have contributed toward this outcome with a low and a high abundance of methanogens in N-deficient and N-supplemented reactors, respectively.

To further explore the possible route of methanogenesis, both N-supplemented and N-deficient reactors were exposed to  $H_2/CO_2$  in the absence of oxalate. Over a 2 d incubation period, the N-supplemented reactor demonstrated continuous production of methane whereas no measurable quantity of methane was produced by the N-deficient reactor (Figure 4.6). The inability of the N-deficient reactor to produce methane with  $H_2/CO_2$  suggested that lack of hydrogenotrophic methanogens and methane production

during fermentation of oxalate possibly occurred via acetoclastic methanogens in this reactor (Strapoć et al., 2011; Susilawati et al., 2016). The methane production rates when fermenting oxalate (0.125 mg/g biomass.h) and when utilising H<sub>2</sub>/CO<sub>2</sub> (0.131 mg/g biomass.h), on the other hand showed a great deal of similarity in the N-supplemented reactor. This indicates that the route of methanogenesis in N-supplemented reactor was perhaps predominantly via hydrogenotrophic methanogens. Although chemical data provides some insight towards route of methanogenesis of both N-supplemented and N-deficient reactors, more in depth microbiological analysis of methanogens in ecosystems similar to that of N-supplemented and N-deficient oxalate degrading reactors is required to better understand the influence of nitrogen on the selection of methanogens during oxalate fermentation.

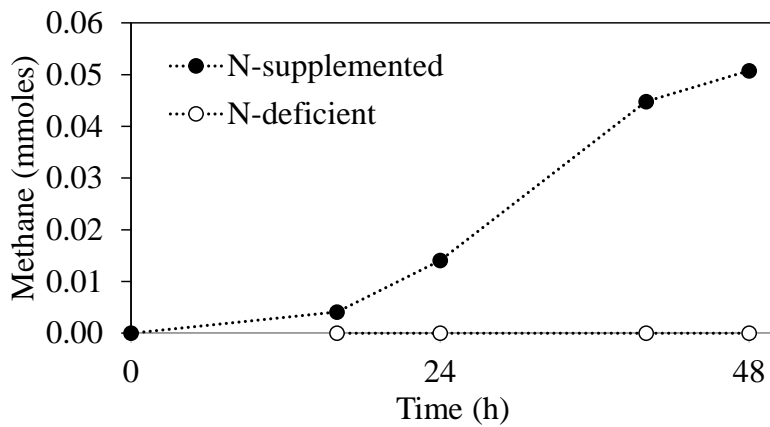


**Figure 4.6.** Production of methane during anaerobic exposure to H<sub>2</sub>/CO<sub>2</sub> in the absence of oxalate.

#### 4.3.4 Are nitrogen requirements of N-deficient reactor fulfilled with atmospheric nitrogen fixation?

The feed of the N-deficient reactor did not contain any inorganic nitrogen source. Frequent measurement of NH<sub>4</sub><sup>+</sup>-N, NO<sub>3</sub><sup>-</sup>-N and NO<sub>2</sub><sup>-</sup>-N confirmed no measureable quantity of NH<sub>4</sub><sup>+</sup>, NO<sub>3</sub><sup>-</sup> or NO<sub>2</sub><sup>-</sup> in the N-deficient reactor. It is common practice to include a trace amount of yeast extract to supplement essential nutrient requirements of N fixing bacteria (Gauthier et al., 2000; Sorokin et al., 2008) and, therefore 10 mg/L yeast extract was added into the feed of the N-deficient reactor. This trace amount of

yeast extract is unlikely to fulfil all nitrogen requirements of the N-deficient reactor. Hence, nitrogen requirements of the N-deficient reactor were likely fulfilled via biological nitrogen fixation.

To confirm the presence of nitrogen fixation activity, acetylene reduction assay was performed, which facilitates an indirect measurement of nitrogen fixation by exploiting the ability of the nitrogenase enzyme to reduce acetylene to ethylene (Hardy et al., 1968). When the acetylene reduction assay was carried out using the biomass of N-deficient reactor, no ethylene was detected over a 48 h incubation period with both 2 % and 100 % of oxygen. Inactivation of nitrogenase enzyme with exposure to high concentration of oxygen is well documented (Compaore & Stal, 2010a; Staal et al., 2007) and there is a possibility that the negative results obtained was a result of the use of 100% oxygen content. With figures 4.3E and 4.3F suggesting limited anaerobic activity in N-deficient reactor when the bulk water DO was 8 mg/L, the biofilm in the reactor was assumed to be tolerant towards oxygen when fixing nitrogen. Specifically, the 2 % oxygen used in the assay was unlikely inhibitory as this has been widely reported in past literature where acetylene reduction assays have been carried out to determine nitrogen fixation (Compaore & Stal, 2010a; Staal et al., 2007).

Although able to oxidise the carbon source, some nitrogen fixing bacteria have been shown to have difficulties in reducing acetylene when exposed to particular carbon sources (Dalton & Whittenbury, 1976; Trinchant et al., 1994). For example, a nitrogen fixing strain *Methylococcus capsulatus*, although able to oxidise both methanol and glutamate, was only able to reduce acetylene when in the presence of methanol and not glutamate (Dalton & Whittenbury, 1976). Accordingly, the negative result obtained with oxalate could also be a result of a substrate inhibition (i.e. Oxalate) on the acetylene reduction. According to figure 4.5, acetate and formate are intermediate by-products of oxalate metabolism and hence, in addition to oxalate, the biofilm of N-deficient reactor is also capable of utilising both acetate and formate. Therefore, the acetylene reduction assay was subsequently carried out replacing oxalate with acetate or formate. When formate was used as the sole source of carbon, the outcome was similar to oxalate i.e. no ethylene was detected. However, when acetate was used as the sole source of carbon in the acetylene reduction assay, ethylene was detected (data not shown) confirming that the biofilm of N-deficient reactor was capable of fixing nitrogen. Similar to what has been observed by Dolton et al. (1976), in this study the

use of both oxalate and formate as substrate inhibited the reduction of acetylene to ethylene by the nitrogen fixing bacteria in the N-deficient reactor.

#### **4.3.5 Implications of findings**

Biological degradation of oxalate is a more environmentally benign approach to removing oxalate from Bayer process wastes when compared to traditional destruction methods such as liquor burning. With a comparative assessment, this study for the very first time experimentally demonstrated that an N-deficient biological process could be used to oxidise oxalate under alkaline conditions. An in-depth assessment of the oxalate degradation efficiency revealed that the oxalate removal relative to oxygen consumption in the N-supplemented reactor was only slightly higher than in N-deficient reactor, indicating that aeration costs would be similar if current N-supplemented systems were to be replaced with N-deficient systems.

The findings also suggest that anaerobic oxalate mineralisation in the biofilm systems tested was inevitable. However, conversion of oxalate to methane is of environmental concern because compared to carbon dioxide, methane is a much more potent (30 times) greenhouse gas. The methane yield per oxalate degraded was lower for N-deficient than N-supplemented reactor, indicating that converting N-supplemented bioreactors to N-deficient ones could potentially reduce methane emissions.

### **4.4 Conclusions**

This study evaluated and compared the effect of DO concentration on oxalate degradation of N-supplemented and N-deficient biofilm reactors under saline and alkaline conditions. Based on the results, N-supplemented reactor performs better in oxalate removal rate and also has a much shorter start-up period compared to the N-deficient reactor. In both reactors, oxalate degradation occurred in absence of DO, and the amount of oxalate removed per oxygen consumed exceeded theoretical aerobic oxalate removal estimates, suggesting that some of the oxalate was degraded anaerobically. Under anaerobic conditions, both reactors produced formate and acetate during fermentation of oxalate.

# **5 INFLUENCES OF PH AND ORGANIC CARBON ON OXALATE REMOVAL BY MIXED BACTERIAL CULTURES ACCLIMATISED TO NITROGEN-DEFICIENT AND SUPPLEMENTED CONDITIONS**

Extended from

Weerasinghe Mohottige, T.N., Cheng, K.Y., Kaksonen, A.H., Sarukkalige, R. and Ginige, M.P. (2017) Influences of pH and organic carbon on oxalate removal by mixed bacterial cultures acclimatized to Nitrogen-deficient and supplemented conditions. Journal of Cleaner Production. Under Review.

## **Chapter Summary**

Microbial oxidation is a low-cost approach to remove organics, but hostile conditions of Bayer liquor ( $\text{pH} > 14$  and nitrogen (N) deficiency) makes it challenging. This study compared oxalate removal efficiencies of two packed bed biofilm reactors (N-supplemented and N-deficient) on exposure to a range of influent pH and simple organic compounds. Both reactors were operated ( $> 265$  days) at pH 9 and pH influence was compared in batch experiments. Results suggested that both biofilms could tolerate a broad pH range (7 - 10). The optimal specific oxalate removal rate of N-supplemented reactor was restricted to pH 9, whereas the maximal rate was maintained over a wider pH range (7 - 8) in N-deficient reactor. In this range, the N-deficient system outperformed the N-supplemented system (105 vs. 130 mg/h.g biomass). Although acclimatized primarily with oxalate, both biofilms simultaneously oxidised other organics (acetate, formate, malonate and succinate) without a noticeable influence on oxalate removal. This study suggests that N-deficient systems are more versatile and better suited to remove organic impurities in Bayer liquor.

## 5.1 Introduction

Bayer process is used to refine alumina ( $\text{Al}_2\text{O}_3$ ) from aluminium (Al) bearing bauxite minerals. In the Bayer process, crushed bauxite is digested in a hot concentrated solution of sodium hydroxide (NaOH) to produce sodium aluminate ( $\text{NaAlO}_2$ ). To recover aluminium trihydroxide ( $\text{Al(OH)}_3$ ), the process liquor is cooled down and an  $\text{Al(OH)}_3$  crystallisation seed is introduced to trigger crystallisation of  $\text{Al(OH)}_3$ . On separation, the spent NaOH is recycled to the process (Meyers, 2004; Whelan et al., 2003). In addition to Al, the bauxite minerals also contain organic impurities and due to continuous re-cycling, these impurities accumulate in process liquor to concentrations that hinder Al recovery. The organics present in bauxite range from very complex high molecular weight humic substances to simple organic acids (Power et al., 2012; Whelan et al., 2003). Of these organic compounds, sodium oxalate ( $\text{Na}_2\text{C}_2\text{O}_4$ ) is the most harmful impurity as it reduces process efficiency and product quality due to its co-precipitation with  $\text{Al(OH)}_3$ .

Some alumina refineries have used biological processes to remove oxalate from Bayer liquor (McKinnon & Baker, 2012). However, high pH ( $> 13$ ) and nitrogen (N) deficiencies of Bayer liquor, makes it a stream to treat biologically, and hence, uptake of the technology is limited possibly due to fears of operational failures. Initial studies that examined biological removal of oxalate, neutralised Bayer liquor to create a suitable environment for oxalate degrading microorganisms (Brassinga et al., 1989). To avoid pH neutralisation, Worsley Alumina Pty Ltd for the first time examined the use of alkaliphilic bacteria to remove oxalate (Morton et al., 1991). A typical alkaliphilic bacterium, has a pH tolerance range of 8.5 – 11 and the use of an alkaliphilic culture (Horikoshi, 1999), therefore helped better manage operational risks and costs of biological oxalate removal.

Although alkaliphilic bacteria have a broader tolerance of pH, their optimum biological activities remain in a much narrow pH range (Banciu et al., 2008; Sorokin et al., 2001). This partially may be a result of ammonia toxicity arising with a higher prevalence of unionised  $\text{NH}_3$  at higher pH values (Sousa et al., 2015). Compared to  $\text{NH}_4^+$  ions, free  $\text{NH}_3$ , readily diffuses through cell membranes and disrupts the proton balance inside cells, interrupting cellular metabolic processes (toxic) (Sousa et al., 2015). At a given alkaline pH, the free  $\text{NH}_3$  concentration is depended on the total

ammonia nitrogen (TAN) concentration and a low TAN concentration results in a low free NH<sub>3</sub> concentration ( $pK_a = 9.25$ ), which is less toxic to microorganisms. However, free NH<sub>3</sub> toxicity and tolerance vary between different bacterial inocula (Wang et al., 2016), and our knowledge around pH and removal rates of oxalate by different cultures is incomplete and this has prevented alumina refineries from having better control of their biological treatment processes.

N is a major essential element that is required for bacterial growth. The issue related to N deficiencies of Bayer liquor is typically circumvented by external supplementation of N (e.g. NH<sub>3</sub>). Loss of N from Bayer liquor due to volatilisation of NH<sub>3</sub> at high pH is an operational challenge for refineries and the current strategy is to maintain an excess concentration, with an overdose of N. As previously mentioned, higher TAN concentrations result in higher NH<sub>3</sub> toxicities, which in turn affects oxalate removal rates of bacteria. On the other hand, a bacterial inoculum able to fix atmospheric nitrogen would negate the need to externally supplement N and thus could minimise operational risks and costs. Haloalkaliphilic diazotrophs and their ability to facilitate removal of oxalate from Bayer liquor was demonstrated for the first time by (Weerasinghe Mohottige et al., 2017a) and this has provided the alumina industry a choice of bacterial cultures to facilitate a costs effective, low risk biological process to remove oxalate.

A typical alumina refinery produces  $> 1000 \text{ m}^3$  Bayer liquor/h (Chen et al., 11-15 March 2007). If a biological process is to maintain a low concentration of oxalate in Bayer liquor, an efficient side stream biological process is needed. In order to facilitate an efficient side stream process, a well-characterised (i.e. physicochemical and kinetically) bacterial culture is needed. Although current alumina refineries have access to two main types of cultures (i.e. an N-supplemented and an N-deficient inoculum) to date no effort has gone towards a comparative assessment to understand which culture would be best suited to reduce operational risks and costs. Considering the very high pH of Bayer liquor ( $> 13$ ) there is an operational need to determine pH range where optimum removal of oxalate takes place. Further, in addition to oxalate, there is accumulation of other simple organic impurities such as sodium acetate, sodium formate, sodium succinate and sodium malonate in Bayer liquor (McKinnon & Baker, 2012; Tilbury, 2003) and implications of these organic compounds on the removal of oxalate is also currently unexplored.

Therefore, in this study we compared oxalate removal efficiencies of two packed bed biofilm reactors (one supplemented and the other not supplemented with N) by exposing the reactors to a range of influent pH values (7 to 12) and simple organic compounds. The two reactors were operated aerobically at pH 9 for a period of 275 days using a synthetic medium that mimicked (i.e. in terms of salinity and alkalinity) the Bayer process liquor. This study offers new insight into pros and cons of using each of the bacterial cultures to remove oxalate in Bayer liquor.

## 5.2 Materials and methods

### 5.2.1 Aerobic bioreactor systems

Experiments were carried out using two identical laboratory-scale aerobic bioreactors as described in chapter 4. As illustrated in Figure 5.1, each reactor was composed of a packed bed glass column and a recirculation bottle. The internal diameter and height of the glass column was 55 mm and 400 mm, respectively and total available bed volume of the reactor was 650 ml. Each column was packed with 480 g of air dried graphite granules (3-5 mm diameter, KAIYU Industrial (HK) Ltd) that made up a bed volume of 600 mL. Once packed in the column, there was a 210 mL void volume in the granular column. The 2 L glass recirculation bottle served as a solution reservoir to enable recirculation of liquid through the granular column. The two reactors were operated in sequencing-batch mode with a cycle length of 4 h. During the first 2 mins of the cycle, 10 times concentrated solutions of carbon and nutrient was pumped into the recirculation bottle together with deionised water to make up a 1.3 L volume of fresh influent. The solution in the recirculation bottle was continuously aerated with a sparger over the entire period of reactor cycle to maintain a near saturation level of dissolved oxygen (DO) in the liquid. The aerated liquor (i.e. a total working volume of approximately 1.5 L) was continuously recirculated through the packed bed column in an upward-flow direction at a flow rate of 9.6 L/h. At the end of each cycle, the liquid (~ 1.3 L) in the 2 L bottle was decanted to replenish with new solution, while the packed bed remained submerged (~ 210 mL).

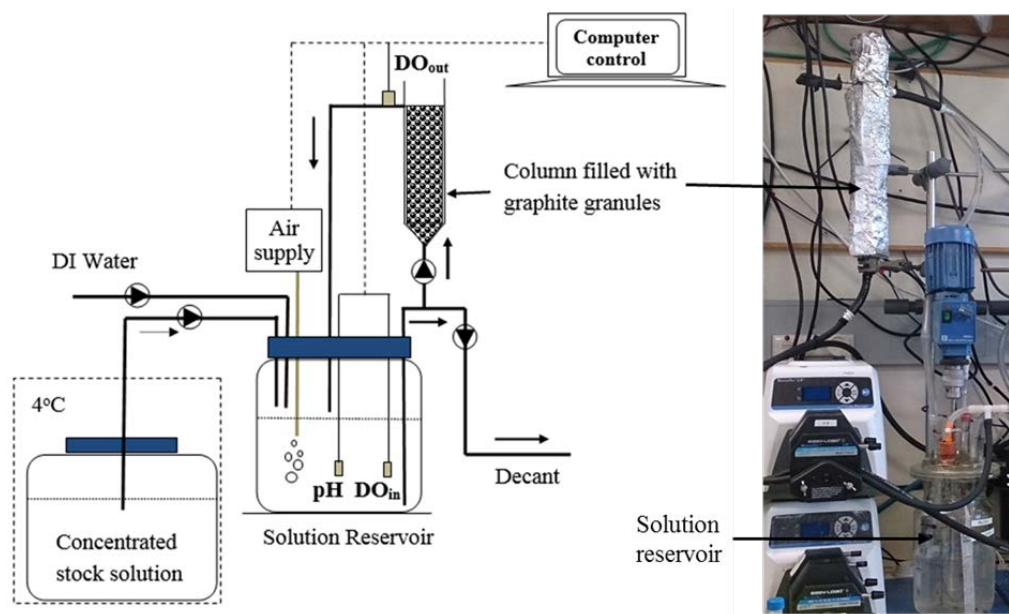


**Figure 5.1.** A schematic diagram and a photographic image of the aerobic packed bed bioreactor.

Data acquisition and control hardware (CompactRio National Instruments, USA) and software (Labview, National Instrument, USA) were used for continuous monitoring and control of the reactors. Online monitoring of DO and pH were carried out using a luminescent DO probe (PDO2, Barben Analyzer Technology, USA) and an intermediate junction pH probe (Ionode IJ44, Ionode Pty Ltd, Australia), respectively. Two DO probes were used to measure the DO concentrations at the inlet and outlet of the packed column, with one immersed in the synthetic solution in the 2 L bottle and the other placed at the outlet of the column reactor (Figure 5.1). All experiments were carried out at room temperature ( $\sim 23^{\circ}\text{C}$ ).

### 5.2.2 Influent for N-supplemented and N-deficient reactors

A highly saline and alkaline synthetic medium was used as the influent to simulate the salinity and alkalinity of Bayer process liquor of the alumina industry. The working solution contained 2.0 g/L  $\text{Na}_2\text{C}_2\text{O}_4$  and 25 g/L NaCl. The pH of the working solution was 9.0 - 9.5 and was adjusted using 2 M NaOH. Additionally, the working solution also contained a nutrient medium.

The nutrient medium was consisted of (per L): 50 mg NH<sub>4</sub>Cl, 125 mg NaHCO<sub>3</sub>, 51 mg MgSO<sub>4</sub>·7H<sub>2</sub>O, 15 mg CaCl<sub>2</sub>·2H<sub>2</sub>O, 20.5 mg K<sub>2</sub>HPO<sub>4</sub>·3H<sub>2</sub>O, and 1.25 ml of trace element solution. The trace element solution contained (Per L): 0.43 g ZnSO<sub>4</sub>·7H<sub>2</sub>O, 5 g FeSO<sub>4</sub>·7H<sub>2</sub>O, 0.24 g CoCl<sub>2</sub>·6H<sub>2</sub>O, 0.99 g MnCl<sub>2</sub>·4H<sub>2</sub>O, 0.25 g CuSO<sub>4</sub>·5H<sub>2</sub>O, 0.22 g NaMoO<sub>4</sub>·2H<sub>2</sub>O, 0.19 g NiCl<sub>2</sub>·6H<sub>2</sub>O, 0.21 g NaSeO<sub>4</sub>·10H<sub>2</sub>O, 15 g ethylenediaminetetraacetic acid (EDTA), 0.014 g H<sub>3</sub>BO<sub>3</sub>, and 0.05 g NaWO<sub>4</sub>·2H<sub>2</sub>O.

Compared to the N-supplemented reactor, the working solution of the N-deficient reactor contained a lower concentration of Na<sub>2</sub>C<sub>2</sub>O<sub>4</sub> (0.8 g/L). NH<sub>4</sub>Cl was removed from the nutrient medium of N-deficient reactor and replaced with 10 mg/L yeast extract. Yeast extract is commonly used to supplement essential nutrients when culturing nitrogen fixing bacteria (Gauthier et al., 2000; Sorokin et al., 2008).

### 5.2.3 Reactor start up

The inoculum for the reactors was sourced from two locations. Since the Bayer liquor is a saline solution (typical NaCl concentration of 0.43 M NaCl) (Hind et al., 1997) and coastal sediments are also known to contain oxalic acid, a sediment sample was collected from a local beach (Floreat beach, Western Australia) for microbial enrichment. Another two samples were collected from a local wetland reserve (Perry Lake reserve, Western Australia). Rhizosphere microorganisms are likely exposed to oxalic acid due to the accumulation of oxalic acid by most plant cells as a metabolic end product. Also, Western Australian soils are highly deficient in N and as such diazotrophs are also likely to dominate the rhizosphere (Bahadur & Tripathi, 1976). Hence, Perry Lake samples were obtained from the vicinity of the rhizosphere of native plants. Equal weights from all three different inocula samples (total weight of 225 g each) were combined and suspended in two separate 2 L glass bottles, which contained 1.5 L of N-supplemented and N-deficient feed solutions, respectively. Initially, the Na<sub>2</sub>C<sub>2</sub>O<sub>4</sub> concentrations in the working solutions were maintained low (100 mg/L) to prevent substrate inhibition of microorganisms. The two vessels were aerated at room temperature for 3 weeks to enrich aerobic oxalate degrading microorganisms. During enrichment, aeration was regularly interrupted for a period of 1 h once per week to allow the contents of both bottles to settle. Subsequently, the supernatant liquid (1 L) was discarded and replenished with respective fresh feed solutions.

After 3 weeks of enrichment, the sediments in both vessels were vigorously disturbed by shaking to dislodge microbial cells from sediment material. Subsequently, the two packed bed column reactors were connected to the vessels as illustrated in figure 5.1 and the reactors were operated in batch mode. The liquid containing the dislodged biomass was re-circulated through the respective reactors to facilitate colonisation and growth of an N-supplemented and an N-deficient biofilm on the carriers. The reactors were operated for another 2-3 d with the sediments in the recirculation bottle. Thereafter, all sediment was completely removed from each of the recirculation bottles. Biofilm enrichment in the column reactors was allowed to continue with weekly replenishment of feed solutions (1.3 L) in the 2 L recirculation bottles.

During enrichment, oxalate removal in the reactors was monitored every two weeks. Depending on the removal of oxalate, the cycle length of the reactors was decreased gradually to 4 h. After the 4 h cycle length was achieved, the oxalate concentration in the feed was increased to coincide with increasing oxalate removal rates. The increase of oxalate loading rate was terminated when no further increase in the rate of oxalate removal was observed. During stable operation, the final  $\text{Na}_2\text{C}_2\text{O}_4$  concentrations in the feed of N-deficient and N-supplemented reactors were 0.8 g/L and 2.0 g/L, respectively.

#### **5.2.4 Cyclic studies**

After 21 days of microbial inoculation, cyclic studies were carried out once every two weeks during the enrichment period to determine the oxalate removal rate of the bioreactors. During steady state of operation, the frequency of sampling was varied based on specific experiments. During routine cyclic studies, hourly sampling was carried out (over the 4 h cycle). During sampling, 3 mL volumes were withdrawn from the 2 L re-cycle bottles and immediately filtered through 0.22  $\mu\text{m}$  pore size syringe filters (Cat. No. SLGN033NK, Merck Pty Ltd, Australia) and the filtrates were collected in a 2 ml Eppendorf tube. The samples were immediately stored at 4 °C until analysed.

### **5.2.5 Effect of in-reactor pH on oxalate degradation rate**

Once the routine cyclic studies revealed stable reactor performance, the impact of in-reactor pH on oxalate removal rate was examined. The normal operation of the reactors was at a pH range of 9 – 9.5. The influence of different in-reactor pH values on oxalate removal rate was examined in a pH range of 7.0 to 12. pH values below 7 were not tested due to practical relevance. During the experiment, in-reactor pH set point was feedback-maintained using the programmable logic controller to dose either acid (1 M HCl) or base (1M NaOH). The biofilm was exposed to each of the in-reactor pH values over a single reactor cycle of 4 h. In the subsequent 5 cycles, the biofilm was allowed to recover under its normal operational conditions (i.e. exposed to a pH of 9 – 9.5). The influent DO during this experiment was maintained at 8 mg/L. The  $\text{Na}_2\text{C}_2\text{O}_4$  concentration introduced at the beginning of the cycle was 2 g/L and 0.8 g/L for N-supplemented and N-deficient reactors, respectively. During the experiment, hourly liquid samples were collected and immediately filtered through 0.22  $\mu\text{m}$  syringe filters (Cat No SLGNO33NK, Merck Millipore, USA) for oxalate measurement.

### **5.2.6 Removal of other organics and their influence on oxalate removal**

Bayer liquor contains other simple organic compounds such as sodium acetate, sodium formate, sodium succinate and sodium malonate (McKinnon & Baker, 2012). In this experiment, the influence of these organics on the removal of oxalate and their individual removal efficiencies were examined in both the N-supplemented and the N-deficient reactors. The effects of sodium acetate, sodium formate, sodium succinate and sodium malonate for each reactor were independently examined in 4 separate batch experiments. In each of the batch experiments, the additional carbon source was included to create an initial in-reactor chemical oxygen demand (COD) molar ratio of 1:1 between the additional carbon source and the oxalate. During these experiments, the influent pH (9.5) and DO (8 mg/L) were maintained at a constant. The removal of carbon sources was monitored over a 4 h cycle length by collecting hourly liquid samples (3 mL). On collection, the samples were immediately filtered through 0.22  $\mu\text{m}$  syringe filters (Cat No SLGNO33NK, Merck Millipore, USA) to enable quantitation of residual carbon. In between exposure to each carbon source, the biofilm

was allowed to recover under normal operational conditions (i.e. exposed to oxalate only) over five consecutive cycles.

### **5.2.7 Assessment of N-deficient conditions**

To confirm the N-deficient and N-supplemented conditions in the two reactors, the following assessments were carried out.

#### **5.2.7.1 In-reactor ammonia-N, nitrite-N and nitrate-N concentrations**

Ammonia-N, nitrite-N and nitrate-N concentrations in both N-deficient and N-supplemented reactors were monitored with frequent analysis of in-reactor liquid samples. Approximately 2 mL volumes of liquid samples were withdrawn and immediately filtered through 0.22 µm syringe filters (Cat No SLGNO33NK, Merck Millipore, USA) and the filtrates were analysed for residual ammonia, nitrite and nitrate using ion chromatography.

#### **5.2.7.2 Acetylene reduction assay**

The acetylene reduction assay was based on a method proposed by Sprent (1990). After 250 days of operation, two media samples were withdrawn from each N-deficient (16 mL) and N-supplemented (20 mL) reactors and were placed in four 150 mL bottles. Thereafter, 50 mL of N-deficient and N-supplemented growth media (pH 9) containing 2 g/L of oxalate were introduced into the respective bottles. The bottles were subsequently capped (using butyl rubber stoppers), crimped (with an aluminium seal) and flushed with helium for 3 min to remove any N<sub>2</sub> from the samples. Subsequently 2 % of the headspace helium was removed and replaced with pure oxygen in one N-deficient and one N-supplemented bottle. In the remaining two bottles, the headspace was completely flushed with pure oxygen. Subsequently, 2 % of the headspace volume of all four bottles was replaced with acetylene (produced by reacting DI water with calcium carbide ~ 1 g in a 1 L conical flask and the acetylene captured with displacement of water in a column). The sample was then incubated in

an environmental shaker at 28 °C. Liquid and headspace gas sampling were carried out on all 4 bottles at time intervals of 3, 16, 24, 40 and 48 h. Once collected, the liquid samples were immediately filtered through 0.22 µm syringe filters (Cat No SLGNO33NK, Merck Millipore, USA) and the filtrates were analysed for residual oxalate.

### **5.2.8 Analysis of samples**

#### **5.2.8.1 Analysis of organic carbon and nitrogen species**

Organic carbon and nitrogen species in samples were analysed using a Dionex ICS-3000 reagent free ion chromatography (RFIC) system equipped with an IonPac® AS18 4 x 250 mm column. The eluent for the system was potassium hydroxide (KOH) and the eluent flow rate was maintained at 1 mL/min. The eluent KOH concentration was 12 - 45 mM from 0 - 5 min, 45 mM from 5 - 8 min, 45 - 60 mM from 8 - 10 min and 60 - 12 mM from 10 - 13 min. Ammonium ( $\text{NH}_4^+ \text{-N}$ ) was measured with the same RFIC but with a IonPac® CG16, CS16, 5 mm column. Methansulfonic acid (30 mM) was used as an eluent with a flow rate of 1 mL/min. The temperature of the two columns was maintained at 30°C. Suppressed conductivity was used as the detection signal (ASRS ULTRA II 4 mm, 150 mA, AutoSuppressioin® recycle mode) for concentration determination. COD measurements of the filtered liquid samples were measured using a closed reflux dichromate method (HACH Method 8000, HACH Ltd).

#### **5.2.8.2 Gas analysis**

Acetylene and ethylene gases in the headspace were analysed using a Trace 1300 gas chromatograph (ThermoFisher Scientific, USA) fitted with a flame ionisation detector (FID). Rt®-U-BOND, (30 m, 0.32 mm ID, 10 µm, Cat.# 19752, Restek, USA) capillary column was used to measure the gases. A 100 µL volume of gas was manually injected using a gas tight syringe into a split injector (split flow 40 mL/min) maintained at 200 °C. Helium was used as the carrier gas and the flow rate through the capillary column was maintained at a constant pressure of 53.1 kPa. The initial oven

temperature was set at 100 °C for 1 min. Subsequently the temperature was raised to 150 °C at a rate of 25 °C/min and was finally held for 4 min. FID temperature was maintained at 230 °C and analysis was carried out using Chromeleon software (Version 7.1.2.1478).

#### **5.2.8.3 Estimation of dry biomass weight in reactors**

Known volumes of graphite biomass carriers were removed from the reactors and immersed in a known volume of deionized water in 50 mL Falcon tubes. Subsequently, the tubes were subjected to ultra-sonication (Sanophon ultrasonic cleaner - 90 watts and 50 Hz) for 3 min to dislodge the attached biofilm from the carriers. The suspensions containing the dislodged cells were then decanted into new 50 mL Falcon tubes and the carriers were sonicated once more for 3 min in deionized water. This final suspension was combined with the previous one and suspended solids (SS) and the volatile suspended solids (VSS) of the suspension were measured using methods detailed in the Standard Methods for Water and Wastewater Analysis (American Public Health, 1995).

### **5.3. Results and Discussion**

#### **5.3.1 Highly alkaline conditions impacted N-deficient reactor more than N-supplemented one**

The performance of the two aerobic reactors during the first six months of operation is summarized in chapter 4. Except when specific batch experiments were carried out, the in-reactor pH of both reactors was maintained at approximately 9 - 9.5 throughout the entire period of the study. The oxalate removal rate of both reactors was low at the start of the experiment. Since the inoculum used in both reactors was sourced from neutral pH environments, the immediate exposure to a highly alkaline environment may have negatively impacted the indigenous microorganisms present in the inoculum. While the negative impact appears to be less with the N-supplemented

reactor, the impact on the N-deficient reactor appears to be profound according to the chapter 4.

The oxalate removal rate of the N-supplemented reactor steadily increased without any notable lag phase. In contrast, a long lag period of 75 days was detected for the N-deficient reactor where oxalate removal remained negligible (Chapter 4, Figure 4.2). Often it is assumed that a lag phase enables adaptation of microorganisms to a new environmental condition (Madigan et al., 2000). This may include the repair of macromolecular damage (Dukan & Nystrom, 1998) and the synthesis of necessary cellular components required for growth.

The specific oxalate removal rate in N-supplemented reactor (110 mg/h.g biomass) was slightly higher than in N-deficient (87 mg/h.g biomass) reactor after 215 d of reactor operation and this difference in specific rates indicated that microorganisms in the N-supplemented reactor were more efficient at oxidising oxalate than those in the N-deficient reactor. The low specific oxalate removal rate on the other hand, could be a result of (1) an inhibition of activity due to exposure to high alkaline conditions and/or (2) a lower oxalate oxidising activity of the microorganisms under N-deficient conditions and /or (3) a lower initial oxalate concentration in N-deficient reactor. In addition to having differences in specific oxidation rates, the overall biomass concentrations in the two reactors were also notably different. The VSS of the N-supplemented reactor (10 mg/mL of graphite media) was 1.25 times higher than that of the N-deficient reactor (8 mg/mL of graphite media) (Refer Chapter 4). The low biomass concentration in the N-deficient reactor is another reason for the observed low rate of oxalate removal in this reactor.

Influence of pH on microbial activity and growth is well demonstrated in literature. For example, a pH value of 8 was noted desirable for ammonia oxidising bacteria, while a pH value greater than 7.5 was completely inhibitory towards nitrite oxidising bacteria (Villaverde et al., 1997). In this instance, the activity of both organisms was found to be dependent on specific free NH<sub>3</sub> concentrations. Accordingly, free NH<sub>3</sub> inhibition and the limitation of ammonia (due to volatilisation) are challenges associated with an N-supplemented reactor when exposed to high pH. Both of the above factors however, may not be causing any impact on the N-supplemented reactor

due to an oversupply of ammonia. However, further studies are required to validate this.

In the absence of an inorganic source of N, the oxalate oxidising activity recorded in the N-deficient reactor suggested that the microorganisms there would have to fulfil their N requirements plausibly via biological fixation of atmospheric N. It is well known that the enzyme responsible for catalysing the fixation of N is nitrogenase (Hernandez et al., 2009). This enzyme is known to be inhibited when exposed to highly alkaline conditions (Yang et al., 2014). According to Hadfield and Bulen (1969) and Igarashi et al. (2005), the pH dependence of nitrogenase activity exhibits a bell-shaped relationship, whereby an optimal activity is at approximately pH 7 - 8. Therefore an increase of pH beyond 8 significantly reduces activity, not due to high pH inactivation of MoFe-proteins in nitrogenase, but rather as a consequence of a complex, mechanism-based reaction (Yang et al., 2014). Accordingly, at pH 9, the N-deficient reactor was likely to have suffered a severe shortage of N (both as a result of limited fixation of atmospheric N and volatilisation of the produced ammonia), specifically impacting the growth of microorganisms. The low biomass concentration that prevailed in the reactor provides an indirect indication towards an inefficient fixation of N in this reactor. Overall, the high pH condition appears to have negatively impacted the performance of the N-deficient reactor, specifically in terms of maintaining a suitable concentration of biomass required for higher loading rates desirable for practical application.

### **5.3.2 The acetylene reduction assay on N-deficient biomass confirmed low nitrogenase activity**

No inorganic source of nitrogen was included in the feed of the N-deficient reactor. Frequent measurement of  $\text{NH}_4^+ \text{-N}$  and  $\text{NO}_x \text{-N}$  showed no measureable concentration of ammonia and  $\text{NO}_x \text{-N}$  in the N-deficient reactor. Although an inorganic source of nitrogen was not included, some organic nitrogen was introduced into the reactor in the form of yeast extract. The 10 mg/L concentration of yeast extract in the feed is unlikely to fulfil all N requirements of the biomass. Hence, nitrogen requirements of the N-deficient reactor were therefore likely fulfilled via biological nitrogen fixation.

Biological nitrogen fixation can be indirectly quantified using acetylene reduction assay (Hardy et al., 1968). Instead of N<sub>2</sub>, in this assay, acetylene is reduced by nitrogenase enzyme to form ethylene and by monitoring ethylene, the activity of nitrogenase can be assessed. When acetylene reduction assay was carried out using biomass from the N-deficient reactor, no ethylene was detected with both 2 and 100 % of oxygen over a 48 h incubation period. Exposure to higher concentration of oxygen is known to inactivate nitrogenase (Compaore & Stal, 2010a; Staal et al., 2007) and this could be one reason for the observed negative result with 100 % oxygen. However, the N-deficient reactor was at all times operated near saturation (8 mg/L) levels of dissolved oxygen. Hence the biofilm in the reactor can be assumed to be tolerant towards oxygen when fixing nitrogen. Specifically, the 2 % oxygen used in the assay was unlikely to cause any inhibitory effect as similar concentrations have been widely used in other acetylene reduction assays reported in the literature (Compaore & Stal, 2010b).

Overall the failure to obtain a measureable quantity of ethylene, suggested very low nitrogenase activity in the biomass of the N-deficient reactor. This supported the hypothesis that a severe nitrogen limitation (due to a low nitrogenase activity) in the N-deficient reactor failed to facilitate a high biomass concentration in N-deficient reactor.

### **5.3.3 The performance of the N-deficient reactor improved at close to neutral pH**

It is well known that proteins (e.g. enzyme) can be denatured at pH values outside the optimal range and this optimal range is largely species dependent. When considering the need to dilute the Bayer process liquor to reduce pH, having an understanding about the optimal pH range of the biological oxalate removal process becomes invaluable, as this would help reduce the treatment costs. Accordingly, the influence of pH on biological oxidation of oxalate under both N-supplemented and N-deficient conditions was examined (Figure 5.2).

Considering that the biomass in both reactors was acclimatised at pH 9, it was expected that both reactors would demonstrate optimal oxalate removal rates at pH 9. As expected, the N-supplemented reactor showed an optimal oxidation rate (105 mg/h.g

biomass) (Figures 5.2A and 5.2B) at pH 9. Interestingly, for the N-deficient reactor, the highest oxalate removal rate (130 mg/h.g biomass) was detected at a slightly lower pH range of 7 - 8 (Figures 5.2C and 5.2D). Compared to the oxalate removal rate at pH 9 (63 mg/h.g biomass), the removal rate at pH 7 was approximately 2 times higher in the N-deficient reactor. At this pH range, the specific oxalate removal rate was even higher than that of the N-supplemented reactor. These results suggested that the microorganisms in both reactors were equally active in oxidising oxalate given that the respective pHs were maintained at an optimal condition. Hence, for the N-deficient reactor to perform similarly to the N-supplement reactor (in terms of treatment load), the biomass needs to be exposed to a lower pH of approximately 7 - 8. However, a lower pH condition would translate into an increased cost of operation (i.e. increased chemical cost for pH reduction) which is undesirable for practical application.

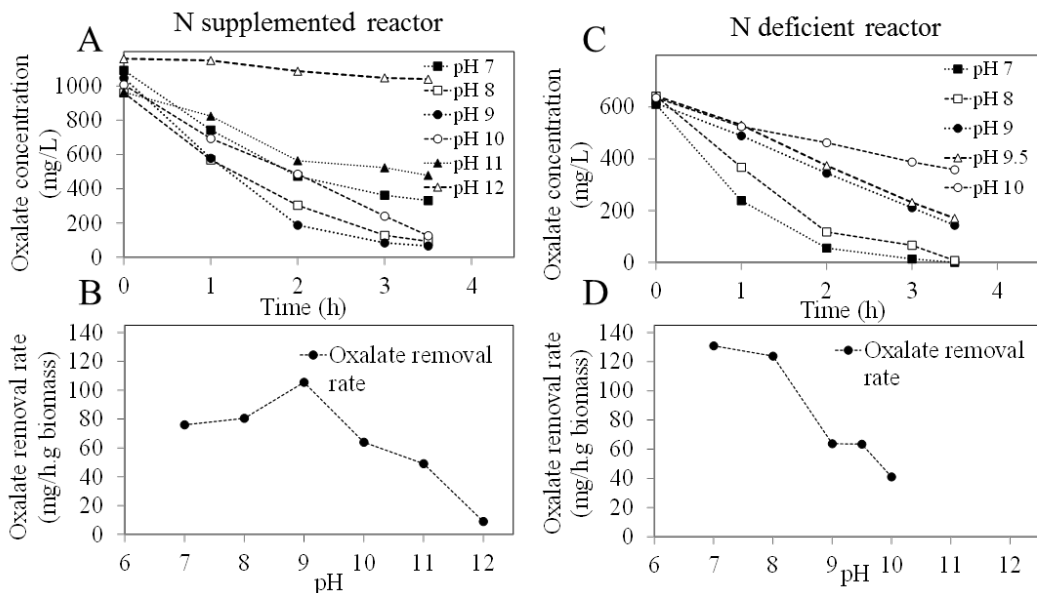


**Figure 5.2.** Oxalate concentrations during oxalate degradation and various initial pH values in the (A) N-supplemented reactor from day 167 and (B) N-deficient reactor from day 267. The influence of pH on oxalate removal rate in (C) N-supplemented and (D) N-deficient reactors as calculated based on initial 2 h of oxalate removal.

### 5.3.4 A continuous influent flow can facilitate the maintenance of optimum pH

Biological oxidation of oxalate generates carbonate resulting in a decrease of pH in the reactor. During a reactor cycle, both N-supplemented and N-deficient reactors

showed a gradual decrease of in-reactor pH from approximately 9 down to 8.5. Hence, in general, if an optimum pH of 9 and 8 is to be maintained in N-supplemented and N-deficient systems respectively, alkaline liquor needs to be continuously fed into both systems to control pH (also facilitates a steady supply of oxalate). As previously mentioned, at respective optimum pH values, the specific oxalate removal rates of both processes were similar. Hence, at optimum pH, both N-supplemented and N-deficient systems are able to produce a similar quantity of carbonate. As a consequence (i.e. with similar biomass concentrations), both systems will demand a similar loading rate of influent to maintain its respective optimum pH levels. Accordingly, by adopting a continuous mode of operation, the N-deficient system has the potential to even outperform the N-supplemented system in terms of the influent load that could be handled, the oxalate removal efficiency that could be achieved and low treatment cost that could be maintained due to no requirements for an external nitrogen source.

The N-deficient process was able to maintain optimal performance even at pH 7 and accordingly, it is even possible to achieve an effluent, which is near pH neutral with an N-deficient system using the above approach. The performance of the N-deficient system increased (from 63 to 130 mg/h.g biomass) when the pH was decreased from 9 to 7. The N-supplemented system on the other hand underperformed at pH 7 as the specific oxalate removal rate decreased from 105 to 76 mg/h.g biomass when the pH was changed from 9 to 7 (Figure 5.2B). The poor performance of the N-supplemented reactor at pH 7 could be a result of acclimatisation of the microorganisms at pH 9. Future studies should examine the specific oxalate removal rates of an N-supplemented and an N-deficient reactor acclimatised at pH 7 in order to understand whether N-deficient reactors would continue to outperform N-supplemented reactors at neutral pH.

### **5.3.5 The N-supplemented reactor was irreversibly impacted when in-reactor pH values exceeded 11**

Microorganisms in the N-supplemented reactor demonstrated two rates of oxalate removal when oxidising oxalate at the optimal pH of 9 (Figure 5.2A). A linear rate of oxalate removal (105.5 mg/h.g biomass) continued until the residual oxalate reached approximately 185 mg/L. Subsequently another lower linear rate (16.9 mg/h.g

biomass) of removal was detected. At pH 8, a similar reduction in oxalate removal rate was detected approximately at the same residual oxalate concentration. The oxalate removal profile at pH 10 did not however show a distinct rate change and maintained a consistent rate of removal (64 mg/h.g biomass) throughout the experiment. The residual oxalate concentration at pH 10 did not reach the 185 mg/L threshold during the entire period of experiment and this may be the reason for the non-occurrence of the second lower rate of oxalate removal. The change of oxalate removal rate from high to low at the above residual oxalate concentration is likely a response of microorganisms to substrate affinity.

The initial oxalate removal rates of both pHs 7 and 11 experiments were approximately 2 times lower compared to the rate observed at pH 9. Due to the reduced removal rates, the residual oxalate concentrations at pH 7 and 11 did not reach the 185 mg/L threshold to trigger a lower oxalate removal rate similar to that observed with pHs 9 and 8 experiments. Nevertheless, pH 7 and 11 experiments showed a reduction in removal rates after 2 h of oxidation and this reduction in oxalate removal rates was likely an inhibitory response to pH. The very low oxalate removal rate observed with the pH 12 experiment confirmed that pH 12 was remarkably detrimental to the biofilm.

A separate experiment was conducted to evaluate whether the observed pH inhibition was reversible (Figure 5.3). The results suggested that the inhibition caused by a short-term (4 h) exposure of the biofilm to pH 7 was reversible, as a subsequent correction of the pH to 9 showed an instantaneous increase of oxalate removal rate (Figure 5.3). However, exposing the biofilm to pH 12 for a similar period (4 h) resulted in an irreversible inhibition of oxalate removal, as a subsequent exposure to pH 9 failed to revert the oxalate removal activity of the biofilm (Figure 5.3). The inhibitory effect on the biofilm, even with such a short-term exposure to pH 12, was noted to be severe, with the biofilm requiring more than 18 reactor cycles (3 days) to regain original stable activity (data not shown).

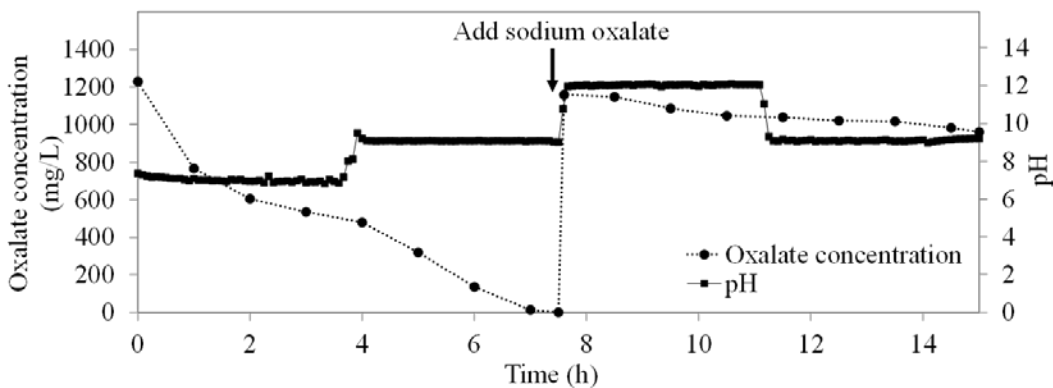


**Figure 5.3.** Reversible and irreversible inhibition of oxalate removal by N-supplemented reactor at in-reactor pH 7 and pH 12, respectively.

### 5.3.6 Short-term exposure to optimal pH conditions has a long-lasting impact with higher rates of oxalate removal in N-deficient reactor

There was a near linear improvement of oxalate removal (increasing by approximately 1.29 mg/L.h each day) after ~ 84 d of operating the N-deficient reactor at an in-reactor pH of 9 (Refer Chapter 4 Figure 4.2). With a decrease of in-reactor pH to 8, there was an instantaneous increase of oxalate removal rate (9.84 mg/L.h per day) (Figure 5.4). As anticipated, when in-reactor pH was returned to pH 9, there was an immediate reduction in the oxalate removal rate. However, after an initial decrease, the oxalate removal continued to increase at a lower rate (4.43 mg/L.h per day) with exposure to pH 9 (Figure 5.4). This improvement in reactor performance at pH 9 after a period of exposure to an in-reactor pH of 8, suggested an improvement in biological activity which was likely a result of an increase in biomass concentration. After 5 days of exposure to pH 9, when the in-reactor pH was once again reduced to 8, the oxalate removal once again increased (16.9 mg/L.h per day) (Figure 5.4).

This experiment hints at a strategy that could be effectively used to increase the biomass activity of an N-deficient biofilm oxidising oxalate exposed to an unfavourable high pH such as pH 9. As previously highlighted, nitrogenase activity is compromised at high pH (Yang et al., 2014), and this likely imposes severe nitrogen limitation, affecting microbial growth. The exposure to favourable pH conditions increases nitrogenase activity reducing limitations of nitrogen for growth and as a consequence, a rapid increase of biomass can be anticipated. With prolonged exposure

to unfavourable pH, the higher rate of oxalate removal is unlikely to be sustainable specifically if the level of nitrogenase activity is not sufficient to maintain the biomass in the reactor. Therefore, an intermittent exposure to a favourable pH such as 8 may be needed if the higher rate of oxalate removal is to be maintained long-term at pH 9. Alternating between a favourable and unfavourable pH facilitates biomass management and future research should examine the development of smart operational strategies that could capitalise on this finding to reap economic benefits from using N-deficient biomass to oxidise oxalate.

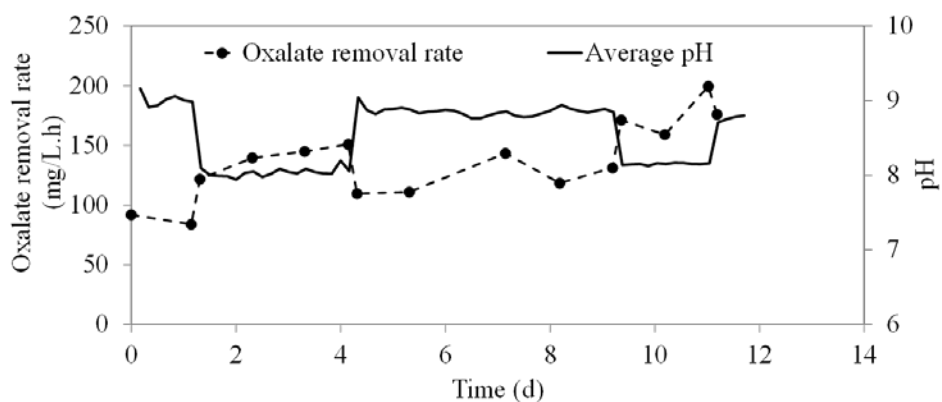


**Figure 5.4.** Intermittent exposure to a favourable pH and its impact on the removal of oxalate after the exposed to an unfavourable pH from day 298.

### 5.3.7 Other organic impurities in Bayer liquor could potentially increase the performance of N-deficient reactor

Power et al. (2011c) provides a summary of the organic compounds detectable in Bayer process liquor. Of the large number of organic compounds in Bayer liquor, oxalate imposes a major impact (due to co-precipitation with aluminium trihydroxide), while other organics tend to have a limited impact on the overall process (Brady, 2011). The increase in concentration of other organics with the recycling of process liquor, however, is of concern and requires management.

Although primarily acclimatised to only oxidise oxalate, both N-supplemented and N-deficient reactors demonstrated the ability to simultaneously oxidise other organic compounds introduced alongside oxalate (Figure 5.5). The impact of other organic compounds on the oxidation of oxalate appeared negligible with both reactors, as the

recorded oxalate oxidation rates remained similar even with the presence of other organics (Figures 5.5).

With the exception of succinate, the oxidation rates of other organic compounds were remarkably lower (approximately half) compared to the oxidation rate of oxalate in the N-supplemented reactor. The oxidation rate of succinate (10 mg-COD/h.g biomass) in the N-supplemented reactor was only marginally different to the oxidation rate of oxalate (14 mg-COD/h.g biomass). Similar results were recorded with the N-deficient reactor. However, instead of succinate, the oxidation rate of acetate (10 mg-COD/h.g biomass) was only marginally different to the oxidation rate of oxalate (12 mg-COD/h.g biomass). Formate was the only carbon source that was completely oxidised in the N-supplemented reactor during the 4 h experiment, whereas acetate was the only carbon source that was completely oxidised in the N-deficient reactor.

The oxidation profiles of oxalate and most other organic carbon sources showed a parallel trend to each other (Figures 5.5C–J) in both of the N-supplemented and N-deficient reactors. This implied a concomitant oxidation of the two substrates (i.e. oxalate and the additional carbon source). Co-metabolism refers to a concomitant oxidation of a non-growth substrate during the growth of a microorganism on an utilisable carbon and energy source (Wackett, 1996) and in this instance, further studies are needed to confirm whether the oxidation of other organic compounds was a result of co-metabolism.

The N-deficient reactor showed an overall lower concentration of biomass. While an inhibition of nitrogenase activity at high pH may have resulted in a lower concentration of biomass, the higher energy demand of nitrogen fixation may also have limited the availability of carbon to facilitate the growth of microorganisms in the N-deficient reactor. The energy gain from the oxidation of oxalate ( $\Delta G^\circ = -608.46 \text{ KJ mol}^{-1}$ ) is 1.5 times lower than what could be gained from acetate ( $\Delta G^\circ = -925.88 \text{ KJ mol}^{-1}$ ) and 2.9 times lower than what could be gained from succinate ( $\Delta G^\circ = -1740.57 \text{ KJ mol}^{-1}$ ). Accordingly, if the high demand of energy for nitrogen fixation was impacting the biomass growth in the N-deficient reactor, this impediment could potentially be eliminated by the N-deficient biofilm's ability to co-oxidise other organic carbon sources present in Bayer liquor. Future research is needed to consolidate fundamental

knowledge about slow growth of biomass in the N-deficient reactor and to examine the effectiveness of the discussed strategies to overcome this limitation.

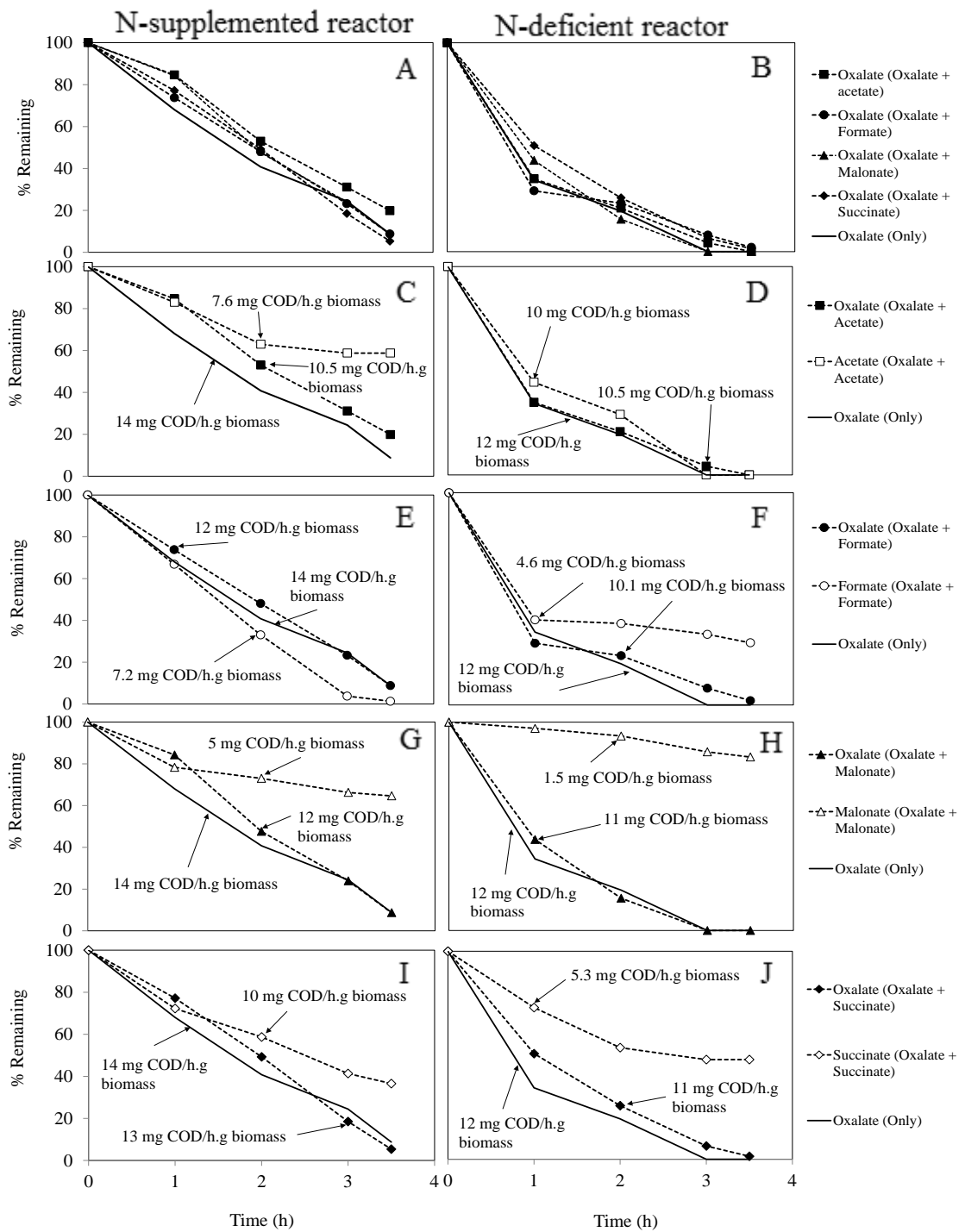


**Figure 5.5.** The efficacy of N-supplemented and N-deficient biofilms to oxidise organics other than oxalate and the influence of other organics on oxalate removal. The tests were carried out for N-supplemented reactor from day 229 and for N-deficient reactor from day 413.

### **5.3.8 Implication of the findings**

As demonstrated, the biological oxidation of oxalate could be facilitated by using both N-supplemented and N-deficient reactors. The tested systems have the potential to effectively treat similar oxalate loads. There are obvious operational savings that could be achieved using N-deficient systems (due to no requirements of an external nitrogen source), but in order to realise these savings, current operational strategies need to be revisited to specifically favour the N-deficient treatment systems. This study highlights some beneficial strategies that could be considered for optimising the efficiency of N-deficient systems, for example by capitalising on the carbonate produced during oxidation of oxalate to impose an in-reactor fluctuation of pH.

The ability of both reactors to co-oxidise other organics present in Bayer liquor is not only beneficial but has the potential to increase the activity of an N-deficient reactor. The extra energy and carbon available as a result of co-oxidation may enable the N-deficient reactor to better respond to the extra energy demand required for nitrogen fixation. In contrast, the N-supplemented reactor could get hampered with an excessive increase of biomass growth, which could lead to operational challenges such as oxygen mass transfer limitation and a build-up of anaerobic pockets (could lead to methane emissions due to the fermentation of oxalate and other organics). In summary, this comparative study provides insight on N-deficient systems and highlights opportunities for the alumina industry to embrace N-deficient systems to remove oxalate from Bayer liquor.

## **5.4. Conclusions**

This study for the first time examined the impact of pH and other organics of Bayer liquor on two biofilm reactors under N-supplemented and N-deficient conditions. Based on the results of this study, N-supplemented reactor performs better in oxalate removal rate and has much shorter start-up period compared to an N-deficient reactor at pH 9 that the biomass was acclimatised. However, when exposed to optimal pH conditions, the N-deficient and N-supplemented reactors achieved similar oxalate removal rates. The N-supplemented reactor was irreversibly impacted when exposed to an in-reactor pH exceeding 11 and the oxalate removal inhibition at pH 7 however,

was reversible. A short-term exposure of the N-deficient biofilm to an optimal pH 8 induced higher oxalate removal rates at pH 9. Accordingly, the carbonate produced during oxidation of oxalate could be used to impose an in-reactor fluctuation of pH, in order to expose the biofilm intermittently to an optimal pH environment promoting growth of biomass. Other organic impurities in Bayer liquor had a negligible effect on oxalate removal rates and potentially could increase the performance of the N-deficient reactor.

# **6 A COMPARATIVE STUDY ON THE KINETICS OF OXALATE DEGRADATION AND MICROBIAL COMMUNITIES OF AEROBIC BIOREACTORS OPERATED UNDER NITROGEN SUPPLEMENTED AND DEFICIENT CONDITIONS**

Extended from

Weerasinghe Mohottige, T.N., Kaksonen, A.H., Cheng, K.Y., Sarukkalige, R. and Ginige, M.P. (2017) A comparative study on the kinetics of oxalate degradation and microbial communities of aerobic bioreactors operated under nitrogen supplemented and deficient conditions. Chemical Engineering Journal. Submitted.

## **Chapter Summary**

Some alumina refineries have embraced biological oxalate degradation as a cost-effective method for oxalate destruction. However, until now, there has been paucity of information available on oxalate degradation kinetics, although it is a key design factor for developing bioreactor processes. Hence, this study determined oxalate degradation kinetics in two aerobic packed bed biofilm reactors under N-supplemented and N-deficient conditions. Michaelis-Menten equation was used to derive kinetic parameters for specific oxalate degradation. The N-deficient culture had a higher affinity ( $K_m$  of 458.4 vs. 541.9 mg/L) towards oxalate and a higher maximum specific oxalate removal rate ( $V_{max}$  of 161.3 vs. 133.3 mg/h.g biomass) compared to the N-supplemented culture, suggesting that the N-deficient culture is better suited to remove oxalate. Microbial community analysis also showed differences in the composition of the two cultures. Based on kinetic parameters derived, a novel two step oxalate removal process was proposed that capitalises on higher specific oxalate removal rates for efficient oxalate destruction from waste streams of alumina industry.

## 6.1 Introduction

Aluminium is one of the most commercially utilized metals in the world due to its light weight, high strength and excellent corrosion resistance (Meyers, 2004). Pure aluminium does not occur in its metallic form and refining is required to produce aluminium from its mineral ore. Bauxite is the most commonly used aluminium ore and it is refined in Bayer process to produce alumina ( $\text{Al}_2\text{O}_3$ ) (Meyers, 2004; Power et al., 2011b). In brief, the major steps of the Bayer process are (1) digestion of bauxite in a hot concentrated caustic solution; (2) recovery of aluminium hydroxide with seeded precipitation at low temperature; and (3) calcination of aluminium hydroxide to produce alumina.

The raw bauxite generally contains organic carbon (0.02 – 0.2 % by weight) and a higher percentage is found in Australian bauxite ores (0.2 – 0.3 % by weight) as compared to those found in other countries (Hind et al., 1999; Power et al., 2012). The organic impurities are released from the ore during digestion and accumulate in the process liquor due its repeated reuse. Among the organic impurities, sodium oxalate severely impacts the productivity and product quality of the Bayer process due to the co-precipitation of oxalate with aluminium hydroxide (Power et al., 2012; Power & Tichbon, 1990). Depending on the plant capacity of an alumina refinery, the daily accumulation of oxalate in spent liquor could be significant. For example, in 2007, an alumina refinery in Western Australia generated 38 - 40 t/d of oxalate while processing 21,000 t/d of bauxite (McSweeney, 2011). To prevent the co-precipitation of oxalate with gibbsite, oxalate concentration in spent liquor is maintained below supersaturation concentrations and a common practise is to maintain a spent liquor oxalate concentration of approximately 2.5 – 2.8 g/L (Barnett et al., 1995; Whelan et al., 2003). The NaOH concentration in spent liquor is approximately 4 M and a direct biological removal of oxalate (~ 40 t/day) from spent liquor would necessitate a reduction of NaOH in spent liquor from 4 M (pH 14.6) down to approximately 0.01 mM (pH 9). A near 99.99975 % removal of NaOH from spent liquor is operationally detrimental to the Bayer process as external addition of NaOH is then needed to increase NaOH concentrations back to 4 M before the effluent could be re-combined with spent liquor. Accordingly, biological removal of oxalate directly from spent liquor is uneconomical. Hence biological oxidation of oxalate is currently practiced by

some refineries to destroy oxalate that had been crystallised (oxalate cake) from spent liquor (McKinnon & Baker, 2012).

Prior to the biological destruction of oxalate, liquor burning has been practiced to not only remove oxalate but also to recover sodium (as Na<sub>2</sub>O) from crystallised oxalate. Compared to energy costs of liquor burning, biological oxalate degradation is economical and as a consequence alumina refineries are increasingly embracing biological processes to remove oxalate (Chinloy et al., 1993; McKinnon & Baker, 2012). For effective onsite management of oxalate, an efficient biological process that has high volumetric removal rates and a small foot print is highly desirable to minimise capital and operating costs (McKinnon & Baker, 2012).

The bioavailable nitrogen (N) content in crystallised oxalate waste is low, and in current biological oxalate removal processes N requirements are met by adding an external N-source. Hence, the currently used bioreactor processes rely microbial communities that demand an external N source to oxidise oxalate. Recently, Weerasinghe Mohottige et al. (Weerasinghe Mohottige et al., 2017a) for the first time demonstrated the feasibility of using N-fixing haloalkaliphilic bacteria to oxidise oxalate alleviating the need for external dose of N. From an operational point of view the use of N-fixing bacteria without the need to externally supplement N would have environmental and cost benefits for the alumina industry. External N sources, specifically as NH<sub>3</sub>, are often supplied in excess, to compensate for the possible loss through volatilisation of NH<sub>3</sub> at high pH. Such operational issues can be avoided with N-deficient systems that utilise N-fixing bacteria. Hence the alumina industry could consider utilising N-fixing bacteria specifically if they are demonstrated comparable or superior in terms of reaction kinetics. However, to date, the degradation kinetics of oxalate under both N-supplemented and N-deficient conditions has not been explored.

In this study, two aerobic packed bed biofilm reactors (one N-supplemented and the other not supplemented (N-deficient)) were operated for a period of 275 days using a synthetic alkaline, saline oxalate-containing medium. The Michaelis-Menten model was applied to comparatively assess oxalate degradation kinetics ( $K_m$  and  $V_{max}$ ) of both cultures to evaluate the suitability of the N-deficient system for industry application. Moreover, the composition of microbial communities in the two reactors

were analysed by next generation sequencing to reveal differences in the dominant microbial groups.

## 6.2 Materials and methods

### 6.2.1 Aerobic bioreactor set up

Two identical laboratory-scale packed bed column reactors (Figure 6.1) were operated under aerobic conditions similar to describe in chapter 4. Each packed bed column had an internal diameter and height of 55 mm and 400 mm, respectively. The columns were packed with graphite granules (3-5 mm diameter, KAIYU Industrial (HK)) to create a bed volume of 600 mL. The weight of the air-dried graphite granules in each reactor was 480 g and once packed, the void volume of the granular column was 210 mL. The granular media in the packed beds were exposed to feed solutions that were continuously aerated in 2 L glass bottles, which were used as solution reservoirs. The feed solutions were recirculated from the reservoirs through the columns in an up-flow direction at a flow rate of 9.6 L/h resulting in a hydraulic retention (HRT) time of 1.3 min in the column reactors. The solution in the reservoirs were changed every 4 h. At the beginning of each 4 h cycle, concentrated stock solutions (carbon and nutrients) were pumped in for 2 min together with deionised water to create a 1.3 L volume of working solution in the reservoirs. To maintain a near saturation level of oxygen in the working solution, compressed air was sparged into the solution reservoirs throughout the entire cycle. At the end of each cycle, the entire volume of the solution reservoirs was decanted, while the graphite granules in the column remained completely submerged. Hence, with retained solution in the column (200 mL), the total volume recirculated in each reactor was 1.5 L.

The reactors were monitored and controlled using data acquisition / control hardware (CompactRio National Instruments, USA) and software (Labview, National Instrument, USA). Online monitoring of dissolved oxygen (DO) and pH were carried out using a luminescent DO probes (PDO2, Barben Analyzer Technology, USA) and an intermediate junction pH probes (Ionode IJ44, Ionode Pty Ltd, Australia), respectively. In each reactor, two DO probes were used, with one immersed in the

liquid of the solution reservoir and the other placed at the outlet of the column reactor. All experiments were carried out at room temperature ( $\sim 23^{\circ}\text{C}$ ).

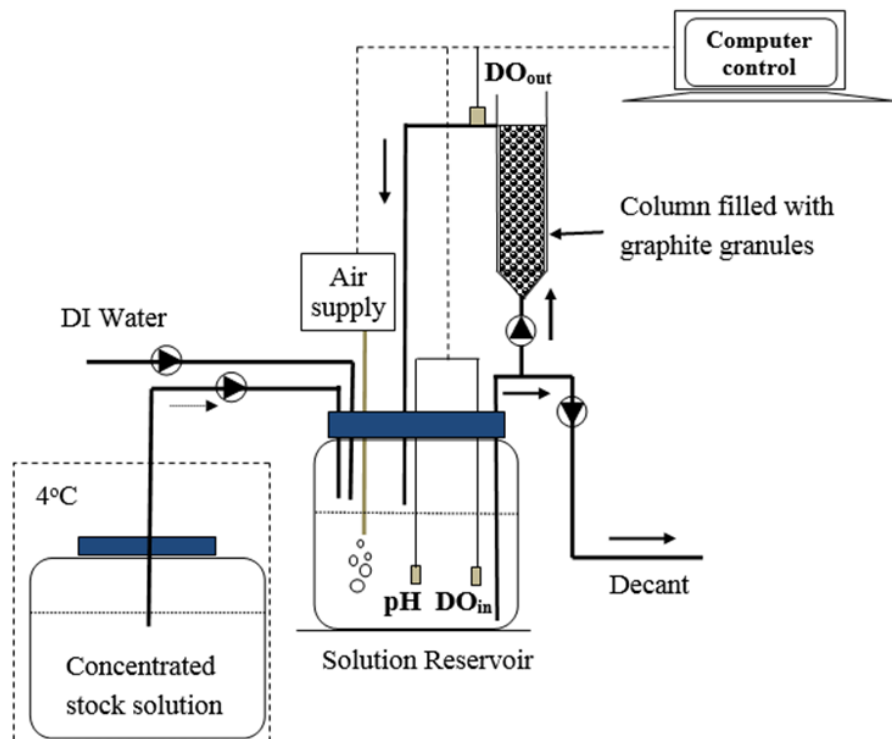


**Figure 6.1.** A schematic diagram of the laboratory-scale aerobic packed bed bioreactor.

### 6.2.2 Synthetic Medium

The working solution for the reactors contained sodium oxalate ( $\text{Na}_2\text{C}_2\text{O}_4$ ) as the carbon source and 25 g/L of NaCl, simulating Bayer liquor in its salinity. The pH of the influent stream was adjusted to 9.0 - 9.5 using 2 M NaOH. Additionally, the working solution also contained a growth medium, which contained (per L): 125 mg  $\text{NaHCO}_3$ , 51 mg  $\text{MgSO}_4 \cdot 7\text{H}_2\text{O}$ , 15 mg  $\text{CaCl}_2 \cdot 2\text{H}_2\text{O}$ , 20.5 mg  $\text{K}_2\text{HPO}_4 \cdot 3\text{H}_2\text{O}$ , and 1.25 mL of trace element solution. The trace element solution contained (per L): 0.43 g  $\text{ZnSO}_4 \cdot 7\text{H}_2\text{O}$ , 5 g  $\text{FeSO}_4 \cdot 7\text{H}_2\text{O}$ , 0.24 g  $\text{CoCl}_2 \cdot 6\text{H}_2\text{O}$ , 0.99 g  $\text{MnCl}_2 \cdot 4\text{H}_2\text{O}$ , 0.25 g  $\text{CuSO}_4 \cdot 5\text{H}_2\text{O}$ , 0.22 g  $\text{NaMoO}_4 \cdot 2\text{H}_2\text{O}$ , 0.19 g  $\text{NiCl}_2 \cdot 6\text{H}_2\text{O}$ , 0.21 g  $\text{NaSeO}_4 \cdot 10\text{H}_2\text{O}$ , 15 g ethylenediaminetetraacetic acid (EDTA), 0.014 g  $\text{H}_3\text{BO}_3$ , and 0.05 g  $\text{NaWO}_4 \cdot 2\text{H}_2\text{O}$ . For the N-supplemented reactor the medium additionally contained 25 mg NH<sub>4</sub>Cl, whereas for the N-deficient reactor medium, 10 mg/L yeast extract was additionally added to supplement nutritional requirements of N-fixing bacteria (Gauthier et al.,

2000; Sorokin et al., 2008). The nitrogen supplemented and deficient reactors were initially operated with sodium oxalate concentrations of 2.0 g/L and 0.8 g/L, respectively, and the concentrations were later varied for the kinetic experiments.

### **6.2.3 Microbial inoculum**

A sediment sample from Floreat Beach and two soil samples from Perry Lake Reserve (Perth, Western Australia) were used as an inoculum. Oxalic acid is well known to exist in both costal sediments and around rhizosphere of plants (most plant cells accumulate oxalic acid). Additionally, the microorganisms in coastal sediments are tolerant to saline conditions and soil samples at near vicinity of rhizosphere of native plants contain N-fixing bacteria (Gupta et al., 2014). An equal weight (75 g) of sediment from the three locations were mixed together and placed in two separate 2 L glass bottles. Thereafter, 1.5 L of N-supplemented and N-deficient feed solutions were placed in the respective bottles and 100 mg/L Na<sub>2</sub>C<sub>2</sub>O<sub>4</sub> was added as a carbon source into each of the bottles. The two bottles were aerated at room temperature for 3 weeks to enrich aerobic oxalate degrading microorganisms. During the enrichment (3 weeks), aeration was interrupted once a week for a period of 1 h to settle suspended solids. Subsequently, the supernatant (1 L) was discarded and replenished with respective fresh feed solutions.

### **6.2.4 Reactor start up**

During the initial 3 weeks, the 2 L bottles were operated without the packed bed column reactors. After 3 weeks of operation, the sediment in each of the bottles were removed upon disturbing the attached biomass vigorously by shaking. Subsequently, the packed bed columns were connected and the bottle contents were recirculated through the respective columns.

The 1 d cycle length of the reactors were gradually reduced to 4 h and subsequently Na<sub>2</sub>C<sub>2</sub>O<sub>4</sub> concentrations in the working solutions were stepwise increased until a steady maximum biofilm activities were achieved. The optimised Na<sub>2</sub>C<sub>2</sub>O<sub>4</sub>

concentrations for the 4 h cycle in the N-supplemented and N-deficient reactors were 2.0 g/L and 0.8 g/L, respectively.

During the microbial enrichment and thereafter, cyclic studies were carried out to determine the oxalate removal rates of the bioreactors. Cyclic studies were carried out once every two weeks and the number and the frequency of sampling depended on cycle length. Hourly sampling was carried out once cyclic length was reduced to 4 h. During sampling, 3 mL volumes were withdrawn from the 2 L solution reservoirs and were immediately filtered through 0.22 µm pore size syringe filters (Cat. No. SLGN033NK, Merck Pty Ltd, Australia) into 2 mL Eppendorf tubes. The samples were then stored at 4°C until analysed.

#### **6.2.5 Investigating the effect of initial oxalate concentration on oxalate degradation**

After reaching stable reactor performance, the effect of initial oxalate concentration on oxalate degradation kinetics was investigated on both packed bed column reactors. Each initial oxalate concentration was tested over a single 4 h cycle. Between each of the initial oxalate concentrations tested, the biofilm was allowed to recover over 5 normal operational cycles. The initial sodium oxalate concentrations tested with N-supplemented and N-deficient reactors ranged 0.2 - 5 g/L and 0.2 - 4 g/L, respectively. During the kinetic studies, hourly liquid samples (3 mL) were collected, immediately filtered (through 0.22 µm syringe filters (Cat No SLGNO33NK, Merck Millipore, USA)) and stored (at 4 °C in 2 mL Eppendorf tubes) for later analysis of oxalate concentrations.

#### **6.2.6 Determination of biomass dry weight**

The dry weight of biofilm in the packed bed columns was determined by using a known volume (50 mL) of packed granules coated with biomass. Known volumes of graphite media were removed from the reactors and placed together with a known volume (13 mL) of deionized water in 50 mL Falcon tubes. Subsequently, the tubes were placed in an ultra-sonication (Sanophon ultrasonic cleaner - 90 watts and 50 Hz) water bath

for 3 min to dislodge attached biofilms. The suspensions with dislodged cells were then decanted into new 50 mL Falcon tubes and the graphite media were sonicated once more for 3 min in fresh deionized water. The respective final suspensions were combined and total suspended solids (TSS) and volatile suspended solids (VSS) were measured using methods detailed in the Standard Methods for Water and Wastewater Analysis (American Public Health Association. et al., 1995).

### **6.2.7 Kinetic calculations**

The oxalate oxidation rates were normalised to the total dry weight of the biomass in the column reactor. Michaelis-Menten equation (Equation 6.1) and three other graphical representations of enzyme kinetics (Equations 6.2-6.4) were used to obtain the kinetic parameters  $V_{max}$  (maximum initial oxalate removal rate) and  $K_m$  (Michaelis constant - numerically equal to the concentration of substrate that facilitates a half maximal initial oxalate removal rate) for oxalate degradation (Cornish-Bowden, 1995; Kaksonen et al., 2003).  $V$  is the degradation rate,  $[S]$  is the substrate concentration,  $V_{max}$  is the maximum degradation rate and  $K_m$  is Michaelis-Menten constant.

Michaelis-Menten equation:

$$V = (V_{max} \times [S]) / (K_m + [S]) \quad (\text{Equation 6.1})$$

Lineweaver-Burk plot:

$$1/V = (K_m/V_{max}) \times (1/[S]) + (1/V_{max}) \quad (\text{Equation 6.2})$$

Hanes Plot:

$$[S]/V = (K_m/V_{max}) + (1/V_{max}) \times [S] \quad (\text{Equation 6.3})$$

Eadie-Hofstee plot:

$$V = V_{max} - K_m \times (V/[S]) \quad (\text{Equation 6.4})$$

### **6.2.8 Assessment of N deficient conditions**

The nitrogen deficient reactor did not receive any form of nitrogen other than 10 mg/L of yeast extract throughout the experimental period. The use of yeast extract is common specifically to supplement essential nutrient requirements for the growth of nitrogen fixing bacteria (Gauthier et al., 2000; Sorokin et al., 2008). To confirm the absence of inorganic nitrogen in the reactor, liquid samples collected from the influent and effluent of the reactor were analysed for soluble nitrate ( $\text{NO}_3^-$ ), nitrite ( $\text{NO}_2^-$ ) and ammonium ( $\text{NH}_4^+$ ) using a Dionex ICS-3000 reagent free ion chromatography (RFIC) system.

### **6.2.9 Chemical analysis**

Oxalate and other anion concentrations were analysed using a Dionex ICS-3000 reagent free ion chromatography (RFIC) system, which was fitted with an IonPac® AS18 4 x 250 mm column. Potassium hydroxide was the eluent for anion separation at a flow rate of 1 mL min<sup>-1</sup>. The eluent concentration was 12 - 45 mM from 0 - 5 min, 45 mM from 5 - 8 min, 45 - 60 mM from 8 - 10 min and 60 - 12 mM from 10 - 13 min. NH<sub>4</sub><sup>+</sup>-N was measured with the same RFIC but with a IonPac® CG16, CS16, 5 mm column using 30 mM methansulfonic acid eluent with a flow rate of 1 mL min<sup>-1</sup> for 29 min. The temperature of the two columns were maintained at 30 °C. Suppressed conductivity was used as the detection signal (ASRS ULTRA II 4 mm, 150 mA, AutoSuppression® recycle mode).

### **6.2.10 Microbial Analysis**

The biofilm coated granules (15 mL) were separately collected from each packed bed column reactor into two 50 mL centrifuge tubes for DNA extraction. Sampling for microbial community analysis was carried out after 3 weeks of reactor start-up (Samples no. NS21D and ND21D from N-supplemented and N-deficient reactor, respectively) and during optimisation of N-supplemented (Samples NS83D, NS141D and NS221D on days 83, 141 and 221, respectively) and N-deficient reactor (Samples ND225D, ND253D and ND280D on days 225, 253 and 280, respectively) operation.

On collection of the granules into the 50 mL centrifuge tubes, deionized water was added and the tubes were sonicated for 2 min using a Sanophon ultrasonic water bath (90 watts, 50 Hz) to detach the biomass. The deionized water (with dislodged biomass) in the sonicated tubes was decanted into fresh 50 mL centrifuge tubes and the granules were re-sonicated once more with an equal volume of fresh deionise water. The deionised water in the sonication tubes were combined with respective previous collections and the biomass in the cells were pelleted via centrifugation (at 6000 g for 5 min). The supernatants were subsequently decanted and the pelleted biomass was used for DNA extraction.

#### **6.2.10.1 DNA extraction**

DNA was extracted from 250 µL of pelleted biomass using Power Soil DNA isolation kit (MO BIO laboratories, USA) following manufacturer's instructions. The extracted DNA was quantified using a Qubit fluorometer and stored at -20°C prior to delivery to the School of Pathology and Laboratory Medicine, University of Western Australia for 454 sequencing.

#### **6.2.10.2 Microbial community analysis**

The 454 sequencing was carried out as describe in (Nagel et al., 2016). In brief, microbial 16S rRNA genes were amplified from 1 ng aliquots of the extracted DNA using V4/5 primers (515F: GTGCCAGCMGCCGCGGTAA and 806R: GGACTACHVGGGTWTCTAAT). A mixture of gene-specific primers and gene-specific primers tagged with Ion Torrent-specific sequencing adaptors and barcodes were used. The tagged and untagged primers were mixed at a ratio of 90:10. Using this method, the amplification of all samples was achieved with 18 - 20 cycles, minimising primer-dimer formation. The amplification was confirmed by agarose gel electrophoresis, and PCR product was quantified using fluorometry. Up to 100 amplicons were diluted to equal concentrations and adjusted to a final concentration of 60 pM. Templated Ion Sphere Particles (ISP) were then generated and loaded onto sequencing chips using an Ion Chef (Thermofisher Scientific) and samples were sequenced on a PGM semiconductor sequencer (Thermofisher Scientific) for 650

cycles using a 400 bp sequencing kit typically yielding a modal read length of 309 bp. Data collection and read trimming/filtering was performed using TorrentSuite 5.0.

Post sequence analysis was carried out using an open source software package QIIME (Quantitative Insights Into Microbial Ecology) (Caporaso et al., 2010b). The fasta, qual and mapping files were analysed using downstream computational pipelines of QIIME. The chimeric reads were identified and filtered using USEARCH and an unaligned reference Greengenes database (gg\_13\_5.fasta obtained from [http://greengenes.secondgenome.com/downloads/database/13\\_5](http://greengenes.secondgenome.com/downloads/database/13_5)). Subsequently operational taxonomic units (OTUs) were assigned at 97 % sequence similarity using the same reference database file from Greengenes. For each OTU picked, a representative sequence was assigned and a final taxonomic assignment was carried out using the RDP classifier version 2 (Wang et al., 2007) with reference to the same Greengenes database. The unprocessed DNA sequences of this study were deposited (accession numbers SRR5982975, SRR5982976 to SRR5982982) in NCBI's (National Centre for Biotechnology) Sequence Read Archive (SRA) (Meyer et al., 2008).

## 6.3 Results and Discussion

### 6.3.1 Bioreactor performance

Both N-supplemented and N-deficient reactors showed a stable removal of oxalate after approximately 200 d of operation. Regular monitoring of inorganic nitrogenous species in N-deficient reactor revealed no detectable concentration of  $\text{NO}_3^-$ -N,  $\text{NO}_2^-$ -N and  $\text{NH}_4^+$ -N in both the influent and effluent of the reactor. In N-supplemented reactor, although no  $\text{NO}_3^-$ -N and  $\text{NO}_2^-$ -N were detected, an  $\text{NH}_4^+$ -N concentration of approximately  $60 \pm 3$  mg/L and  $< 8$  mg/L was detected in the influent and effluent, respectively. The low  $\text{NH}_4^+$ -N concentration in the effluent was likely due to volatilisation of  $\text{NH}_3$  at high pH and usage by microorganisms for growth and cell maintenance. The N demand of the N-deficient reactor, on the other hand, was likely fulfilled with atmospheric fixation of  $\text{N}_2$ .

After 3 weeks of enrichment, the oxalate removal rates of N-supplemented and N-deficient reactors were 34 mg/L.h and 1 mg/L.h, respectively. The oxalate removal rate of the N-supplemented reactor showed a linear increase (from 34 to 364 mg/L.h ( $R^2 = 0.98$ )) during the optimisation of reactor operation. In contrast, a much slower linear increase of oxalate removal was recorded for N-deficient reactor and during stable operation of reactor, a steady removal rate of 187 mg/L.h was achieved. A typical cyclic study, of N-supplemented and N-deficient reactors (Figure 6.2) showed a linear decrease of oxalate over time. During the 3.5 h reaction time, alongside removal of oxalate, a gradual decrease of pH was noted (a reduction of pH from 9.5 to 8.7 and 9.3 to 8.8 in N-supplemented and N-deficient reactors, respectively) in both reactors. Biological degradation of oxalate generates carbonate, and this resulted in a decrease of pH in the reactors (Figure 6.2). Unlike pH, the oxygen uptake rate (OUR) of both reactors remained steady (285 mg O<sub>2</sub>/L.h and 140 mg O<sub>2</sub>/L.h in N-supplemented and in N-deficient reactors, respectively) throughout the cycle and the OUR only decreased (to 75 mg O<sub>2</sub>/L.h and 70 mg O<sub>2</sub>/L.h in N-supplemented and in N-deficient reactors respectively (Data not shown)) on complete exhaustion of oxalate in both reactors. The reduced OUR values represent endogenous respiration rates of the reactors.

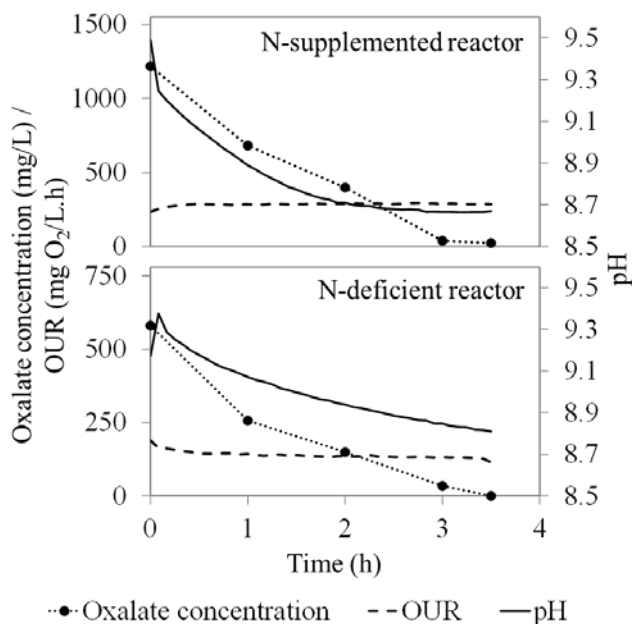


**Figure 6.2.** Profiles of in-reactor oxalate concentration, oxygen uptake rate (OUR) and pH during a 3.5 h aerobic reactor reaction time.

### 6.3.2 Oxalate degradation kinetics

In this study, a sequencing batch mode of operation was used with both N-supplemented and N-deficient reactors. Sequencing batch reactors are highly beneficial specifically when enforcing strict hydraulic boundaries. However, continuous flow reactors are desired specifically to minimise complexities of operation. In order to conceptualise oxalate removal in continuous flow reactors with these two cultures, kinetic parameters were derived for oxalate degradation using Michaelis-Menten equation for both N-supplemented and N-deficient reactors.

Specific oxalate removal rates for different initial in-reactor oxalate concentrations are shown in Figure 6.3A (Figure S6.1 in appendix 2 reflects data used to derive initial specific oxalate removal rates). There was no decline of specific oxalate removal rates, when initial in-reactor concentrations were increased and hence a substrate level inhibition was not evident with in-reactor concentrations tested in this study. Since the relationship between the independent variable, initial oxalate concentration (S), and the dependent variable, initial specific rate of oxalate removal (V) was curvilinear, the estimation of the two parameters ( $V_{max}$  and  $K_m$ ) were derived using three linear transformations (Lineweaver-Burk plot, Hanes Plot and Eadie-Hofstee plot) of equation 6.1. Equations 6.2, 6.3, and 6.4 are all variants of Equation 6.1 and theoretically all three linear transformations should result in identical values for  $V_{max}$  and  $K_m$ . However, this is never the case simply due to measurement errors of V and S (Dowd & Riggs, 1965).

The  $V_{max}$  and  $K_m$  values derived in this study using the three linear transformations of Michaelis-Menten equation are summarised in Table 6.1, which also reports the coefficient of determination ( $R^2$ ) for each of the three linear transformations (Figures 6.3B – D). Both Lineweaver-Burk and Hanes Plots showed a good fit to the data ( $R^2$  values of  $> 0.92$ ), while a poor fit was noted with Eadie-Hofstee plot ( $R^2$  values of  $< 0.87$ ). The  $R^2$  values reflect measurement errors associated with V and S and a low  $R^2$  value with Eadie-Hofstee plot suggested that  $V_{max}$  and  $K_m$  should not be derived using Eadie-Hofstee plot. Although a good fit can be observed with Lineweaver-Burk plot, it also has been sometimes reported to give deceptively good fits according to Dowd and Riggs (1965). Based on Hanes plot, which gave the highest  $R^2$  value of  $>0.97$ , the  $V_{max}$  values of the N-supplemented and N-deficient reactors were 133.3 and 161.3

mg/h.g biomass, respectively and the corresponding  $K_m$  values were 541.9 and 458.4 mg/L, respectively. Hence, in this study,  $V_{max}$  and  $K_m$  values derived using the Hanes Plot ( $R^2$  values of > 0.97) were used in future calculations. From an operational perspective, the  $K_m$  value is of significance as it reflects the affinity of the culture to the substrate (oxalate). A low  $K_m$  value indicates that the culture has a high affinity towards a substrate and vice versa. Accordingly, the N-deficient culture has a higher affinity towards oxalate and as a consequence is able to reach closer to its maximum oxalate removal rates at lower oxalate concentrations. To achieve a similar specific removal rate of oxalate, the N-supplemented reactor required exposure to a higher in-reactor oxalate concentration. Hence, when a low concentration of oxalate is desired in bioreactor effluent, the N-deficient culture is likely to facilitate it with a shorter HRT. A shorter HRT on the other hand helps to reduce reactor foot-print, and capital and operating costs.

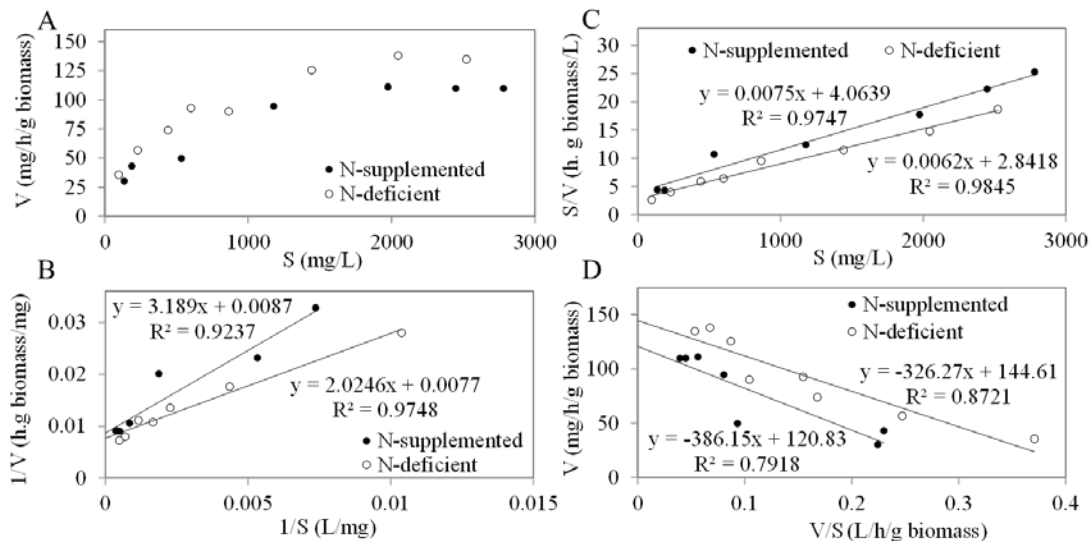


**Figure 6.3.** (A) Effect of initial oxalate concentration ( $S$ ) on specific oxalate degradation rate ( $V$ ) in N-supplemented and N-deficient reactors. Linearization of results with (B) Lineweaver-Burk plot (C) Hanes plot, and (D) Eadie-Hofstee plot. The experimental tests were carried out for N-supplemented reactor from day 196 and for N-deficient reactor from day 360.

**Table 6.1.** Michaelis-Menten constants ( $K_m$ ) and maximum specific oxalate degradation rates ( $V_{max}$ ) for N-supplemented and N-deficient reactor systems obtained with three different linearization approaches.

Linearization Approach	$K_m$ (mg/L)		$V_{max}$ (mg/h/g biomass)		$R^2$	
	N-supplemented	N-deficient	N-supplemented	N-deficient	N-supplemented	N-deficient
Lineweaver-Burk plot	366.6	262.9	114.9	129.9	0.9237	0.9748
Hanes Plot	541.9	458.4	133.3	161.3	0.9747	0.9845
Eadie-Hofstee plot	386.2	326.3	120.8	144.6	0.7918	0.8721

### 6.3.3 A side stream two-step continuous biological treatment process for efficient removal of oxalate

According to Michaelis-Menten kinetics, higher oxalate removal rates can only be achieved with higher in-reactor oxalate concentrations. Accordingly, a two-stage biological treatment process (Figure 6.5) is proposed to utilise the higher degradation rates at higher oxalate concentrations to achieve efficient oxalate removal. When considering saturation concentrations, the maximum in-reactor oxalate concentration that could be maintained is approximately 3 g/L (Hiralal et al., 1994). At such an in-reactor concentration of oxalate, a specific oxalate removal rate of 112.9 or 139.9 mg/h.g biomass can be facilitated with either N-supplemented or N-deficient reactor biomass, respectively (Table 6.2). The second reactor (polish-up reactor) could then be operated to polish up bulk of the remaining oxalate to reduce the effluent concentration to 0.4 g/L for the effluent to be discharged into alkaline lakes in the refinery (Tilbury, 2003). At this effluent concentration the oxalate degradation rates would be 56.6 and 75.2 mg/h.g biomass in the N-supplemented and N-deficient reactor, respectively (Table 6.2).

If 40 t/d of oxalate is to be biologically destructed using influent oxalate concentration of 100 g/L oxalate, the total HRT of the two-stage bioreactor would be 1.43 and 1.57

d for N-supplemented and N-deficient systems, respectively. In comparison, corresponding single stage systems would require HRTs of 2.52 and 2.87 d for N-supplemented and N-deficient systems respectively (Table 6.2). Even though the N-deficient biofilm has a higher specific oxalate removal rate ( $V$ ), the biofilm density was lower than the N-supplemented reactor. Consequently, a low volumetric oxalate degradation rate per media volume in N-deficient reactor. This low volumetric oxalate degradation rate has caused for the higher HRT in N-deficient reactor compared to N-supplemented reactor. The differences in HRT would translate to required total reactor volumes to be 1626 m<sup>3</sup> and 1648 m<sup>3</sup> for the two stage systems operated under N-supplemented and N-deficient conditions, respectively, while the corresponding one-stage systems (Figure 6.4) would require volumes of 3060 m<sup>3</sup> and 2904 m<sup>3</sup>, respectively. Hence the use of the two-stage system would allow the total reactor volume to be decreased by nearly 55 % (from approximately one Olympic size swimming pool to half a pool) while still allowing equally good effluent quality. This would considerably reduce the footprint of biological oxalate destruction, and likely decrease capital and operating costs (Table 6.2).

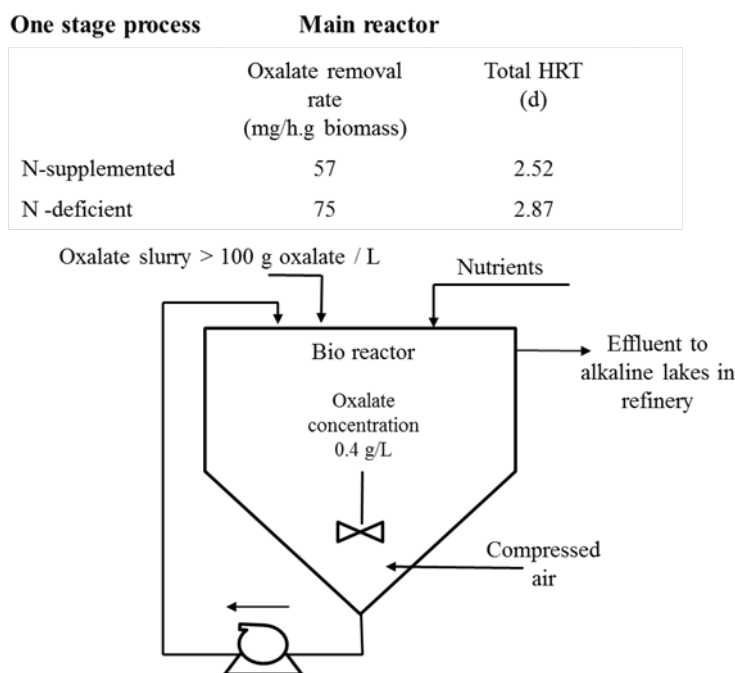


**Figure 6.4.** A schematic diagram of a side stream continuous biological oxalate removal one-stage process.

Two stage process	Main reactor	Polish-up reactor	
	Oxalate removal rate (mg/h.g biomass)	Total HRT (d)	
N-supplemented	113	57	1.43
N -deficient	140	75	1.57

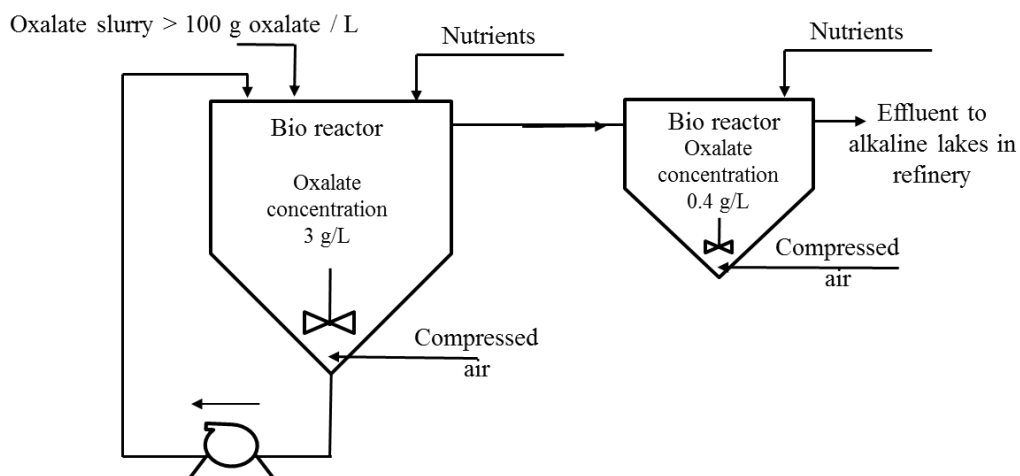


**Figure 6.5.** A schematic diagram of a side stream continuous biological oxalate removal two-stage process.

**Table 6.2.** Design parameters for one stage and two stage bioreactor processes assuming oxalate generation of 40 t/d (McSweeney, 2011) and influent oxalate concentration of 100 g/L.

Parameter	Unit	Two-stage process		
		One-stage process	Main reactor	Polish-up reactor
Oxalate Loading	t/d	40	40	1.2
Influent oxalate concentration	g/L	100	100	3
Influent flow rate	m <sup>3</sup> /d	400	400	400
<b>N-supplemented process</b>				
Maximum specific Oxalate removal rate ( $V_{max}$ )	g/h.g biomass	0.133	0.133	0.133
Michaelis-Menten constants ( $K_m$ )	g/L	0.542	0.542	0.542
Effluent [Oxalate] - [S]	g/L	0.40	3.00	0.40
Specific Oxalate removal rate (V)*	g/h.g biomass	0.057	0.113	0.057

Biomass density per media volume (based on lab reactor)	g biomass/m <sup>3</sup>	9622	9622	9622
Oxalate degradation rate (based on media volume)	g/d.m <sup>3</sup>	13071	26072	13071
Media to liquid volume ratio (based on lab reactor)		3.0	3.0	3.0
HRT	d	2.52	1.23	0.07
Effective reactor liquid volume	m <sup>3</sup>	1,008	492	26
Biological media (Granules) volume (Reactor Volume)	m <sup>3</sup>	3060	1534	92
Size equivalent to an Olympic size swimming pool (2500 m <sup>3</sup> )		1.22	0.61	0.04

#### **N-deficient process**

Maximum specific Oxalate removal rate ( $V_{max}$ )	g/h.g biomass	0.161	0.161	0.161
Michaelis-Menten constants ( $K_m$ )	g/L	0.4584	0.4584	0.4584
Effluent [Oxalate] - [S]	g/L	0.40	3.00	0.40
Specific Oxalate removal rate ( $V$ )*	g/h.g biomass	0.075	0.140	0.075
Biomass density per media volume (based on lab reactor)	g biomass/m <sup>3</sup>	7632	7632	7632
Oxalate degradation rate (based on media volume)	g/d.m <sup>3</sup>	13768	25629	13768
Media to liquid volume ratio (based on lab reactor)		2.5	2.5	2.5
HRT	d	2.87	1.50	0.07
Effective reactor liquid volume	m <sup>3</sup>	1,147	600	30
Biological media (Granules) volume (Reactor Volume)	m <sup>3</sup>	2905	1561	87
Size equivalent to an Olympic size swimming pool (2500 m <sup>3</sup> )		1.16	0.62	0.03

\* Calculated based on Hanes plot linearization for the in-reactor oxalate concentration (i.e. effluent oxalate concentration)

### **6.3.4 Kinetic differences reflect the differences in microbial community composition**

What is noteworthy of Table 6.2 is approximate equal media volume requirements from either N-supplemented or N-deficient reactor to treat 40 t/d of oxalate. Despite similar media volume requirements, the associated biomass in media volume of N-supplemented reactor was approximately 1.3 times higher than that of N-deficient reactor. The high and low specific removal rates of N-deficient and N-supplemented biomass respectively were likely due to the differences in microbial community composition between the N-deficient and N-supplemented reactors.

The start-up inoculum of both N-supplemented and N-deficient reactors was identical. The microbial community changes of both reactors were examined from start-up until stable reactor performance using 454 pyrosequencing of 16S rRNA genes. Rarefaction curves of all samples sequenced indicated that sequencing depth was adequate to capture bacterial diversity present in the samples (Figure S6.2 in appendix 2). The Principal coordinate analysis (PCoA) of unweighted Unifrac distances (which measures similarity of microbial communities based on phylogenetic diversity), showed clustering of microorganisms according to the availability of N in the reactors (Figure 6.6A). A similar clustering was noted with the unweighted pair group method with arithmetic mean (UPGMA) tree (Figure 6.6B). Both analyses demonstrate clustering of all samples into three groups. The samples collected from both reactors after 3 weeks of inoculation clustered together, indicating a greater phylogenetic similarity between microbial communities of the N-supplemented and N-deficient reactors than during later stages of operation when each reactor appeared to have microbial communities that were uniquely different to one another. As a consequence, latter samples obtained from both N-supplemented and N-deficient reactors clustered independently from each other (Figures 6.6A and 6.6B). When examining the single cluster formed by samples of N-deficient reactor (Figure 6.6B), it is evident that microbial community composition continued to change between samples taken on days 225 and 253. There was however, no major change in the composition beyond 253 d, suggesting the reactor achieved a stable community. In contrast, the microbial community composition of the N-supplemented reactor did not appear to have achieved stability even after 221 d of reactor operation. In terms of microbial community composition, samples taken on day 21 from both reactors showed closer

similarity to the samples of N-deficient reactor even once the reactor achieved stable performance than the later samples obtained from the N-supplemented reactor. The Western Australian soil and ocean sediment used to inoculate the reactors were from environments that are highly deficient of nitrogen and the indigenous microorganisms in the inoculum, perhaps were dominant of nitrogen fixing bacteria. Hence, the higher phylogenetic similarity observed between 21 d samples and the N-deficient reactor samples is not surprising.

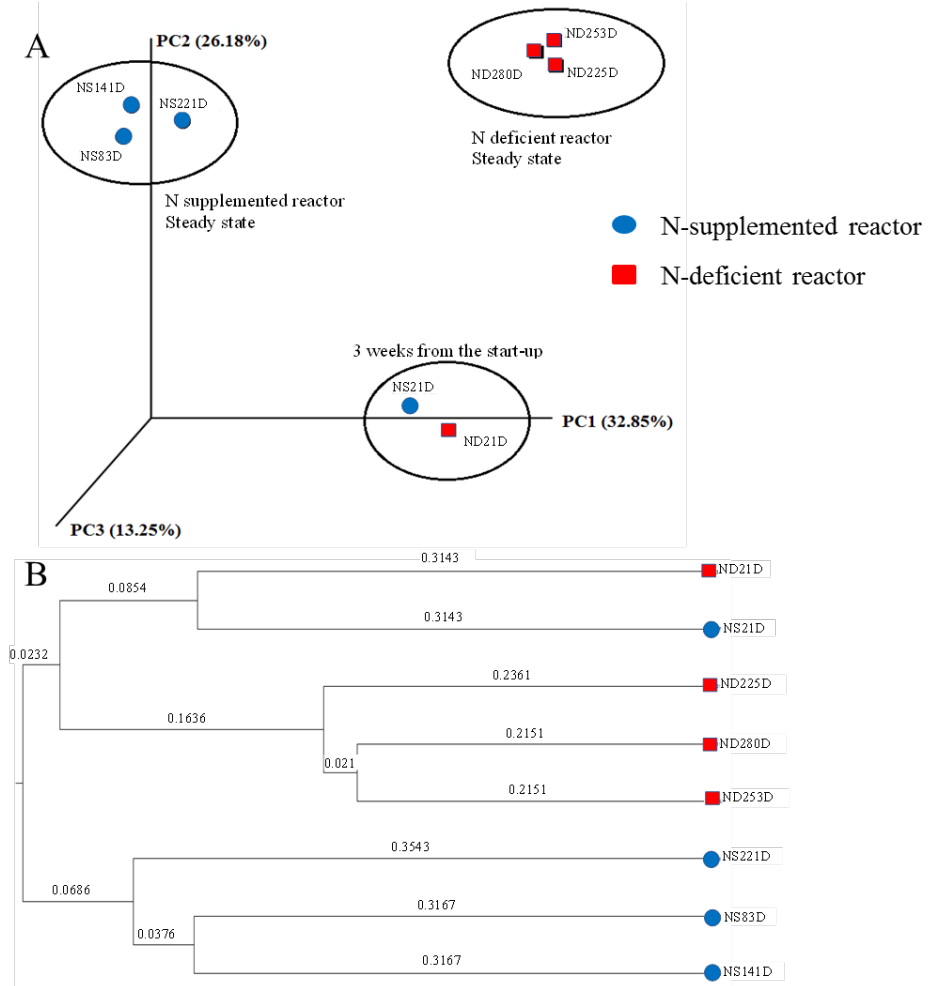


**Figure 6.6.** Similarity analysis (at 97% sequences similarity) of microbial communities in N-supplemented and N-deficient reactors 3 weeks after inoculation and during stable operation based on unweighted Unifrac. (A) Principal coordinates analysis (PCoA). (B) Unweighted pair group method with arithmetic mean (UPGMA) cluster analysis. The values on branches show the similarity of the microbial communities.

Although there is a higher level of similarity between the microbial community compositions of samples collected on day 21 from N-supplemented and N-deficient reactors, the dominant taxa in these samples differed considerably (Figure 6.7A). In N-supplemented reactor, 87 % of 16S rRNA gene sequences were found spread across 4 bacterial classes, namely Alphaproteobacteria (46 %), Betaproteobacteria (19 %), Saprospirae (13 %) and Deinococci (9 %). In contrast in the N-deficient reactor, 85 % of sequences were spread across bacterial classes Betaproteobacteria (46 %), Alphaproteobacteria (16 %), Cytophagia (14 %) and Gammaproteobacteria (10 %). Once stable reactor performance was achieved, approximately 90 % of sequences in N-supplemented reactor were associated with bacterial classes Alphaproteobacteria (~53 %), Betaproteobacteria (~24 %), Gammaproteobacteria (~9 %) and Bacilli (~4 %). In contrast in the N-deficient reactor 78 % of sequences were evenly spread across bacterial classes Alphaproteobacteria (~23 %), Gammaproteobacteria (~23 %), Betaproteobacteria (~18 %) and Cytophaga (~14 %). In the N-supplemented reactor, there was a positive linear increase (Pearson correlation  $r = 0.9977$ ) of Alphaproteobacteria relative abundance during the 200 d of reactor operation. A similar positive linear increase (Pearson correlation  $r = 0.9037$ ) in relative abundance was observed for Gammaproteobacteria in the N-deficient reactor during 256 d of reactor operation.

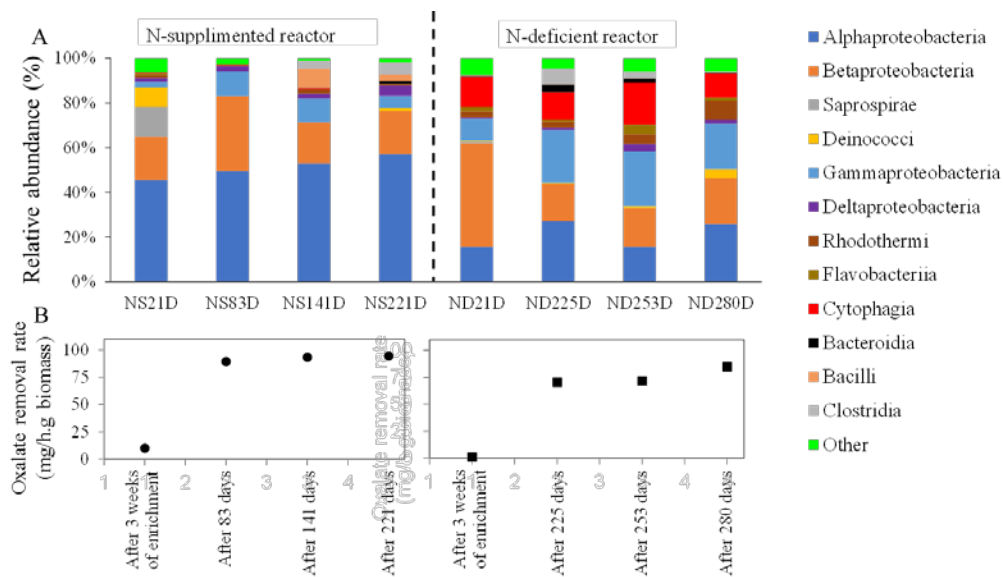


**Figure 6.7.** (A) Relative abundance of microbial class (having a  $\geq 3\%$  abundance) observed in N-supplemented and N-deficient reactors. (B) Specific oxalate removal

rates of the two reactors at the time sample collection for microbial community analysis.

When the abundance of microbial taxa was examined at a genus level, *Paracoccus* and *Azoarcus* of bacterial classes Alphaproteobacteria and Betaproteobacteria, respectively appeared dominant in both reactors (Figure 6.8A). During the study period, the relative abundance of *Paracoccus* and *Azoarcus* increased from 28 % to 46 % and 10 % to 17 %, respectively in the N-supplemented reactor. In contrast, the increase of genus *Paracoccus* in the N-deficient reactor was low (from 1 % to 6 %). Compared to the N-deficient reactor, the dominance of *Paracoccus* in N-supplemented reactor suggested a possible dependence of this genus on a ready source of nitrogen. The *Paracoccus* spp. associated with roots of Amorphophallus plants have been demonstrated capable of oxidising oxalate (Anbazhagan et al., 2007). Hence, *Paracoccus* may also be responsible for oxidation of some oxalate in both reactors. Compared to *Paracoccus*, genus *Azoarcus*, showed a similar level of dominance in both reactors. Genus *Azoarcus* is known for its nitrogen-fixing capabilities specifically associated with plant roots in soil (Reinholdhurek et al., 1993). Some species of genus *Azoarcus* have also been demonstrated capable of oxidising oxalate (Mechichi et al., 2002) and McSweeney et al. (McSweeney et al., 2011b) demonstrated the abundance of *Azoarcus* in a pilot and in a full-scale moving bed bioreactor operated for biological oxalate destruction. Accordingly, oxidation of oxalate in both reactors may also be facilitated by genus *Azoarcus*. Nitrogen fixation is extremely energy intensive, and hence, when ammonia is readily available, nitrogen fixing bacteria directly utilise ammonia to fulfil nitrogen requirements without fixing atmospheric nitrogen (Kanamori et al., 1989). Accordingly, the presence of *Azoarcus* in both reactors is not surprising.

Genus *Alkaliphilus* of family *Clostridiaceae* and an unknown genus of family *Rhodobacteraceae* also showed an increase in abundance during the operation of the N-supplemented reactor (Figure 6.8B). Similar increasing trends were observed for bacterial taxon *KSA1* of family *Balneolaceae* and unknown bacterial genera of families *Rhodobacteraceae*, *Flammeovirgaceae* and *Marinicellaceae* of the N-deficient reactor (Figure 6.8C). Accordingly, in addition to *Azoarcus* and *Paracoccus* other bacteria also appear to influence degradation of oxalate (directly or indirectly) in both the N-supplemented and the N-deficient reactors.

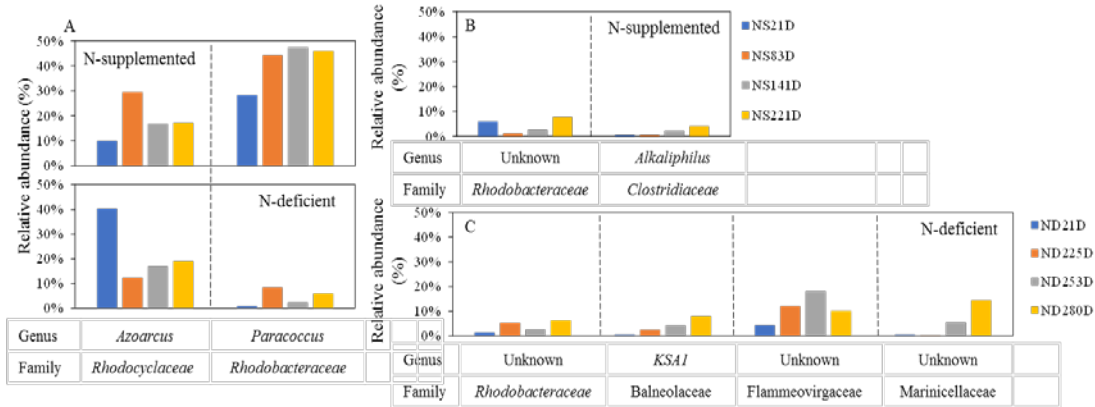


**Figure 6.8.** Change of abundance of microbial genera during the operation of N-supplemented and N-deficient reactors. (A) A comparison of relative abundance of genera *Azoarcus* and *Paracoccus*. (B) Other bacterial genera that showed a positive increase of abundance - N-supplemented reactor. (C) Other bacterial genera that showed a positive increase of abundance - N-deficient reactor.

## 6.4 Conclusions

The kinetics of oxalate degradation under N-supplemented and N-deficient conditions was comparatively examined to explore the feasibility of facilitating side-stream removal of oxalate from alumina refineries without external nitrogen supplementation. The N-deficient culture had a higher affinity (a low  $K_m$ ) towards oxalate than the N-supplemented culture. Additionally, the same culture showed a higher  $V_{max}$ , suggesting that compared to the N-supplemented culture, the N-deficient culture was better suited for oxalate destruction. Even with a low biomass density, the foot-print of the N-deficient bioreactor was found to be similar to the N-supplemented bioreactor and this was primarily due to the differences of reaction kinetics in the two microbial communities. Molecular analysis of the microbial communities also showed that the two cultures were uniquely different. A number of bacterial genera that could be directly or indirectly responsible for the removal of oxalate in both cultures were detected. To capitalise on higher specific oxalate removal rates, this study also proposed a two-step treatment process to remove oxalate waste generated by alumina industry. The prospective bioreactor will require two units, yet with a smaller reactor foot print, especially suitable for a low oxalate discharge with effluent.

# **7 RAPID START-UP OF A BIOELECTROCHEMICAL SYSTEM UNDER ALKALINE AND SALINE CONDITIONS FOR EFFICIENT OXALATE REMOVAL**

Extended from

Weerasinghe Mohottige, T.N., Ginige, M.P., Kaksonen, A.H., Sarukkalige, R. and Cheng, K.Y. (2017) Rapid start-up of a bioelectrochemical system under alkaline and saline conditions for efficient oxalate removal. Chemical Engineering Journal. Submitted.

## **Chapter Summary**

This study examined a new approach for starting up a bioelectrochemical system (BES) for oxalate removal from an alkaline ( $\text{pH} > 12$ ) and saline ( $\text{NaCl } 25\text{g/L}$ ) wastewater. An oxalotrophic biofilm pre-grown aerobically onto graphite carriers was used directly as both the microbial inoculum and the BES anode. At anode potential of +200 mV (Ag/AgCl) the biofilm readily switched from using oxygen to graphite as sole electron acceptor for oxalate oxidation. BES performance was characterized at various hydraulic retention times (HRTs, 3 - 24 h), anode potentials (-600 to +200 mV vs. Ag/AgCl) and influent oxalate (25 mM) acetate (0 - 30 mM) ratios. Maximum current density recorded was  $363 \text{ A/m}^2$  at 3 h HRT with a high coulombic efficiency (CE) of 70%. The biofilm could concurrently degrade acetate and oxalate (CE 80%) without apparent preference towards acetate. Pyro-sequencing analysis revealed that known oxalate degraders *Oxalobacteraceae* became abundant signifying their role in this novel BES process.

## 7.1 Introduction

Smelting grade alumina ( $\text{Al}_2\text{O}_3$ ) is refined from Al-containing bauxite minerals through Bayer process (Meyers, 2004). In the Bayer process, crushed bauxite is digested in a concentrated caustic solution (~ 3 M NaOH) at high temperature (140 °C – 250 °C) in a pressurised reactor (~ 3.5 MPa) (Balomenos et al., 2011). After the product aluminium hydroxide (gibbsite,  $\text{Al}(\text{OH})_3$ ) is separated from the process liquor, the remaining caustic solution (spent liquor) is recycled to the digestion reactors to minimise caustic consumption (Hind et al., 1999; Meyers, 2004). With the continuous recycling of the spent liquor during the Bayer process, organic substances extracted from the bauxite also accumulate in the process liquor (Hind et al., 1999; Power et al., 2011c). These organics consist of various compounds ranging from very complex high molecular weight humic substances to simple organic acids (Power et al., 2012).

Among the organics present in the Bayer process liquor, sodium oxalate ( $\text{Na}_2\text{C}_2\text{O}_4$ ) is a key organic impurity (Power et al., 2012). It causes detrimental impact to the quality and yield of the alumina products. Depending on the digestion conditions, 5 - 10% of the organic carbon is typically converted into sodium oxalate (Sipos et al., 1999). If not controlled, sodium oxalate affects the settling of gibbsite and scaling of pipes and tanks (Gnyra & Lever, 1979; Turhan et al., 2011). The most widely used industrial technique for oxalate removal involves crystallisation of sodium oxalate in a Bayer process side stream and disposal of the solid residues in residue areas (Brown, 1991; Rosenberg et al., 2004). Since Australian bauxite typically contains high organic content, Australian alumina refineries (particularly those in Western Australia) can produce up to 40 t/day of oxalate, which requires treatment and storage (McSweeney, 2011). The storage of oxalate in alkaline residue lakes poses significant risk on the environment such as groundwater contamination and dusting, demanding strict handling and disposal guidelines (Power et al., 2011a).

Biological oxalate degradation has been increasingly considered as an environmentally friendly option to destroy oxalate in alumina refineries. However, microbial degradation of oxalate is challenging due to the strict requirement of unique enzymes only present in specific microbial cultures (Allison et al., 1995; Miller & Dearing, 2013; Sahin, 2003). Three main enzymes, namely oxalate oxidase, oxalate decarboxylase and oxalyl-CoA decarboxylase present in oxalotrophic bacterial strains

are known to be responsible for catalysing the cleavage of the C-C bond of oxalate, which is the crucial first step of oxalate biodegradation (Svedruzic et al., 2005). Different bacterial strains capable of using oxalate as carbon source and or energy source have been isolated from various living organisms and environmental sources such as human gastrointestinal tracts, sheep rumen, rhizosphere soil and aquatic sediments (Sahin, 2003). The most commonly found oxalate degrading bacterial genus is *Oxalobacter* within the family *Oxalobacteraceae* (Baldani et al., 2014).

Recently, Bonmati et al. (2013) have reported a successful use of a cation exchange membrane (CEM)-equipped bioelectrochemical system (BES) for the removal of oxalate from a low salinity liquor (sodium and potassium concentrations were ~ 2 g/L). Their BES was inoculated with an active anodophilic mixed microbial culture collected from a separate acetate-fed microbial fuel cell (MFC) and a mixed culture obtained from an upflow anaerobic sludge blanket (UASB) reactor treating brewery wastewater. During process start-up, acetate was used as a co-substrate to stimulate oxalate degradation. When oxalate was tested as the sole substrate, their anodic biofilm could efficiently (almost completely) remove oxalate from the anodic influent ( $10.3 \text{ kg/m}^3\text{.d}$  at hydraulic retention of 7 h) (Bonmati et al., 2013). However, only low coulombic efficiency (CE) of  $21 \pm 2\%$  was achieved, and because the operational pH was not reported it was unclear if their oxalotrophic biofilm would remain active under alkaline conditions.

In our previous study, the use of BES for removing oxalate under alkaline and saline conditions was investigated for the first time (Weerasinghe Mohottige et al., 2017b). Activated sludge was chosen as a microbial inoculum considering that it can be easily sourced in large quantity from domestic sewage treatment plants, and that microbes in activated sludge are generally capable of degrading different types of organics. However, start-up of the BES was unsuccessful when oxalate was used as the sole carbon and energy source. Even with acetate added as a co-substrate as practiced by Bonmati et al. (2013), the maximal oxalate removal was only marginal (<10% at a removal rate of  $0.4 \text{ kg/m}^3\text{.d}$ ). Microbial community analysis of the anodic biofilm suggested that the inefficient oxalate removal was possibly associated with a paucity of microorganisms responsible for catalysing decarboxylation of oxalate into formate (Weerasinghe Mohottige et al., 2017b). Hence, it was concluded that activated sludge

was not a suitable BES inoculum for oxalate removal under the alkaline and saline conditions used.

To address this microbial inoculation issue, we postulated that microorganisms habituated in existing oxalate degrading reactors or oxalate-rich environment (e.g. soda lake or residue lake within an alumina plant) are likely having the enzymes required for catalysing the crucial first step of oxalate biodegradation (C-C bond cleavage), and are thus a more suitable inoculum for the described BES process. However, to be efficient in BES these microorganisms must also be able to readily grow as a biofilm on the anode and be electrochemically active. One conceivable strategy to accomplish this is to first expose the electrode material to an oxalate enriched environment (e.g. an aerobic bioreactor), facilitating the formation of an active oxalate-degrading biofilm onto the electrode carrier. Subsequently, this so-called “biofilm-electrode assemblage” may directly serve as both the microbial inoculum and the anode of a BES to facilitate bioelectrochemical oxidation of oxalate.

In this work, the concept of using this “biofilm-electrode assemblage” for starting up an oxalate removing BES was studied. Such an assemblage was prepared by growing an aerobic biofilm onto graphite carriers (granules) within an aerobic bioreactor operated under both saline (NaCl 25 g/L) and alkaline (pH 9) conditions, and with oxalate as the sole carbon and energy source (> 250 days) (Weerasinghe Mohottige et al., 2017a). For the first time, the following questions were examined: (1) Can a metabolically active aerobic oxalate-degrading biofilm be readily acclimatised to generate anodic current under saline-alkaline conditions? (2) How long would it take for the aerobic biofilm to become anodically active with oxalate as the sole source of carbon and electrons under saline-alkaline conditions? (3) What would be the changes in the biofilm microbial community over the transition from aerobic- into anodic-(anaerobic) oxalate degradation? These questions were answered by operating a dual chamber BES reactor inoculated with an aerobically pre-grown active oxalotrophic biofilm (> 130 d) under alkaline-saline conditions.

## 7.2 Materials and methods

### 7.2.1 Bioelectrochemical systems and general process operation

A dual-chamber BES consisted of two identical half cells ( $14\text{ cm} \times 12\text{ cm} \times 2\text{ cm}$ ), which were separated by a cation exchange membrane (Ultrex CMI-7000, Membrane International Inc., surface area  $168\text{ cm}^2$ ) was used in this study. The anodic chamber (working chamber) was loaded with  $300\text{ mL}$  volume of biofilm coated graphite granules (anode material, 3-5 mm diameter, KAIYU Industrial (HK) Ltd.) collected from an nitrogen supplemented aerobic bioreactor operated with oxalate as a sole carbon source for over 250 days. The start-up, acclimatisation and oxalate removal performance of the aerobic biofilm was reported in our earlier study (Weerasinghe Mohottige et al., 2017a). The total biomass dry weight on the granules was  $9.6\text{ mg/mL}$  packed volume of biofilm coated graphite granules, and the biomass had an initial aerobic oxalate degradation activity of  $111\text{ mg/h.g}$  biomass. The cathodic chamber was loaded with similar type and quantity of graphite granules but without any biomass. After loaded with the granules, the void volume of each half cell reduced from  $336$  to  $250\text{ mL}$ . Four graphite rods (5 mm diameter, length 12 cm) were used as current collectors in each half cell to enable electric connection between the graphite granules and the external circuit. The BES was operated as a three-electrode system coupled to a potentiostat (VMP3, BioLogic) (Cheng et al., 2010). The working electrode (anode) was polarized against a silver-silver chloride (Ag/AgCl) reference electrode (MF-2079 Bioanalytical Systems, USA) at a defined potential using the potentiostat. The reference electrode was inserted (ca. 1 cm from the top) within the granular graphite working electrode bed to minimise ohmic resistance. Total liquid volumes of  $0.5$  and  $2.0\text{ L}$  were continuously recirculated (at recirculation rate of approximately  $14\text{ L/h}$ ) through the anodic and the cathodic half cells via two separate external bottles ( $0.25$  and  $2.0\text{ L}$ ), respectively (Figure 7.1). The headspace of the anodic recirculation bottle was intermittently flushed with nitrogen gas (every 20 min for 30 second) to create an anaerobic environment in the anodic half cell. The process was operated at ambient temperature ( $22 \pm 2^\circ\text{C}$ ).

Unless specified otherwise, the anodic chamber of the BES was operated predominately in continuous mode. Fresh anolyte (maintained at  $4\text{ }^\circ\text{C}$  in a refrigerator)

was introduced at a specified flow rate into the external recirculation bottle and an equal volume of the old anolyte was withdrawn (and discarded) from the recirculation line using a peristaltic pump (Masterflex® Cole-Parmer L/S pump drive fitted with a Model 77202-60 Masterflex® pump head; Norprene® tubing 06404-14). Throughout the experimental period, the cathodic chamber of the BES was operated in batch mode, and the catholyte was occasionally renewed as per experimental requirements (approximately once per week). The BES process was continuously monitored and was controlled using a computer program (LabVIEW). The working electrode potential and the current of the BES were monitored via the potentiostat. All electrode potentials (mV) reported in this paper refer to values against Ag/AgCl reference electrode (ca. +197 mV vs. standard hydrogen electrode (Bard & Faulkner, 2001)). The pH of the working electrolyte was continuously monitored using in-line pH sensors (TPS Ltd. Co., Australia). All signals were regularly recorded to an Excel spreadsheet via the computer programme interfaced with a National InstrumentTM data acquisition card.

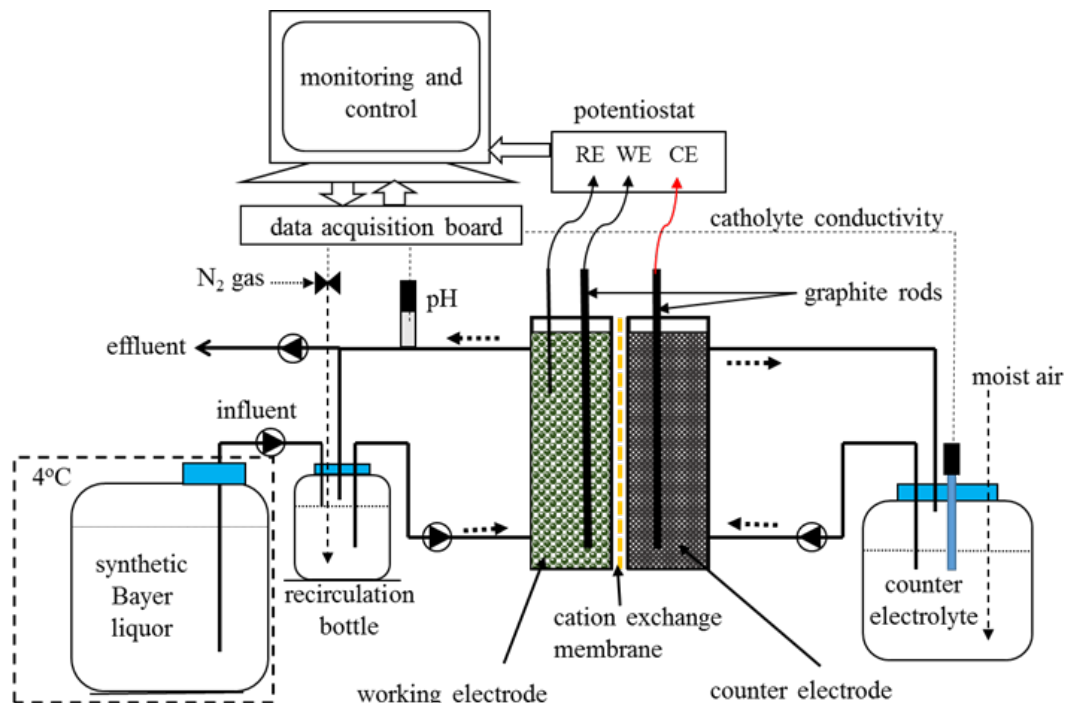


**Figure 7.1.** A schematic diagram of the BES process consisting of anodic cell and cathodic cell filled with graphite granules, a recirculation line and a computer for process monitoring and control.

## **7.2.2 Synthetic refinery process water (anolyte) and BES catholyte**

A synthetic medium, which simulated an alumina refinery process water stream in terms of its salinity and pH was used as the influent of the BES anode. Unless specified otherwise, sodium oxalate (3.35 g/L as  $\text{Na}_2\text{C}_2\text{O}_4$ , 25 mM) was used as the only carbon source, and  $\text{NaCl}$  (25 g/L) was added to increase the solution salinity equivalent to a typical Bayer liquor (Hind et al., 1997). Stock solution of  $\text{NaOH}$  (2 M) was used to maintained the feed solution pH (> 12). The nutrient medium used for the BES anolyte consisted of (mg/L): 130  $\text{NH}_4\text{Cl}$ ; 125  $\text{NaHCO}_3$ ; 51  $\text{MgSO}_4 \cdot 7\text{H}_2\text{O}$ ; 15  $\text{CaCl}_2 \cdot 2\text{H}_2\text{O}$ ; and 20.5  $\text{K}_2\text{HPO}_4 \cdot 3\text{H}_2\text{O}$  and 1.25 ml/L of trace element solution which had the composition of (g/L): 0.43  $\text{ZnSO}_4 \cdot 7\text{H}_2\text{O}$ ; 5  $\text{FeSO}_4 \cdot 7\text{H}_2\text{O}$ ; 0.24  $\text{CoCl}_2 \cdot 6\text{H}_2\text{O}$ ; 0.99  $\text{MnCl}_2 \cdot 4\text{H}_2\text{O}$ ; 0.25  $\text{CuSO}_4 \cdot 5\text{H}_2\text{O}$ ; 0.22  $\text{NaMoO}_4 \cdot 2\text{H}_2\text{O}$ ; 0.19  $\text{NiCl}_2 \cdot 6\text{H}_2\text{O}$ ; 0.21  $\text{NaSeO}_4 \cdot 10\text{H}_2\text{O}$ ; 15 ethylenediaminetetraacetic acid (EDTA); 0.014  $\text{H}_3\text{BO}_3$ ; and 0.05  $\text{NaWO}_4 \cdot 2\text{H}_2\text{O}$ . (Cheng et al., 2010). Unless otherwise stated, this medium was used as the electrolyte in the anodic chamber throughout the entire study. A similar  $\text{NaCl}$  concentration (25 g/L) as the anolyte was used as the catholyte medium of the BES. The catholyte recirculation bottle was exposed to air during the operation.

## **7.2.3 Experimental Procedures**

### **7.2.3.1 Process start-up with the aerobic biofilm coated graphite granules**

After the BES was setup, the synthetic medium was continuously fed into the anodic chamber to obtain a hydraulic retention time (HRT) of one day. Soon after loading the medium into the reactor (within an equilibration period of ~ 1h), the working electrode (anode) was poised at a constant potential of +200 mV, which was similar to the one used in our previous work for process start up (Weerasinghe Mohottige et al., 2017b). Over this period, sodium oxalate was used as the sole carbon and electron source and the influent pH was maintained at  $10 \pm 0.2$ . Anodic current production and oxalate removal in the anolyte were used as the parameters to indicate the establishment of biofilm activity after initiation of the process. The following sections summarise the experimental procedures of evaluating the effects of HRT in the anodic chamber, anode potential and supplementation of various acetate concentrations as a co-substrate on the BES performance.

### **7.2.3.2 Effect of Hydraulic Retention Time (HRT) on BES performance**

The effect of HRT on current production and oxalate removal rate of the biofilm was studied using different HRTs for anodic chamber ranging from 24 to 1 h (24, 12, 6, 3, 1 h) on days between 15 to 23, corresponding to COD loading rates of  $1.76 \text{ kg/m}^3\text{.d}$  to  $13.7 \text{ kg/m}^3\text{.d}$ , respectively. The BES was operated at a fixed HRT until it generated stable current over time ( $\geq$  one HRT). During this experiment, the BES was operated with an influent pH of 12.5 resulting in an in-reactor pH between 9.0 and 9.5 at a constant anode potential of -300mV, which was similar to process operation in our previous study (Weerasinghe Mohottige et al., 2017b). The CE (%) of the anodic reaction was calculated based on the electrons recovered as anodic current versus the theoretical amount of electrons liberated from the removed oxalate (assuming two moles of electrons per mole of oxalate oxidised).

### **7.2.3.3 Effect of anode potential on BES performance**

To test the performance of the established biofilm at different poised anode potentials, the following experiment was carried out after day 61. The BES anode was operated in continuous mode with 6 h HRT throughout this experiment. Initially the BES was operated in open circuit mode for more than 12 h until the open circuit voltage became stable. Thereafter, the anode potential was increased stepwise from -300 mV to +200 mV and then was decreased from +200 mV to -600 mV. The BES was operated at a poised anode potential until the current become stable for  $\geq 12$  h. Throughout the experiment, pH (influent pH 12.5, in-reactor pH 9 - 9.5) and feed composition (25 mM oxalate as the sole carbon and electron source) remained constant.

### **7.2.3.4 Effect of increasing acetate concentration on oxalate degradation rate and BES performance**

The effect of acetate, another organic compound present in Bayer liquor, on the oxalate degradation and coulombic efficiency of the BES was investigated by various concentrations of sodium acetate to the BES influent after day 95. At the beginning of the experiment, the BES was operated with 25 mM oxalate in the influent and acetate

concentration was gradually increased from 0 mM to 30 mM (0 mg/L to 1500 mg/L). During the study, the BES was operated at an anode potential of -300 mV and HRT in the anodic compartment of 12 h. The influent pH was ranging from 12.5 to 13.4 resulting in in-reactor pH 9 – 9.5. Both acetate and oxalate removal were considered for CE calculation.

#### **7.2.4 Chemical analyses**

During these experiments, liquid samples were collected and immediately filtered through 0.22 µm syringe filters (Cat No SLGNO33NK, Merck Millipore, USA) for oxalate and acetate measurements, which were carried out using a Dionex ICS-3000 reagent free ion chromatography (RFIC) system equipped with an IonPac® AS18 4 × 250 mm column. Potassium hydroxide was used as an eluent at a flow rate of 1 ml/min. The eluent concentration was 12 - 45 mM from 0 - 5 min, 45 mM from 5 - 8 min, 45 - 60 mM from 8 - 10 min and 60 - 12 mM from 10 - 13 min. The temperature of the column was maintained at 30°C. Suppressed conductivity was used as the detection signal (ASRS ULTRA II 4 mm, 150 mA, AutoSuppression® recycle mode).

#### **7.2.5 Biofilm samples collection and DNA extraction**

Biofilm samples for microbial analysis were collected from the aerobic biofilm granules, which were used as the inoculum, and the anodic biofilm granules from the BES anodic chamber for DNA extraction and microbial community analysis. Before sampling, the biofilm inside the BES was dislodged from the granules within the reactor by forward-backward flushing with a syringe as described in Wong et al. (2014). The biomass samples were collected on days 21 (BES-21D) (HRT of 6h and anode potential of -300mV) and 75 (BES-75D) (HRT of 1d and anode potential of -300mV) after the BES had shown stable performance with oxalate as the sole substrate. Another two samples were collected at and after adding the acetate as co-substrate on days 99 (BES-99D) (1 day after addition of 5 mM acetate) and 103 (BES-103D) (5 days after addition of acetate). For comparison, two biofilm samples (BR-1 and BR2) were also collected from the aerobic bioreactor that was operated more than 250 days

with oxalate as the only carbon source at pH 9 - 9.5 before taking the biofilm-coated granules to inoculate the BES.

DNA was extracted from 250 µL of suspended biomass dislodged from the graphite granules by using Power Soil DNA isolation kit from MO BIO laboratories, Inc. according to the manufacturer's instructions. The extracted DNA was stored at -20°C prior to sending to the School of Pathology and Laboratory Medicine, University of Western Australia for 454 sequencing.

#### **7.2.5.1 Microbial community analysis**

The 454 sequencing was carried out as described by Nagel et al. (2016). In brief, microbial 16S rRNA genes were amplified from 1 ng aliquots of the extracted DNA using V4/5 primers (515F: GTGCCAGCMGCCGCGGTAA and 806R: GGACTACHVGGGTWTCTAAT). A mixture of gene-specific primers and gene-specific primers tagged with Ion Torrent-specific sequencing adaptors and barcodes were used. The tagged and untagged primers were mixed at a ratio of 90:10. Using this method, the amplification of all samples was achieved using 18-20 cycles, thus minimising primer-dimer formation and allowing streamlined downstream purification. Amplification was confirmed by agarose gel electrophoresis, and product formation was quantified by fluorometry. Up to 100 amplicons were diluted to equal concentrations and adjusted to a final concentration of 60 pM. Templatized Ion Sphere Particles (ISP) were generated and loaded onto sequencing chips using an Ion Chef (Thermofisher Scientific) and sequenced on a PGM semiconductor sequencer (Thermofisher Scientific) for 650 cycles using a 400 bp sequencing kit yielding a modal read length of 309 bp. Data collection and read trimming/filtering was performed using TorrentSuite 5.0.

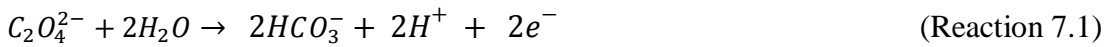
The open source software package QIIME (Quantitative Insights Into Microbial Ecology) was used for the post sequence analysis. The fasta, qual and mapping files were analysed using the downstream computational pipelines of QIIME. USEARCH61 was used for identification of chimeric sequences and was carried out in reference to an unaligned database (Greengene). On removal of chimeric sequences, the sequences were assigned operational taxonomic units (OTU) using the same

reference database. The sequence similarity threshold was set at 97 %. Then a representative sequence was assigned from each OTU and taxonomies were assigned to each of the selected representative sequences using RDP classifier and the same Greengenes reference database. Subsequently a phylogenetic tree was created on aligning all sequences against the same reference database using the Greengenes core alignment. Diversity analysis were finally carried out using the BIOM table, mapping file and the phylogenetic tree.

## 7.3 Results and Discussion

### 7.3.1 The aerobic oxalotrophic biofilm could readily switch from using oxygen to graphite as electron acceptor

Soon after loading the BES anodic chamber with the graphite granules acclimatised from the aerobic bioreactor, the BES was continuously fed with the synthetic medium (containing only oxalate as organic electron donor) and the potential of the granules were poised at +200 mV (Figure 7.2). Unexpectedly, anodic current was recorded immediately, reaching a peak of approximately 20 mA (Figure 7.2A, at ~6 h). Although, the current declined gradually thereafter plausibly due to a concomitant decrease in the anolyte pH (from 9.2 to ~8), it was apparent that the biofilm could readily use the graphite granules (growth surface) as an electron acceptor without any lag period. The current production also coincided with a slight decrease in the anolyte pH (Figure 7.2A), as the anodic oxidation of oxalate would liberate protons (Reaction 7.1). Resuming the anolyte pH to ~9.2 by adding NaOH (i.e. the optimal pH for the aerobic biofilm) resulted in a sharp increase in current, asserting that the biofilm was alkalophilic (Figure 7.2A).



Oxalate measurement further confirmed that the current production was associated with oxalate removal (Figure 7.2B). Clearly, the biofilm could degrade oxalate immediately even when the electron acceptor was drastically switched (from oxygen to graphite anode). Noteworthy, such a rapid onset of biofilm activity is opposing our previous finding, in which under the same conditions (i.e. anodic potential, pH, salinity

and anolyte composition) activated sludge inoculum failed to adapt as an anodic oxalotrophic biofilm for efficient oxalate removal (Weerasinghe Mohottige et al., 2017b). The fact that in this study, a pre-acclimatised aerobic oxalate-degrading biofilm could rapidly (instantly) start up a BES for oxalate removal under saline and alkaline conditions is promising.

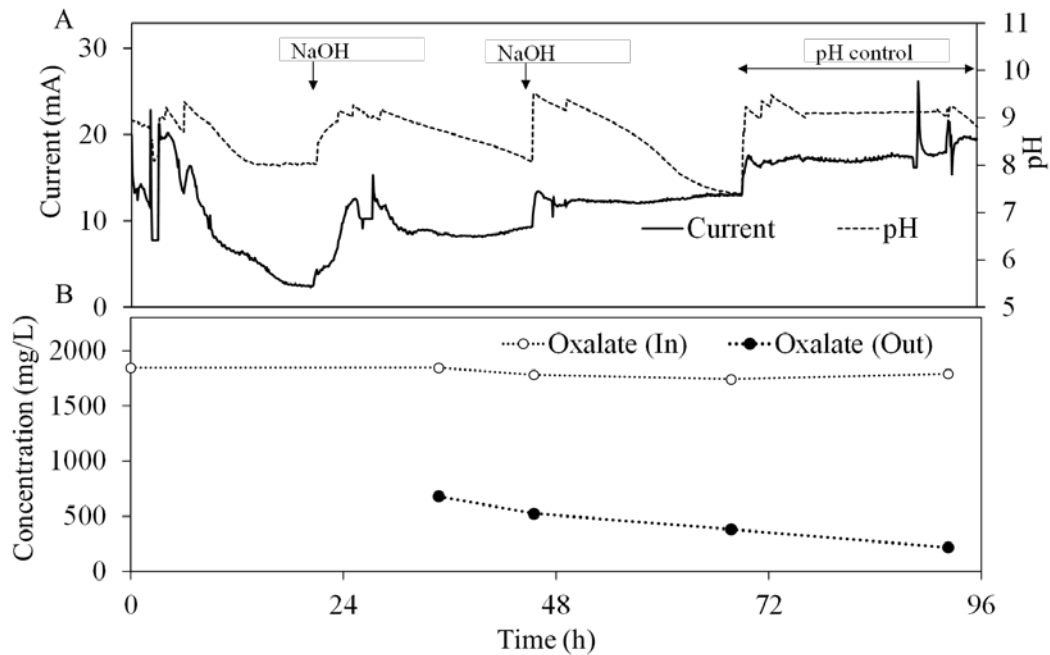


**Figure 7.2.** (A) BES current generation and pH profile during start up with biofilm granules from aerobic bioreactor, using influent with 25 mM sodium oxalate. The anode potential was +200 mV and HRT of 1 day for first 4 days. (B) Oxalate concentration in anolyte inflow and outflow streams for the first 4 days.

### 7.3.2. Increasing hydraulic loading increased current and oxalate removal when the anolyte had a pH of ~9.

The biofilm was further characterised for its ability to convert (remove) oxalate into current at various HRTs (Figure 7.3). Decreasing HRT (from 24 to 3 h) increased the current (Figure 7.3A). This suggested that the anodic biofilm activity was limited by the oxalate availability. In fact, increasing the oxalate loading rate (decreasing HRT) resulted in linear increases in both the current ( $R^2 > 0.99$ ) and the oxalate removal rate ( $R^2 > 0.99$ ) (Figure 7.3D). The maximum current production was  $122 \pm 0.6$  mA ( $363 \text{ A/m}^3$ ) as recorded at a HRT of 3 h. The results were reproducible as the biofilm was able to reproduce similar current (e.g. at HRTs of 12 h and 6 h).

Notably, at a very low HRT of 1 h the current was drastically reduced (Figure 7.3C). Figure 7.3B shows that after the HRT was reduced from 12 h to 1 h, the current initially increased as expected due to increased oxalate loading (from 27 mA to 111 mA). However, the current only lasted for a short period (~ 80 min) and then a collapse was recorded (Figure 7.3B). Such a collapse was likely due to an increasing anolyte pH initiated by the higher flux of the alkaline influent (pH 12.5). As such, the acidity generated from the oxalate oxidation (Reaction 7.1) was not sufficient to sustain the anolyte pH at ~ 9. Clearly, the gradual increase (within 20 mins) in the anolyte pH to 10 coincided with a current drop (from 106 mA to 42 mA), and with further increase in the anolyte pH to 11.3 (maximal), the current drastically decreased to 5 mA (Figure 7.3B). Overall, this suggested that at anolyte pH higher than ~ 9.7, the biofilm became less proficient to convert oxalate into current. Hence, the optimal pH of the anodic biofilm was lower than 9.7, aligned with the optimum pH (pH 9) recorded for the aerobic biofilm prior to inoculation and acclimatisation in the BES (Weerasinghe Mohottige et al., 2017a).

To rectify the suppression caused by the pH rise (i.e. due to the overloading of alkalinity at elevated influent load), and to test if the now impacted anodic biofilm activity could be readily revived, the HRT was reverted to 12 h (Figure 7.3B, at ~ day 6.3). As expected, with a higher HRT the anolyte pH gradually returned to ~ 9 again, and the current was also gradually increased to a similar level (~ 26 mA) as noted earlier with the same HRT (Figure 7.3A).

In terms of coulombic conversion, a reasonably high and stable CE of ~ 70% was recorded at most tested HRTs (Figure 7.3C). This suggested a good ability of the biofilm to electrochemically oxidise the oxalate. As near complete oxalate removal was recorded at most HRTs tested (Figure 7.3D), a CE of 70% means that 30% of the oxalate was removed via non-bioelectrochemical pathways such as fermentation or methanogenesis. Since prior to this study methanogenic activities were detected with the aerobic biofilm (Weerasinghe Mohottige et al., 2017a), this unaccountable loss of oxalate in the BES may also be due to methanogenesis. However, further studies are required to elucidate these losses.

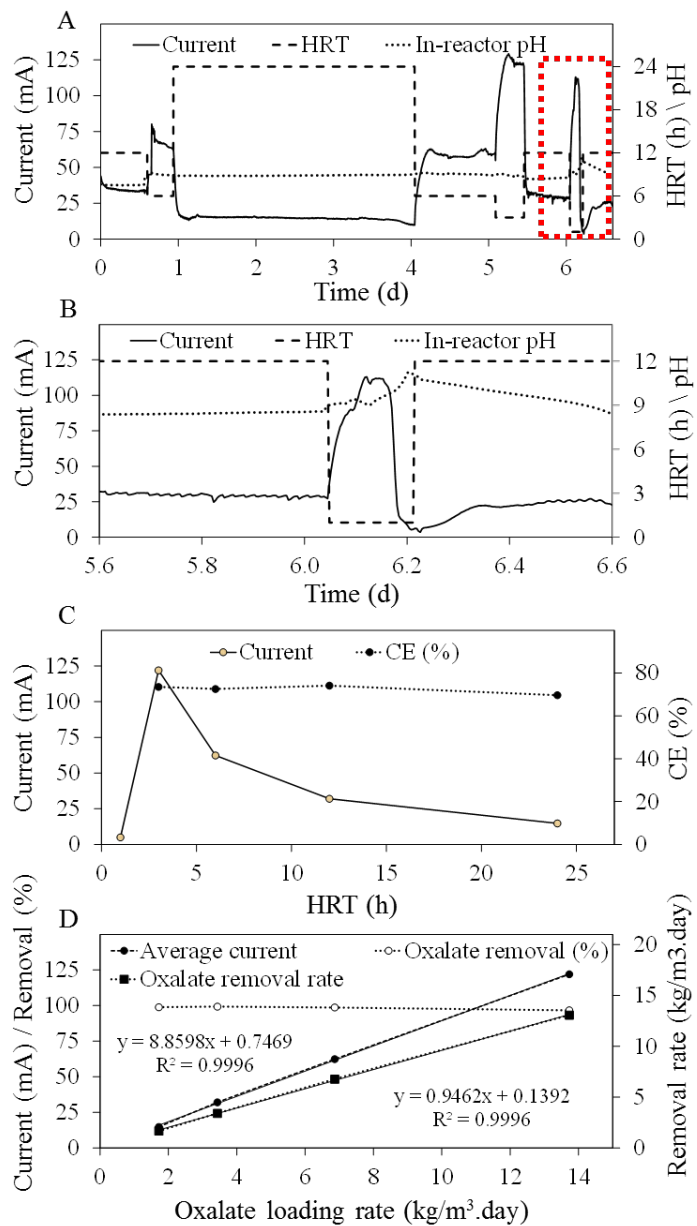


**Figure 7.3.** BES performance at various HRTs at an anode potential of -300 mV vs. Ag/AgCl, in-reactor pH of ~ 9 and with sodium oxalate as only electron donor. (A) Variation of HRT and current production over time. An enlarged view of area covered by red dotted box is given in (B). (C) Average current and CE (%) at various HRTs. (D) Oxalate removal percentage and average current produced at various COD loading rates.

### **7.3.3. The oxalotrophic biofilm remained proficient in generating current even at low anode potentials**

Anode potential is a critical factor determining the performance of a BES process. Typically, a more positive anode potential is favourable for microbial energy gain (Torres et al., 2009; Wagner et al., 2010). However, some studies showed that lower anode potentials enabled higher anodic current (Aelterman et al., 2008; Torres et al., 2009). From a BES operational standpoint, it is desirable if an anodic biofilm could produce maximal current at a low anode potential as this would minimise the energy loss in the anodic process (Aelterman et al., 2008). Hence, it would be meaningful to determine the effect of anode potential on the performance of our oxalate-degrading BES (Figure 7.4).

When the anode potential was varied between -300 mV and +200 mV, no noticeable changes in current ( $68\pm2$  mA) and cathode potentials (~ -1250 mV) were recorded (Figure 7.4A), suggesting that the anodic activity of the biofilm remained stable. However, current began to decrease when the potential reduced to below -300 mV (Figure 7.4A, ~ 4.5 d). Even at a very low potential of -600 mV, the biofilm could still generate a notable current ( $10.5\pm0.8$  mA). This was not surprising because under the tested condition (pH 9, oxalate 25 mM), oxalate oxidation is thermodynamically feasible as long as the anode potential was higher than -644 mV (see Appendix 3 equation S7.5). The ability of the biofilm to anodically oxidise oxalate was also evident from the relationship between steady-state currents and anode potentials (Figure 7.4B). Such relationship again confirmed that the biofilm was proficient in generating current even at a very low anode potential (e.g. at -500 mV), and both the oxalate removal and CE could be sustained at a relatively stable range (near 100% and 60%, respectively) in all the tested conditions (Figure 7.4B). In terms of oxalate removal rate, when the BES was operated in open circuit mode a notable rate was recorded ( $3 \text{ kg/m}^3\text{.d}$ ), plausibly due to alternative degradation pathways as previously mentioned. Nevertheless, with increasing anode potentials (from -600 mV to -300 mV) oxalate removal rate remarkably increased from  $4.2 \text{ kg/m}^3\text{.d}$  to  $8.75 \text{ kg/m}^3\text{.d}$  (Figure 7.4C).

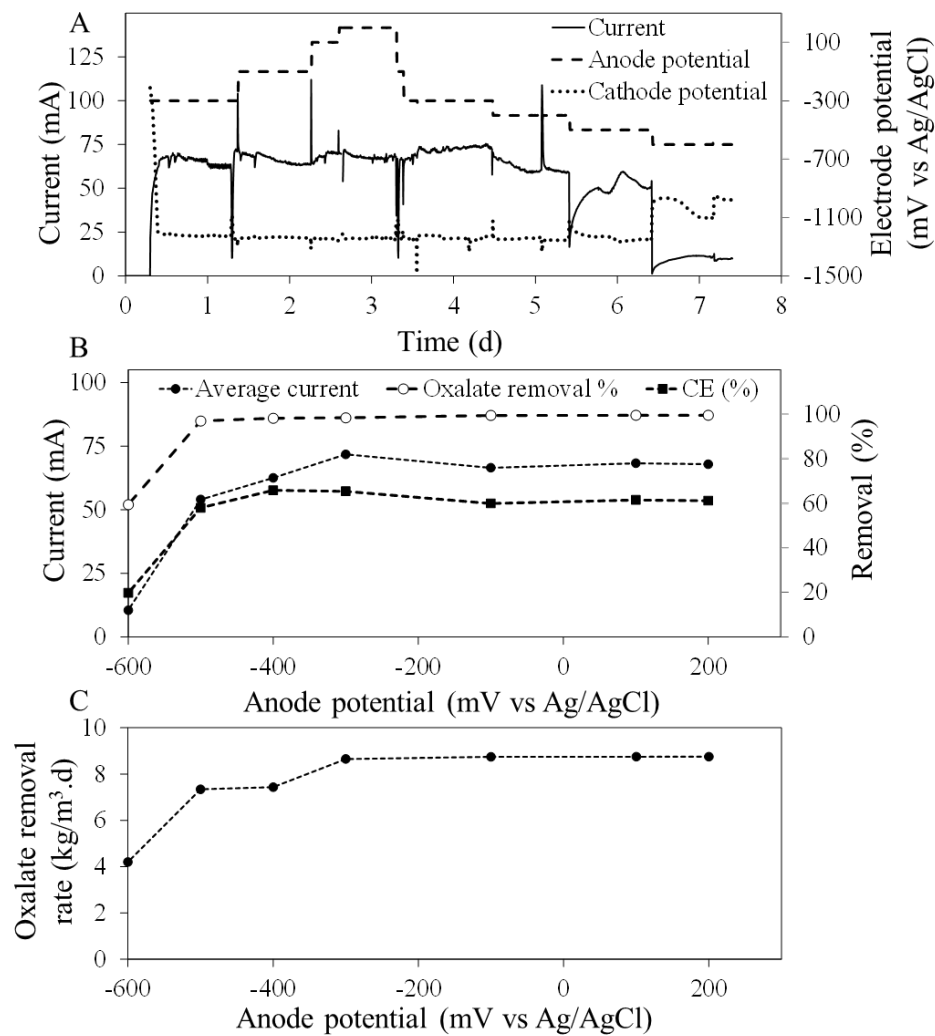


**Figure 7.4.** BES performance at various poised anode potentials from -600 mV to +200 mV vs. Ag/AgCl at in-reactor pH of 9 – 9.5 with 25 mM sodium oxalate as only electron donor and anodic chamber HRT of 6 h. (A) Current production and electrode potentials over time. (B) Average current produced, oxalate removal percentage and CE (%) at various poised anode potentials. (C) Positive linear relationship between current and oxalate removal rate.

### 7.3.4. Simultaneous acetate degradation by the established oxalotrophic anodic biofilm

Apart from oxalate, other simple organics such as acetate are also commonly present in alumina refinery process water (McKinnon & Baker, 2012; Tilbury, 2003). Unlike oxalate that directly affects the alumina product quality and yield (Power et al., 2012), these compounds may affect oxalate degradation in a microbial treatment process. In

the presence of acetate and oxalate, oxalotrophic microorganisms may prefer to metabolise acetate over oxalate for cell growth (a metabolic phenomenon known as diauxic growth) (Dijkhuizen et al., 1978; Krulwich & Ensign, 1969; Whiting et al., 1976). For example, Dijkhuizen et al. (1978) found that *Pseudomonas oxalaticus*, an oxalate metabolizing microorganism, preferred to metabolise acetate over oxalate when both substrates were present in anaerobic condition. Hence, in this study the effect of acetate on oxalate degradation in the BES was investigated by gradually increasing acetate concentration in the influent (from 0 to 30 mM), while maintaining the oxalate concentration constant (25 mM) (Figure 7.5A).

The results showed that increasing acetate concentration increased the current almost instantly and linearly (Figures 7.5B and D), suggesting that in the presence of oxalate the established oxalotrophic anodic biofilm could also readily convert acetate into anodic current. Apparently, there was no sign of diauxic metabolism recorded. The addition of acetate did not affect the oxalate removal rate, and the biofilm concurrently removed both oxalate and acetate at efficiencies of nearly 100% (Figure 7.5C).

To test if the addition of acetate would affect the overall coulombic conversion efficiency of the anodic process, the CE% was calculated (based on the total amount of electrons retrieved as current versus the amount of electrons dissipated as substrate removal (both acetate and oxalate) in the BES anode) (Figure 7.5D). Compared with the previous experiment where oxalate was used as the sole substrate, the CE% increased from 71% to 80% with the increasing molar ratio of acetate in the feed (Figure 7.5D). However, although with nearly complete removals of both acetate and oxalate (Figure 7.5C), it remained uncertain whether the improved CE% was due to a more proficient anodic conversion of oxalate or acetate. Nonetheless, the result confirmed that the anodic oxalate removal was highly efficient and was not impacted by the presence of acetate. Indeed, the anodic biofilm could efficiently oxidise both substrates.

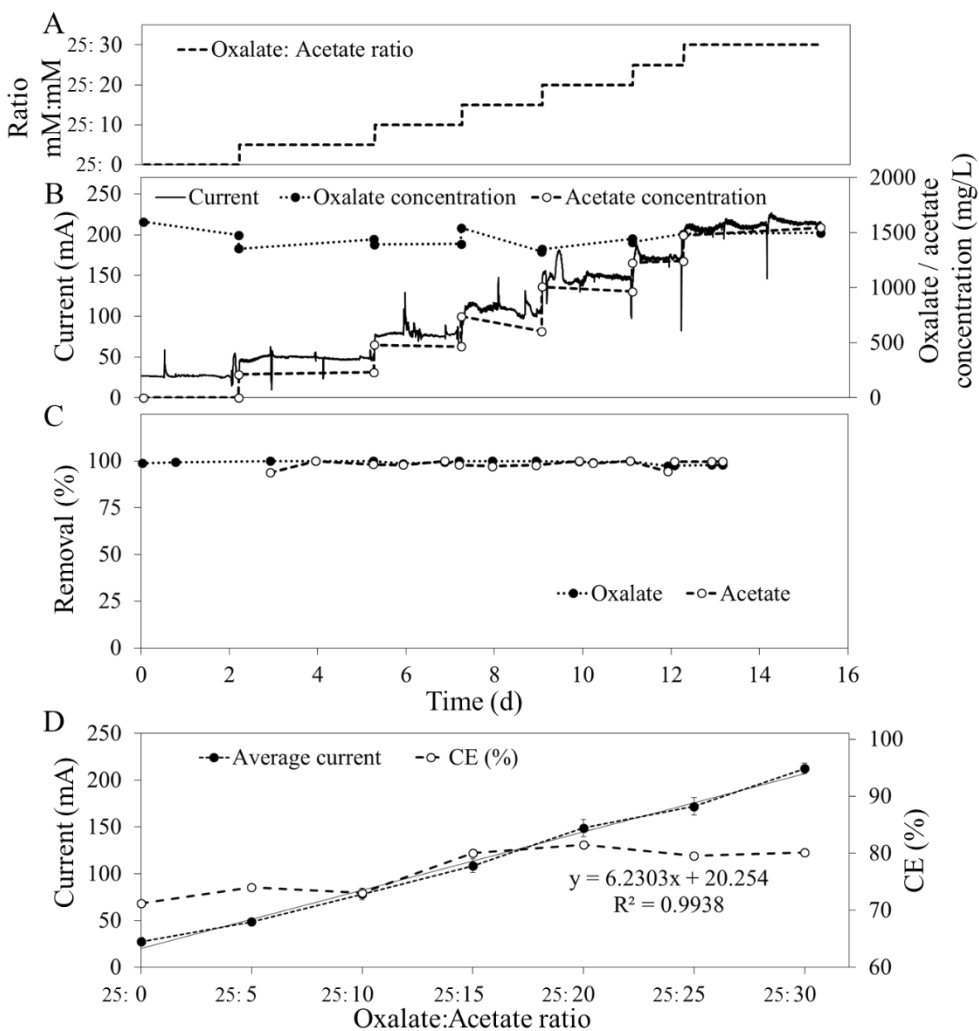


**Figure 7.5.** Increase in current production with increasing acetate concentrations in the feed with sodium oxalate (25 mM) at anode potential of -300 mV vs. Ag/AgCl, HRT of 12 h and in-reactor pH of 9.5. (A) Increase in oxalate to acetate ratio over time. (B) Current production, and influent oxalate and acetate concentrations over time. (C) Oxalate and acetate removal efficiencies over time. (D) Relationship of average current production and CE with oxalate to acetate ratio.

### 7.3.5. Changes in microbial community compositions at different stages of the BES operation

The effectiveness of the strategy of using the so-called “aerobic biofilm-electrode assemblage” to start up a BES for oxalate removal was demonstrated. Understanding the temporal changes in the microbial communities involved in this process would be valuable to develop this effective strategy. Hence, the microbial communities of the

biofilm at different stages (1st: prior to inoculation; 2nd: during active BES operation with oxalate as the sole substrate; and 3rd: during active BES operation with both oxalate and acetate as the substrate) were characterised and compared (Figure 7.6).

Rarefaction curves of all samples sequenced indicated that sequencing depth was adequate to capture bacterial diversity present in the samples (Appendix 3 Figure S7.1). The microbial communities of the six biofilm samples were compared using principal coordinate analysis (PCoA), which measured the similarity amongst the samples based on phylogenetic diversity (Figure 7.6A). Each point on the PCoA plot represents a sample and a closer distance between two points indicates smaller differences between the two microbial communities. In general, the sequences of all tested samples were distinctively clustered based on the aforesaid three operational stages (Figure 7.6A). A notable shift of the clusters occurred after the aerobic biofilm (BR-1 and BR-2) was inoculated to the BES (BES-21D and BES-75D), suggesting that the microbial composition was remarkably changed when the biofilm was forced to use an anode instead of oxygen as an electron acceptor to oxidise the oxalate. When both acetate and oxalate were made available as substrates, the microbial composition of the biofilm shifted again to form a new distinct cluster (BES-99D and BES-103D) (Figure 7.6A). This affirmed that the substrate characteristic was influential on microbial composition of the anodic biofilm. Similar conclusion could be derived from the unweighted pair group method with arithmetic mean (UPGMA) clustering (Figure 7.6B). Again, the microbial communities in all samples were clustered according to the three distinct stages, signifying that the biofilms at these unique operational stages were phylogenetically different.

The relative abundances of microbial families of the aerobic biofilm (inoculum) and those acclimatized in the BES are depicted in Figure 7.6C. Before inoculated into the BES, the dominant microbial families in the aerobic biofilm inoculum were *Rhodobacteraceae* (~50%) and *Rhodocyclaceae* (~18%). Among the members of the *Rhodobacteraceae* family, *Paracoccus* was the dominant genus (47%) in the aerobic reactor biofilm. Microorganisms belonging to this genus have been shown as being able to oxidise oxalate. For instance, Anbazhagan et al. (2007) isolated a *Paracoccus* strain capable of oxidising oxalate under aerobic and alkaline (pH 8) condition (Anbazhagan et al., 2007). Another pure culture of *Paracoccus* (*P. homiensis DRR-*

3) was also found to be electrochemically active and was able to produce anodic current in a microbial fuel cell (Jothinathan & Wilson, 2017).

After inoculation and acclimatisation in the BES, the abundances of families *Rhodobacteraceae* (20%) and *Rhodocyclaceae* (12%) in the biofilms decreased remarkably (Figure 7.6C). During the time when the BES was operated with oxalate as the sole electron donating substrate, the abundance of *Oxalobacteraceae*, *Idiomarinaceae*, *Clostridiaceae* and *Balneolaceae* increased considerably. As expected, after the BES influent was supplemented with acetate, the microbial community became more diverse with several families becoming more abundant (from <3% to >10%) (e.g. *Rhodobacteraceae*, *Oxalobacteraceae* and *Marinicellaceae*). Of special interest among these bacterial families is *Oxalobacteraceae*, which is a well-known oxalotrophic bacterial family containing both aerobic and anaerobic strains characterised in past studies (Baldani et al., 2014; Sahin, 2003). Further, under the family *Oxalobacteraceae*, genera *Oxalicibacterium* and *Oxalobacter* are known oxalate degraders, of which, *Oxalobacter sp.* are known to be obligatory anaerobic (Baldani et al., 2014). Since the abundance of *Oxalobacteraceae* remarkably increased after the aerobic biofilm was inoculated to the BES (under anaerobic condition), it is plausible that the increased abundance of *Oxalobacteraceae* was attributed to an increased growth of *Oxalobacter sp.* Indeed, *Oxalobacter formigenes* is a widely studied oxalotrophic strain that requires acetate as a growth supplement (Allison et al., 1985; Baldani et al., 2014). The increased abundance of *Oxalobacteraceae* (from 7.3% to 11.4%) recorded after the BES influent was supplemented with acetate was a result of the enrichment of this species. Although, no report had so far confirmed that *Oxalobacteraceae* strains were electrochemically active, the fact that our biofilm could efficiently convert both oxalate and acetate into current (CE 80%) suggests that *Oxalobacteraceae* strains might play a role in producing current in the described BES process. However, further studies are required to confirm this.

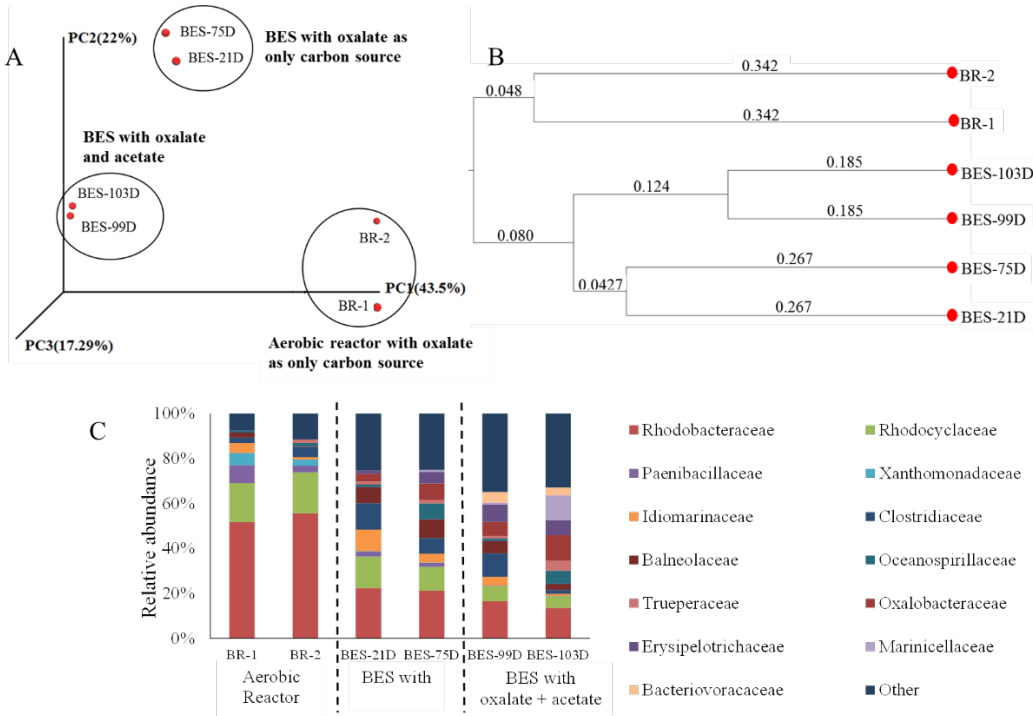


**Figure 7.6.** (A) Principle component analysis (PcoA) profile (unweighted Unifrac) for samples collected from the aerobic bioreactor (BR-1 and BR-2) and BES (BES-21D, BES-75D, BES-99D to BES-103D) indicating clustering of samples. (B) Unweighted pair group method with arithmetic mean (UPGMA) dendrogram of unweighted unifrac distances sample set. The values at the branches show the similarity of the samples. The two plots highlight the clustering of samples according to reactor type and carbon source available. (C) Stacked bar plot of the relative abundance bacterial families in the aerobic bioreactor and BES fed with oxalate and oxalate + acetate. Family that represent less than 3% of the total microbial community composition were classified as “others”.

### 7.3.6. Implication of the findings

Overall, this study offered a number of new findings. The most notable one is that an aerobic oxalotrophic biofilm could rapidly switch their final electron acceptor from oxygen to an electrode for oxalate oxidation, enabling a rapid and successful start-up of a BES process. Second, the BES could efficiently remove oxalate (> 97%) from an alkaline and saline influent, and allowed a coulombic conversion of oxalate into current at the highest efficiency reported in the literature (CE >70%). Third, the well-known oxalate degrading bacterial family *Oxalobacteraceae* became more abundant

over time in the oxalate-degrading BES. Fourth, the established oxalotrophic biofilm could simultaneously convert both acetate and oxalate into anodic current at a high CE of 80%. These are new knowledge that have not been previously reported.

The practical implication of these findings can be appreciated by comparing the performance of the described BES process with other industrial scale oxalate-removing bioprocesses (Table 7.1). Here, the selected aerobic processes in the comparison were operated with alkaline alumina refinery spent liquor and residue lake water, and are considered as benchmark for this comparison. In terms of oxalate removal, it is clear that all aerobic bioprocesses were better than the BES processes, with the highest rate (41.2 kg/m<sup>3</sup>.d) recorded from a pilot scale bioreactor. However, the recovery of resources (such as energy and caustic) are not allowed in aerobic reactors. Although the laboratory-scale bioreactor (from which the aerobic oxalotrophic biofilm-graphite granules were harvested for this work) removed oxalate at a lower rate (23.5 kg/m<sup>3</sup>.d), it could be operated at a considerably higher hydraulic loading rate (HRT 3.5 h vs. ≥14.7 h) (Table 7.1). This is attractive because a lower operational HRT enables a smaller reactor foot-print, and hence a lower capital investment.

In the literature, only limited studies have explored the use of BES for oxalate removal. Bonmati et al. (2013) reported for the first time that oxalate could be completely removed in a BES. However, only a very poor anodic conversion of oxalate was recorded (CE 21%), and it was unclear if the anodic oxalate removal could be carried out under alkaline and saline conditions. Under industrial relevant conditions (high alkalinity and salinity), the BES established in the current study enabled oxalate removal at a rate comparable to the laboratory-scale aerobic process (19.6 vs. 23.5 kg/m<sup>3</sup>.d) (Table 7.1). To this end, using BES for treating alumina refineries liquor can be considered attractive.

The start-up strategy adopted in this study also deemed practically attractive. In our previous study, a similar BES loaded with plain graphite granules was seeded with activated sludge. However, start-up was not successful even after a prolonged period (> 50 days), with only negligible oxalate removal recorded (0.4 kg/m<sup>3</sup>.day) (Weerasinghe Mohottige et al., 2017b). Having an effective and reliable source of microbial inocula is highly desirable for any industrial microbial processes. A process

demanding a long start-up period requires high operational cost, which is obviously undesirable. The fact that an aerobic oxalotrophic biofilm could readily start up a BES process is encouraging, as this can reduce down time operation of the process (e.g. during circumstances such as reactor failure, process inhibition (see Appendix 3 Figure S7.3)).

Last but not the least, the described BES processes could also facilitate caustic production, which can be considered apart from oxalate removal, as an additional benefit for the alumina industry. Since the industry is well known for its high demand for caustic, this aspect should be further researched. Finally, as with many other novel processes, further optimisation and development of the described BES process are desired.

**Table 7.1.** Comparison of oxalate removal performance of various aerobic and bioelectrochemical reactor processes.

\* = Normalised to active void volume of the bioreactor (i.e. anodic chamber of BES). ^ = In-reactor anolyte pH value is not available

Process	Electron acceptor	Influent	Reactor size (m <sup>3</sup> or L)	HRT h	In-reactor pH	Oxalate removal rate* kg/m <sup>3</sup> .d	Oxalate removal %	Current density* A/m <sup>3</sup>	CE %	Reference
<b><i>Aerobic reactor</i></b>										
Pilot scale aerobic biofilm reactor	Oxygen	Refinery lake water	3.8 m <sup>3</sup>	20	9.6	41.2	100	n.a	n.a	(McSweeney, 2011)
Full scale aerobic biofilm reactor	Oxygen	Refinery lake water	450 m <sup>3</sup>	14.7	9.7	30.6	100	n.a	n.a	(McSweeney, 2011)
Full scale aerobic reactor	Oxygen	Refinery lake water + oxalate thickener discharge	270 m <sup>3</sup>	20	10	40.3	100	n.a	n.a	(McKinnon & Baker, 2012)
Lab scale aerobic biofilm reactor	Oxygen	Synthetic liquor	1.5 L	3.5	9.2±3	23.5	100	n.a	n.a	(Weerasinghe Mohottige et al., 2017a)
<b><i>BES reactor</i></b>										
Dual chamber BES reactor	Graphite granules anode	Synthetic liquor	0.34 L	6.96	-^	10.3	100	29.8	21±2	(Bonmati et al., 2013)
Dual chamber BES reactor	Graphite granules anode	Synthetic liquor	0.5 L	24	9	0.4	2	3.0	39	(Weerasinghe Mohottige et al., 2017b)
Dual chamber BES reactor	Graphite granules anode	Synthetic liquor	0.5 L	3	9.1±4	19.6	97	363.1	73.5	This study

## **7.4 Conclusions**

For the first time, an aerobic oxalotrophic biofilm pre-grown on a graphite carrier was demonstrated as an effective agent to readily start-up a BES under alkaline and saline conditions. The biofilm could rapidly switch from using oxygen to graphite as electron acceptor for efficient anodic oxalate oxidation (CE 70%). The established biofilm could simultaneously degrade both oxalate (25 mM) and acetate (30 mM) with removal of 97 – 99 % removal efficacy (HRT 12 h). The microbial community of the established anodic biofilm deviated notably from that of the initial aerobic biofilm, with known oxalotrophic families (e.g. *Oxalobacteraceae*) became increasingly abundant over time.

# **8 CONCLUSIONS AND SUGGESTIONS FOR FUTURE RESEARCH**

Overall, this thesis reveals the BES as a promising technology for organics removal and caustic recovery from alkaline, saline and N-deficient liquors. Another important outcome of this thesis is that the N-fixing bacteria hold promise for enhancing the performance and economics of aerobic bioreactors used for destructing organics. The thesis provides new knowledge and alternative process options for biological organics removal and resource recovery in Alumina industry.

This final chapter summarises the main findings of the study, discusses the potential applications to alumina refinery process and provides suggestions for future research.

## **8.1 Main findings of the study**

In six experimental chapters, biological removal of organics, effect of different operational parameters on organics removal and recovery of caustic from alkaline-saline wastewater were discussed in both bioelectrochemical systems and aerobic bioreactor technology.

The first experiment explored and compared oxalate degradation in BES under N-supplemented and N-deficient conditions using an alkaline and saline synthetic medium. However, the reactors inoculated with activated sludge were unable to remove oxalate or produce any significant current from oxalate (Chapter 2) due to the paucity of oxalotrophic bacteria regardless of N availability. Unlike the low oxalate degradation, the biofilms readily responded to other organic substrates common for Bayer process liquors, such as sodium acetate and sodium formate. Another main aspect of this thesis was to explore the recovery of caustic which is the main chemical used in the Bayer processing. Thus, the chapter 3 was mainly focused on the caustic recovery efficiency of the established BES reactors. The N-deficient BES allowed the recovery of caustic stream that had less unwanted cations such as  $\text{NH}_4^+$  than the N-supplemented BES reactor.

As aerobic bioreactors are commercially operated to degrade oxalate in Alumina refinery plants, two lab scale packed bed aerobic reactors were used to enrich oxalate degrading biofilms by using soil microorganisms as the inoculum under N-supplemented and N-deficient conditions (Chapter 4). For the first time, this study revealed the use of haloalkaline bacterial culture grown in N-deficient medium to degrade oxalate completely. At the beginning, the N-deficient bioreactor had a long lag phase than the N-supplemented reactor. The importance of DO on oxalate removal efficiency was explored in Chapter 4. In the N-supplemented reactor, a positive linear correlation was recorded between the oxalate removal rate and the DO concentration across the DO concentrations tested. In contrast, the oxalate removal rate became plateau above 3 mg/L DO in the N-deficient reactor. However, simultaneous aerobic and anaerobic removal of oxalate was recorded in every tested DO concentration in both N-supplemented and N-deficient conditions. From further studies, formate, acetate and methane were detected as the by-products of oxalate degradation in both reactors. The established aerobic biofilms were further characterised in Chapter 5, under various alkaline pH conditions and in the presence of various simple organic compounds. Although biomass was acclimatised at pH 9, the optimal oxalate removal rate in the N-deficient reactor was at a pH range of 7-8. In contrast, the optimal removal rate of the N-supplemented reactor was at the same pH at which the biomass was acclimatised (pH 9). The specific oxalate removal rates of the both reactors were similar at optimal pH conditions. However, the intermittent exposure of N-deficient biofilm to the optimal pH environment improved the oxalate removal rate at pH 9. Other simple organic impurities common for Bayer liquor (acetate, formate, succinate and malonate) had a negligible effect on oxalate removal rates and potentially could increase the performance of the N-deficient reactor. Based on the improved performance of the N-deficient biofilm, the oxalate oxidation kinetics were studied in both biofilms using Michaelis-Menten model (Chapter 6). The N-deficient biofilm showed a higher maximum oxalate degradation rate and higher affinity towards oxalate compared to N-supplemented biofilm. The differences in the two biofilms were further confirmed by microbial community analysis. The microbial community of the N-deficient reactor appeared more diverse than that of the N-supplemented reactor. Members of the oxalotrophic bacterial genus *Paracoccus* from family *Rhodobacteraceae* were dominant in the N-supplemented biofilm, whereas the N-

deficient biofilm was dominated by members of the N-fixing genus *Azoarcus* from family *Rhodocyclaceae*.

The difficulty in establishing an oxalate degrading biofilm in BES anode in Chapter 2 was overcome in Chapter 7. This study examined the use of aerobically grown biofilm coated graphite granules in the BES as the inoculum and the anode. The pre-grown biofilm in aerobic reactor was able to instantly switch from oxygen to anode as the electron acceptor and produced current from electrochemical oxidation of oxalate. The successful establishment of oxalate degrading BES biofilm (Oxalate removal > 98%, CE > 70%) was reinforced by 454 sequencing of the 16S rRNA gene of the microbial community. The microbial analysis revealed that the members of the oxalate degrading *Oxalobacteraceae* family were present in the biofilm.

## **8.2 The practical implementation of biological oxalate removal processes in alumina refinery**

As discussed throughout the previous chapters, the organic contaminants in the Bayer process liquor can cause significant economic losses and process problems by reducing the product ( $\text{Al(OH)}_3$ ) quality and yield. The presence of organics in the process liquor reduce the alumina yield by approximately 0.4 g/L for each 1 g/L TOC (Tilbury, 2003). The hostile conditions (pH > 13, Temperature > 60°C, caustic content and aluminium ion content) of the Bayer process liquor hinder the applicability of biological processes for complete degradation of oxalate and other organics in the main Bayer process stream. However, there are several potential locations within the refinery where biological processes can be applied to treat the refinery water.

One suitable location with less harsh conditions is the refinery lake water which is used as a water source to slurry fresh bauxite for the Bayer circuit at some refineries. The organics content of the lake water is often elevated as a result of disposal of red mud, which contains residual organics, near the refinery lakes. As lake water is more diluted (pH < 13), the biological treatment of lake water to remove organics is possible and would reduce the organics concentration in the process water.

Another appropriate location within the alumina refinery for application of biological processes is the oxalate cake or slurry that is separated from the Bayer circuit. In the current practice, the unwanted oxalate is precipitated from the Bayer process liquor by physiochemical methods. This separated oxalate slurry is stored in residue areas or storage tanks within the refinery. The disposal of this oxalate residue is a large problem due to limited space, undesirable emissions and environmental contamination. Microbial oxalate degradation allows complete destruction of oxalate in environmentally feasible way.

Based on the experimental results on oxalate removal rates in Chapter 4 (aerobic reactor) and Chapter 7 (BES reactor) the foot print of the potential reactor application was calculated for the oxalate degradation capacity of 40 t/d. The concentration of the oxalate slurry was considered as 100 g/L for the calculation. As indicated in the table 8.1, when degrading oxalate at the rate of 111.3 mg/h.g biomass, the required reactor media volume for the aerobic reactor was 1556 m<sup>3</sup> with HRT 1.29 d. However, the required bioanode volume for BES reactor was higher than the aerobic reactor media volume. Considering the maximum experimentally achieved oxalate removal rate of 94.5 mg/h.g biomass in BES operation, the required bioanode volume was 1832 m<sup>3</sup> for the degradation of daily oxalate production of 40 tonne. Even though, the BES configuration requires a higher footprint, the feasibility of alkalinity recovery from BES reactor is beneficial to alumina industry.

**Table 8.1.** Estimated footprint for the removal of daily oxalate production of 40 t/day – A comparison of aerobic reactor and BES.

Parameter	Unit	Aerobic Reactor (Chapter 4)	BES process (Chapter 7)	Remarks
Oxalate production	T/d	40	40	(McSweeney, 2011)
Influent oxalate concentration	g/L	100	100	(McKinnon & Baker, 2012)
Influent flow rate	m <sup>3</sup> /d	400	400	
Maximum experimental oxalate removal rate	mg/h.g biomass	111.3	94.5	
Biomass density in lab scale reactor (per media volume)	g/m <sup>3</sup>	9622	9622	
Volumetric oxalate degradation rate per media volume	kg/d.m <sup>3</sup>	25.7	21.8	
Media to liquid volume ratio in lab scale reactor		3.0	3.0	Considered the same ratio in both systems
HRT	d	1.29	1.51	
Effective reactor liquid volume	m <sup>3</sup>	515	606	
Biological media required	m <sup>3</sup>	1556	1832*	

\*BES reactor anode volume

Despite of being easy to operate and having a smaller foot print than the BES, the main shortcoming of the aerobic reactor application in alumina industry is the reduction of alkalinity due to CO<sub>2</sub> production. Moreover, unlike in BES processes, the aerobic bioreactor processes do not facilitate the recovery of alkalinity. The recovery of alkalinity is important for the economics of alumina production. Therefore a basic cost comparison was carried out to understand the benefit of caustic recovery from BES processes. Even though many other factors influence the cost of BES application in commercial scale, the comparison in table 8.2 considered only the cost related to input energy requirement for the BES process (based on Chapter 3 experimental results). Even with higher energy requirement, the N-deficient reactor was able to produce a

cleaner caustic solution absent of unwanted cations ( $\text{NH}_4^+$ ). For the comparison, the current market price of the 1 tonne of caustic was considered to fluctuate 250 to 500 (AUS\$). The cost associated with the energy input to BES operation was lower than the market price of 1 T of caustic in both N-deficient and N-supplemented BES processes.

**Table 8.2.** Comparison of energy input cost for BES to produce 1 T of caustic with the market price of caustic.

Reactor (Based on chapter 3)	Energy Input (kWh/kg caustic)	Energy cost (AUS\$/ kWh)	Energy cost (AUS\$/t caustic)	Cost of caustic (AUS\$/t) (Approximately)	Remarks
N-supplemented	0.85	0.26	221	250-500	Energy cost – Based on Synergy (Western Australia energy provider)
N-deficient	0.91	0.26	236	250-500	Cost of caustic based on market prices

### 8.3 Suggestions for Future Research

This thesis demonstrated the feasibility of lab scale application of both BES and aerobic reactor for efficient removal of oxalate and other organics from synthetic alkaline, saline and N-deficient wastewater. However, further experiments and investigations are required for the application of the technology in industrial scale.

The future research could focus on demonstrating the BES technology in pilot scale or full for treating real liquors derived from Bayer process. Possible future research questions are outlined below.

- **Can the BES reactor be used to treat the real samples of Bayer spent liquor (after Al(OH)<sub>3</sub> precipitation) and residue lake water?**

Due to the unavailability of real Bayer liquors at the time of the study, the experiments were conducted with synthetic medium which may not represent the complex chemistry of the real Bayer liquor. Hence the possible effects of Bayer liquor on the BES process were not fully demonstrated. For instance, the media used contained no alumina/ aluminium, and as such it may not allow a true reflection of the process performance. Future work or process development should include experiments with real liquor samples sourced from alumina industry.

- **Can the aerobically pre-grown biofilm degrade oxalate in BES under N-deficient conditions?**

Chapter 7 described the successful start-up of BES reactor with aerobically pre-grown oxalotrophic biofilm under N-supplemented conditions. However, due to time constrain the N-deficient aerobic biofilm (discussed in chapter 4, 5 and 6) was not investigated in a BES reactor to study the oxalate degradation capability. Hence, a similar study for N-deficient biofilm is required to compare the oxalate degradation performance to the performance of the N-supplemented biofilm.

- **Can the BES cathodic operation be optimised to increase the strength of caustic solution?**

Increasing the strength of recovered caustic stream is important for practical application of the technology as the recovered caustic could be readily used in the Bayer process. Hence, it is necessary to optimize the operational parameters of the cathodic chamber, such as HRT and volume, to maximise the cathodic caustic strength.

- **What microorganisms are actively involved in oxalate oxidation in BES reactor and aerobic reactor?**

The biofilms in the aerobic reactor and BES consisted of mixed bacterial communities. Hence, isolation and characterisation of the members of the microbial communities in the aerobic and anaerobic biofilms would allow to identify the key microorganisms involved in oxalate degradation in N-supplemented and N-deficient systems. Moreover the determination of the pH and temperature ranges of the isolated microorganisms would allow the optimisation of the operating conditions for maximum process performance.

- **Can oxalate in Bayer process liquor be treated in a fermenter?**

As discussed in Chapter 4, the microbial community in the aerobic reactor was able to degrade oxalate anaerobically. Hence, experiments could be conducted to explore oxalate fermentation under anaerobic conditions in a fermenter. The existing commercial scale aerobic bioreactors produce sodium carbonate as a results of aerobic oxalate oxidation. The sodium carbonate contained effluent is subjected to further causticisation process to form sodium hydroxide for reuse in the Bayer circuit. In this context, it is worth to explore the possibility to convert oxalate into CO<sub>2</sub> and CH<sub>4</sub> to minimise carbonate production.

## Reference

- Aelterman, P., Freguia, S., Keller, J., Verstraete, W., Rabaey, K. 2008. The anode potential regulates bacterial activity in microbial fuel cells. *Applied Microbiology and Biotechnology*, **78**(3), 409-418.
- Ahn, Y., Hatzell, M.C., Zhang, F., Logan, B.E. 2014. Different electrode configurations to optimize performance of multi-electrode microbial fuel cells for generating power or treating domestic wastewater. *Journal of Power Sources*, **249**, 440-445.
- Albuquerque, L., da Costa, M.S. 2014. The Family *Idiomarinaceae*. *The Prokaryotes: Gammaproteobacteria*, 361-385.
- Allen, R.M., Bennetto, H.P. 1993. Microbial fuel-cells - Electricity production from carbohydrates. *Applied Biochemistry and Biotechnology*, **39**, 27-40.
- Allison, M., Dawson, K., Mayberry, W., Foss, J. 1985. *Oxalobacter formigenes* gen. nov., sp. nov.: oxalate-degrading anaerobes that inhabit the gastrointestinal tract. *Archives of Microbiology*, **141**(1), 1-7.
- Allison, M.J., Daniel, S.L., Cornick, N.A. 1995. Oxalate-degrading bacteria. in: *Calcium Oxalate in biological systems*, (Ed.) S.R. Khan, CRC press. USA, pp. 131-168.
- American Public Health, A. 1995. *Standard methods for the examination of water and wastewater / prepared and published jointly by American Public Health Association, American Water Works Association. 19th ed.. ed.* Washington, DC : American Public Health Association, Washington, DC.
- American Public Health Association., American Water Works Association., Water Environment Federation. 1995. *Standard methods for the examination of water and wastewater. 19th ed.* American Public Health Association, American Water Works Association, and Water Environment Federation, Washington, D.C.
- Anbazhagan, K., Raja, C.E., Selvam, G.S. 2007. *Oxalotrophic Paracoccus alcaliphilus* isolated from Amorphophallus sp rhizoplane. *World Journal of Microbiology & Biotechnology*, **23**(11), 1529-1535.
- Antunes, A. 2014. The Family Haloplasmataceae. in: *The Prokaryotes: Firmicutes and Tenericutes*, (Eds.) E. Rosenberg, E.F. DeLong, S. Lory, E. Stackebrandt, F. Thompson, Springer Berlin Heidelberg. Berlin, Heidelberg, pp. 179-184.

- Atasoy, A. 2005. An investigation on characterization and thermal analysis of the Aughinish red mud. *Journal of Thermal Analysis and Calorimetry*, **81**(2), 357-361.
- Atkinson, D.E. 1977. Cellular energy metabolism and its regulation, Academic Press. San Diego.
- Australian Aluminium Council, L. 2010. Australian aluminium council position on climate change policy.
- Badalamenti, J.P., Krajmalnik-Brown, R., Torres, C.I. 2013. Generation of high current densities by pure cultures of anode-respiring *Geoalkalibacter* spp. under alkaline and saline conditions in microbial electrochemical cells. *Mbio*, **4**(3).
- Bahadur, K., Tripathi, P. 1976. Nitrogen fixation by microbial cultures with sodium salt of organic acids as carbon source. *Zentralblatt für Bakteriologie, Parasitenkunde, Infektionskrankheiten und Hygiene. Zweite Naturwissenschaftliche Abteilung: Allgemeine, Landwirtschaftliche und Technische Mikrobiologie*, **131**(4), 375-377.
- Baldani, J.I., Rouws, L., Cruz, L.M., Olivares, F.L., Schmid, M., Hartmann, A. 2014. The Family *Oxalobacteraceae*. in: *The Prokaryotes: Alphaproteobacteria and Betaproteobacteria*, (Eds.) E. Rosenberg, E.F. DeLong, S. Lory, E. Stackebrandt, F. Thompson, Springer Berlin Heidelberg. Berlin, Heidelberg, pp. 919-974.
- Balomenos, E., Panias, D., Paspaliaris, I. 2011. Energy and exergy analysis of the primary aluminum production processes: A review on current and future sustainability. *Mineral Processing and Extractive Metallurgy Review*, **32**(2), 69-89.
- Banciu, H.L., Sorokin, D.Y., Tourova, T.P., Galinski, E.A., Muntyan, M.S., Kuenen, J.G., Muyzer, G. 2008. Influence of salts and pH on growth and activity of a novel facultatively alkaliphilic, extremely salt-tolerant, obligately chemolithoautotrophic sulfur-oxidizing Gammaproteobacterium *Thioalkalibacter halophilus* gen. nov., sp nov from South-Western Siberian soda lakes. *Extremophiles*, **12**(3), 391-404.
- Bard, A.J., Faulkner, L.R. 2001. *Electrochemical methods: fundamentals and applications*. 2 ed. John Wiley & Sons, Inc., New York, USA.

- Barnett, N.W., Bowser, T.A., Russell, R.A. 1995. Determination of oxalate in alumina process liquors by ion chromatography with post column chemiluminescence detection. *Analytical Proceedings including Analytical Communications*. The Royal Society of Chemistry. pp. 57-59.
- Beyenal, H., Lewandowski, Z. 2005. Modeling mass transport and microbial activity in stratified biofilms. *Chemical Engineering Science*, **60**(15), 4337-4348.
- Bezerra, R.P., Matsudo, M.C., Sato, S., Perego, P., Converti, A., Carvalho, J.C.M.d. 2012. Effects of photobioreactor configuration, nitrogen source and light intensity on the fed-batch cultivation of Arthrospira (Spirulina) platensis. Bioenergetic aspects. *Biomass and Bioenergy*, **37**, 309-317.
- Bishop, P.L., Zhang, T.C., Fu, Y.C. 1995. Effects of biofilm structure, microbial distributions and mass-transport on biodegradation processes *Water Science and Technology*, **31**(1), 143-152.
- Bogatyrev, B.A., Zhukov, V.V., Tsekhovsky, Y.G. 2009. Formation conditions and regularities of the distribution of large and superlarge bauxite deposits. *Lithology and Mineral Resources*, **44**(2), 135-151.
- Bonmati, A., Sotres, A., Mu, Y., Rozendal, R., Rabaey, K. 2013. Oxalate degradation in a bioelectrochemical system: Reactor performance and microbial community characterization. *Bioresource Technology*, **143**, 147-153.
- Brady, J.P. 2011. An examination of the applicability of hydrotalcite for removing oxalate anions from Bayer process solutions, Queensland University of Technology.
- Brassinga, R.D., Fulford, G.D., Lang, R.G., McCready, R.G.L., Gould, W.D., Beaudette, L. 1989. Biodegradation of oxalate ions in Bayer process - removes oxalate-contg. compsn. from processing liquor, modifies pH and sodium concn. and introduces to bio-reactor contg. microorganism, Alcan Int Ltd (Alcn-C).
- Brown, N. 1991. Method for removing sodium oxalate from caustic aluminate liquors, Google Patents.
- Caporaso, J.G., Bittinger, K., Bushman, F.D., DeSantis, T.Z., Andersen, G.L., Knight, R. 2010a. PyNAST: a flexible tool for aligning sequences to a template alignment. *Bioinformatics*, **26**(2), 266-267.
- Caporaso, J.G., Kuczynski, J., Stombaugh, J., Bittinger, K., Bushman, F.D., Costello, E.K., Fierer, N., Pena, A.G., Goodrich, J.K., Gordon, J.I., Huttley, G.A.,

- Kelley, S.T., Knights, D., Koenig, J.E., Ley, R.E., Lozupone, C.A., McDonald, D., Muegge, B.D., Pirrung, M., Reeder, J., Sevinsky, J.R., Tumbaugh, P.J., Walters, W.A., Widmann, J., Yatsunenko, T., Zaneveld, J., Knight, R. 2010b. QIIME allows analysis of high-throughput community sequencing data. *Nature Methods*, **7**(5), 335-336.
- Cardwell, T.J., Laughton, W.R. 1994. Analysis of fluoride, acetate and formate in Bayer liquors by ion chromatography. *Journal of Chromatography A*, **678**(2), 364-369.
- Casey, E., Glennon, B., Hamer, G. 1999. Oxygen mass transfer characteristics in a membrane-aerated biofilm reactor. *Biotechnology and bioengineering*, **62**(2), 183-192.
- Chang, I.S., Moon, H., Bretschger, O., Jang, J.K., Park, H.I., Nealson, K.H., Kim, B.H. 2006. Electrochemically active bacteria (EAB) and mediator-less microbial fuel cells. *Journal of Microbiology and Biotechnology*, **16**(2), 163-177.
- Chen, H.L., Spitzer, D., Rothenberg, A., Lewellyn, M., Chamberlain, O., Heitner, H., Kula, F., Dai, Q., Franz, C. 11-15 March 2007. Sodalite scale control In alumina Bayer process. in: *Corrosion Conference and Expo (CORROSION 2007)* NACE International. Nashville, Tennessee, USA.
- Cheng, K.Y. 2009. Exploring the potential of bioelectrochemical systems for energy recovery from waste water. *Ph.D. Thesis*.
- Cheng, K.Y., Ho, G., Cord-Ruwisch, R. 2008. Affinity of microbial fuel cell biofilm for the anodic potential. *Environmental Science & Technology*, **42**(10), 3828-3834.
- Cheng, K.Y., Ho, G., Cord-Ruwisch, R. 2010. Anodophilic biofilm catalyzes cathodic oxygen reduction. *Environ. Sci. Technol.*, **44**(1), 518-525.
- Cheng, K.Y., Ho, G., Cord-Ruwisch, R. 2012. Energy-efficient treatment of organic wastewater streams using a rotatable bioelectrochemical contactor (RBEC). *Bioresource Technology*, **126**, 431-436.
- Cheng, S., Liu, H., Logan, B.E. 2006. Increased power generation in a continuous flow MFC with advective flow through the porous anode and reduced electrode spacing. *Environmental Science & Technology*, **40**(7), 2426-2432.
- Cheng, S.A., Ye, Y.L., Ding, W.J., Pan, B. 2014. Enhancing power generation of scale-up microbial fuel cells by optimizing the leading-out terminal of anode. *Journal of Power Sources*, **248**, 931-938.

- Chinloy, D.R., Doucet, J., McKenzie, M.A., The, K.I. 1993. Processes for the alkaline biodegradation of organic impurities, Google Patents.
- Compaore, J., Stal, L.J. 2010a. Effect of temperature on the sensitivity of nitrogenase to oxygen in two Heterocystous cyanobacteria *Journal of Phycology*, **46**(6), 1172-1179.
- Compaore, J., Stal, L.J. 2010b. Oxygen and the light-dark cycle of nitrogenase activity in two unicellular cyanobacteria. *Environmental Microbiology*, **12**(1), 54-62.
- Cornish-Bowden, A. 1995. *Fundamentals of enzyme kinetics. Revised edition ed.* Portland Press Ltd, London.
- Dalton, H., Whittenbury, R. 1976. The acetylene reduction technique as an assay for nitrogenase activity in the methane oxidizing bacterium *Methylococcus capsulatus* strain bath. *Archives of Microbiology*, **109**(1), 147-151.
- Das, S., Mangwani, N. 2010. Recent developments in microbial fuel cells: a review. *Journal of Scientific & Industrial Research*, **69**(10), 727-731.
- Davis, J.B., Yarbrough, H.F. 1962. Preliminary experiments on a microbial fuel cell. *Science*, **137**(3530), 615-&.
- Dawson, K.A., Allison, M.J., Hartman, P.A. 1980a. Characteristics of anaerobic oxalate-degrading enrichment cultures from the rumen *Applied and Environmental Microbiology*, **40**(4), 840-846.
- Dawson, K.A., Allison, M.J., Hartman, P.A. 1980b. Isolation and some characteristics of anaerobic oxalate-degrading bacteria from the rumen. *Applied and Environmental Microbiology*, **40**(4), 833-839.
- Dehning, I., Schink, B. 1989. Two new species of anaerobic oxalate-fermenting bacteria, *Oxalobacter vibrioformis* sp. nov. and *Clostridium oxalicum* sp. nov., from sediment samples. *Archives of Microbiology*, **153**(1), 79-84.
- Den Hond, R., Hiralal, I., Rijkeboer, A. 2007. Alumina yield in the Bayer process past, present and prospects. *Light metals*, 37-41.
- Dhar, B.R., Lee, H.-S. 2013. Membranes for bioelectrochemical systems: challenges and research advances. *Environmental Technology*, **34**(13-14), 1751-1764.
- Dijkhuizen, L., Knight, M., Harder, W. 1978. Metabolic regulation in *Pseudomonas oxalaticus* OX1. *Archives of Microbiology*, **116**(1), 77-83.

- Dowd, J.E., Riggs, D.S. 1965. A comparison of estimates of Michaelis-Menten kinetic constants from various linear transformations *Journal of Biological Chemistry*, **240**(2), 863-&.
- Dukan, S., Nystrom, T. 1998. Bacterial senescence: stasis results in increased and differential oxidation of cytoplasmic proteins leading to developmental induction of the heat shock regulon. *Genes Dev*, **12**, 3431–3441.
- Erable, B., Roncato, M.A., Achouak, W., Bergel, A. 2009. Sampling natural biofilms: A new route to build efficient microbial anodes. *Environmental Science & Technology*, **43**(9), 3194-3199.
- Gauthier, F., Neufeld, J.D., Driscoll, B.T., Archibald, F.S. 2000. Coliform bacteria and nitrogen fixation in pulp and paper mill effluent treatment systems. *Applied and Environmental Microbiology*, **66**(12), 5155-5160.
- Ghulam, J., Abida, A., Ali, R.M., Hafeez, F.Y., Shamsi, I.H., Chaudhry, A.N., Chaudhry, A.G. 2007. Enhancing crop growth, nutrients availability, economics and beneficial rhizosphere microflora through organic and biofertilizers. *Annals of Microbiology*, **57**(2), 177-184.
- Gil, G.C., Chang, I.S., Kim, B.H., Kim, M., Jang, J.K., Park, H.S., Kim, H.J. 2003. Operational parameters affecting the performance of a mediator-less microbial fuel cell. *Biosensors & Bioelectronics*, **18**(4), 327-334.
- Gnyra, B., Lever, G. 1979. Review of Bayer organics - Oxalate control processes. *Light Metals.*, **1**, 151-161.
- Gräfe, M., Power, G., Klauber, C. 2009. Review of bauxite residue alkalinity and associated chemistry. *Clay Miner. Karawara, WA, Australia*.
- Gupta, V.V.S.R., Kroker, S.J., Hicks, M., Davoren, C.W., Descheemaeker, K., Llewellyn, R. 2014. Nitrogen cycling in summer active perennial grass systems in South Australia: non-symbiotic nitrogen fixation. *Crop and Pasture Science*, **65**(10), 1044-1056.
- Guyot, J.P., Brauman, A. 1986. Methane production from formate by syntrophic association of *Methanobacterium-bryantii* and *Desulfovibrio-vulgaris-jj*. *Applied and Environmental Microbiology*, **52**(6), 1436-1437.
- Hadfield, K.L., Bulen, W.A. 1969. Adenosine triphosphate requirement of nitrogenase from *Azotobacter vinelandii*. *Biochemistry*, **8**, 5103–5108.

- Hardy, R.W., Holsten, R., Jackson, E., Burns, R. 1968. The acetylene-ethylene assay for N<sub>2</sub> fixation: laboratory and field evaluation. *Plant physiology*, **43**(8), 1185-1207.
- He, Z., Huang, Y.L., Manohar, A.K., Mansfeld, F. 2008. Effect of electrolyte pH on the rate of the anodic and cathodic reactions in an air-cathode microbial fuel cell. *Bioelectrochemistry*, **74**(1), 78-82.
- Hernandez, J.A., George, S.J., Rubio, L.M. 2009. Molybdenum trafficking for nitrogen fixation. *Biochemistry*, **48**(41), 9711-9721.
- Hind, A.R., Bhargava, S.K., Grocott, S.C. 1997. Quantitation of alkyltrimethylammonium bromides in Bayer process liquors by gas chromatography and gas chromatography mass spectrometry. *Journal of Chromatography A*, **765**(2), 287-293.
- Hind, A.R., Bhargava, S.K., Grocott, S.C. 1999. The surface chemistry of Bayer process solids: a review. *Colloids and Surfaces a-Physicochemical and Engineering Aspects*, **146**(1-3), 359-374.
- Hiralal, I.D.K., Holewijn, J.E., Moretto, K. 1994. Critical oxalate concentration (COC) determination in Bayer plant liquors using a turbidity method *Light Metals 1994*, 53-57.
- Horikoshi, K. 1999. Alkaliphiles: Some applications of their products for biotechnology. *Microbiology and Molecular Biology Reviews*, **63**(4), 735-750.
- Igarashi, R.Y., Laryukhin, M., Dos Santos, P.C., Lee, H.I., Dean, D.R., Seefeldt, L.C., Hoffman, B.M. 2005. Trapping H(-) bound to the nitrogenase FeMo-Cofactor active site during H(2) evolution: Characterization by ENDOR spectroscopy. *Journal of the American Chemical Society*, **127**(17), 6231-6241.
- International Aluminium, I. 2017. <http://www.world-aluminium.org/>.
- International Aluminium Institute and European Aluminium, A. 2014. Bauxite Residue Management: Best Practice.
- Ishii, S., Suzuki, S., Norden-Krichmar, T.M., Wu, A., Yamanaka, Y., Nealson, K.H., Bretschger, O. 2013. Identifying the microbial communities and operational conditions for optimized wastewater treatment in microbial fuel cells. *Water Research*, **47**(19), 7120-7130.
- Jin, X.D., Angelidaki, I., Zhang, Y.F. 2016. Microbial electrochemical monitoring of volatile fatty acids during anaerobic digestion. *Environmental Science & Technology*, **50**(8), 4422-4429.

- Joshi, A., Thite, S., Kulkarni, G., Dhotre, D., Joseph, N., Ramana, V.V., Polkade, A., Shouche, Y. 2016. *Nitrincola alkalisediminis* sp nov., an alkaliphilic bacterium isolated from an alkaline lake. *International Journal of Systematic and Evolutionary Microbiology*, **66**, 1254-1259.
- Jothinathan, D., Wilson, R.T. 2017. Comparative analysis of power production of pure, coculture, and mixed culture in a microbial fuel cell. *Energy Sources, Part A: Recovery, Utilization, and Environmental Effects*, **39**(5), 520-527.
- Kaksonen, A.H., Franzmann, P.D., Puhakka, J.A. 2003. Performance and ethanol oxidation kinetics of a sulfate-reducing fluidized-bed reactor treating acidic metal-containing wastewater. *Biodegradation*, **14**(3), 207-217.
- Kanamori, K., Weiss, R.L., Roberts, J.D. 1989. Ammonia assimilation pathways in nitrogen-fixing *Clostridium-Kluyverii* and *Clostridium-Butyricum*. *Journal of Bacteriology*, **171**(4), 2148-2154.
- Kim, B., Chang, I., Gadd, G. 2007. Challenges in microbial fuel cell development and operation. *Applied Microbiology and Biotechnology*, **76**(3), 485-494.
- Krulwich, T.A., Ensign, J.C. 1969. Alteration of glucose metabolism of arthrobacter crystallopoietes by compounds which induce sphere to rod morphogenesis. *Journal of Bacteriology*, **97**(2), 526-534.
- Larrosa-Guerrero, A., Scott, K., Head, I.M., Mateo, F., Ginesta, A., Godinez, C. 2010. Effect of temperature on the performance of microbial fuel cells. *Fuel*, **89**(12), 3985-3994.
- Liu, M., Yuan, Y., Zhang, L.X., Zhuang, L., Zhou, S.G., Ni, J.R. 2010. Bioelectricity generation by a gram-positive *Corynebacterium* sp strain *MFC03* under alkaline condition in microbial fuel cells. *Bioresource Technology*, **101**(6), 1807-1811.
- Logan, B.E., Hamelers, B., Rozendal, R.A., Schrorder, U., Keller, J., Freguia, S., Aelterman, P., Verstraete, W., Rabaey, K. 2006. Microbial fuel cells: Methodology and technology. *Environmental Science & Technology*, **40**(17), 5181-5192.
- Ma, C., Zhuang, L., Zhou, S.G., Yang, G.Q., Yuan, Y., Xu, R.X. 2012. Alkaline extracellular reduction: isolation and characterization of an alkaliphilic and halotolerant bacterium, *Bacillus pseudofirmus MC02*. *Journal of Applied Microbiology*, **112**(5), 883-891.

- Madigan, M.T., Parker, J., Martinko, J.M. 2000. *Biology of Microorganisms*. Prentice Hall, London.
- Margaria, V., Tommasi, T., Pentassuglia, S., Agostino, V., Sacco, A., Armato, C., Chiodoni, A., Schiliro, T., Quaglio, M. 2017. Effects of pH variations on anodic marine consortia in a dual chamber microbial fuel cell. *International Journal of Hydrogen Energy*, **42**(3), 1820-1829.
- McKinlay, J.B., Zeikus, J.G. 2004. Extracellular iron reduction is mediated in part by neutral red and hydrogenase in *Escherichia coli*. *Applied and Environmental Microbiology*, **70**(6), 3467-3474.
- McKinnon, A.J., Baker, C.L. 2012. Process for the destruction of organics in a Bayer process stream, Alcoa Australia Ltd (Alum-C), pp. 28.
- McSweeney, N.J. 2011. The microbiology of oxalate degradation in bioreactors treating Bayer liquor organic wastes. in: *School of biomedical, biomolecular chemical sciences, Microbiology and Immunology*, Vol. PhD, University of Western Australia. Australia, pp. 53-58.
- McSweeney, N.J., Plumb, J.J., Tilbury, A.L., Nyeboer, H.J., Sumich, M.E., McKinnon, A.J., Franzmann, P.D., Sutton, D.C., Kaksonen, A.H. 2011a. Comparison of microbial communities in pilot-scale bioreactors treating Bayer liquor organic wastes. *Biodegradation*, **22**(2), 397-407.
- McSweeney, N.J., Tilbury, A.L., Nyeboer, H.J., McKinnon, A.J., Sutton, D.C., Franzmann, P.D., Kaksonen, A.H. 2011b. Molecular characterisation of the microbial community of a full-scale bioreactor treating Bayer liquor organic waste. *Minerals Engineering*, **24**(11), 1094-1099.
- Mechichi, T., Stackebrandt, E., Gad'on, N., Fuchs, G. 2002. Phylogenetic and metabolic diversity of bacteria degrading aromatic compounds under denitrifying conditions, and description of *Thauera phenylacetica* sp nov., *Thauera aminoaromatica* sp nov., and *Azoarcus buckelii* sp nov. *Archives of Microbiology*, **178**(1), 26-35.
- Meyer, F., Paarmann, D., D'Souza, M., Olson, R., Glass, E.M., Kubal, M., Paczian, T., Rodriguez, A., Stevens, R., Wilke, A., Wilkening, J., Edwards, R.A. 2008. The metagenomics RAST server - a public resource for the automatic phylogenetic and functional analysis of metagenomes. *Bmc Bioinformatics*, **9**.
- Meyers, R.A.E. 2004. Encyclopedia of physical science and technology:Third edition. in: *Materials Chapter : Aluminum*, Academic Press. New York, pp. 495-518.

- Miller, A.W., Dearing, D. 2013. The metabolic and ecological interactions of oxalate-degrading bacteria in the Mammalian gut. *Pathogens (Basel, Switzerland)*, **2**(4), 636-52.
- Miller, L.G., Oremland, R.S. 2008. Electricity generation by anaerobic bacteria and anoxic sediments from hypersaline soda lakes. *Extremophiles*, **12**(6), 837-848.
- Miller, W.S., Zhuang, L., Bottema, J., Wittebrood, A.J., De Smet, P., Haszler, A., Vieregge, A. 2000. Recent development in aluminium alloys for the automotive industry. *Materials Science and Engineering: A*, **280**(1), 37-49.
- Morton, R.A., Dilworth, M.J., Wienecke, B. 1991. Biological disposal of oxalate - by introducing oxalate into reactor contg. aq. soln. in which oxalate-degrading aerobic microorganism is present, etc, Worsley Alumina Pty (WORS-Non-standard) Worsley Alumina Pty Ltd (WORS-Non-standard) pp. 12.
- Nagel, R., Traub, R.J., Allock, R.J.N., Kwan, M.M.S., Bielefeldt-Ohmann, H. 2016. Comparison of faecal microbiota in Blastocystis-positive and Blastocystisnegative irritable bowel syndrome patients. *Microbiome*, **4**:47.
- Nair, A.R. 2010. *Principals of Biotechnology*. Swastik Publishers and Distributors, New Delhi.
- Nappi, C. 2013. The global aluminium industry 40 years from 1972. International Aluminium Institute.
- Paul, V.G., Minteer, S.D., Treu, B.L., Mormile, M.R. 2014. Ability of a haloalkaliphilic bacterium isolated from Soap Lake, Washington to generate electricity at pH 11.0 and 7% salinity. *Environmental Technology*, **35**(8), 1003-1011.
- Pei-Yuan, Z., Zhong-Liang, L. 2010. Experimental study of the microbial fuel cell internal resistance. *Journal of Power Sources*, **195**(24), 8013-8018.
- Peoples, M.B., Herridge, D.F., Ladha, J.K. 1995. Biological nitrogen-fixation - An efficient source of nitrogen for sustainable agricultural production. *Plant and Soil*, **174**(1-2), 3-28.
- Pikaar, I., Rozendal, R.A., Rabaey, K., Yuan, Z. 2013. In-situ caustic generation from sewage: The impact of caustic strength and sewage composition. *Water Research*, **47**(15), 5828-5835.
- Pikaar, I., Rozendal, R.A., Yuan, Z., Rabaey, K. 2011. Electrochemical caustic generation from sewage. *Electrochemistry Communications*, **13**(11), 1202-1204.

- Piña, R.G., Cervantes, C. 1996. Microbial interactions with aluminium. *Biometals*, **9**(3), 311-316.
- Power, G., Gräfe, M., Klauber, C. 2011a. Bauxite residue issues: I. Current management, disposal and storage practices. *Hydrometallurgy*, **108**(1–2), 33-45.
- Power, G., Loh, J. 2010. Organic compounds in the processing of lateritic bauxites to alumina Part 1: Origins and chemistry of organics in the Bayer process. *Hydrometallurgy*, **105**(1-2), 1-29.
- Power, G., Loh, J.S.C., Niemela, K. 2011b. Organic compounds in the processing of lateritic bauxites to alumina Addendum to Part 1: Origins and chemistry of organics in the Bayer process. *Hydrometallurgy*, **108**(1-2), 149-151.
- Power, G., Loh, J.S.C., Vernon, C. 2012. Organic compounds in the processing of lateritic bauxites to alumina Part 2: Effects of organics in the Bayer process. *Hydrometallurgy*, **127**, 125-149.
- Power, G., Loh, J.S.C., Wajon, J.E., Busetti, F., Joll, C. 2011c. A review of the determination of organic compounds in Bayer process liquors. *Analytica Chimica Acta*, **689**(1), 8-21.
- Power, G., Tichbon, W. 1990. Sodium oxalate in the Bayer process: Its origin and effects. in: *Second International Alumina Quality Workshop*. Perth, pp. 99-115.
- Rabaey, K., Butzer, S., Brown, S., Keller, J., Rozendal, R.A. 2010. High current generation coupled to caustic production using a lamellar bioelectrochemical system. *Environmental Science & Technology*, **44**(11), 4315-4321.
- Rabaey, K., Clauwaert, P., Aelterman, P., Verstraete, W. 2005. Tubular microbial fuel cells for efficient electricity generation. *Environmental Science & Technology*, **39**(20), 8077-8082.
- Rabaey, K., Rodriguez, J., Blackall, L.L., Keller, J., Gross, P., Batstone, D., Verstraete, W., Nealson, K.H. 2007. Microbial ecology meets electrochemistry: electricity-driven and driving communities. *Isme Journal*, **1**(1), 9-18.
- Raghavan, P.K.N., Kshatriya, N.K., Dasgupta, S. 2011. Digestion Studies on Central Indian Bauxite. in: *Light Metals 2011*, John Wiley & Sons, Inc., pp. 29-32.
- Raghavulu, S.V., Mohan, S.V., Reddy, M.V., Mohanakrishna, G., Sarma, P.N. 2009. Behavior of single chambered mediatorless microbial fuel cell (MFC) at acidophilic, neutral and alkaline microenvironments during chemical

- wastewater treatment. *International Journal of Hydrogen Energy*, **34**(17), 7547-7554.
- Rao, J.R., Richter, G.J., Von Sturm, F., Weidlich, E. 1976. The performance of glucose electrodes and the characteristics of different biofuel cell constructions. *Bioelectrochemistry and Bioenergetics*, **3**(1), 139-150.
- Reinholdhurek, B., Hurek, T., Gillis, M., Hoste, B., Vancanneyt, M., Kersters, K., Deley, J. 1993. *Azoarcus* gen-nov, nitrogen-fixing proteobacteria associated with roots of Kallar grass (*Leptochloa-fusca* (L) kunth), and description of 2 species, *Azoarcus-Indigens* sp-nov and *Azoarcus-Communis* sp-nov. *International Journal of Systematic Bacteriology*, **43**(3), 574-584.
- Rosenberg, S.P., Tichbon, W., Wilson, D.J., Heath, C.A. 2004. Process for the removal of oxalate and/or sulphate from Bayer liquors, Google Patents.
- Rousseau, R., Dominguez-Benetton, X., Delia, M.L., Bergel, A. 2013. Microbial bioanodes with high salinity tolerance for microbial fuel cells and microbial electrolysis cells. *Electrochemistry Communications*, **33**, 1-4.
- Rozendal, R.A., Hamelers, H.V.M., Buisman, C.J.N. 2006. Effects of membrane cation transport on pH and microbial fuel cell performance. *Environmental Science & Technology*, **40**(17), 5206-5211.
- Rozendal, R.A., Hamelers, H.V.M., Rabaey, K., Keller, J., Buisman, C.J.N. 2008. Towards practical implementation of bioelectrochemical wastewater treatment. *Trends in Biotechnology*, **26**(8), 450-459.
- Sahin, N. 2003. Oxalotrophic bacteria. *Research in Microbiology*, **154**(6), 399-407.
- Sakai, S., Conrad, R., Liesack, W., Imachi, H. 2010. *Methanocella arvoryzae* sp nov., a hydrogenotrophic methanogen isolated from rice field soil. *International Journal of Systematic and Evolutionary Microbiology*, **60**, 2918-2923.
- Santegoeds, C.M., Ferdelman, T.G., Muyzer, G., de Beer, D. 1998. Structural and functional dynamics of sulfate-reducing populations in bacterial biofilms. *Applied and Environmental Microbiology*, **64**(10), 3731-3739.
- Schulze, J., Adgo, E., Schilling, G. 1994. The influence of N<sub>2</sub>-fixation on the carbon balance of leguminous plants *Experientia*, **50**(10), 906-912.
- Sipos, G., Kildea, J.D., Parkinson, G.M. 1999. The role of quaternary amines in the inhibition of sodium oxalate crystal growth in Bayer liquor. in: *14th International symposium on industrial crystallization*, Institute of chemical engineers, UK. University of Cambridge, UK.

- Songqing, G. 2013. Bayer process efficiency improvement. in: *Light Metals 2013*, John Wiley & Sons, Inc., pp. 163-167.
- Sorokin, D., Tourova, T., Schmid, M.C., Wagner, M., Koops, H.P., Kuenen, J.G., Jetten, M. 2001. Isolation and properties of obligately chemolithoautotrophic and extremely alkali-tolerant ammonia-oxidizing bacteria from Mongolian soda lakes. *Archives of Microbiology*, **176**(3), 170-177.
- Sorokin, I.D., Kravchenko, I.K., Doroshenko, E.V., Boulygina, E.S., Zadorina, E.V., Tourova, T.P., Sorokin, D.Y. 2008. Haloalkaliphilic diazotrophs in soda solonchak soils. *FEMS Microbiology Ecology*, **65**(3), 425-433.
- Soucy, G., Larocque, J.E., Forté, G. 2013. Organic control technologies in Bayer process. *Essential Readings in Light Metals*, 291-296.
- Sousa, J.A.B., Sorokin, D.Y., Bijmans, M.F.M., Plugge, C.M., Stams, A.J.M. 2015. Ecology and application of haloalkaliphilic anaerobic microbial communities. *Applied Microbiology and Biotechnology*, **99**(22), 9331-9336.
- Sprent, P. 1990. *Nitrogen fixing organisms: pure and applied aspects*. Chapman and Hall, London.
- Staal, M., Rabouille, S., Stal, L.J. 2007. On the role of oxygen for nitrogen fixation in the marine cyanobacterium *Trichodesmium* sp. *Environmental Microbiology*, **9**(3), 727-736.
- Stewart, C.S., Duncan, S.H., Cave, D.R. 2004. *Oxalobacter formigenes* and its role in oxalate metabolism in the human gut. *FEMS Microbiology Letters*, **230**(1), 1-7.
- Strapoć, D., Mastalerz, M., Dawson, K., Macalady, J., Callaghan, A.V., Wawrik, B., Turich, C., Ashby, M. 2011. Biogeochemistry of microbial coal-bed methane. *Annual Review of Earth and Planetary Sciences*, **39**, 617-656.
- Susan Hill, J.W.D.a.J.R.P. 1972. Environmental effects on the growth of nitrogen-fixing bacteria. *Journal of Applied Chemical Technology and Biotechnology*(22), 541-558.
- Susilawati, R., Golding, S.D., Baublys, K.A., Esterle, J.S., Hamilton, S.K. 2016. Carbon and hydrogen isotope fractionation during methanogenesis: A laboratory study using coal and formation water. *International Journal of Coal Geology*, **162**, 108-122.
- Svedruzic, D., Jonsson, S., Toyota, C.G., Reinhardt, L.A., Ricagno, S., Linqvist, Y., Richards, N.G.J. 2005. The enzymes of oxalate metabolism: unexpected

- structures and mechanisms. *Archives of Biochemistry and Biophysics*, **433**(1), 176-192.
- Tadanori, H., Kazuhiko, N., Koichi, Y. 1975. Method for the removal of organic substances from sodium aluminate solution, Google Patents.
- Tilbury, A. 2003. Biodegradation of Bayer organics in residue disposal systems. in: *Department of Chemistry*, Vol. Doctor of Philosophy, University of Western Australia.
- Torres, C.I., Kato Marcus, A., Rittmann, B.E. 2008. Proton transport inside the biofilm limits electrical current generation by anode-respiring bacteria. *Biotechnology and Bioengineering*, **100**(5), 872-881.
- Torres, C.I., Krajmalnik-Brown, R., Parameswaran, P., Marcus, A.K., Wanger, G., Gorby, Y.A., Rittmann, B.E. 2009. Selecting anode-respiring bacteria based on anode potential: phylogenetic, electrochemical, and microscopic characterization. *Environmental Science & Technology*, **43**(24), 9519-9524.
- Trinchant, J.C., Guerin, V., Rigaud, J. 1994. Acetylene reduction by symbiosomes and free bacteroids from broad bean (*Vicia faba L.*) nodules (Role of oxalate). *Plant Physiology*, **105**(2), 555-561.
- Turhan, S., Usta, B., Şahin, Y., Uysal, O. 2011. Determination of oxalate ion in Bayer liquor using electrochemical method. in: *Light Metals 2011*, John Wiley & Sons, Inc., pp. 215-217.
- Villaverde, S., GarciaEncina, P.A., FdzPolanco, F. 1997. Influence of pH over nitrifying biofilm activity in submerged biofilters. *Water Research*, **31**(5), 1180-1186.
- Virdis, B., Freguia, S., Rozendal, R.A., Rabaey, K., Yuan, Z., Keller, J. 2011. Microbial fuel cells. in: *Treatise on Water Science*, (Ed.) P. Wilderer, Elsevier. Oxford, pp. 641-665.
- Wackett, L.P. 1996. Co-metabolism: is the emperor wearing any clothes? *Current Opinion in Biotechnology*, **7**(3), 321-325.
- Wagner, R.C., Call, D.F., Logan, B.E. 2010. Optimal set anode potentials vary in bioelectrochemical systems. *Environmental Science & Technology*, **44**(16), 6036-6041.
- Wang, H., Zhang, Y., Angelidaki, I. 2016. Ammonia inhibition on hydrogen enriched anaerobic digestion of manure under mesophilic and thermophilic conditions. *Water Research*, **105**, 314-319.

- Wang, Q., Garrity, G.M., Tiedje, J.M., Cole, J.R. 2007. Naive Bayesian classifier for rapid assignment of rRNA sequences into the new bacterial taxonomy. *Applied and Environmental Microbiology*, **73**(16), 5261-5267.
- Weerasinghe Mohottige, T.N., Cheng, K.Y., Kaksonen, A.H., Sarukkalige, R., Ginige, M.P. 2017a. Oxalate degradation by alkaliphilic biofilms acclimatised to nitrogen-supplemented and nitrogen-deficient conditions. *Journal of chemical technology and biotechnology*.
- Weerasinghe Mohottige, T.N., Ginige, M.P., Kaksonen, A.H., Sarukkalige, R., Cheng, K.Y. 2017b. Bioelectrochemical oxidation of organics by alkali-halotolerant anodophilic biofilm under nitrogen-deficient, alkaline and saline conditions. *Bioresource Technology*.
- Wellington, M., Valcin, F. 2007. Impact of Bayer process liquor impurities on causticization. *Industrial & Engineering Chemistry Research*, **46**(15), 5094-5099.
- Whelan, T.J., Ellis, A., Kannangara, G.S.K., Marshall, C.P., Smeulders, D., Wilson, M.A. 2003. Macromolecules in the Bayer process. *Reviews in Chemical Engineering*, **19**(Issue 5), Pages 431–472.
- Whiting, P.H., Midgley, M., Dawes, E.A. 1976. The regulation of transport of glucose, gluconate and 2-oxogluconate and of glucose catabolism in *Pseudomonas aeruginosa*. *Biochemical Journal*, **154**(3), 659-668.
- Williams, F.S., Perrotta, A.J. 1998. Adsorbent combinations for enhanced removal of sodium oxalate from bayer process spent liquor, Google Patents.
- Wong, P.Y., Cheng, K.Y., Kaksonen, A.H., Sutton, D.C., Ginige, M.P. 2014. Enrichment of anodophilic nitrogen fixing bacteria in a bioelectrochemical system. *Water Research*, **64**, 73-81.
- Xie, C.H., Yokota, A. 2006. *Zoogloea oryzae* sp nov., a nitrogen-fixing bacterium isolated from rice paddy soil, and reclassification of the strain ATCC 19623 as *Crabtreella saccharophila* gen. nov., sp nov. *International Journal of Systematic and Evolutionary Microbiology*, **56**, 619-624.
- Yamada, K., Harato, T., Kato, H. 1980. Method for the separation of precipitated aluminum hydroxide from sodium aluminate solution, Google Patents.
- Yang, K.Y., Haynes, C.A., Spatzal, T., Rees, D.C., Howard, J.B. 2014. Turnover-dependent inactivation of the nitrogenase MoFe-Protein at high pH. *Biochemistry*, **53**(2), 333-343.

- Yingwei, B., Mingliang, S., Junqi, L., Fei, Z. 2011. A new method for removal organics in the Bayer process. *Light Metals 2011*, 51-55.
- Yong, Y.-C., Cai, Z., Yu, Y.-Y., Chen, P., Jiang, R., Cao, B., Sun, J.-Z., Wang, J.-Y., Song, H. 2013. Increase of riboflavin biosynthesis underlies enhancement of extracellular electron transfer of Shewanella in alkaline microbial fuel cells. *Bioresource Technology*, **130**, 763-768.
- Zhang, E.R., Zhai, W.J., Luo, Y., Scott, K., Wang, X., Diao, G.W. 2016. Acclimatization of microbial consortia to alkaline conditions and enhanced electricity generation. *Bioresource Technology*, **211**, 736-742.
- Zhuang, L., Zhou, S., Li, Y., Yuan, Y. 2010a. Enhanced performance of air-cathode two-chamber microbial fuel cells with high-pH anode and low-pH cathode. *Bioresource Technology*, **101**(10), 3514-3519.
- Zhuang, L., Zhou, S.G., Li, Y.T., Yuan, Y. 2010b. Enhanced performance of air-cathode two-chamber microbial fuel cells with high-pH anode and low-pH cathode. *Bioresource Technology*, **101**(10), 3514-3519.

# Appendix 1

## Supplementary Information to Chapter 2.

**Table S2.1.** Step changes to the R1 (nitrogen supplemented) during the entire operational period.

Days	Sodium oxalate concentration (mM)	Sodium acetate Concentration (mM)	HRT (h)	Influent pH	Anode potential (mV vs Ag/AgCl)	Experimental objective
1 to 26	25	-	24	10	+200	
27 to 37	25	-	Batch	10	+200	Reactor start-up period with sodium oxalate as the only carbon source
38 to 44	25	-	48	10	+200	
44 to 54	25	-	Batch	10	+200	
55 to 61	25	5	48	10	+200	
62 to 72	25	5	48	10	+200	
73 to 80	25	5	48	10	+200	
81 to 90	25	-	Batch	10	+200	To study the response to sodium acetate and the response to sodium formate
91 to 110	25	5	1-48	10	+200	To Study the effect of HRT on BES performance
111 to 127	25	5	3	10	Varied	To study the effect of poised anode potential on BES performance
128 to 132	25	5	48	10	-300	
133 to 141	25	5	1-48	10	-300	To Study the effect of HRT on BES performance
142 to 156	25	5	3	10	-300	To Study the alkalinity increase and caustic production in the catholyte
157 to 167	25	5	Batch	10	-300	
168 to 203	25	5	48	10	-300	
204 to 213	25	5	24	10	-300	
214 to 226	25	Varied	6	10	-300	To study the microbial activity at reducing sodium acetate concentrations
227 to 237	25	-	Batch	10	-300	To study the response to other organics in Bayer liquor - sodium succinate and sodium malonate
238 to 256	25	-	48 and 6	10	-300	

**Table S2.2.** Step changes to R2 (nitrogen deficient) during the entire operational period.

Days	Sodium oxalate concentration (mM)	Sodium acetate Concentration (mM)	HRT (h)	Anode Influent pH	potential (mV vs Ag/AgCl)	Experimental objective
1 to 26	25	-	24	10	+200	Reactor start-up period with sodium oxalate as the only carbon source
27 to 37	25		Batch	10	+200	
38 to 44	25	-	48	10	+200	
44 to 54	25	-	Batch	10	+200	
55 to 61	25	5	48	10	+200	Reactor operation with sodium oxalate and sodium acetate
62 to 72						Biofilm was inactive
73 to 80	25	5	48	10	+200	
81 to 90	25	5	Batch	10	+200	To study the response to sodium acetate and the response to sodium formate
91 to 110	25	5	Varied	10	+200	To Study the effect of HRT on BES performance
111 to 127	25	5	48	10	+200	
128 to 132	25	5	48	10	+200	
134 to 135	25	5	Batch	10	+200	
136 to 154	25	5	48	10	+200	
155 to 169	25	5	3-48	10	+200	To Study the effect of HRT on BES performance
170 to 175	25	5	3	10	Varies	To study the effect of poised anode potential on BES performance
176 to 187	25	5	1-48	10	-300	To Study the effect of HRT on BES performance
188 to 198	25	5	3	10	-300	To Study the alkalinity increase and caustic production in the catholyte
199 to 210	25	5	24	10	-300	
211 to 222						Biofilm was inactive
223 to 259	25	5	48 and 24	10	-300	To study the response to other organics in Bayer liquor - sodium succinate and sodium malonate

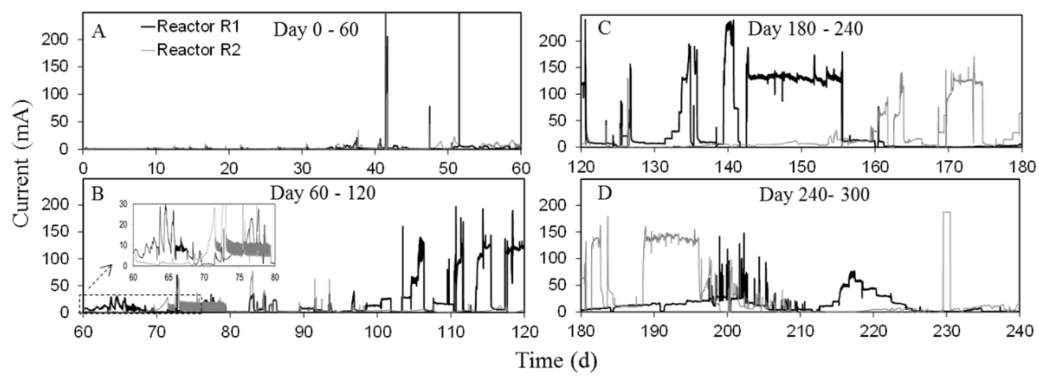


**Figure S2.1.** Long term current generation profiles for the two BES reactors (R1: reactor with nitrogen supplementation; R2: reactor without nitrogen supplementation). Operational parameters and details of different periods are given in Table S2.1 and S2.2.

**Relationship between the rate of electrical conductivity increment in the catholyte and electrical current in both R1 and R2**

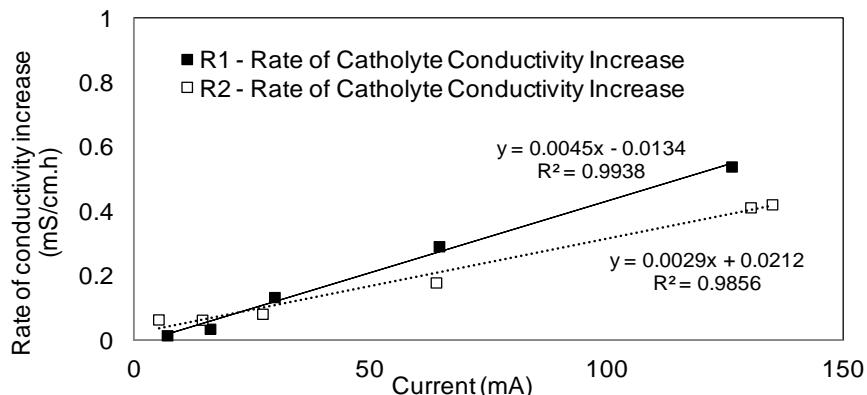


**Figure S2.2.** Relationship between the rate of electrical conductivity increment in the catholyte and electrical current of the bioelectrochemical system. Data were calculated from the experiments as shown in Figure 2.4 and 2.5.

During the study, it was observed that the catholyte conductivity increased proportionally with an increase in current mostly likely due to increased flux of cations across the cation exchange membrane (Figure S2.2). Since sodium was the predominate cation in the anolyte, it was likely that sodium was the key species accounting for such migration. The rate of catholyte conductivity increase is linearly related to the current production in both reactors. Figure S2.2 shows the linear relationship of rate of catholyte conductivity increase and current production. This result suggests that the process is also promising for recovering caustic soda.

## Appendix 2

### Supplementary Information to Chapter 6.

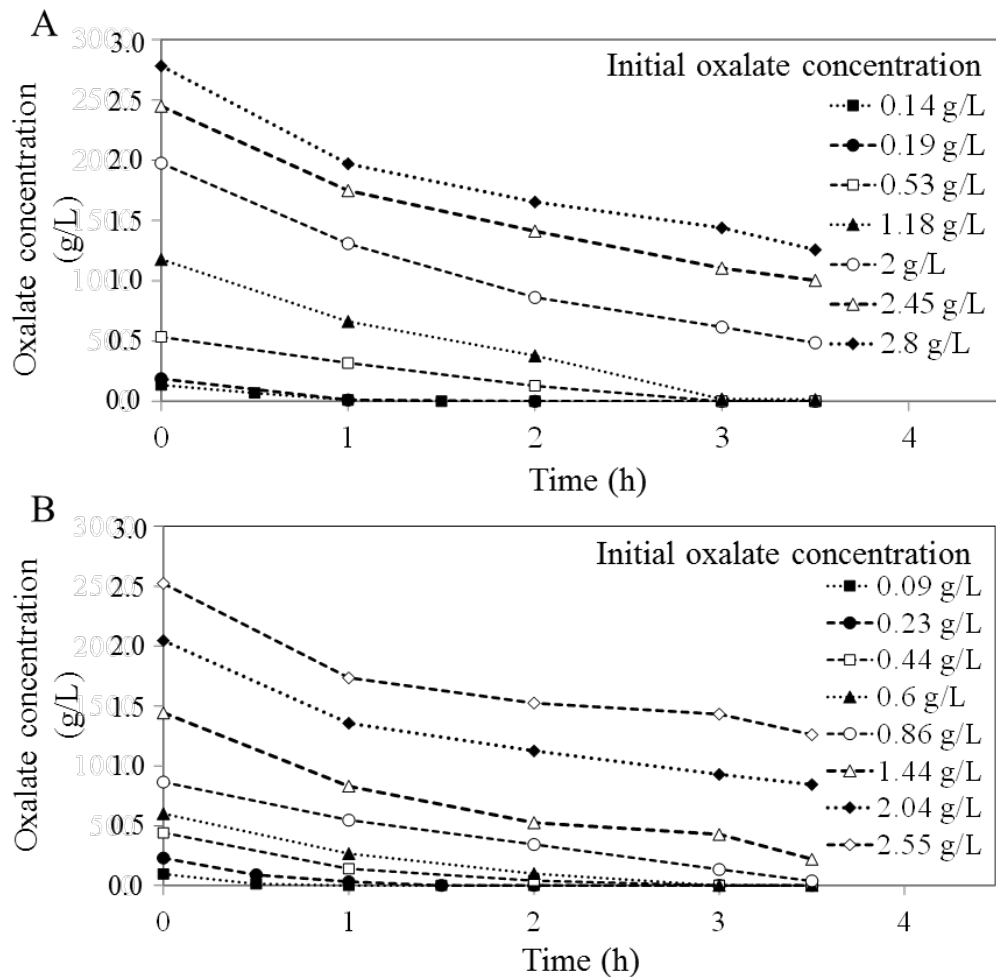


**Figure S6.1.** Oxidation of oxalate during batch experiments with various initial oxalate concentrations in (A) N-supplemented and (B) N-deficient reactor system.

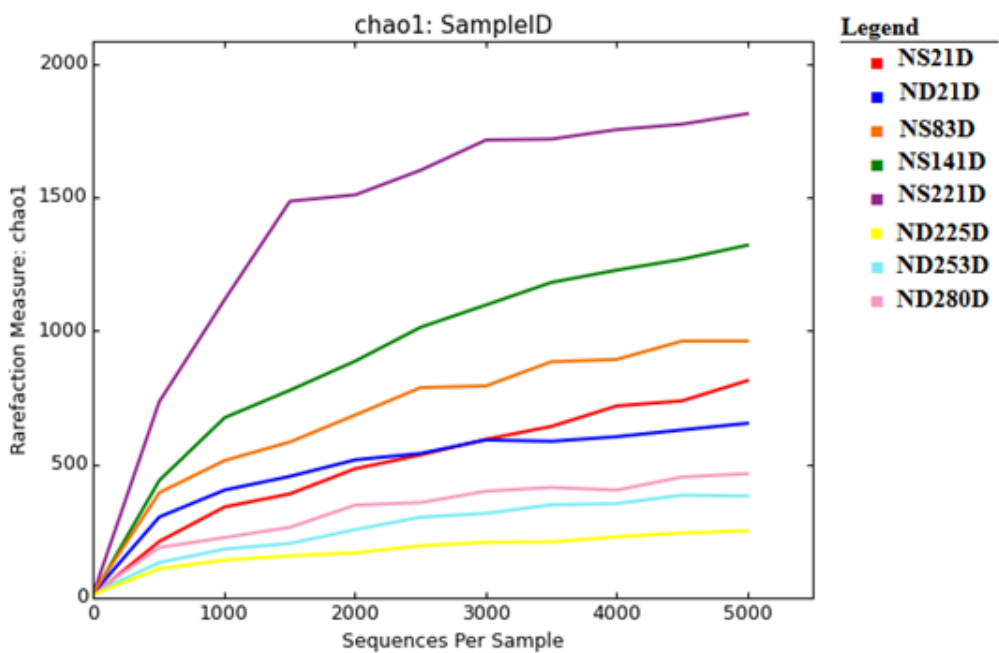


**Figure S6.2.** Alpha diversity rarefaction detected in the N-supplemented and N-deficient reactors as determined by 454 sequencing of 16S rRNA genes.

## Appendix 3

### Supplementary Information to Chapter 7.

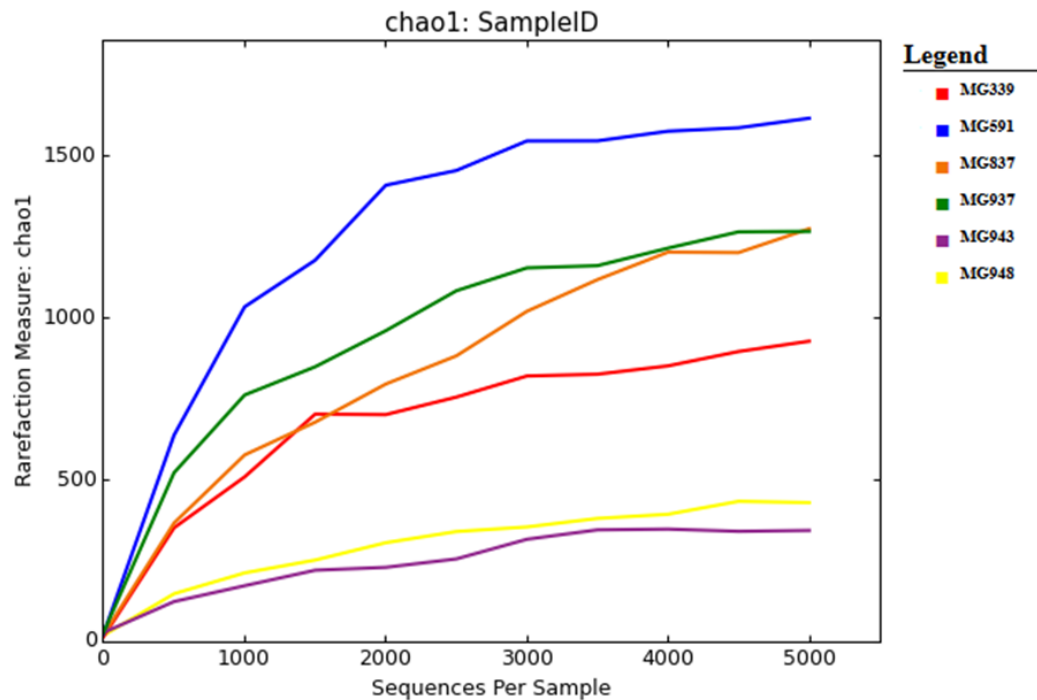


**Figure S7.1.** Alpha diversity rarefaction curves for microbial community analysis of samples determined by 454 sequencing of 16S rRNA genes.

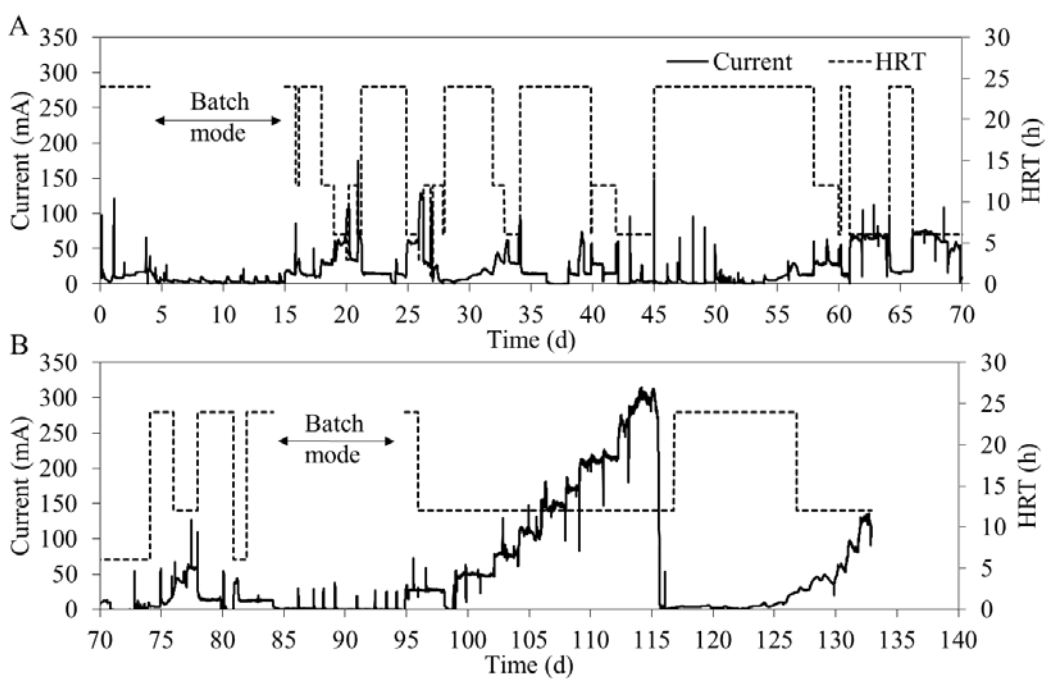


**Figure S7.2.** Long-term current generation and HRT profiles for the BES reactor.

## Further confirmation of rapid start-up of the BES reactor inoculated with aerobic reactor biomass

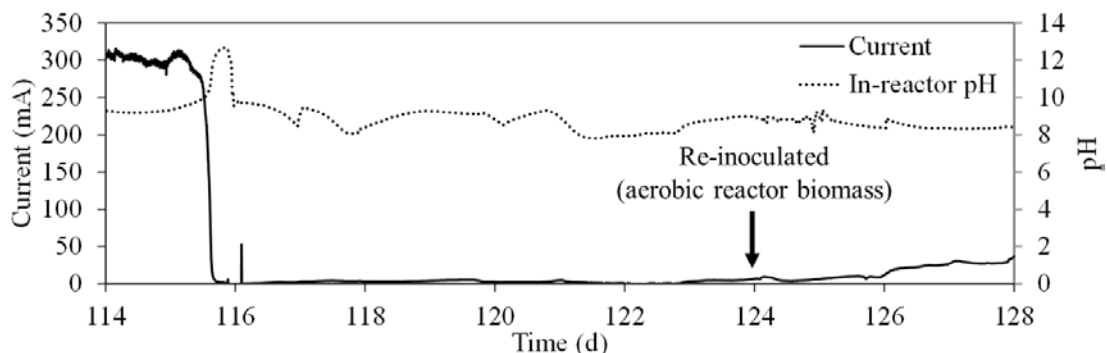
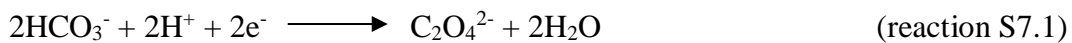


**Figure S7.3.** Recovery of biofilm after inoculated with aerobic reactor biomass at anode potential -300mV vs Ag/AgCl, pH 9.0.

In this study, the observed rapid start-up of the BES reactor inoculated with oxalate degrading aerobic reactor biofilm was further confirmed. On day 115, the reactor was fed with both oxalate and acetate to produce high current and then the biofilm was challenged by increasing pH ( $\text{pH} > 12$ ) to investigate the recovery of established biofilm (Fig. S3). After day 116, the feed solution was changed with oxalate as the sole substrate and the reactor was operated at 24 h HRT for 8 days to allow the inhibited biofilm to recover its activity. During this period, the current production remained low ( $< 5 \text{ mA}$ ) indicating a lack of activity of the biofilm. On day 124, the reactor was re-inoculated with biomass obtained from the parent aerobic reactor. Clearly, the re-inoculation had triggered an onset of the biofilm activity within 2 days and the current increased to 10 mA at the end of day 126. On day 127, the HRT was changed back to 12 h and the reactor was able to produce respective maximum current ( $\sim 27 \text{ mA}$ ) with the oxalate as the only carbon source (Fig. S3). This result confirmed that the aerobic reactor biomass could not only allow a rapid start-up of the BES, but also allow a ready revival of the anodophilic activity of the biofilm in a BES.

## Calculation of anode potential for oxalate oxidation

The expected anode potential was calculated based on half-cell reactions. According to IUPAC convention the standard reduction potential is written as electron consuming process as shown for oxalate in Reaction S7.1 (Logan et al., 2006).



Standard free energy ( $\Delta G^\circ$ ) of the half cell reaction at standard conditions of substrate concentration of 1 M, pH 7 at 25°C was calculated as follows (Equation S7.2).

$$\begin{aligned}\Delta G^\circ &= 2\Delta G_f^\circ(\text{HCO}_3^-) - [\Delta G_f^\circ(\text{C}_2\text{O}_4^{2-}) - 2\Delta G_f^\circ(\text{H}_2\text{O})] \\ &= (2 \times -586.85) - [(-674.04) + 2 \times (-237.13)] \\ &= -25.4 \text{ kJ/mol}\end{aligned} \quad (\text{equation S7.2})$$

Where  $\Delta G^\circ_f$  is the standard Gibbs free energy of formation.

Standard electrode potentials are reported relative to the normal hydrogen electrode, which has a potential zero at standard conditions of 1 M, pH<sub>2</sub> 1 bar at 298 K. Standard anode potential at substrate concentration of 1 M, pH 7 at 298 K was calculated as follows (Equation S7.3).

$$\begin{aligned}E^\circ_{\text{AN}} &= -\Delta G^\circ / nF \\ &= -(-25.4 \times 10^3) / (2 \times 96485.3) \\ &= 0.131 \text{ V}\end{aligned} \quad (\text{equation S7.3})$$

Where n = number of electrons per reaction mol and F = Faraday's constant.

Hence, anode potential for oxalate oxidation in our study at  $[\text{C}_2\text{O}_4^{2-}] = 25 \text{ mM}$ ,  $[\text{HCO}_3^-] = 25 \text{ mM}$  and pH 9 was calculated based on (Logan et al., 2006) as follows (Equation S7.4):

$$\begin{aligned}E_{\text{AN}} &= E^\circ_{\text{AN}} - (RT/nF) \times \ln((\text{C}_2\text{O}_4^{2-}) / ([\text{HCO}_3^-]^2 \times (\text{H}^+)^2]) \\ E_{\text{AN}} &= \\ &= 0.13 - (8.3145 \times 298 / 2 \times 96485.3) \times \ln(25 \times 10^{-3} / [(25 \times 10^{-3})^2 \times (1 \times 10^{-9})^2]) \\ &= 0.13 - (0.0128 \times 45.135) \\ &= -0.447 \text{ V}\end{aligned} \quad (\text{equation S7.4})$$

Where, R = 8.3145 J/mol.K and T = 298 K

The potential was converted to Ag/AgCl electrode potential as follows (Equation S7.5):

$$E_{\text{AN-Ag/AgCl}} = E_{\text{AN}} - 0.197 \text{ mV} = -0.644 \text{ V} \quad (\text{equation S7.5})$$